

**IN SITU FORMING BIODEGRADABLE
HYDROGELS AND THEIR APPLICATION
FOR PROTEIN DELIVERY**

PROEFSCHRIFT

**ter verkrijging van
de graad van doctor aan de Universiteit Twente,
op gezag van de rector magnificus,
prof. dr. W. H. M. Zijm,
volgens besluit van het College voor Promoties
in het openbaar te verdedigen
op vrijdag 1 juni 2007 om 16.45 uur**

door

Christine Hiemstra

**geboren op 15 februari 1978
te Drogeham**

Dit proefschrift is goedgekeurd door:

Promotor: Prof. dr. J. Feijen

Co-promotor: Prof. dr. Z. Y. Zhong

Het weten heft het geheim niet op, maar verdiept het.

Dietrich Bonhoeffer (1906-1945)

Committee

Chairman:	prof. dr. ir. W. P. M. Van Swaaij	University of Twente
Promotor:	prof. dr. J. Feijen	University of Twente
Co-promotor:	prof. dr. Z. Y. Zhong	University of Twente
Members:	dr. P. J. Dijkstra	University of Twente
	prof. dr. J. F. J. Engbersen	University of Twente
	prof. dr. ing. M. Wessling	University of Twente
	prof. dr. W. Briels	University of Twente
	prof. dr. W. E. Hennink	University of Utrecht
	prof dr. ir. J. C. M. van Hest	Radboud University

The research described in this thesis was financially supported by the Netherlands Organization for Scientific Research (NWO).

This publication was sponsored by the Dutch Society for Biomaterials (NVB).

In situ forming biodegradable hydrogels and their application for protein delivery.

Ph. D. Thesis – With references; summary in English and Dutch.

University of Twente, Enschede, The Netherlands

ISBN 978-90-9021890-8

Copyright © 2007 by C. Hiemstra

All rights reserved.

Printed by PrintPartners Ipskamp, Enschede, The Netherlands, 2007.

The cover was designed by Adriaan de Haan

Voorwoord

Al weer bijna vijf jaar geleden begon ik met afstuderen bij de vakgroep Polymeer Chemie en Biomaterialen van professor Feijen aan de Universiteit Twente. In heb begin had ik het moeilijk, ik moest nog wennen aan de 9 tot 5 tijden. Toch werd ik enthousiast voor het onderzoek en besloot ik om assistent in opleiding (AIO) te worden bij deze vakgroep. Er zijn momenten waarop ik dacht, was ik daar maar nooit aan begonnen, maar het is ook een leerzame en erg leuke periode geweest. En dat mede dankzij de mensen ik hieronder noem.

Allereerst wil ik mijn promotor Jan Feijen bedanken. Vooral in het laatste jaar heb ik vaak bij u aan de tafel gezeten, vaak waren het lange vergaderingen. Ik heb er erg veel in geleerd en besepte me helaas te laat het grote nut van deze besprekingen. Bedankt voor uw blijvende enthousiasme en inzet.

Since my co-promotor Zhiyuan Zhong still has not learned Dutch yet, I will proceed in English. Thanks Zhiyuan for your patience and your help to lift my research to a higher level. When sometimes I thought I obtained data of less use, you saw opportunities and helped me to see the greater picture. Often I received my articles back after correction containing many red remarks. Though this may have been frustrating, it did teach me to be more critic and precise.

Ik wil ook graag Piet Dijkstra bedanken. In mijn eerste jaar als AIO was jij mijn begeleider en ook na de tijd ben ik jouw kantoor nog regelmatig binnengevallen om het een of ander te vragen. Bedankt voor al je hulp en tijd.

Tijdens mijn onderzoek heb ik de hulp gehad van ontzettend veel mensen zonder wie ik dit niet had kunnen doen. Ik heb veel van mijn resultaten te danken aan mijn studenten, Wei Zhou en Hans van der Aa. Wei, you maybe had to get used to polymers, since your background was organic chemistry, but you learned quickly. Also you worked very hard, even at Sunday you could be found in the Chemical Technology building. In the end you obtained very nice results, which can be found in Chapter 4 of this thesis. Hans, ook jij hebt erg hard gewerkt, ik stond versteld wat je in korte tijd voor elkaar kon krijgen. Ook was je veel handiger op het lab dan ik, ik heb nog veel van je op kunnen steken. Helaas deelden we wel onze handigheid met glaswerk. Van jouw werk kon ik maar liefst twee

hoofdstukken schrijven, Hoofdstuk 7 en 8 van dit proefschrift. Jasper, jouw werk heb ik nog kunnen presenteren op het NVB congres. Bedankt voor je inzet. Henriëtte en Marloes, bedankt voor jullie inzet voor het meten van de groeifactor activiteit. Helaas lukte het door de te korte tijd niet om de bepaling lopende te krijgen. Na vier en een half jaar is het ook tijd om het onderzoek af te sluiten.

Ook heb ik veel hulp gehad van mensen buiten onze universiteit. Liangbin Li, thanks for doing the WAXS experiments. It was very nice to be able to prove the existence of the stereocomplex crystals in the PEG-PLA hydrogels. Sophie Van Tomme, enorm bedankt voor al je tijd en hulp bij het opzetten van de eiwitafgifte proef van de PEG-PLA hydrogelen. We hebben erg mooie resultaten behaald, deze staan in Hoofdstuk 5 van dit proefschrift. Mies van Steenbergen, jou moet ik ook zeker niet vergeten. Bedankt voor je hulp bij of zelfs het uitvoeren van de HPLC experimenten. Professor Hennink, bedankt dat ik een tijdje in uw groep mocht werken. Ook wil ik u bedanken voor het bespreken van de eiwitafgifte resultaten en voor alle nuttige tips. John Jacobs en Wim den Otter, jullie wil ik bedanken voor het uitvoeren van de dierexperimenten. Het was voor mij wel even slikken, ik was blij dat ik het aan jullie over kon laten. Wim, bedankt voor het mogelijk maken van de experimenten en John, bedankt voor je hulp bij het schrijven. Xulin Jiang, thanks for the GPC measurements on the PEG-PLA multiblock copolymers you performed for me. They were very useful and enabled me to write Appendix 1 of this thesis. Haike Ruijters, het duurde even voor ik je naam goed had in het begin, maar gedurende mijn hele promotieonderzoek kon ik bij jou terecht voor vragen over reologie. Bedankt voor je blijvende interesse, hulp en tijd. Op jouw verwijzing heb ik contact gezocht met Mariëlle Wouters voor het doen van UV-reologie metingen. Mariëlle, je had het ontzettend druk, dus we konden maar een beperkt aantal metingen doen. Deze metingen gaven echter wel zeer goede resultaten (zie Hoofdstuk 6), zo goed dat we een patent hebben aangevraagd. Bedankt voor je inzet! Voor Appendix 2 heb ik hulp gehad van meerdere mensen. Richard Heenan, Ann Terry of the ISIS SANS facility Rutherford and Dirk Visser of the NWO, thanks for helping me with the measurements. Dirk, also thanks for the nice and interesting conversations over dinner. Johan Padding, Wim Briels en Menno Bokdam, dankzij jullie heb ik nog een deel aan Appendix 2 kunnen toevoegen over computational modeling. Bedankt voor jullie hulp en inzet. De resultaten zijn nog voorlopig, maar ik hoop dat we

samen met de SANS metingen een beter beeld kunnen krijgen van hoe stervormige PEG-PLA moleculen zich gedragen in water.

Dan mijn eigen vakgroep. Ingrid, Lanti, Wei, Priscilla, Laura, Fenghua, Anita en niet te vergeten Boon Hua. Jullie waren mijn kantoorgenootjes van de 'Chicken Room'. (Boon Hua, you fitted in perfectly, since I have never met a woman who could talk as much as you do.) Thanks for all the talks and fun we had together! Ingrid en Priscilla, met jullie heb ik nogal eens het vertrouwde rondje rond de Campus gelopen in de middagpauze. Dat was niet alleen sportief, maar ook erg gezellig. Zalata, bedankt voor al je hulp en de social talks bij de koffie. Karin, bedankt voor al het regelen! Zheng, I think I talked to you mostly during birthday parties. I enjoyed being your paranimf. Ik wil ook nog iedereen van PBM, STEP, RBT en MTP bedanken voor de gezellige tijd. De borrels, etentjes, triatlon, Sinterklaas feest...enz. en natuurlijk de altijd gezellige koffiepauzes. In het speciaal wil ik bedanken: Ingrid, Priscilla, Mark, Lanti, Wei, Andries (wat hadden wij toch een goede snert gemaakt!), Marc, Moniek, Anita, Laura, Fenghua, Boon Hua, Kinsuk, Hans, Debbie, Zalata en Karin.

Mark en Susanne, jullie zijn mijn paranimfen. Mark, ik kon altijd terecht voor raad bij jou, hopelijk heb je ook nog iets gehad aan mijn raad. Je had al genoeg ideeën over hoe het 'stukje' moest gaan, ik ben benieuwd (heb je genoeg glaswerk achterover kunnen drukken tijdens de verhuizing?). Susanne, jou ken ik al sinds mijn veertiende en we hebben veel dingen samen meegemaakt. We kletsen samen heel wat af en je bent een hele steun, ik hoop dat we nog heel lang vrienden mogen blijven.

Ik wil mijn familie en vrienden bedanken voor hun interesse en steun. In het bijzonder wil ik Cees en Jantine bedanken. Bedankt dat ik bij jullie kon logeren tijdens mijn onderzoek in Utrecht en voor de gezellige tijd (ik maak nu nog cryptogrammen).

Heit en mem, Jacobien, Johannes en Annemarie, jullie hebben mij gesteund en vertrouwen gegeven in mijzelf. Bedankt voor al jullie warmte en aandacht. Jacobien, je bent mijn oudere zus, maar eigenlijk meer een vriendin voor mij. Bedankt voor je luisterend oor en voor alle gezellige en goede gesprekken die we hebben.

Ik ben om nog een reden blij dat ik AIO ben geworden, anders had ik jou, Adriaan misschien nooit ontmoet. Misschien zonder het zelf te weten, ben jij een grote steun voor

mij geweest. We zijn samen gegroeid in die jaren en ik kan me nu mijn leven niet meer voorstellen zonder jou.

Christine

Contents

Chapter 1 General Introduction	1
Chapter 2 In situ forming hydrogels for biomedical applications	9
Chapter 3 Stereocomplex mediated gelation of PLA-PEG-PLA and PEG-(PLA) ₈ block copolymers	49
Chapter 4 In situ formation of biodegradable hydrogels by stereocomplexation of PEG-(PLLA) ₈ and PEG-(PDLA) ₈ star block copolymers	67
Chapter 5 In vitro and in vivo protein delivery from in situ forming poly(ethylene glycol)-poly(lactide) hydrogels	87
Chapter 6 Rapidly in situ forming biodegradable robust hydrogels by combining stereocomplexation and photocrosslinking	109
Chapter 7 Novel in situ forming, degradable dextran hydrogels by Michael addition chemistry: Synthesis, rheology and degradation	139
Chapter 8 Rapidly in situ forming degradable hydrogels from dextran thiols through Michael addition	167
Chapter 9 Release of model proteins and basic fibroblast growth factor from in situ forming degradable dextran hydrogels	191
Appendix 1 PEG-PLLA and PEG-PDLA multiblock copolymers: Synthesis and in situ hydrogel formation by stereocomplexation	213

Appendix 2	221
Computational modeling of aqueous solutions of poly(ethylene glycol)- poly(lactide) star block copolymers	
Summary	241
Samenvatting	246
Curriculum Vitae	253

Chapter 1

General introduction

1.1 Hydrogels and biomedical applications

Hydrogels are hydrated networks. Hydrogels have been widely applied in biomedical applications, such as drug delivery¹⁻⁴ and tissue engineering⁵⁻⁷, due to their many favorable characteristics. Their high water content renders them compatible with living tissues and proteins and their rubbery nature minimizes damage to the surrounding tissue. Their mechanical properties parallel those of soft tissues, making them particularly appealing for engineering of these tissues. Hydrogels used for biomedical applications are preferably biodegradable, thus a second surgery after the hydrogel has performed its function is not required. Also, biodegradable hydrogels allow for the replacement of the hydrogel in time by the extracellular matrix produced by the incorporated cells. Hydrogels are formed by physical or chemical crosslinking. Physical crosslinks may be formed by ionic interactions, van der Waals interactions, hydrophobic interactions and stereocomplexation. Physical crosslinking generally proceeds under mild conditions, thus allowing for the immobilization of labile compounds, such as proteins. However, in general physically crosslinked hydrogels are mechanically weak compared to chemically crosslinked hydrogels and changes in the external environment (i.e. pH, temperature and ionic strength) may give rise to disruption of the hydrogel network. Chemically crosslinked hydrogels have been mostly formed by radical chain polymerization initiated by photo-irradiation or a redox system. In addition, chemically crosslinked hydrogels have been formed by reactions between complementary groups, including reactions between thiols and acrylates or vinyl sulfones, and amines and activated esters or aldehydes.

1.2 *In situ forming hydrogels*

Hydrogels that are formed *in situ*^{1, 8, 9} are preferred over preformed hydrogels, since cells and bioactive compounds, such as drugs, may be easily mixed with the precursor solutions prior to gelation to give homogeneously loaded gels. Moreover, *in situ* gelation allows for minimally invasive surgery and for the preparation of complex shapes. *In situ* forming, physically crosslinked hydrogels have been mostly prepared by self-assembly of thermosensitive amphiphilic block copolymers.¹⁰⁻¹³ Recently, physically crosslinked hydrogels have been formed *in situ* by stereocomplexation of water-soluble poly(L-lactide) and poly(D-lactide) copolymers.^{14, 15} Chemically crosslinked hydrogels may also be formed *in situ*. The gel precursors, however, should be non-toxic and the gelation reaction does not cause any toxicity or substantial temperature rise. Photopolymerization has been mostly used for the *in situ* formation of chemically crosslinked hydrogels.¹⁶⁻¹⁸ More recently, chemically crosslinked hydrogels have been formed *in situ* by Michael addition between thiols and acrylates or vinyl sulfones.¹⁹⁻²⁴

1.3 *Aim of the study*

The aim of this study is to prepare biodegradable hydrogels that are rapidly formed *in situ* under physiological conditions. The hydrogels should be based on biocompatible materials and should degrade into biocompatible products. The hydrogel degradation time should be well-controlled by the choice of the base polymers and their concentration, thus allowing design of a hydrogel for a particular application. The hydrogels should have good mechanical properties to withstand the forces which act upon the gel after its formation in the body. Furthermore, the hydrogels should allow easy incorporation of bioactive moieties, such as cell adhesion peptides, to obtain biomimetic hydrogels.

1.4 *Outline of the thesis*

In this thesis *in situ* forming hydrogels and their application as controlled protein delivery systems are described. Parts of this thesis have been published elsewhere or have been

submitted for publication.²⁵⁻³⁴ In **Chapter 2** a literature overview is given on in situ forming hydrogels used for biomedical applications, with emphasis on in situ gel formation via stereocomplexation, photopolymerization and Michael addition. In **Chapter 3** the in situ formation and rheology of stereocomplexed hydrogels based on PLA-PEG-PLA triblock or eight-arm PEG-PLA star block copolymers is described. PEG-PLA copolymers could be readily prepared with controlled compositions by ring opening polymerization of lactide initiated by the hydroxyl groups of PEG, using a zinc complex as a catalyst. Hydrogels were rapidly formed in situ under physiological conditions by mixing aqueous solutions of PEG-PLLA and PEG-PDLA copolymers due to stereocomplexation of the PLLA and PDLA blocks. Stereocomplexed hydrogels based on eight-arm PEG-PLA showed improved mechanical properties as compared to the hydrogels based on PLA-PEG-PLA, due to its higher crosslinking functionality. In **Chapter 4** the dependence of the gelation rate and the mechanical properties of stereocomplexed hydrogels depending on the PLA block length and concentration of eight-arm PEG-PLA star block copolymers are studied in detail. The hydrogel storage modulus increased with increasing PLA block length or concentration. Also, the gelation mechanism is studied. In **Chapter 5** the release of model proteins with different sizes, as well as the pharmaceutically active protein recombinant human interleukin-2 (rhIL-2), from stereocomplexed hydrogels based on eight-arm PEG-PLA star block copolymers is studied. Protein loaded hydrogels can be easily prepared by mixing protein containing aqueous solutions of PEG-PLLA and PEG-PDLA. Released lysozyme retained its enzymatic activity, emphasizing the protein-friendly hydrogel preparation method. An almost constant release of rhIL-2 can be achieved using these hydrogels. The therapeutic efficacy of rhIL-2 loaded stereocomplexed hydrogels is demonstrated using mice bearing fast growing, large malignant tumors. In **Chapter 6** PEG-PLA hydrogels that are crosslinked by combining stereocomplexation and photopolymerization are described. These hydrogels form rapidly in situ under physiological conditions due to stereocomplexation and may be subsequently slowly photopolymerized at low initiator concentrations or light intensities, thus preventing an excessive local temperature rise. Interestingly, stereocomplexation aids in photopolymerization, yielding hydrogels with increased storage modulus and degradation time. In **Chapter 7** hydrogels that are rapidly formed in situ under physiological conditions by Michael addition between dextran vinyl sulfone conjugates and multi-

functional mercapto PEGs are described. The hydrogel storage modulus and degradation time are well-controlled by the DS, dextran molecular weight, polymer concentration and length of the spacer between the thioether and ester bonds. Degradable hydrogels that are rapidly formed in situ under physiological conditions by Michael addition upon mixing aqueous solutions of dextran thiol conjugates and PEG tetra-acrylate or a dextran vinyl sulfone conjugate are described in **Chapter 8**. These dextran thiol hydrogels degraded much slower compared to the dextran vinyl sulfone hydrogels, rendering them particularly interesting for applications such as tissue engineering of cartilage or release of proteins over an extended period of time. In **Chapter 9** the release of model proteins with different sizes, as well as basic fibroblast growth factor (bFGF) from dextran hydrogels, is described. Protein loaded hydrogels can be easily prepared by mixing protein containing aqueous solutions of dextran vinyl sulfone conjugates and tetrafunctional mercapto PEG. Importantly, bFGF was quantitatively released in 28 days without a burst-effect. In **Appendix 1** stereocomplexed hydrogels based on PEG-PLA multi-block copolymers is described. These hydrogels have improved mechanical properties compared to PLA-PEG-PLA triblock copolymers due to their higher crosslinking functionality. In **Appendix 2** preliminary results are given on the phase behavior of eight-arm PEG-PLA star block copolymers in water as studied by computational modeling and small angle neutron scattering (SANS).

1.5 References

1. Chitkara, D.; Shikanov, A.; Kumar, N.; Domb, A. J., Biodegradable injectable in situ depot-forming drug delivery systems. *Macromol. Biosci.* 2006, 6, 977-990.
2. Kashyap, N.; Kumar, N.; Kumar, M., Hydrogels for pharmaceutical and biomedical applications. *Crit. Rev. Ther. Drug Carrier Syst.* 2005, 22, 107-149.
3. Peppas, N.; Bures, P.; Ichikawa, H., Hydrogels in pharmaceutical formulations. *Eur. J. Pharm. Biopharm.* 2000, 50, 27-46.
4. Malmsten, M., Soft drug delivery systems. *Soft Matter* 2006, 2, 760-769.
5. Hubbell, J. A., Materials as morphogenetic guides in tissue engineering. *Curr. Opin. Biotechn.* 2003, 14, 551-558.

6. Nerem, R. M., Tissue engineering: The hope, the hype, and the future. *Tissue Eng.* 2006, 12, 1143-1150.
7. Lavik, E.; Langer, R., Tissue engineering: current state and perspectives. *Appl. Microbiol. Biotechnol.* 2004, 65, 1-8.
8. Ruel-Gariepy, E.; Leroux, J. C., In situ-forming hydrogels - review of temperature-sensitive systems. *Eur. J. Pharm. Biopharm.* 2004, 58, 409-426.
9. Temenoff, J. S.; Mikos, A. G., Injectable biodegradable materials for orthopedic tissue engineering. *Biomaterials* 2000, 21, 2405-2412.
10. Jeong, B.; Bae, Y. H.; Lee, D. S.; Kim, S. W., Biodegradable block copolymers as injectable drug-delivery systems. *Nature* 1997, 388, 860-862.
11. Jeong, B.; Bae, Y. H.; Kim, S. W., Thermoreversible gelation of PEG-PLGA-PEG triblock copolymer aqueous solutions. *Macromolecules* 1999, 32, 7064-7069.
12. Shim, W. S.; Kim, J. H.; Park, H.; Kim, K.; Kwon, I. C.; Lee, D. S., Biodegradability and biocompatibility of a pH- and thermo-sensitive hydrogel formed from a sulfonamide-modified poly(epsilon-caprolactone-co-lactide)-poly(ethylene glycol)-poly(epsilon-caprolactone-co-lactide) block copolymer. *Biomaterials* 2006, 27, 5178-5185.
13. Bae, S. J.; Joo, M. K.; Jeong, Y.; Kim, S. W.; Lee, W. K.; Sohn, Y. S.; Jeong, B., Gelation behavior of poly(ethylene glycol) and polycaprolactone triblock and multiblock copolymer aqueous solutions. *Macromolecules* 2006, 39, 4873-4879.
14. de Jong, S. J.; van Eerdenbrugh, B.; van Nostrum, C. F.; Kettenes-van de Bosch, J. J.; Hennink, W. E., Physically crosslinked dextran hydrogels by stereocomplex formation of lactic acid oligomers: degradation and protein release behavior. *J. Controlled Release* 2001, 71, 261-275.
15. Li, S.; Vert, M., Synthesis, characterization, and stereocomplexation-induced gelation of block copolymers prepared by ring-opening polymerization of L(D)-lactide in the presence of poly(ethylene glycol). *Macromolecules* 2003, 36, 8008-8014.
16. Lu, S. X.; Anseth, K. S., Release behavior of high molecular weight solutes from poly(ethylene glycol)-based degradable networks. *Macromolecules* 2000, 33, 2509-2515.

17. West, J. L.; Hubbell, J. A., Polymeric biomaterials with degradation sites for proteases involved in cell migration. *Macromolecules* 1999, 32, 241-244.
18. Zhu, J.; Beamish, J.; Tang, C.; Kottke-Marchant, K.; Marcant, R., Extracellular Matrix-like Cell-Adhesive Hydrogels from RGD-Containing Poly(ethylene glycol) Diacrylate. *Macromolecules* 2006, 39, 1305-1307.
19. Metters, A.; Hubbell, J., Network formation and degradation behavior of hydrogels formed by Michael-type addition reactions. *Biomacromolecules* 2005, 6, 290-301.
20. van de Wetering, P.; Metters, A. T.; Schoenmakers, R. G.; Hubbell, J. A., Poly(ethylene glycol) hydrogels formed by conjugate addition with controllable swelling, degradation, and release of pharmaceutically active proteins. *J. Controlled Release* 2005, 102, 619-627.
21. Raeber, G. P.; Lutolf, M. P.; Hubbell, J. A., Molecularly engineered PEG hydrogels: A novel model system for proteolytically mediated cell migration. *Biophys. J.* 2005, 89, 1374-1388.
22. DuBose, J.; Cutshall, C.; Metters, A., Controlled release of tethered molecules via engineered hydrogel degradation: Model development and validation. *J. Biomed. Mater. Res.* 2005, 74A, 104-116.
23. Cai, S. S.; Liu, Y. C.; Shu, X. Z.; Prestwich, G. D., Injectable glycosaminoglycan hydrogels for controlled release of human basic fibroblast growth factor. *Biomaterials* 2005, 26, 6054-6067.
24. Shu, X. Z.; Ghosh, K.; Liu, Y. C.; Palumbo, F. S.; Luo, Y.; Clark, R. A.; Prestwich, G. D., Attachment and spreading of fibroblasts on an RGD peptide-modified injectable hyaluronan hydrogel. *J. Biomed. Mater. Res.* 2004, 68A, 365-375.
25. Hiemstra, C.; Zhong, Z.; Dijkstra, P. J.; Feijen, J., PEG-PLA hydrogels by stereocomplexation for tissue engineering of cartilage. *J. Controlled Release* 2005, 101, 332-334.
26. Hiemstra, C.; Zhong, Z. Y.; Dijkstra, P. J.; Feijen, J., Stereocomplex mediated gelation of PEG-(PLA)₂ and PEG-(PLA)₈ block copolymers. *Macromol. Symp.* 2005, 224, 119-131.
27. Hiemstra, C.; Zhong, Z. Y.; Li, L.; Dijkstra, P. J.; Feijen, J., In-situ formation of biodegradable hydrogels by stereocomplexation of PEG-(PLLA)₈ and PEG-(PDLA)₈ star block copolymers. *Biomacromolecules* 2006, 7, 2790-2795.

28. Hiemstra, C.; van der Aa, L. J.; Zhong, Z. Y.; Dijkstra, P. J.; Feijen, J., Novel in situ forming, degradable dextran hydrogels by Michael addition chemistry: Synthesis, rheology and degradation. *Macromolecules* 2007, 40, 1165-1173.
29. Hiemstra, C.; Zhong, Z. Y.; Van Tomme, S. R.; Jacobs, J. J. L.; Den Otter, W.; Hennink, W. E.; Feijen, J., In vitro and in vivo protein delivery from in situ forming poly(ethylene glycol)-poly(lactide) hydrogels. *J. Controlled Release* 2007, *accepted*.
30. Hiemstra, C.; Wouters, M. E. L.; Zhong, Z. Y.; Feijen, J., Rapidly in situ forming PEG-PLA hydrogels prepared by combined stereocomplexation and photocrosslinking. *JACS* 2007, *submitted*.
31. Hiemstra, C.; van der Aa, L. J.; Zhong, Z. Y.; Feijen, J., Rapidly in situ forming degradable hydrogels from dextran thiols through Michael addition. *Biomacromolecules* 2007, *accepted*.
32. Hiemstra, C.; Zhong, Z. Y.; van Steenberg, M. J.; Hennink, W. E.; Feijen, J., Release of model proteins and basic fibroblast growth factor from in situ forming degradable dextran hydrogels. *J. Controlled Release* 2007, *submitted*.
33. Hiemstra, C.; Zhong, Z. Y.; Liang, X. L.; Dijkstra, P. J.; Feijen, J., PEG-PLLA and PEG-PDLA multiblock copolymers: Synthesis and in situ hydrogel formation by stereocomplexation. *J. Controlled Release* 2006, 116, e17-e19.
34. Hiemstra, C.; Zhong, Z. Y.; Van Tomme, S. R.; Hennink, W. E.; Dijkstra, P. J.; Feijen, J., Protein release from injectable stereocomplexed hydrogels based on PEG-PDLA and PEG-PLLA star block copolymers. *J. Controlled Release* 2006, 116, e19-e21.

Chapter 2

In situ forming hydrogels for biomedical applications

Christine Hiemstra, Zhiyuan Zhong, and Jan Feijen

Department of Polymer Chemistry and Biomaterials, Faculty of Science and Technology, Institute for Biomedical Technology, University of Twente, P. O. Box 217, 7500 AE Enschede, The Netherlands

2.1 Introduction

Hydrogels are water-swollen, insoluble networks of crosslinked hydrophilic polymers. Due to their similarity with the extracellular matrix, hydrogels have been investigated for use in biology and medicine since Wichterle and Lim discovered them in the early 1960s.¹ They are important materials for biomedical applications², such as drug delivery³⁻⁵ and tissue engineering⁶⁻⁸. Many hydrogels have been found to be biocompatible with strongly reduced protein interaction, and their soft and rubbery nature minimizes damage to surrounding tissue.⁹ The mechanical properties of hydrogels parallel those of soft tissues, such as cartilage, making hydrogels especially suitable for engineering of these tissues.

Recently, in situ forming hydrogels have been prepared for biomedical applications. In situ forming hydrogels are preferred over preformed hydrogels, since in situ formation allows homogeneous mixing of e.g. cells and proteins with the polymer solutions prior to gelation. Moreover, in situ formation allows for preparation of complex shapes and applications using minimally invasive surgery.

Hydrogels can be classified in several ways. According to their composition, they can be classified into synthetic, natural or hybrid hydrogels. According to the crosslinking mechanism, hydrogels can be classified into chemically and physically crosslinked hydrogels. In chemical crosslinking covalent bonds are formed, while in physical crosslinking non-covalent interactions, such as hydrophobic and ionic interactions, are established. Furthermore, hydrogels can be classified into in situ forming or preformed

hydrogels. In situ forming hydrogels form in the body after injection of the precursors, in contrast to preformed hydrogels that have to be implanted by surgery.

In section 2.2.1 general requirements, biocompatibility and biodegradability, of hydrogels used for biomedical applications are discussed. Polymers used for hydrogel preparation and hydrogel crosslinking methods are described in section 2.2.2 and section 2.2.3, respectively. Section 2.3 deals with biomedical applications of hydrogels, such as controlled drug delivery and tissue engineering.

2.2 Hydrogels

2.2.1 General requirements

Materials used for biomedical applications should be biocompatible. The materials should not elicit an unresolved inflammatory reaction and should not demonstrate immunogenicity or cytotoxicity. In addition, this must be true for any unreacted compounds or additives and in case of biodegradable materials, also for their degradation products.

It is important that hydrogels can degrade in the body, in order to avoid a second surgery to remove the implant after it has performed its function. The degradation products should be either metabolized or excreted by the kidneys. Excretion of such products is limited to a certain size. For instance, the cut-off molecular weight of globular proteins is approximately 60,000.¹⁰ In particular, for tissue engineering applications the progressive loss of mechanical strength of the material simulates the healing process of the tissues.¹¹⁻¹³

The best known synthetic, degradable polymers are the poly(hydroxy acid)s, including poly(glycolide) (PGA), poly(lactide) (PLA), poly(glycolide-*co*-lactide) (PLGA) and poly(ϵ -caprolactone) (PCL). These polymers degrade via hydrolytic cleavage of the ester bonds, finally resulting in the corresponding hydroxy acids as non-toxic degradation products. Many natural materials, such as collagen and fibrin, have specific peptide sequences that can be cleaved by enzymes.

2.2.2 Polymers used for hydrogel preparation

2.2.2.1 Hydrogels based on natural polymers

Both natural^{14, 15} and synthetic¹⁶ polymers have been applied for the preparation of hydrogels for biomedical applications. Natural biodegradable polymers, such as hyaluronic acid¹⁷⁻¹⁹, fibrin²⁰⁻²², collagen²³, gelatin (produced by partial hydrolysis of collagen)²⁴ and chondroitin sulfate²⁵, have inherent biocompatibility and induce specific cell-material interactions. Fibrin, collagen and gelatin are proteins, while hyaluronic acid and chondroitin sulfate are polysaccharides. Other polysaccharides such as alginate²⁶⁻²⁸, dextran²⁹⁻⁴¹, chitosan^{27, 42-51} and pullulan⁵²⁻⁵⁴ have also often been applied. Many of these polymers are biocompatible and depending on their molecular weight they may be excreted by the kidneys. Structural elements of several important polysaccharides are shown in Figure 1. Although natural polymers have shown promise, their chemical structure is less defined compared to synthetic polymers, and therefore their mechanical and degradation properties are less controlled. Also, they may provoke a serious immune response or harbor microbes or viruses and their supply from one source may be limited.²³ Some natural polymers, such as dextran and hyaluronic acid, can be produced by genetic engineering, thus alleviating problems concerning immunogenicity and supply to some extent. Peptide sequences, synthesized by solid-phase peptide synthesis or by genetic engineering, are increasingly used as components for the preparation of hydrogels.⁵⁵⁻⁶⁰ Peptides used for the preparation of hydrogels can perform a specific function, such as crosslinking, cell adhesion, enzymatic degradation and heparin binding. The main drawback of these peptide containing biomaterials is their time-consuming and costly synthesis.

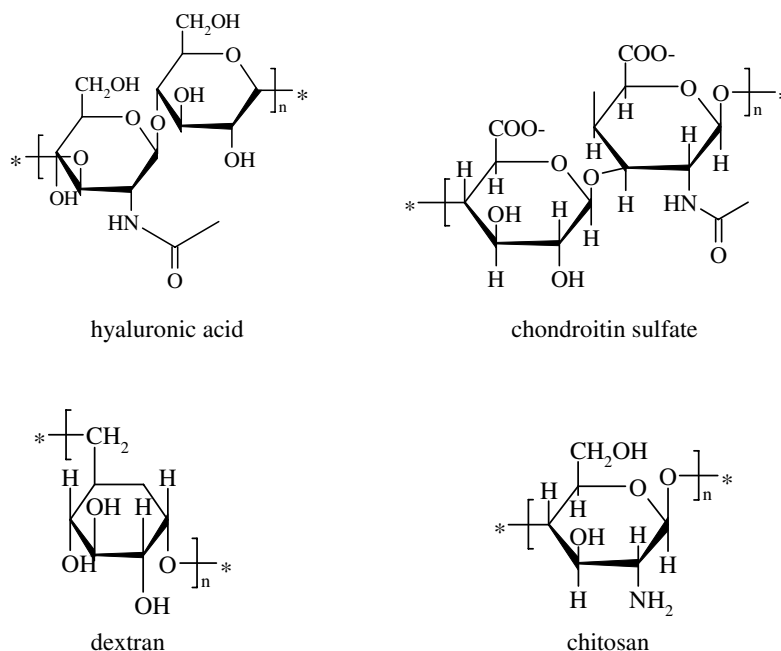


Figure 1. Structural elements of polysaccharides used for hydrogel preparation.

2.2.2.2 Hydrogels based on synthetic materials

Synthetic hydrogels can be tailored to have a much wider range of mechanical and chemical properties than their natural counterparts. However, cell-material interactions and biocompatibility may be an issue and have to be taken into account in the development of these hydrogels. The most commonly used synthetic hydrogels are based on poly(ethylene glycol) (PEG).^{12, 13, 61-75} Due to its high hydrophilicity PEG shows hardly any interactions with proteins and can be excreted through the kidneys up to molecular weights of approximately 30,000.¹⁰ Amphiphilic block copolymers, consisting of hydrophilic PEG blocks and hydrophobic blocks have been widely applied for the preparation of hydrogels (Figure 2). PLA⁷⁶ and PLGA⁷⁷ have been mostly used as the hydrophobic blocks. Other hydrophobic blocks include PCL⁷⁸ and poly(D,L-3-methylglycolide) (PMG)⁷⁹. These amphiphilic block copolymers self-assemble in water due to hydrophobic interactions and may form physically crosslinked hydrogels. PEG has also been derivatized with

polymerizable (meth)acrylate groups for the formation of hydrogels by photoirradiation or redox initiation.

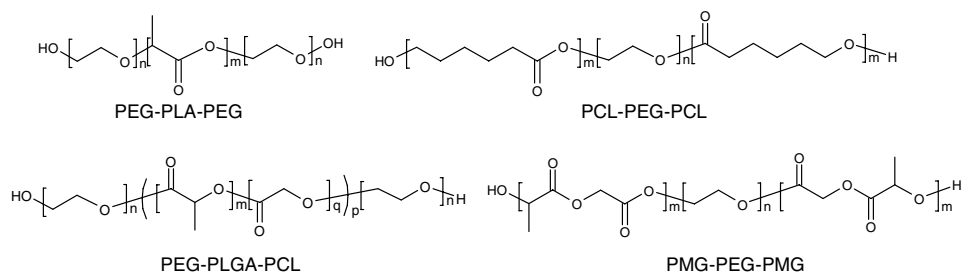


Figure 2. PEG- poly(hydroxy acid) block copolymers used for hydrogel preparation.

Another often used biocompatible polymer is poly(vinyl alcohol) (PVA).⁸⁰⁻⁸⁴ Similar to PEG, this polymer is protein repellent with the additional advantage that its many hydroxyl groups allow for easy chemical modification. PVA hydrogels have been mostly formed by photopolymerization of (degradable) PVA (meth)acrylate derivatives (Figure 3).⁸¹⁻⁸³ Poly(N-isopropylacrylamide) (PNIPAAm) (co)polymers have also been investigated as biomaterials.⁸⁵⁻⁹³ These polymers are thermosensitive, having a lower critical solution temperature (LCST) in water around body temperature. The biocompatibility of PNIPAAm has been studied. Several authors have reported good biocompatibility for PNIPAAm based hydrogels^{48, 86, 94}, though PNIPAAm polymers themselves showed some cytotoxicity.⁹⁵ Poly(organophosphazenes) present a new type of materials that degrade through hydrolysis.⁹⁶⁻⁹⁸ They may be prepared with a variety of side groups, thus offering a wide range of material properties. Although hydrophilic polymers may be excreted by the kidneys dependent on their molecular weight, they become non-soluble when they are chemically crosslinked to form hydrogels. To allow for the degradation of hydrogels based on water-soluble, non-biodegradable polymers, such as PEG, PVA and PNIPAAm, biodegradable sequences, such as PLA⁹⁹⁻¹⁰¹ or degradable peptide sequences^{62, 64, 85, 102}, have to be incorporated in the hydrogel network.

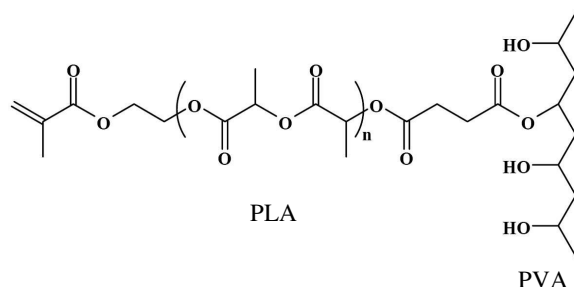


Figure 3. Degradable, photocrosslinkable PVA-PLA macromer.⁹⁹ Reprinted with permission from Elsevier.

2.2.2.3 Hybrid hydrogels based on both synthetic and natural materials

Hybrid hydrogels based on both natural and synthetic polymers have been designed to combine the advantages of both synthetic and natural hydrogels, control over properties and specific cell-material interaction.^{20, 23} Cell-responsive hybrid hydrogels have been prepared by using a combination of PEG and additives such as chondroitin sulfate¹⁰³, collagen mimetic peptide⁶⁷ and cell-adhesion and enzyme cleavable peptides^{102, 104}. Temperature-responsive hybrid hydrogels have been prepared by combining natural polymers with PNIPAAm.^{47, 54, 105, 106} Hybrid hydrogels that are pH-sensitive have been prepared by combining natural polymers with poly(acrylic acid).^{75, 87, 107} Natural polymers have also been combined with PLA to obtain degradable hydrogels and to tune the swelling properties.^{108, 109}

2.2.3 Crosslinking methods

Hydrogels are either physically crosslinked by noncovalent interactions or chemically crosslinked by covalent bonds. Several physical and chemical crosslinking methods are discussed, with emphasis on hydrogels formed by stereocomplexation, photopolymerization and Michael addition.

2.2.3.1 In situ forming hydrogels

In situ forming hydrogels are those that can form in the body, i.e. under (near) physiological conditions, wherein the gel precursors should be non-toxic and the gelation reaction should not cause any toxicity or substantial temperature rise. In the past few years an increasing number of in situ forming hydrogels have been reported in literature. These hydrogels offer several advantages over preformed hydrogels, which are shaped into their final form before implantation. The precursors of in situ forming hydrogels are injectable fluids that can be introduced into the body in a minimally invasive manner prior to gelation within the desired tissue, organ or body cavity. Their flowing nature ensures a good fit and contact with surrounding tissue. Since hydrogels are fluid prior to gelation, bioactive components, such as cells, proteins and drugs, can be easily mixed with the polymer solutions, ensuring high loading and homogeneous distribution. The gelation should occur within a few minutes to prevent leakage of the gelling solution to the surrounding tissue and to minimize the length of the procedure, while on the other hand allowing surgeons ample time for placement before hardening.¹¹⁰

In situ hydrogels have been formed by physical or chemical crosslinking methods. Since the conditions for physical crosslinking are generally mild, most physically crosslinked hydrogels can be formed in situ. For the in situ formation of chemically crosslinked hydrogels often a compromise needs to be found between fast gelation (i.e. crosslinking reaction rate) and reaction conditions (such as temperature and pH). For instance, photopolymerization, which is a common method for in situ preparation of chemically crosslinked hydrogels, can give rise to substantial heat effects due to the polymerization exotherm. Furthermore, toxicity may be an issue in chemical crosslinking, since the gel precursors have reactive groups and often auxiliary compounds such as initiators, co-crosslinkers and organic solvents are needed.

Besides in situ hydrogel formation, injectable systems may also be obtained by hydrogels that become fluid-like when subjected to shear stress when injected through a needle, so-called injectable hydrogels.^{31, 59, 111} However, these hydrogels are generally mechanically weak. In contrast, in situ hydrogel formation offers both the ability for minimally invasive surgery by injection as well as good mechanical properties of the hydrogel. Therefore, in

situ forming hydrogels are much more promising compared to injectable hydrogels that are preformed.

2.2.3.2 Physical crosslinking

Physical crosslinking offers the advantage that the crosslinking conditions are generally mild compared to chemical crosslinking, since no reactive groups, crosslinking agents, (photo)initiators or photoirradiation are needed. These mild crosslinking conditions allow for in situ hydrogel formation and entrapment of labile compounds, such as proteins. Moreover, many physical interactions are reversible, allowing for repeated gelation and sol formation. In general however, physical hydrogels are mechanically weak compared to chemically crosslinked hydrogels and changes in the external environment (e.g. ionic strength, pH, temperature) may give rise to disruption of the hydrogel network.

Thermosensitive hydrogels

Physically crosslinked hydrogels have been prepared by a variety of noncovalent interactions. Most commonly, hydrogels have been formed by self-assembly of thermosensitive polymers. The hydrophobicity of these polymers increases upon increasing the temperature to around body temperature, causing decreased hydrogen bonding with the surrounding water and increased hydrophobic interactions. Subsequently, the polymers self-assemble and form physical crosslinks. Water-soluble, amphiphilic block copolymers with both hydrophobic and hydrophilic blocks (as discussed in section 2.2.2.2) represent an important class of thermosensitive polymers, including PEG-PLA-PEG⁷⁶, PEG-PLGA-PEG⁷⁷, and PCL-PEG-PCL^{78, 112} triblock copolymers. In these hydrogels the crosslinks are formed by the hydrophobic blocks. A schematic representation of proposed self-assembly mechanisms of amphiphilic PEG-PLGA-PEG⁷⁷ and PCL-PEG-PCL¹¹³ triblock copolymers is shown in Figure 4. The gelation for PEG-PLGA-PEG copolymers is thought to be due to self-assembly into closely packed micelles, while the gelation of PCL-PEG-PCL copolymers is thought to be due to self-assembly of micelle aggregates that are bridged by polymers having both hydrophobic ends in different micelles. Other well-known thermosensitive hydrogels are those based on PNIPAAm and its copolymers, which have an LCST around body temperature.⁸⁶⁻⁸⁸ More recently, thermosensitive hydrogels

based on elastin-like peptides⁵⁸, hydroxybutyl chitosan¹¹⁴, PEG-grafted chitosan¹¹⁵, mixtures of chitosan with anionic polyol salts⁵¹ and poly(organophosphazenes) bearing thermosensitive side groups^{97, 98} have been reported. Thermosensitive hydrogels are generally rapidly formed upon increasing the temperature and have been applied as in situ forming hydrogels.

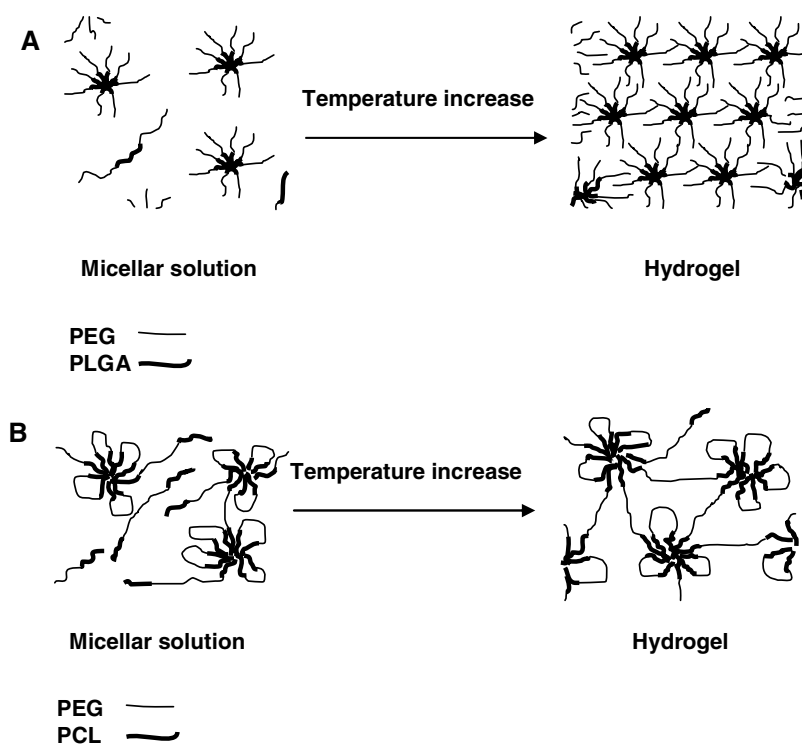


Figure 4. Self-assembly of amphiphilic PEG-PLGA-PEG⁷⁷ (A) and PCL-PEG-PCL¹¹³ (B) triblock copolymers upon temperature increase in water.

Stereocomplexation

Stereocomplexation refers to co-crystallization of poly(L-lactide) (PLLA) and poly(D-lactide) (PDLA). Recently, this type of physical interaction has been used for in situ hydrogel formation. It is well-known that blending of PLLA and PDLA results in the formation of stereocomplex crystals, having a melting temperature of approximately 230 °C, which is 50 °C above the melting temperature of homocrystallites of non-blended

PLLA or PDLA.¹¹⁶ The PLLA and PDLA chains in a stereocomplex crystal are packed side-by-side as shown in Figure 5.¹¹⁷ The higher melting point of the stereocomplex crystals is ascribed to a denser packing of the PLLA and PDLA helices as compared to the packing of the single enantiomer helices. PLLA forms a left-handed helix and PDLA forms a right-handed helix. The van der Waals forces between opposite oxygen atoms and hydrogen atoms of the two helices are suggested to be the driving force for the dense packing of the helices in the stereocomplex.¹¹⁸ A mixture of both polyenantiomers crystallizes in a triclinic unit cell, to form a 3_1 (3 Å rise/1 monomer unit) helical conformation known as the β -form, with each unit cell comprising three L-lactyl and three D-lactyl units.¹¹⁹ In contrast, PLLA (or PDLA) crystallizes mainly in a pseudo-orthorhombic system with two 10_3 -helices (known as the α -form).¹²⁰ The major difference between the two helical forms is that in the 3_1 conformation the helix winds a little tighter compared to the 10_3 conformation, going from 108° to 120° rotation per monomer unit.¹²¹

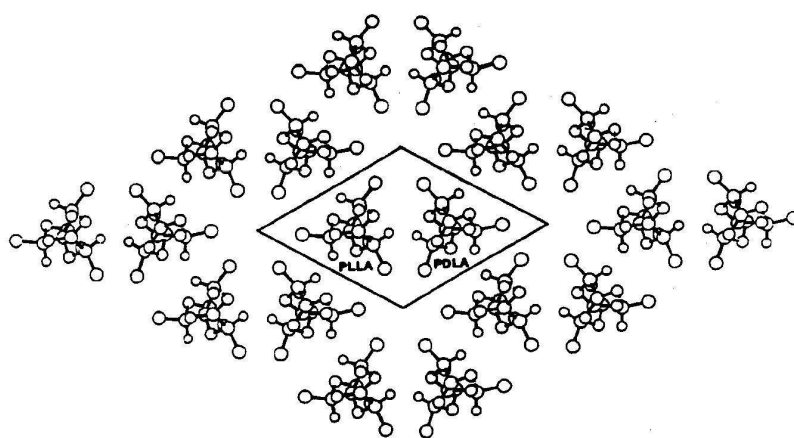


Figure 5. PLLA and PDLA molecular arrangements in a stereocomplex crystal projected on the plane normal to the chain axis.¹¹⁷ Reprinted with permission from Wiley-VCH Verlag GmbH & Co KGaA.

Stereocomplexation offers an attractive crosslinking method for in situ hydrogel formation using water-soluble PLLA and PDLA block copolymers. Since stereocomplex formation takes place at shorter block lengths than for homocrystallization, an operation window

exists in which mixing of aqueous solutions of these block copolymers results in hydrogel formation through stereocomplexation. De Jong et al. formed hydrogels by stereocomplexation of dextran grafted with monodisperse L-lactic acid and D-lactic acid oligomers (Figure 6). At least 11 lactyl units were required to form stereocomplex crystals.^{122, 123} Monodisperse lactate oligomers formed stereocomplex crystals starting from 7 lactyl units, indicating that the longer critical block length for dextran-(lactic acid oligomer) graft copolymers is most likely due to sterical hindrance of dextran.

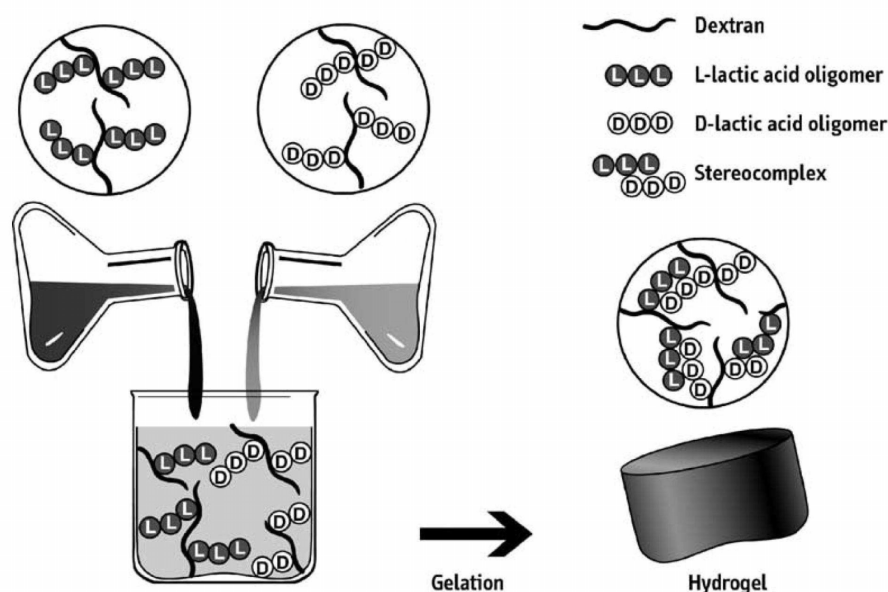


Figure 6. Formation of hydrogels by stereocomplexation of dextran-(L-lactic acid oligomer) and dextran-(D-lactic acid oligomer).¹²⁴ Reprinted with permission from Elsevier.

These dextran-(lactic acid oligomer) hydrogels quantitatively released lysozyme over a period of one week, wherein the lysozyme retained its enzymatic activity.³⁵ Moreover, *in vivo* tests showed that these stereocomplexed hydrogels are biocompatible and effective tools for local delivery of the cytokine interleukin-2.¹⁹⁰ Li et al.¹⁸⁹ prepared stereocomplexed PLA-PEG-PLA triblock copolymer hydrogels and showed that bovine serum albumin (BSA) can be released from these hydrogels over a prolonged period of time without denaturation (up to 15 days).

Inclusion complexation

Inclusion complexation between α -cyclodextrins (CDs) and biopolymers, including linear¹²⁵ and star PEG¹²⁶, PEG grafted chitosan¹²⁷ and dextran¹²⁸ and poly(ϵ -lysine) grafted dextran¹²⁹, represents another often used type of physical crosslinking. Linear polymers can penetrate the inner cavity of CDs, upon which the CDs self-assemble due to hydrophobic interactions, thus providing physical crosslinks (Figure 7). These hydrogels often have low stability in aqueous environment¹²⁵ and/or the gelation is very slow (typically several hours). Recently, more stable hydrogels (stable for up to 1 month) have been prepared by mixing aqueous solutions of PEG-poly([R]-3-hydroxybutyrate)-PEG (PEG-PHB-PEG)¹³⁰ triblock copolymers with CDs (Figure 7). Rapid gelation (within 1 min) was obtained by mixing aqueous solutions of PCL-PEG-PCL triblock copolymers with CDs¹³¹. These PEG-PHB-PEG and PCL-PEG-PCL hydrogels are thought to form via a combination of inclusion complexation and micelle formation of the triblock copolymers.

Ionic interactions

Alginate hydrogels crosslinked by various types of cations are the best known examples of hydrogels crosslinked through ionic interactions.^{26, 132} More recently, in situ hydrogel formation through ionic interactions between negatively charged peptide amphiphiles and a positively charged basic fibroblast growth factor (bFGF) was reported.⁵⁵ Preformed hydrogels have been prepared by ionic interactions between oppositely charged decapeptides⁵⁹ or microparticles based on dextran-(2-hydroxyethyl methacrylate) copolymerized with methacrylic acid (MAA) or dimethylaminoethyl methacrylate (DMAEMA)³¹. These hydrogels were injectable through shear-thinning.

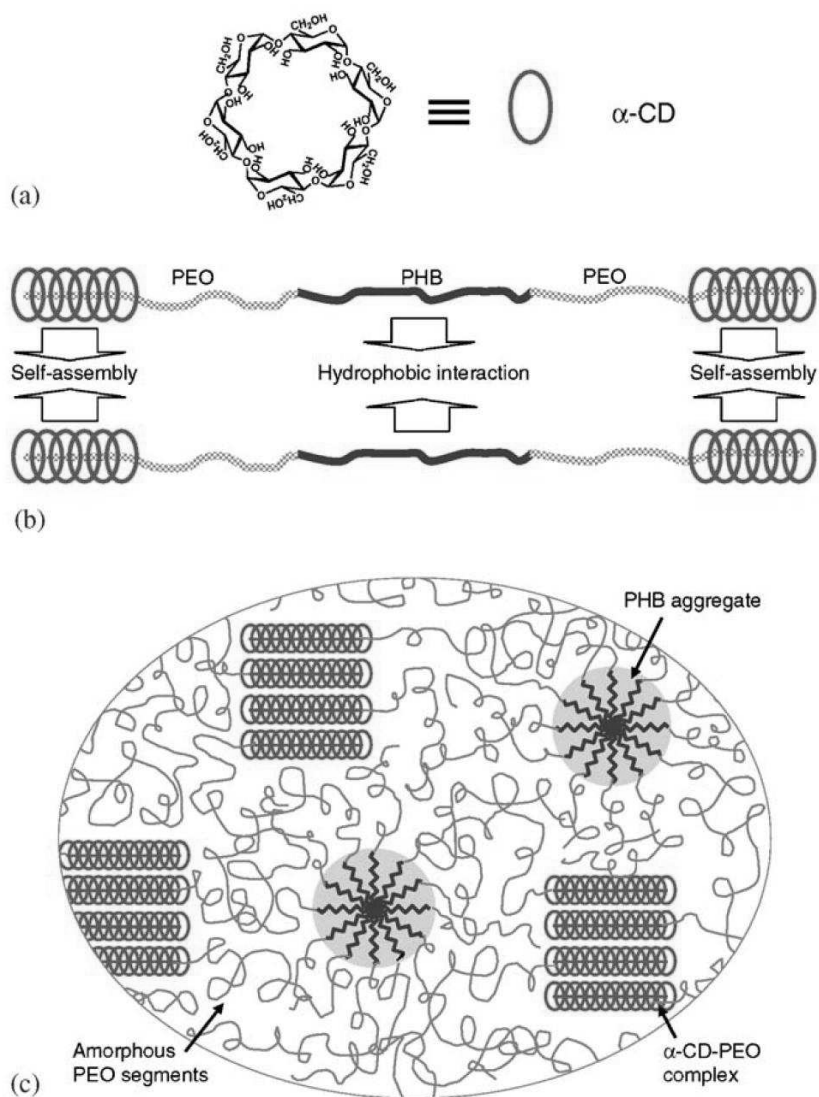


Figure 7. The structure of α -CD (a), the schematic illustration of the proposed structures of α -CD-PEG-PHB-PEG inclusion complex (b), and α -CD-PEG-PHB-PEG hydrogel (c).¹³⁰ Reprinted with permission from Elsevier.

2.2.3.3 Chemical crosslinking

Chemical crosslinking generally yields more stable hydrogels and better mechanical properties compared to physical crosslinking. The main issue of chemical crosslinking is that reactive compounds and/or photoirradiation are needed, which may cause toxicity problems. However, recently several chemical crosslinking methods have been developed that proceed under mild reaction conditions, allowing in situ hydrogel formation.

Photopolymerization

Chemically crosslinked hydrogels have been mostly prepared via photopolymerization^{11, 133}, in particular by UV-irradiation of (meth)acrylate functionalized PEG^{71, 100, 134}. Other materials include (meth)acrylate functionalized PVA⁸¹⁻⁸³ and dextran^{36, 135}. Alternatively, polymers have been crosslinked by visible light.^{18, 64, 101, 136-138} Photopolymerization offers the advantage of spatial and temporal control, polymerization takes place where and when the polymer is exposed to the light. The main disadvantage is that its *in vivo* application, i.e. transdermal photopolymerization, is hampered by the absorption of the UV-light by the skin (> 99%).¹³⁹ Visible light is less attenuated by the skin, but more efficient and cytocompatible initiators are needed.^{140, 141} Another drawback of photopolymerization is that the energy of the polymerizing light, the heat and the radical species produced during the polymerization and the toxicity of the photoinitiators and monomers may damage the surrounding tissue and/or the entrapped molecules.¹³³ Photopolymerization has been combined with Michael addition¹⁴² and redox initiation^{141, 143}, to alleviate some of these problems.

Hubbell et al. were the first to report on photopolymerized, hydrolytically degradable PEG-PLA diacrylate hydrogels (Figure 8).¹⁰¹ More recently, they developed protease biodegradable PEG-peptide diacrylate hydrogels.¹³⁴ These hydrogels supported the three-dimensional outgrowth of photo-encapsulated fibroblasts.⁶⁴ Later, Anseth et al. reported on biodegradable PEG-PLA dimethacrylate hydrogels.¹⁰⁰ It was shown that by using combinations of PEG and PEG-PLA dimethacrylates and/or by changing the PLA block length, the hydrogel degradation rate, compressive modulus and crosslinking density could be tuned to provide suitable scaffolds for cartilage tissue engineering.¹⁴⁴ Though

photopolymerization has been proposed for in situ hydrogel formation by transdermal photoirradiation, photopolymerized hydrogels have mostly been preformed and subsequently implanted. Currently, there are still problems with efficient in situ formation of hydrogels by photopolymerization *in vivo* due to the UV absorption by the skin. Elisseff et al. have formed hydrogels by transdermal irradiation of an aqueous PEG methacrylate solution with UV-light, which were successfully applied for the generation of cartilage in nude mice.¹⁴⁵

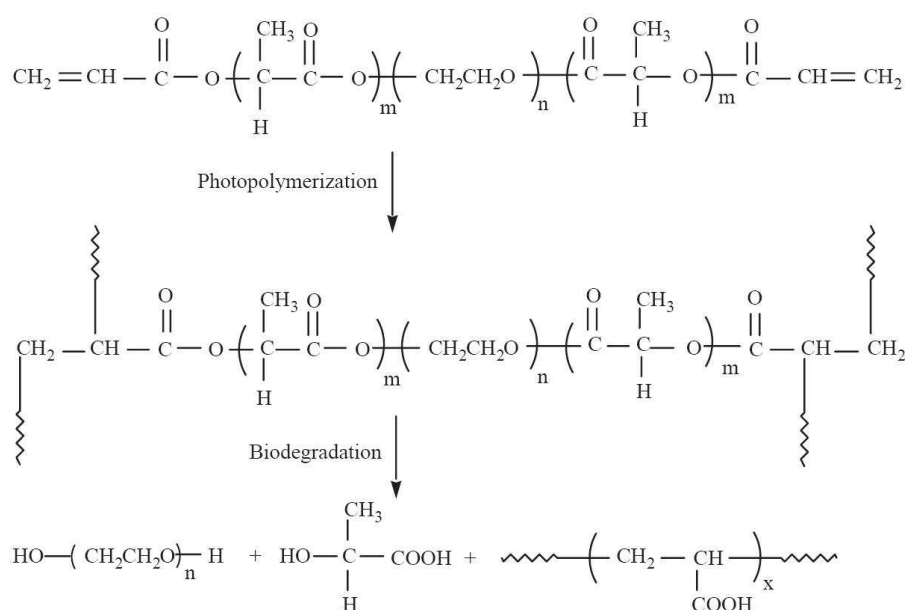


Figure 8. Photopolymerization and degradation of PEG-PLA diacrylate hydrogels.¹⁰¹ Reprinted with permission from the American Chemical Society. Copyright 1993 American Chemical Society.

Redox polymerization

Alternatively, the polymerization of (meth)acrylate functionalized polymers has been initiated by redox reaction.^{34, 89, 146-148} Mikos et al. prepared oligopoly(ethylene glycol) fumarate hydrogels using an ammonium persulfate (APS)/N,N,N,N'-tetramethylethylenediamine (TEMED) redox initiator system and N,N'-methylenebisacrylamide as a crosslinker (Figure 9).¹⁴⁸ These gels were proposed as injectable hydrogels, wherein gelation occurred within 4 min. Hennink et al. have prepared dextran-(hydroxyethyl)methacrylate (dextran-(HE)MA)⁴⁰ and dextran-lactate-HEMA¹⁴⁹ hydrogels using a potassium peroxydisulfate (KPS)/TEMED initiator system. The gelation was rather slow (typically 1 h was used to allow polymerization).

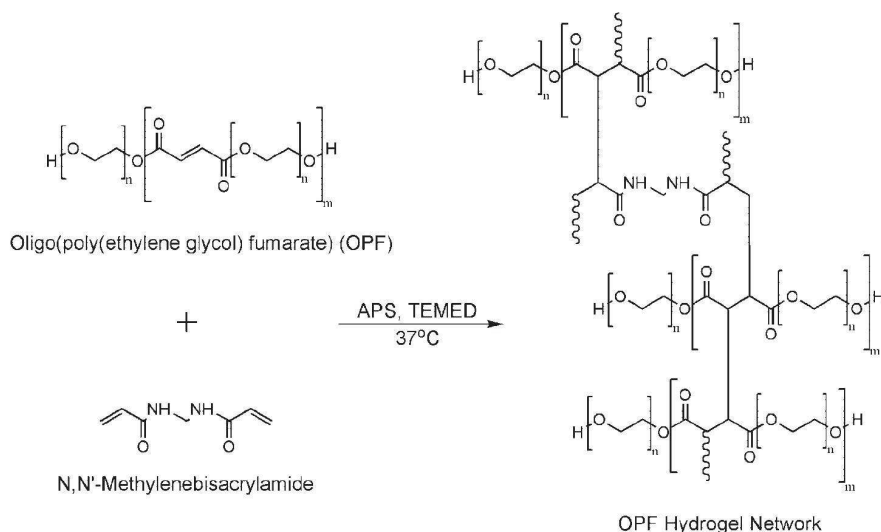


Figure 9. Preparation of an oligopoly(ethylene glycol) fumarate hydrogel using an APS/TEMED initiator system.¹⁵⁰ Reprinted with permission from John Wiley & Sons, Inc.

Michael type addition

More recently, hydrogels have been prepared by Michael type addition between thiols and acrylates or vinyl sulfones¹⁵¹⁻¹⁵⁸ Michael type addition offers several advantages in the preparation of hydrogels. The reaction is selective towards thiols under physiological conditions, thus minimizing side reactions with amines present in the body.^{159, 160} The Michael type addition is catalyzed by a (weak) base, which is present in a physiological environment, making this type of crosslinking very well suited for in situ hydrogel formation. When using acrylate as the unsaturated group, degradable hydrogels are formed, since the ester bond of the acrylate group can be hydrolyzed. Hubbell et al. were the first to report on hydrogels prepared by Michael addition.¹⁶¹ These hydrogels were formed by Michael addition between multifunctional PEG acrylate and PEG dithiol or dithioerythritol (DTT). The hydrogel degradation time could be varied from approximately 1 week to several months, by varying the functionality and molecular weight of the PEG acrylate.^{151, 161} These hydrogels released human growth hormone *in vitro* for up to a few months with preservation of the protein integrity.¹⁵² On the other hand, the use of vinyl sulfone compounds offers the advantage of controlling the hydrogel degradation by incorporation of degradable linkers. By using Michael addition, biomimetic scaffolds can easily be obtained by incorporation of thiol-bearing biomolecules. Such scaffolds are particularly attractive for tissue engineering applications. Hubbell et al. prepared cell-responsive hydrogels by Michael addition between PEG tetravinyl sulfones and bifunctional thiol peptide sequences that can be cleaved by metalloproteinases (MMPs) secreted by the encapsulated cells (Figure 10).¹⁰² As such, the hydrogel degradation is closely matched to the cellular activity.¹⁶² In addition, a cell adhesion sequence could be easily incorporated into the hydrogel by Michael addition in the presence of a monocysteine cell adhesion peptide sequence (Figure 10). Fibroblasts adhered to these hydrogels and were able to migrate into the hydrogel.¹⁰² Prestwich et al. have recently reported on hydrogels prepared by Michael addition between thiol-modified hyaluronic acid and PEG diacrylate.¹⁶³ These hydrogels were degradable by the enzyme hyaluronase and were shown to quantitatively release basic fibroblast growth factor (bFGF) for 28 days, wherein bFGF retained 55% of its original biological activity.¹⁵⁷ When loaded with vascular endothelial growth factor (VEGF) and keratinocyte growth factor (KGF), these hydrogels

induced angiogenesis *in vivo*.¹⁶⁴ When a fibronectin functional domain was incorporated into the hydrogel by Michael addition in the presence of a mono-cysteine derivative fibronectin functional domain, these hydrogels recruited fibroblasts *in vivo*.¹⁰⁴

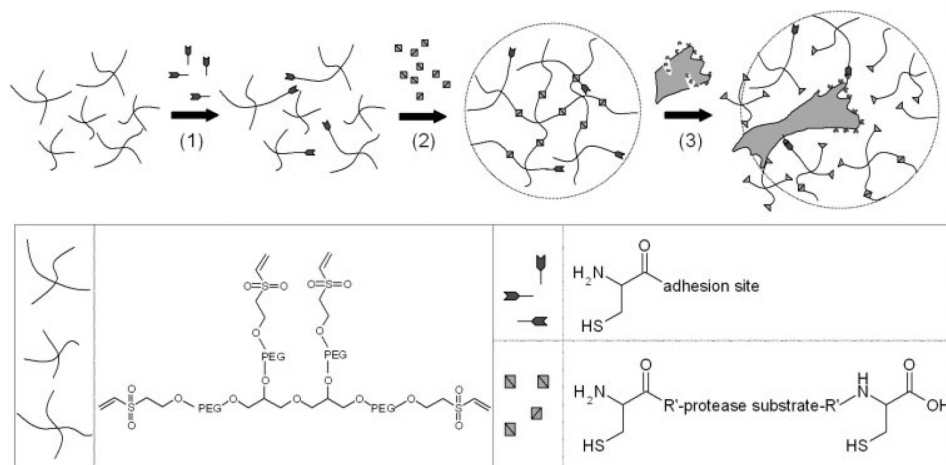


Figure 10. A Michael-type addition reaction between VS-functionalized multi-arm PEGs and mono-cysteine adhesion peptides (step 1) or bis-cysteine MMP substrate peptides (step 2) was used to form gels from aqueous solutions in the presence of cells. These elastic networks were designed to locally respond to protease activity at the cell surface (step 3).¹⁰² Reprinted with permission from Wiley-VCH Verlag GmbH & Co KGaA.

Other crosslinking reactions between complementary reactive groups

Several groups have formed chemically crosslinked hydrogels by reaction between complementary reactive groups under (near) physiological conditions. The gelation reaction of these hydrogels was fast, rendering them suitable as *in situ* forming hydrogels. A well-known example is the fibrin hydrogel that is formed by crosslinking of fibrinogen with thrombin.²² These gels are however generally mechanically weak. Biodegradable hydrogels have also been formed by reaction between aldehyde modified dextran and adipic acid dihydrazide compounds³⁰, reaction of amine groups of gelatin with aldehyde-modified alginate in the presence of small amounts of sodium tetraborate¹⁶⁵ or activated

ester-modified PNIPAAm with amine terminated poly(amino acid)-modified PNIPAAm¹⁶⁶.

2.3 Hydrogels for biomedical applications

2.3.1 Controlled drug delivery

Parental administration is hampered by rapid clearance of the bioactive agent, while oral administration is generally not successful due to the degradation of the bioactive agent in the gastro-intestinal tract. Moreover, since the delivery is not localized, relatively high doses are needed to have a therapeutic effect. The administration of pharmaceuticals, such as drugs and proteins may be greatly improved by the use of controlled delivery systems. Controlled delivery systems allow for sustained and localized release of the bioactive agent, thereby decreasing the number of administrations, preventing damage to the bioactive agent and allowing for relatively low doses. Hydrogels have been widely applied as “intelligent” carriers in controlled delivery systems. Their high water content makes them compatible with encapsulated proteins and living tissue.² In addition, in situ hydrogel formation allows easy and homogeneous loading of bioactive molecules.

Bioactive agents may be physically entrapped or may be covalently conjugated to the hydrogel.¹⁶⁷ Release of physically entrapped bioactive agents may be controlled by diffusion and hydrogel degradation or swelling, or a combination of these factors.⁴ The release of covalently attached compounds is governed by the hydrolysis rate of the linker of the compound to the hydrogel network.^{70, 156} This is particularly favorable for prolonged delivery of small drugs that would quickly diffuse away when they are physically entrapped.

From what was once just a modality to achieve zero order release kinetics (i.e. constant release rate), controlled delivery is now being used to enhance tissue engineering and gene therapy applications, while providing novel strategies for therapeutic angiogenesis.²⁴ Stimuli-responsive hydrogels have been developed to have release controlled by the conditions of the environment.^{168, 169} Temperature-responsive hydrogels (often based on PNIPAAm) have been developed to create drug-delivery systems that exhibit a pulsatile release in response to temperature changes.^{105, 170-172} In addition, pH-responsive hydrogels

have been applied in numerous controlled-release applications.^{75, 87} By incorporating enzymes, researchers have created drug-delivery systems that are responsive to biological analytes.² For instance, glucose-responsive hydrogels have been prepared for self-regulated insulin release.^{32, 173, 174}

2.3.2 Tissue engineering

Tissue engineering has emerged as a promising approach to treat the loss or malfunction of an organ or tissue without the limitations of the current therapies. Broadly defined, tissue engineering is the process of creating living, functional, three-dimensional tissues and organs starting with populations of individual cells. The goal is to create new tissue either directly in the patient via cell transplantation or directed growth from endogenous healthy tissue, or by growing tissue outside the body for transplantation into the patient.

Typically, three-dimensional matrices (i.e. scaffolds) are used in tissue engineering to provide the cells with a physical means for attachment and mechanical support until the newly formed tissue is structurally stabilized. The matrices guide new tissue growth and organization, and may provide specific signals intended to retain tissue-specific gene expression.¹⁷⁵ The matrix should be biocompatible, to avoid detrimental immune response reactions. It should also be biodegradable so the ECM deposited by the cells can replace the scaffold in time. The mechanical properties should be tuned to the specific application, as cells have been shown to respond to the stiffness of the matrix.^{68, 176, 177}

Hydrogels have been extensively used as matrices for tissue engineering applications, since their high water content renders them highly compatible with living tissue and facilitates diffusion of nutrients and waste compounds.^{2, 11, 176, 178} Moreover, in situ forming hydrogels can be easily loaded with cells prior to gelation. In the past years attempts have been made to prepare matrices that more closely resemble the natural ECM. Here, next to supporting cells during their growth, also biochemical cell-matrix interactions contribute to the (re)generation of the tissue. Due to their high hydrophilicity, hydrogels show hardly any interactions with proteins. Since cell adhesion is mediated by proteins, hydrogels also show low cell-adhesion. Hydrogels that support cell-adhesion have been prepared by incorporation of peptide sequences, mostly RGD sequences.^{18, 64, 82, 179-181} Hydrogels that only support adhesion of (a) specific cell type(s) can be prepared by incorporation of the

particular cell-adhesion moieties. For instance, West et al. have shown specific adhesion of endothelial cells onto PEG hydrogels by incorporation of VAPG (Val-Ala-Pro-Gly) peptide sequences.¹⁸² Patterned adhesion of fibroblasts onto PEG hydrogels was obtained by patterning of RGD peptides onto the hydrogels using a photolithographic method.¹⁸³ Cell migration could be directed by cell culture on PEG hydrogels with bFGF gradients.¹⁸⁴ Besides incorporation of cell-adhesion peptides, West and Hubbell et al. have prepared cell-responsive hydrogels by incorporation of peptide sequences that are cleaved by enzymes (proteases) produced by the cells.^{20, 62, 64, 102, 134} The cell-dependent degradation allows invasion of cells, and remodeling and degradation of the hydrogel depending on the cellular activity. Such hydrogels also allow for cell-demanded, local delivery of bioactive agents.¹⁸⁵ Growth factors have been introduced into hydrogels by physical entrapment or by physical interaction with heparin (or heparin-like molecules) to enhance the (re)generation of the tissue. Depending on the type of growth factor, they may have several functions, such as preservation of the cell phenotype, stimulation of extracellular matrix production, cell proliferation and angiogenesis.^{66, 157, 179, 186-188}

2.4 Discussion and conclusions

Hydrogels are important materials for biomedical applications, such as drug or protein delivery and tissue engineering. Besides serving as a depot or support, hydrogels are more and more designed with additional functionalities, such as cell-adhesion and cell-dependent degradation and release, thus mimicking the natural ECM. Hydrogels are formed by physical or chemical crosslinking. Stereocomplexation is an attractive method to form physically crosslinked hydrogels, since hydrogels can be rapidly formed in situ in the presence of proteins, without damaging the proteins.^{35, 189, 190} Furthermore, stereocomplexed hydrogels are degradable due to the presence of the PLA blocks. However, stereocomplexed hydrogels that are based on PLA-PEG-PLA triblock copolymers show weak mechanical properties.¹⁸⁹ Dextran-lactate based stereocomplexed hydrogels require involved synthesis of dextran-lactate graft copolymers.³⁵ Therefore, it will be interesting to design new types of stereocomplexed hydrogels, of which the base

polymers can be easily synthesized, while yielding hydrogels with a high crosslinking density.

Chemically crosslinked hydrogels are generally stronger and may have increased degradation times compared to physically crosslinked hydrogels. Photopolymerization has been mostly used for preparation of robust chemically crosslinked hydrogels.¹⁰¹ However, in situ formation is limited by the significant absorption of UV-light by the skin. Moreover, photopolymerization may cause substantial heat effects. Therefore, we will focus on the combination of photopolymerization with a fast in situ crosslinking method, thus allowing lower photopolymerization rates, preventing temperature rise and potentiating the use of low light intensities.

More recently, in situ forming chemically crosslinked hydrogels prepared by Michael type addition between thiols and vinyl sulfones or acrylates have been reported. Michael type addition is very well suited for in situ hydrogel preparation, since the reaction is rapid and selective towards thiols under physiological conditions. PEG has been often used for this type of hydrogels.¹⁶¹ The main drawback of these hydrogels is that the functionality of PEG is limited by the number of hydroxyl end groups, thus limiting control over the hydrogel properties. Michael addition hydrogels have also been based on the polysaccharide hyaluronic acid, thus allowing a much wider range of crosslinking functionality.¹⁶³ Dextran is another highly water-soluble polysaccharide that has been used for the preparation of hydrogels for biomedical applications.^{30, 35, 191, 192} Unlike hyaluronic acid, dextran is soluble in organic solvents, thus broadening the scope for synthesis of crosslinkable derivatives. Hyaluronic acid is rapidly degraded in the body by the enzyme hyaluronase.^{18, 163, 193} In contrast, dextran is not degradable (except for in the colon, where the enzyme dextranase is present¹⁹⁴), thus allowing the degradation rate to be controlled by the incorporation of degradable sequences (e.g. peptide sequences or hydrolytically labile bonds). Therefore, it will be interesting to design dextran based, biodegradable hydrogels that are formed in situ by Michael addition.

2.5 References

1. Wichterle O, Lim D, Dreifus M., On the problem of contact lenses. *Cesk. Oftalmol.* 1961, 17, 70-75.

2. Peppas, N. A.; Hilt, J. Z.; Khademhosseini, A.; Langer, R., Hydrogels in biology and medicine: From molecular principles to bionanotechnology. *Adv. Mater.* 2006, 18, 1345-1360.
3. Kashyap, N.; Kumar, N.; Kumar, M., Hydrogels for pharmaceutical and biomedical applications. *Crit. Rev. Ther. Drug Carrier Syst.* 2005, 22, 107-149.
4. Peppas, N.; Bures, P.; Ichikawa, H., Hydrogels in pharmaceutical formulations. *Eur. J. Pharm. Biopharm.* 2000, 50, 27-46.
5. Malmsten, M., Soft drug delivery systems. *Soft Matter* 2006, 2, 760-769.
6. Hubbell, J. A., Materials as morphogenetic guides in tissue engineering. *Curr. Opin. Biotech.* 2003, 14, 551-558.
7. Nerem, R. M., Tissue engineering: The hope, the hype, and the future. *Tissue Eng.* 2006, 12, 1143-1150.
8. Lavik, E.; Langer, R., Tissue engineering: current state and perspectives. *Appl. Microbiol. Biotechnol.* 2004, 65, 1-8.
9. Hennink, W. E.; van Nostrum, C. F., Novel crosslinking methods to design hydrogels. *Adv. Drug Deliv. Rev.* 2002, 54, 13-36.
10. Yamaoka, T.; Tabata, Y.; Ikada, Y., Distribution and tissue uptake of poly(ethylene glycol) with different molecular weights after intravenous administration to mice. *J. Pharm. Sci.* 1994, 83, 601-606.
11. Nguyen, K. T.; West, J. L., Photopolymerizable hydrogels for tissue engineering applications. *Biomaterials* 2002, 23, 4307-4314.
12. Benoit, D. S. W.; Durney, A. R.; Anseth, K. S., Manipulations in hydrogel degradation behavior enhance osteoblast function and mineralized tissue formation. *Tissue Eng.* 2006, 12, 1663-1673.
13. Patel, P. N.; Gobin, A. S.; West, J. L.; Patrick, C. W., Poly(ethylene glycol) hydrogel system supports preadipocyte viability, adhesion, and proliferation. *Tissue Eng.* 2005, 11, 1498-1505.
14. Dang, J. M.; Leong, K. W., Natural polymers for gene delivery and tissue engineering. *Adv. Drug Deliv. Rev.* 2006, 58, 487-499.
15. Schmidt, C. E.; Baier, J. M., Acellular vascular tissues: natural biomaterials for tissue repair and tissue engineering. *Biomaterials* 2000, 21, 2215-2231.

16. Whitaker, M. J.; Quirk, R. A.; Howdle, S. M.; Shakesheff, K. M., Growth factor release from tissue engineering scaffolds. *J. Pharm. Pharmacol.* 2001, 53, 1427-1437.
17. Allison, D. D.; Grande-Allen, K. J., Review. Hyaluronan: A powerful tissue engineering tool. *Tissue Eng.* 2006, 12, 2131-2140.
18. Park, Y. D.; Tirelli, N.; Hubbell, J. A., Photopolymerized hyaluronic acid-based hydrogels and interpenetrating networks. *Biomaterials* 2003, 24, 893-900.
19. Miyamoto, K.; Sasaki, M.; Minamisawa, Y.; Kurahashi, Y.; Kano, H.; Ishikawa, S., Evaluation of in vivo biocompatibility and biodegradation of photocrosslinked hyaluronate hydrogels (HADgels). *J. Biomed. Mater. Res.* 2004, 70A, 550-559.
20. Rosso, F.; Marino, G.; Giordano, A.; Barbarisi, M.; Parmeggiani, D.; Barbarisi, A., Smart materials as scaffolds for tissue engineering. *J. Cell. Physiol.* 2005, 203, 465-470.
21. Peretti, G. M.; Xu, J. W.; Bonassar, L. J.; Kirchhoff, C. H.; Yaremchuk, M. J.; Randolph, M. A., Review of injectable cartilage engineering using fibrin gel in mice and swine models. *Tissue Eng.* 2006, 12, 1151-1168.
22. MacGillivray, T. E., Fibrin sealants and glues. *J. Card. Surg.* 2003, 18, 480-485.
23. Lee, C. H.; Singla, A.; Lee, Y., Biomedical applications of collagen. *Int. J. Pharm.* 2001, 221, 1-22.
24. Young, S.; Wong, M.; Tabata, Y.; Mikos, A. G., Gelatin as a delivery vehicle for the controlled release of bioactive molecules. *J. Controlled Release* 2005, 109, 256-274.
25. Li, Q.; Williams, C. G.; Sun, D. D. N.; Wang, J.; Leong, K.; Elisseff, J. H., Photocrosslinkable polysaccharides based on chondroitin sulfate. *J. Biomed. Mater. Res.* 2004, 68A, 28-33.
26. Gombotz, W. R.; Wee, S. F., Protein release from alginate matrices. *Adv. Drug Deliv. Rev.* 1998, 31, 267-285.
27. George, M.; Abraham, T. E., Polyionic hydrocolloids for the intestinal delivery of protein drugs: Alginate and chitosan - a review. *J. Controlled Release* 2006, 114, 1-14.
28. Luginbuehl, V.; Wenk, E.; Koch, A.; Gander, B.; Merkle, H. P.; Meinel, L., Insulin-like growth factor I-releasing alginate-tricalciumphosphate composites for bone regeneration. *Pharm. Res.* 2005, 22, 940-950.

29. Ferreira, L.; Rafael, A.; Lamghari, M.; Barbosa, M. A.; Gil, M. H.; Cabrita, A. M.; Dordick, J. S., Biocompatibility of chemoenzymatically derived dextran-acrylate hydrogels. *J. Biomed. Mater. Res.* 2004, 68A, 584-596.
30. Maia, J.; Ferreira, L.; Carvalho, R.; Ramos, M.; Gil, M., Synthesis and characterization of new injectable and degradable dextran-based hydrogels. *Polymer* 2005, 46, 9604-9614.
31. Van Tomme, S. R.; van Steenberg, M. J.; De Smedt, S. C.; van Nostrum, C. F.; Hennink, W. E., Self-gelling hydrogels based on oppositely charged dextran microspheres. *Biomaterials* 2005, 26, 2129-2135.
32. Tanna, S.; Taylor, M. J.; Sahota, T. S.; Sawicka, K., Glucose-responsive UV polymerised dextran-concanavalin A acrylic derivatised mixtures for closed-loop insulin delivery. *Biomaterials* 2006, 27, 1586-1597.
33. Zhang, R. S.; Tang, M. G.; Bowyer, A.; Eisenthal, R.; Hubble, J., A novel pH- and ionic-strength-sensitive carboxy methyl dextran hydrogel. *Biomaterials* 2005, 26, 4677-4683.
34. Cadee, J. A.; De Kerf, M.; De Groot, C. J.; Den Otter, W.; Hennink, W. E. Synthesis, characterization of 2-(methacryloyloxy)ethyl-(di-)-lactate and their application in dextran-based hydrogels. *Polymer* 1999, 40, 6877-6881.
35. de Jong, S. J.; van Eerdenbrugh, B.; van Nostrum, C. F.; Kettenes-van de Bosch, J. J.; Hennink, W. E., Physically crosslinked dextran hydrogels by stereocomplex formation of lactic acid oligomers: degradation and protein release behavior. *J. Controlled Release* 2001, 71, 261-275.
36. Kim, S. H.; Won, C. Y.; Chu, C. C., Synthesis and characterization of dextran-based hydrogel prepared by photocrosslinking. *Carbohydr. Polym.* 1999, 40, 183-190.
37. Moriyama, K.; Yui, N., Regulated insulin release from biodegradable dextran hydrogels containing poly(ethylene glycol). *J. Controlled Release* 1996, 42, 237-248.
38. Brondsted, H.; Andersen, C.; Hovgaard, L., Crosslinked dextran - a new capsule material for colon targeting of drugs. *J. Controlled Release* 1998, 53, 7-13.
39. Hennink, W. E.; Franssen, O.; vanDijkWolthuis, W. N. E.; Talsma, H., Dextran hydrogels for the controlled release of proteins. *J. Controlled Release* 1997, 48, 107-114.

40. vanDijkWolthuis, W. N. E.; Hoogeboom, J. A. M.; vanSteenbergen, M. J.; Tsang, S. K. Y.; Hennink, W. E., Degradation and release behavior of dextran-based hydrogels. *Macromolecules* 1997, 30, 4639-4645.
41. Levesque, S. G.; Shoichet, M. S., Synthesis of cell-adhesive dextran hydrogels and macroporous scaffolds. *Biomaterials* 2006, 27, 5277-5285.
42. Shi, C. M.; Zhu, Y.; Ran, X. Z.; Wang, M.; Su, Y. P.; Cheng, T. M., Therapeutic potential of chitosan and its derivatives in regenerative medicine. *J. Surg. Res.* 2006, 133, 185-192.
43. Dutta, P. K.; Dutta, J.; Tripathi, V. S., Chitin and chitosan: Chemistry, properties and applications. *J. Sci. Ind. Res.* 2004, 63, 20-31.
44. Berger, J.; Reist, M.; Mayer, J. M.; Felt, O.; Peppas, N. A.; Gurny, R., Structure and interactions in covalently and ionically crosslinked chitosan hydrogels for biomedical applications. *Eur. J. Pharm. Biopharm.* 2004, 57, 19-34.
45. Berger, J.; Reist, M.; Mayer, J. M.; Felt, O.; Gurny, R., Structure and interactions in chitosan hydrogels formed by complexation or aggregation for biomedical applications. *Eur. J. Pharm. Biopharm.* 2004, 57, 35-52.
46. Suh, J. K. F.; Matthew, H. W. T., Application of chitosan-based polysaccharide biomaterials in cartilage tissue engineering: a review. *Biomaterials* 2000, 21, 2589-2598.
47. Kim, S. Y.; Cho, S. M.; Lee, Y. M.; Kim, S. J., Thermo- and pH-responsive behaviors of graft copolymer and blend based on chitosan and N-isopropylacrylamide. *J. Appl. Polym. Sci.* 2000, 78, 1381-1391.
48. Cho, J. H.; Kim, S. H.; Park, K. D.; Jung, M. C.; Yang, W. I.; Han, S. W.; Noh, J. Y.; Lee, J. W., Chondrogenic differentiation of human mesenchymal stem cells using a thermosensitive poly(N-isopropylacrylamide) and water-soluble chitosan copolymer. *Biomaterials* 2004, 25, 5743-5751.
49. Chenite, A.; Gori, S.; Shive, M.; Desrosiers, E.; Buschmann, M. D., Monolithic gelation of chitosan solutions via enzymatic hydrolysis of urea. *Carbohydr. Polym.* 2006, 64, 419-424.
50. Shim, W. S.; Yoo, J. S.; Bae, Y. H.; Lee, D. S., Novel injectable pH and temperature sensitive block copolymer hydrogel. *Biomacromolecules* 2005, 6, 2930-2934.

51. Chenite, A.; Chaput, C.; Wang, D.; Combes, C.; Buschmann, M. D.; Hoemann, C. D.; Leroux, J. C.; Atkinson, B. L.; Binette, F.; Selmani, A., Novel injectable neutral solutions of chitosan form biodegradable gels in situ. *Biomaterials* 2000, 21, 2155-2161.
52. Nomura, Y.; Sasaki, Y.; Takagi, M.; Narita, T.; Aoyama, Y.; Akiyoshi, K., Thermoresponsive controlled association of protein with a dynamic nanogel of hydrophobized polysaccharide and cyclodextrin: Heat shock protein-like activity of artificial molecular chaperone. *Biomacromolecules* 2005, 6, 447-452.
53. Gupta, M.; Gupta, A. K., Hydrogel pullulan nanoparticles encapsulating pBUDLacZ plasmid as an efficient gene delivery carrier. *J. Controlled Release* 2004, 99, 157-166.
54. Masci, G.; Bontempo, D.; Crescenzi, V., Synthesis and characterization of thermoresponsive N-isopropylacrylamide/methacrylated pullulan hydrogels. *Polymer* 2002, 43, 5587-5593.
55. Hosseinkhani, H.; Hosseinkhani, M.; Khademhosseini, A.; Kobayashi, H.; Tabata, Y., Enhanced angiogenesis through controlled release of basic fibroblast growth factor from peptide amphiphile for tissue regeneration. *Biomaterials* 2006, 27, 5836-5844.
56. Collier, J. H.; Hu, B.-H.; Ruberti, J. W.; Zhang, J.; Shum, P.; Thompson, D. H.; Messersmith, P. B., Thermally and photochemically triggered self-assembly of peptide hydrogels. *JACS* 2001, 123, 9463-9464.
57. Yan, H.; Saiani, A.; Gough, J. E.; Miller, A. F., Thermoreversible protein hydrogel as cell scaffold. *Biomacromolecules* 2006, 7, 2776-2782.
58. Betre, H.; Setton, L. A.; Meyer, D. E.; Chilkoti, A., Characterization of a genetically engineered elastin-like polypeptide for cartilaginous tissue repair. *Biomacromolecules* 2002, 3, 910-916.
59. Ramachandran, S.; Tseng, Y.; Yu, Y. B., Repeated rapid shear-responsiveness of peptide hydrogels with tunable shear modulus. *Biomacromolecules* 2005, 6, 1316-1321.
60. Kisiday, J.; Jin, M.; Kurz, B.; H., H.; Semino, C.; Zhang, S.; Grodzinsky, A. J., Self-assembling peptide hydrogel fosters chondrocyte extracellular matrix production and cell division: Implications for cartilage tissue repair. *PNAS* 2002, 99, 9996-10001.

61. Watanabe, J.; Ooya, T.; Nitta, K. H.; Park, K. D.; Kim, Y. H.; Yui, N., Fibroblast adhesion and proliferation on poly(ethylene glycol) hydrogels crosslinked by hydrolyzable polyrotaxane. *Biomaterials* 2002, 23, 4041-4048.
62. Mann, B. K.; Gobin, A. S.; Tsai, A. T.; Schmedlen, R. H.; West, J. L., Smooth muscle cell growth in photopolymerized hydrogels with cell adhesive and proteolytically degradable domains: synthetic ECM analogs for tissue engineering. *Biomaterials* 2001, 22, 3045-3051.
63. Burdick, J. A.; Mason, M. N.; Hinman, A. D.; Thorne, K.; Anseth, K. S., Delivery of osteoinductive growth factors from degradable PEG hydrogels influences osteoblast differentiation and mineralization. *J. Controlled Release* 2002, 83, 53-63.
64. Halstenberg, S.; Panitch, A.; Rizzi, S.; Hall, H.; Hubbell, J. A., Biologically engineered protein-graft-poly(ethylene glycol) hydrogels: A cell adhesive and plasm in-degradable biosynthetic material for tissue repair. *Biomacromolecules* 2002, 3, 710-723.
65. Elbert, D. L.; Hubbell, J. A., Conjugate addition reactions combined with free-radical cross-linking for the design of materials for tissue engineering. *Biomacromolecules* 2001, 2, 430-441.
66. Elisseff, J.; McIntosh, W.; Fu, K.; Blunk, T.; Langer, R., Controlled-release of IGF-I and TGF-beta 1 in a photopolymerizing hydrogel for cartilage tissue engineering. *J. Orthop. Res.* 2001, 19, 1098-1104.
67. Lee, H. J.; Lee, J. S.; Chansakul, T.; Yu, C.; Elisseff, J. H.; Yu, S. M., Collagen mimetic peptide-conjugated photopolymerizable PEG hydrogel. *Biomaterials* 2006, 27, 5268-5276.
68. Peyton, S. R.; Raub, C. B.; Keschrums, V. P.; Putnam, A. J., The use of poly(ethylene glycol) hydrogels to investigate the impact of ECM chemistry and mechanics on smooth muscle cells. *Biomaterials* 2006, 27, 4881-4893.
69. Nuttelman, C. R.; Benoit, D. S. W.; Tripodi, M. C.; Anseth, K. S., The effect of ethylene glycol methacrylate phosphate in PEG hydrogels on mineralization and viability of encapsulated hMSCs. *Biomaterials* 2006, 27, 1377-1386.
70. Nuttelman, C. R.; Tripodi, M. C.; Anseth, K. S., Dexamethasone-functionalized gels induce osteogenic differentiation of encapsulated hMSCs. *J. Biomed. Mater. Res.* 2006, 76A, 183-195.

71. Zhu, J.; Beamish, J.; Tang, C.; Kottke-Marchant, K.; Marcant, R., Extracellular Matrix-like Cell-Adhesive Hydrogels from RGD-Containing Poly(ethylene glycol) Diacrylate. *Macromolecules* 2006, 39, 1305-1307.
72. Laloo, A.; Chao, P.; Hu, P.; Stein, S.; Sinko, P. J., Pharmacokinetic and pharmacodynamic evaluation of a novel in situ forming poly(ethylene glycol)-based hydrogel for the controlled delivery of the camptothecins. *J. Controlled Release* 2006, 112, 333-342.
73. Yamaguchi, N.; Kiick, K. L., Polysaccharide-poly(ethylene glycol) star copolymer as a scaffold for the production of bioactive hydrogels. *Biomacromolecules* 2005, 6, 1921-1930.
74. Fujimoto, M.; Isobe, M.; Yamaguchi, S.; Amagasa, T.; Watanabe, A.; Ooya, T.; Yui, N., Poly(ethylene glycol) hydrogels cross-linked by hydrolyzable polyrotaxane containing hydroxyapatite particles as scaffolds for bone regeneration. *J. Biomater. Sci.-Polym. Ed.* 2005, 16, 1611-1621.
75. Serra, L.; Domenech, J.; Peppas, N. A., Drug transport mechanisms and release kinetics from molecularly designed poly(acrylic acid-g-ethylene glycol) hydrogels. *Biomaterials* 2006, 27, 5440-5451.
76. Jeong, B.; Bae, Y. H.; Lee, D. S.; Kim, S. W., Biodegradable block copolymers as injectable drug-delivery systems. *Nature* 1997, 388, 860-862.
77. Jeong, B.; Bae, Y. H.; Kim, S. W., Thermoreversible gelation of PEG-PLGA-PEG triblock copolymer aqueous solutions. *Macromolecules* 1999, 32, 7064-7069.
78. Bae, S. J.; Joo, M. K.; Jeong, Y.; Kim, S. W.; Lee, W. K.; Sohn, Y. S.; Jeong, B., Gelation behavior of poly(ethylene glycol) and polycaprolactone triblock and multiblock copolymer aqueous solutions. *Macromolecules* 2006, 39, 4873-4879.
79. Zhong, Z. Y.; Dijkstra, P. J.; Feijen, J.; Kwon, Y. M.; Bae, Y. H.; Kim, S. W., Synthesis and aqueous phase behavior of thermoresponsive biodegradable poly(D,L-3-methylglycolide)-block-poly(ethylene glycol)-block-poly(D,L-3-methylglycolide) triblock copolymers. *Macromol. Chem. Phys.* 2002, 203, 1797-1803.
80. Paradossi, G.; Cavalieri, F.; Chiessi, E., Poly(vinyl alcohol) as versatile biomaterial for potential biomedical applications. *J. Mater. Sci.-Mater. Med.* 2003, 14, 687-691.

81. Muhlebach, A.; Muller, B.; Pharisa, C.; Hofmann, M.; Seiferling, B.; Guerry, D., New water-soluble photo crosslinkable polymers based on modified poly(vinyl alcohol). *J. Polym. Sci. Pol. Chem.* 1997, 35, 3603-3611.
82. Schmedlen, K. H.; Masters, K. S.; West, J. L., Photocrosslinkable polyvinyl alcohol hydrogels that can be modified with cell adhesion peptides for use in tissue engineering. *Biomaterials* 2002, 23, 4325-4332.
83. Martens, P. J.; Bryant, S. J.; Anseth, K. S., Tailoring the degradation of hydrogels formed from multivinyl poly(ethylene glycol) and poly(vinyl alcohol) macromers for cartilage tissue engineering. *Biomacromolecules* 2003, 4, 283-292.
84. Hassan, C. M.; Peppas, N. A., Structure and morphology of freeze/thawed PVA hydrogels. *Macromolecules* 2000, 33, 2472-2479.
85. Kim, S.; Healy, K. E., Synthesis and characterization of injectable poly(N-isopropylacrylamide-co-acrylic acid) hydrogels with proteolytically degradable cross-links. *Biomacromolecules* 2003, 4, 1214-1223.
86. Lee, B. H.; West, B.; McLemore, R.; Pauken, C.; Vernon, B. L., In-situ injectable physically and chemically gelling NIPAAm-based copolymer system for embolization. *Biomacromolecules* 2006, 7, 2059-2064.
87. Liu, Y. Y.; Shao, Y. H.; Lu, J., Preparation, properties and controlled release behaviors of pH-induced thermosensitive amphiphilic gels. *Biomaterials* 2006, 27, 4016-4024.
88. Xu, F. J.; Kang, E. T.; Neoh, K. G., pH- and temperature-responsive hydrogels from crosslinked triblock copolymers prepared via consecutive atom transfer radical polymerizations. *Biomaterials* 2006, 27, 2787-2797.
89. Kim, S.; Chung, E. H.; Gilbert, M.; Healy, K. E., Synthetic MMP-13 degradable ECMs based on poly(N-isopropylacrylamide-co-acrylic acid) semi-interpenetrating polymer networks. I. Degradation and cell migration. *J. Biomed. Mater. Res.* 2005, 75A, 73-88.
90. Feil, H.; Bae, Y. H.; Feijen, J.; Kim, S. W., Effect of polyelectrolytes on the lower critical solution temperature of ionizable, thermosensitive polymers. *Makromol. Chem.-Rapid Comm.* 1993, 14, 465-470.

91. Feil, H.; Bae, Y. H.; Jan, F. J.; Kim, S. W., Effect of comonomer hydrophilicity and ionization on the lower critical solution temperature of N-isopropylacrylamide copolymers. *Macromolecules* 1993, 26, 2496-2500.
92. Feil, H.; Bae, Y. H.; Feijen, J.; Kim, S. W., Mutual influence of pH and temperature on the swelling of ionizable and thermosensitive hydrogels. *Macromolecules* 1992, 25, 5528-5530.
93. Feil, H.; Bae, Y. H.; Feijen, J.; Kim, S. W., Molecular separation by thermosensitive hydrogel membranes. *J. Membr. Sci.* 1991, 64, 283-294.
94. Kwon, I. K.; Matsuda, T., Photo-iniferter-based thermoresponsive block copolymers composed of poly(ethylene glycol) and poly(N-isopropylacrylamide) and chondrocyte immobilization. *Biomaterials* 2006, 27, 986-995.
95. Vihola, H.; Laukkanen, A.; Valtola, L.; Tenhu, H.; Hirvonen, J., Cytotoxicity of thermosensitive polymers poly(N-isopropylacrylamide), poly(N-vinylcaprolactam) and amphiphilically modified poly(N-vinylcaprolactam). *Biomaterials* 2005, 26, 3055-3064.
96. Sohn, Y. S.; Cho, Y. H.; Baek, H.; Jung, O. S., Synthesis and properties of low-molecular-weight polyphosphazenes. *Macromolecules* 1995, 28, 7566-7568.
97. Lee, B. H.; Lee, Y. M.; Sohn, Y. S.; Song, S. C., A thermosensitive poly(organo-phosphazene) gel. *Macromolecules* 2002, 35, 3876-3879.
98. Seong, J. Y.; Jun, Y. J.; Jeong, B.; Sohn, Y. S., New thermogelling poly(organo-phosphazenes) with methoxypoly(ethylene glycol) and oligopeptide as side groups. *Polymer* 2005, 46, 5075-5081.
99. Nuttelman, C. R.; Henry, S. M.; Anseth, K. S., Synthesis and characterization of photocrosslinkable, degradable poly(vinyl alcohol)-based tissue engineering scaffolds. *Biomaterials* 2002, 23, 3617-3626.
100. Lu, S. X.; Anseth, K. S., Release behavior of high molecular weight solutes from poly(ethylene glycol)-based degradable networks. *Macromolecules* 2000, 33, 2509-2515.
101. Sawhney, A. S.; Pathak, C. P.; Hubbell, J. A., Bioerodible hydrogels based on photopolymerized poly(ethylene glycol)-co-poly(alpha-hydroxy acid) diacrylate macromers. *Macromolecules* 1993, 26, 581-587.

102. Lutolf, M. P.; Raeber, G. P.; Zisch, A. H.; Tirelli, N.; Hubbell, J. A., Cell-responsive synthetic hydrogels. *Adv. Mater.* 2003, 15, 888-892.
103. Bryant, S. J.; Arthur, J. A.; Anseth, K. S., Incorporation of tissue-specific molecules alters chondrocyte metabolism and gene expression in photocrosslinked hydrogels. *Acta Biomaterialia* 2005, 1, 243-252.
104. Ghosh, K.; Ren, X. D.; Shu, X. Z.; Prestwich, G. D.; Clark, R. A. F., Fibronectin functional domains coupled to hyaluronan stimulate adult human dermal fibroblast responses critical for wound healing. *Tissue Eng.* 2006, 12, 601-613.
105. Huang, X.; Lowe, T. L., Biodegradable thermoresponsive hydrogels for aqueous encapsulation and controlled release of hydrophilic model drugs. *Biomacromolecules* 2005, 6, 2131-2139.
106. Zhang, R. S., Synthesis, characterization and reversible transport of thermo-sensitive carboxyl methyl dextran/poly (N-isopropylacrylamide) hydrogel. *Polymer* 2005, 46, 2443-2451.
107. Chiu, H. C.; Lin, Y. F.; Hung, S. H., Equilibrium swelling of copolymerized acrylic acid- methacrylated dextran networks: Effects of pH and neutral salt. *Macromolecules* 2002, 35, 5235-5242.
108. Zhang, Y. L.; Chu, C. C., Biodegradable dextran-poly lactide hydrogel networks: Their swelling, morphology and the controlled release of indomethacin. *J. Biomed. Mater. Res.* 2002, 59, 318-328.
109. Cho, S. M.; Kim, S. Y.; Lee, Y. M.; Sung, Y. K.; Cho, C. S., Synthesis, properties, and permeation of solutes through hydrogels based on poly(ethylene glycol)-copoly(lactones) diacrylate macromers and chitosan. *J. Appl. Polym. Sci.* 1999, 73, 2151-2158.
110. Temenoff, J. S.; Mikos, A. G., Injectable biodegradable materials for orthopedic tissue engineering. *Biomaterials* 2000, 21, 2405-2412.
111. Barbucci, R.; Leone, G.; Lamponi, S., Thixotrophy property of hydrogels to evaluate the cell growing on the inside of the material bulk (Amber effect). *J. Biomed. Mater. Res. Part B* 2006, 76B, 33-40.
112. Shim, W. S.; Kim, J. H.; Park, H.; Kim, K.; Kwon, I. C.; Lee, D. S., Biodegradability and biocompatibility of a pH- and thermo-sensitive hydrogel formed from a sulfonamide-modified poly(epsilon-caprolactone-co-lactide)-poly(ethylene glycol)-

- poly(epsilon-caprolactone-co-lactide) block copolymer. *Biomaterials* 2006, 27, 5178-5185.
113. Bae, S.; Sug, J.; Sohn, Y.; Bae, Y.; Kim, S.; Jeong, B., Thermogelling poly(caprolactone-b-ethylene glycol-b-caprolactone) aqueous solutions. *Macromolecules* 2005, 38, 5260, 5265.
114. Dang, J. M.; Sun, D. D. N.; Shin-Ya, Y.; Sieber, A. N.; Kostuik, J. P.; Leong, K. W., Temperature-responsive hydroxybutyl chitosan for the culture of mesenchymal stem cells and intervertebral disk cells. *Biomaterials* 2006, 27, 406-418.
115. Bhattarai, N.; Ramay, H. R.; Gunn, J.; Matsen, F. A.; Zhang, M. Q., PEG-grafted chitosan as an injectable thermosensitive hydrogel for sustained protein release. *J. Controlled Release* 2005, 103, 609-624.
116. Garlotta, D., A literature review of poly(lactic acid). *J. Polym. Environ.* 2001, 9, 63-84.
117. Ikada, Y.; Tsuji, H., Biodegradable polyesters for medical and ecological applications. *Macromol. Rapid Commun.* 2000, 21, 117-132.
118. de Jong, S. J.; van Nostrum, C. F.; Kroon-Batenburg, L. M. J.; Kettenes-van den Bosch, J. J.; Hennink, W. E., Oligolactate-grafted dextran hydrogels: Detection of stereocomplex crosslinks by X-ray diffraction. *J. Appl. Polym. Sci.* 2002, 86, 289-293.
119. Okihara, T.; Tsuji, M.; Kawaguchi, A.; Katayama, K.; Tsuji, H.; Hyon, S. H.; Ikada, Y., Crystal-structure of stereocomplex of poly(L-lactide) and poly(D-lactide). *J. Macromol. Sci.-Phys.* 1991, B30, 119-140.
120. Bourque, H.; Laurin, I.; Pezolet, M.; Klass, J. M.; Lennox, R. B.; Brown, G. R., Investigation of the poly(L-lactide)/poly(D-lactide) stereocomplex at the air-water interface by polarization modulation infrared reflection absorption spectroscopy. *Langmuir* 2001, 17, 5842-5849.
121. Spinu, M.; Jackson, C.; Keating, M. Y.; Gardner, K. H., Material design in poly(lactic acid) systems: Block copolymers, star homo- and copolymers, and stereocomplexes. *J. Macromol. Sci.-Pure Appl. Chem.* 1996, A33, 1497-1530.
122. de Jong, S. J., Stereocomplex formation of lactic acid oligomers for the design of biodegradable hydrogels. Utrecht, 2001.

123. de Jong, S. J.; De Smedt, S. C.; Wahls, M. W. C.; Demeester, J.; Kettenes-van den Bosch, J. J.; Hennink, W. E., Novel self-assembled hydrogels by stereocomplex formation in aqueous solution of enantiomeric lactic acid oligomers grafted to dextran. *Macromolecules* 2000, 33, 3680-3686.
124. Hennink, W. E.; De Jong, S. J.; Bos, G. W.; Veldhuis, T. F. J.; van Nostrum, C. F., Biodegradable dextran hydrogels crosslinked by stereocomplex formation for the controlled release of pharmaceutical proteins. *Int. J. Pharm.* 2004, 277, 99-104.
125. Li, J.; Ni, X. P.; Leong, K. W., Injectable drug-delivery systems based on supramolecular hydrogels formed by poly(ethylene oxide) and alpha-cyclodextrin. *J. Biomed. Mater. Res.* 2003, 65A, 196-202.
126. Sabadini, E.; Cosgrove, T., Inclusion complex formed between star-poly(ethylene glycol) and cyclodextrins. *Langmuir* 2003, 19, 9680-9683.
127. Huh, K. M.; Cho, Y. W.; Chung, H.; Kwon, I. C.; Jeong, S. Y.; Ooya, T.; Lee, W. K.; Sasaki, S.; Yui, N., Supramolecular hydrogel formation based on inclusion complexation between poly(ethylene glycol)-modified chitosan and alpha-cyclodextrin. *Macromol. Biosci.* 2004, 4, 92-99.
128. Huh, K. M.; Ooya, T.; Lee, W. K.; Sasaki, S.; Kwon, I. C.; Jeong, S. Y.; Yui, N., Supramolecular-structured hydrogels showing a reversible phase transition by inclusion complexation between poly(ethylene glycol) grafted dextran and alpha-cyclodextrin. *Macromolecules* 2001, 34, 8657-8662.
129. Choi, H. S.; Yamamoto, K.; Ooya, T.; Yui, N., Synthesis of poly(epsilon-lysine)-grafted dextrans and their pH- and thermosensitive hydrogelation with cyclodextrins. *ChemPhysChem* 2005, 6, 1081-1086.
130. Li, J.; Li, X.; Ni, X. P.; Wang, X.; Li, H. Z.; Leong, K. W., Self-assembled supramolecular hydrogels formed by biodegradable PEO-PHB-PEO triblock copolymers and alpha-cyclodextrin for controlled drug delivery. *Biomaterials* 2006, 27, 4132-4140.
131. Zhao, S. P.; Zhang, L. M.; Ma, D., Supramolecular hydrogels induced rapidly by inclusion complexation of poly(epsilon-caprolactone)-poly(ethylene glycol)-poly(epsilon-caprolactone) block copolymers with alpha-cyclodextrin in aqueous solutions. *J. Phys. Chem. B* 2006, 110, 12225-12229.

132. Rowley, J. A.; Madlambayan, G.; Mooney, D. J., Alginate hydrogels as synthetic extracellular matrix materials. *Biomaterials* 1999, 20, 45-53.
133. Baroli, B., Photopolymerization of biomaterials: issues and potentialities in drug delivery, tissue engineering, and cell encapsulation applications. *J. Chem. Technol. Biotechnol.* 2006, 81, 491-499.
134. West, J. L.; Hubbell, J. A., Polymeric biomaterials with degradation sites for proteases involved in cell migration. *Macromolecules* 1999, 32, 241-244.
135. Kim, S. H.; Chu, C. C., Synthesis and characterization of dextran-methacrylate hydrogels and structural study by SEM. *J. Biomed. Mater. Res.* 1999, 49, 517-527.
136. An, Y. J.; Hubbell, J. A., Intraarterial protein delivery via intimately-adherent bilayer hydrogels. *J. Controlled Release* 2000, 64, 205-215.
137. Nakayama, Y.; Kameo, T.; Ohtaka, A.; Hirano, Y., Enhancement of visible light-induced gelation of photocurable gelatin by addition of polymeric amine. *J. Photochem. Photobiol. A-Chem.* 2006, 177, 205-211.
138. Sontjens, S. H. M.; Nettles, D. L.; Carnahan, M. A.; Setton, L. A.; Grinstaff, M. W., Biodendrimer-based hydrogel scaffolds for cartilage tissue repair. *Biomacromolecules* 2006, 7, 310-316.
139. Elisseff, J.; Anseth, K.; Sims, D.; McIntosh, W.; Randolph, M.; Langer, R., Transdermal photopolymerization for minimally invasive implantation. *PNAS* 1999, 96, 3104-3107.
140. Bryant, S.; Nuttelman, C.; Anseth, K., Cytocompatibility of UV and visible light photoinitiating systems on cultured NIH/3T3 fibroblasts in vitro. *J. Biomater. Sci. Polym. Ed.* 2000, 11, 439-457.
141. Muggli, D. S.; Burkoth, A. K.; Keyser, S. A.; Lee, H. R.; Anseth, K. S., Reaction behavior of biodegradable, photo-cross-linkable polyanhydrides. *Macromolecules* 1998, 31, 4120-4125.
142. Rydholm, A. E.; Bowman, C. N.; Anseth, K. S., Degradable thiol-acrylate photopolymers: polymerization and degradation behavior of an in situ forming biomaterial. *Biomaterials* 2005, 26, 4495-4506.
143. Burdick, J. A.; Peterson, A. J.; Anseth, K. S., Conversion and temperature profiles during the photoinitiated polymerization of thick orthopaedic biomaterials. *Biomaterials* 2001, 22, 1779-1786.

144. Bryant, S. J.; Bender, R. J.; Durand, K. L.; Anseth, K. S., Encapsulating Chondrocytes in degrading PEG hydrogels with high modulus: Engineering gel structural changes to facilitate cartilaginous tissue production. *Biotechnol. Bioeng.* 2004, 86, 747-755.
145. Elisseeff, J.; Anseth, K. S.; Sims, D.; McIntosh, W.; Randolph, M.; Yaremchuk, M.; Langer, R., Transdermal photopolymerization of poly(ethylene oxide)-based injectable hydrogels for tissue-engineered cartilage. *Plast. Reconstr. Surg.* 1999, 104, 1014-1022.
146. Kasper, F. K.; Seidlits, S. K.; Tang, A.; Crowther, R. S.; Carney, D. H.; Barry, M. A.; Mikos, A. G., In vitro release of plasmid DNA from oligo(poly(ethylene glycol) fumarate) hydrogels. *J. Controlled Release* 2005, 104, 521-539.
147. Oudshoorn, M. H. M.; Rissmann, R.; Bouwstra, J. A.; Hennink, W. E., Synthesis and characterization of hyperbranched polyglycerol hydrogels. *Biomaterials* 2006, 27, 5471-5479.
148. Temenoff, J. S.; Park, H.; Jabbari, E.; Conway, D. E.; Sheffield, T. L.; Ambrose, C. G.; Mikos, A. G., Thermally cross-linked oligo(poly(ethylene glycol) fumarate) hydrogels support osteogenic differentiation of encapsulated marrow stromal cells in vitro. *Biomacromolecules* 2004, 5, 5-10.
149. vanDijkWolthuis, W. N. E.; Tsang, S. K. Y.; KettenesvandenBosch, J. J.; Hennink, W. E., A new class of polymerizable dextrans with hydrolyzable groups: hydroxyethyl methacrylated dextran with and without oligolactate spacer. *Polymer* 1997, 38, 6235-6242.
150. Kasper, F. K.; Jerkins, E.; Tanahashi, K.; Barry, M. A.; Tabata, Y.; Mikos, A. G., Characterization of DNA release from composites of oligo(poly(ethylene glycol) fumarate) and cationized gelatin microspheres in vitro. *J. Biomed. Mater. Res.* 2006, 78A, 823-835.
151. Metters, A.; Hubbell, J., Network formation and degradation behavior of hydrogels formed by Michael-type addition reactions. *Biomacromolecules* 2005, 6, 290-301.
152. van de Wetering, P.; Metters, A. T.; Schoenmakers, R. G.; Hubbell, J. A., Poly(ethylene glycol) hydrogels formed by conjugate addition with controllable swelling, degradation, and release of pharmaceutically active proteins. *J. Controlled Release* 2005, 102, 619-627.

153. Rizzi, S. C.; Hubbell, J. A., Recombinant protein-co-PEG networks as cell-adhesive and proteolytically degradable hydrogel matrixes. Part 1: Development and physicochemical characteristics. *Biomacromolecules* 2005, 6, (3), 1226-1238.
154. Seliktar, D.; Zisch, A. H.; Lutolf, M. P.; Wrana, J. L.; Hubbell, J. A., MMP-2 sensitive, VEGF-bearing bioactive hydrogels for promotion of vascular healing. *J. Biomed. Mater. Res.* 2004, 68A, 704-716.
155. Raeber, G. P.; Lutolf, M. P.; Hubbell, J. A., Molecularly engineered PEG hydrogels: A novel model system for proteolytically mediated cell migration. *Biophys. J.* 2005, 89, 1374-1388.
156. DuBose, J.; Cutshall, C.; Metters, A., Controlled release of tethered molecules via engineered hydrogel degradation: Model development and validation. *J. Biomed. Mater. Res.* 2005, 74A, 104-116.
157. Cai, S. S.; Liu, Y. C.; Shu, X. Z.; Prestwich, G. D., Injectable glycosaminoglycan hydrogels for controlled release of human basic fibroblast growth factor. *Biomaterials* 2005, 26, 6054-6067.
158. Shu, X. Z.; Ghosh, K.; Liu, Y. C.; Palumbo, F. S.; Luo, Y.; Clark, R. A.; Prestwich, G. D., Attachment and spreading of fibroblasts on an RGD peptide-modified injectable hyaluronan hydrogel. *J. Biomed. Mater. Res.* 2004, 68A, 365-375.
159. Kunath, K.; Merdan, T.; Hegener, O.; Haberlein, H.; Kissel, T., Integrin targeting using RGD-PEI conjugates for in vitro gene transfer. *J. Gene. Med.* 2003, 5, 588-599.
160. Sagara, K.; Kim, S. W., A new synthesis of galactose-poly(ethylene glycol)-polyethylenimine for gene delivery to hepatocytes. *J. Controlled Release* 2002, 79, 271-281.
161. Elbert, D. L.; Pratt, A. B.; Lutolf, M. P.; Halstenberg, S.; Hubbell, J. A., Protein delivery from materials formed by self-selective conjugate addition reactions. *J. Controlled Release* 2001, 76, 11-25.
162. Hubbell, J. A., Bioactive biomaterials. *Curr. Opin. Biotech.* 1999, 10, 123-129.
163. Shu, X. Z.; Liu, Y. C.; Palumbo, F. S.; Lu, Y.; Prestwich, G. D., In situ crosslinkable hyaluronan hydrogels for tissue engineering. *Biomaterials* 2004, 25, 1339-1348.

164. Peattie, R. A.; Rieke, E. R.; Hewett, E. M.; Fisher, R. J.; Shu, X. Z.; Prestwich, G. D., Dual growth factor-induced angiogenesis in vivo using hyaluronan hydrogel implants. *Biomaterials* 2006, 27, 1868-1875.
165. Balakrishnan, B.; Jayakrishnan, A., Self-cross-linking biopolymers as injectable in situ forming biodegradable scaffolds. *Biomaterials* 2005, 26, 3941-3951.
166. Yoshida, T.; Aoyagi, T.; Kokufuta, E.; Okano, T., Newly designed hydrogel with both sensitive thermoresponse and biodegradability. *J. Polym. Sci. Pol. Chem.* 2003, 41, 779-787.
167. Khandare, J.; Minko, T., Polymer-drug conjugates: Progress in polymeric prodrugs. *Prog. Polym. Sci.* 2006, 31, 359-397.
168. Roy, I.; Gupta, M. N., Smart polymeric materials: Emerging biochemical applications. *Chem. Biol.* 2003, 10, 1161-1171.
169. Qiu, Y.; Park, K., Environment-sensitive hydrogels for drug delivery. *Adv. Drug Deliv. Rev.* 2001, 53, 321-339.
170. Katono, H.; Maruyama, A.; Sanui, K.; Ogata, N.; Okano, T.; Sakurai, Y., Thermoresponsive swelling and drug release switching of interpenetrating polymer networks composed of poly(acrylamide-co-butyl methacrylate) and poly(acrylic acid). *J. Controlled Release* 1991, 16, 215-227.
171. Gutowska, A.; Bae, Y. H.; Feijen, J.; Kim, S. W., Heparin release from thermosensitive hydrogels. *J. Controlled Release* 1992, 22, 95-104.
172. Gutowska, A.; Bark, J. S.; Kwon, I. C.; Bae, Y. H.; Cha, Y.; Kim, S. W., Squeezing hydrogels for controlled oral drug delivery. *J. Controlled Release* 1997, 48, 141-148.
173. Gemeinhart, R. A.; Chen, J.; Park, H.; Park, K., pH-sensitivity of fast responsive superporous hydrogels. *J. Biomater. Sci.-Polym. Ed.* 2000, 11, 1371-1380.
174. Zhang, R.; Tang, M.; Bowyer, A.; Eisenthal, R.; Hubble, J., Synthesis and characterization of a D-glucose sensitive hydrogel based on CM-dextran and concanavalin A. *React. Funct. Polym.* 2006, 66, 757-767.
175. Kim, B. S.; Mooney, D. J., Development of biocompatible synthetic extracellular matrices for tissue engineering. *Trends Biotechnol.* 1998, 16, 224-230.
176. Brandl, F.; Sommer, F.; Goepferich, A., Rational design of hydrogels for tissue engineering: Impact of physical factors on cell behavior. *Biomaterials* 2007, 28, 134-146.

177. Genes, N. G.; Rowley, J. A.; Mooney, D. J.; Bonassar, L. J., Effect of substrate mechanics on chondrocyte adhesion to modified alginate surfaces. *Arch. Biochem. Biophys.* 2004, 422, 161-167.
178. Drury, J.; Mooney, D., Hydrogels for tissue engineering: scaffold design variables and applications. *Biomaterials* 2003, 24, 4337-4351.
179. Mann, B. K.; Schmedlen, R. H.; West, J. L., Tethered-TGF-beta increases extracellular matrix production of vascular smooth muscle cells. *Biomaterials* 2001, 22, 439-444.
180. Hern, D. L.; Hubbell, J. A., Incorporation of adhesion peptides into nonadhesive hydrogels useful for tissue resurfacing. *J. Biomed. Mater. Res.* 1998, 39, 266-276.
181. Schense, J. C.; Hubbell, J. A., Cross-linking exogenous bifunctional peptides into fibrin gels with factor XIIIa. *Bioconjugate Chem.* 1999, 10, 75-81.
182. Gobin, A. S.; West, J. L., Val-ala-pro-gly, an elastin-derived non-integrin ligand: Smooth muscle cell adhesion and specificity. *J. Biomed. Mater. Res.* 2003, 67A, 255-259.
183. Hahn, M. S.; Taite, L. J.; Moon, J. J.; Rowland, M. C.; Ruffino, K. A.; West, J. L., Photolithographic patterning of polyethylene glycol hydrogels. *Biomaterials* 2006, 27, 2519-2524.
184. DeLong, S. A.; Moon, J. J.; West, J. L., Covalently immobilized gradients of bFGF on hydrogel scaffolds for directed cell migration. *Biomaterials* 2005, 26, 3227-3234.
185. Zisch, A. H.; Schenk, U.; Schense, J. C.; Sakiyama-Elbert, S. E.; Hubbell, J. A., Covalently conjugated VEGF-fibrin matrices for endothelialization. *J. Controlled Release* 2001, 72, 101-113.
186. Babensee, J.; McIntire, L.; Mikos, A., Growth Factor Delivery for Tissue Engineering. *Pharm. Res.* 2000, 17, 497-504.
187. Tanihara, M.; Suzuki, Y.; Yamamoto, E.; Noguchi, A.; Mizushima, Y., Sustained release of basic fibroblast growth factor and angiogenesis in a novel covalently crosslinked gel of heparin and alginate. *J. Biomed. Mater. Res.* 2001, 56, 216-221.
188. Kimura, Y.; Ozeki, M.; Inamoto, T.; Tabata, Y., Time course of de novo adipogenesis in Matrigel by gelatin microspheres incorporating basic fibroblast growth factor. *Tissue Eng.* 2002, 8, 603-613.

189. Li, S.; Vert, M., Synthesis, characterization, and stereocomplexation-induced gelation of block copolymers prepared by ring-opening polymerization of L(D)-lactide in the presence of poly(ethylene glycol). *Macromolecules* 2003, 36, 8008-8014.
190. Bos, G. W.; Jacobs, J. J. L.; Koten, J. W.; Van Tomme, S. R.; Veldhuis, T. F. J.; van Nostrum, C. F.; Den Otter, W.; Hennink, W. E., In situ crosslinked biodegradable hydrogels loaded with IL-2 are effective tools for local IL-2 therapy. *Eur. J. Pharm. Sci.* 2004, 21, 561-567.
191. Cadee, J. A.; de Groot, C. J.; Jiskoot, W.; den Otter, W.; Hennink, W. E., Release of recombinant human interleukin-2 from dextran-based hydrogels. *J. Controlled Release* 2002, 78, 1-13.
192. Zhang, Y. L.; Chu, C. C., Biodegradable dextran-poly(lactide) hydrogel network and its controlled release of albumin. *J. Biomed. Mater. Res.* 2001, 54, 1-11.
193. Bulpitt, P.; Aeschlimann, D., New strategy for chemical modification of hyaluronic acid: Preparation of functionalized derivatives and their use in the formation of novel biocompatible hydrogels. *J. Biomed. Mater. Res.* 1999, 47, 152-169.
194. Hovgaard, L.; Brondsted, H., Evaluation of biodegradable hydrogels for colon-specific drug delivery. *Macromol. Symp.* 1997, 123, 189-194.

Chapter 3

Stereocomplex mediated gelation of PLA-PEG-PLA and PEG-(PLA)₈ block copolymers¹

*Christine Hiemstra, Zhiyuan Zhong, Pieter J. Dijkstra, and Jan Feijen**

Department of Polymer Chemistry and Biomaterials, Faculty of Science and Technology, Institute for Biomedical Technology, University of Twente, P. O. Box 217, 7500 AE Enschede, The Netherlands

3.1 Abstract

Stereocomplex mediated hydrogels have been prepared by mixing solutions of polymers of opposite chirality of either PLA-PEG-PLA triblock copolymers or PEG-(PLA)₈ star block copolymers. The critical gel concentrations of the mixed enantiomer solutions were considerably lower compared to polymer solutions containing only the single enantiomer. Moreover, gel-sol transition temperatures were increased and gel regions were expanded due to stereocomplexation. Rheology measurements showed that stereocomplexed hydrogels based on PEG-(PLA)₈ have higher storage moduli compared to those based on PLA-PEG-PLA. Stereocomplexed hydrogels prepared from 13 w/v% PLA-PEG-PLA solutions in PBS showed a storage modulus of 0.9 kPa at 37 °C, while at similar conditions stereocomplexed hydrogels of PEG-(PLA)₈ showed a storage modulus of 1.9 kPa at 10 w/v%.

3.2 Introduction

Hydrogels are highly attractive materials for use in biomedical applications, such as tissue engineering and drug delivery, since they possess good biocompatibility due to their

¹ This chapter has been published in *Macromolecular Symposia*, 2005, 224, 119-131.

high hydrophilicity. Block copolymers of PEG and aliphatic polyesters are of interest in this respect, since PEG is known to have excellent antifouling properties and biocompatibility and is excreted by the kidney at molecular weights up to approximately 30,000.¹ Aliphatic polyesters such as poly(lactide) (PLA) and poly(lactide-*co*-glycolide) (PLGA) are known to be biocompatible and are biodegradable. Block copolymers of PEG and PLA or PLGA form physically crosslinked hydrogels at relatively high concentrations and show a gel to sol transition close to body temperature.^{2,3} Recently, several research groups have shown that hydrogels can be prepared from water-soluble PDLA and PLLA based block copolymers, in which the physical crosslinks are provided by stereocomplexation between the enantiomeric PDLA and PLLA blocks. Examples of such physically crosslinked hydrogels include dextran-lactate hydrogels⁴ and hydrogels based on PEG-PLA triblock copolymers with either a central PEG⁵⁻⁷ or PLA⁸ block. Recently, Li et al. showed that upon mixing 15 w/v% polymer solutions containing equimolar amounts of PDLA₂₀-PEG8000-PDLA₂₀ and PLLA₁₈-PEG8000-PLLA₁₈ a turbid hydrogel was obtained up to at least 37 °C.⁶ This gel has storage moduli of 1.1 kPa and ~0.2 kPa at 20 and 37 °C, respectively. The formation of stereocomplexes within the hydrogels was confirmed by Raman spectroscopy on the hydrogels and X-ray on the lyophilized hydrogels. Fujiwara et al. prepared PDLA₁₅-PEG4600-PDLA₁₅ and PLLA₁₈-PEG4600-PLLA₁₈ block copolymers and showed that gelation occurred after mixing 10 w/v% polymer solutions containing equimolar amounts of both enantiomers and heating to 37 °C.⁷ They ascribed the gelation at 37 °C to weakening of the hydrophobic PLA core at increased temperature, which allows mixing of D- and L-enantiomeric blocks. This gel has a storage modulus of ~1 kPa between 37 and 70 °C. WAXS experiments confirmed the presence of the stereocomplexes within the hydrogel at 37 °C and also at 75 °C. Mukose et al. prepared hydrogels by mixing 35 w/v% aqueous solutions containing equimolar amounts of PEG2000-PDLA₂₈-PEG2000 and PEG2000-PLLA₂₈-PEG2000, and heating the mixed solution to 37 °C.⁸ Gelation was thought to be due to the complementary helix formation of the PEG chains induced by the complementary PDLA and PLLA helices. This gel has a relatively high storage modulus of 31 kPa, which was attributed to the high polymer concentration. The stereocomplexed PEG-PLA hydrogels may be useful materials for biomedical applications, such as drug delivery and tissue engineering. Regarding PEG-

PLA block copolymer systems with PLA end blocks, materials with improved mechanical properties are of interest. In this paper we describe the synthesis, characterization and hydrogel formation of PLA-PEG-PLA triblock and PEG-(PLA)₈ star block copolymers and the effect of the number of stereocomplex interaction sites on the gelation behavior.

3.3 Materials and methods

Materials. D-lactide and L-lactide were obtained from Purac and recrystallised from dry toluene. Dihydroxyl PEG ($M_{n, NMR} = 12500$, denoted as PEG12500) and eight-arm star PEG ($M_{n, NMR} = 21800$, denoted as PEG21800) were supplied by Fluka and Nektar, respectively, and were dried by azeotropic distillation from toluene. Stannous octoate (tin(II) bis(2-ethylhexanoate), Sn(Oct)₂, was purchased from Sigma and used as received. The single site Zn-complex catalyst Zn(Et)[SC₆H₄(CH(Me)NC₅H₁₀)-2] was kindly provided by Professor G. van Koten of the University of Utrecht (The Netherlands).

Synthesis. All reactions were performed using Schlenck techniques. PLA-PEG-PLA block copolymers were prepared by the Sn(Oct)₂ catalyzed ring opening polymerization of D- or L-lactide initiated by hydroxyl groups of PEG21500 at 105 °C in toluene for 4 h under an argon atmosphere. In a typical experiment PEG12500 (2.490 g, 0.199 mmol) and lactide (0.510 g, 3.54 mmol) were dissolved in 7.1 ml of toluene at 105 °C (monomer concentration is 0.5 M). To this solution 1 drop of Sn(Oct)₂ was added and the polymerization mixture was stirred for 4 h. The polymerization was terminated by the addition of a small amount of glacial acetic acid under stirring. The solution was concentrated under reduced pressure and the polymer was precipitated in a mixture of cold diethyl ether/methanol (20/1 v/v). After filtration, the polymer was dried under reduced pressure for 2 days at room temperature. Conversion: 89%, yield: 75%. ¹H NMR (CDCl₃): 1.5 (m, CH₃CH), 1.4 (m, CH₃CHOH end group PLA), 3.6 (m, CH₂O), 4.2-4.3 (m, CH₂CO, linking unit PEG), 4.3-4.4 (q, CHOH end group PLA), (m, CHCO)

PEG-(PLA)₈ star block copolymers were prepared similarly at room temperature in dichloromethane for 4 h using the single site Zn-complex catalyst Zn(Et)[SC₆H₄(CH(Me)NC₅H₁₀)-2]. In a typical experiment PEG21800 (0.730 g, 0.0335 mmol) and lactide (0.270 g, 1.88 mmol) were dissolved in 7.5 ml of dichloromethane at

room temperature (monomer concentration is 0.25 M). To this solution, a solution of single site Zn-complex catalyst (0.040 g, 0.134 mmol) in 1 ml of dichloromethane was added and the reaction mixture was stirred for 4 h (molar ratio of hydroxyl groups of PEG21800 to Zn-complex catalyst is 2 : 1). Termination, precipitation and drying methods were similar to those used for the PLA-PEG-PLA block copolymers, as described above. Conversion: 98%, yield: 89%. $^1\text{H NMR}$ (CDCl_3): 1.5 (m, CH_3CH), 1.4 (m, CH_3CHOH end group PLA), 3.6 (m, CH_2O), 4.2-4.3 (m, CH_2CO , linking unit PEG), 4.3-4.4 (q, CHOH end group PLA), (m, CHCO)

Characterization. $^1\text{H NMR}$ spectra (CDCl_3) were recorded on a Varian Inova Spectrometer (Varian, Palo, Alto, USA) operating at 300 MHz. The number of lactyl units per PLA block were calculated rationing the respective areas of the peaks corresponding to the methyl group of lactyl units at δ 1.5 and the methylene groups of PEG at δ 3.6.

Differential Scanning Calorimetry (DSC) measurements were performed using a DSC7 (Perkin-Elmer). The polymer was first heated from 30 to 200 °C, kept at 200 °C for 2 min, quenched to 30 °C, kept at 30 °C for 2 min and heated to 200 °C. Heating and cooling rate were always 20 °C /min. The second heating curve was used for thermal analysis.

For the determination of gel-sol transitions, aqueous polymer solutions were prepared by dissolving the appropriate amount of polymer in distilled water at room temperature. Solutions containing equimolar amounts of enantiomeric block copolymers were prepared by mixing polymer solutions and vigorously stirring for ~2 min. For both single enantiomer solutions and polymer solutions containing both D- and L-enantiomer, temperature dependent phase behavior was studied using the vial tilting method at temperatures between 5 and 70 °C with intervals of 2 °C. At each temperature, the samples were allowed to equilibrate for at least 10 min. No flow within 20 s while inverting the vial was regarded as a gel state.

Rheology experiments were performed on a US 200 Rheometer (Anton Paar). Aqueous polymer solutions of PDLA₁₅-PEG12500-PDLA₁₅, PLLA₁₅-PEG12500-PLLA₁₅, PEG21800-(PDLA₁₄)₈ and PEG21800-(PLLA₁₄)₈ were prepared by dissolving the appropriate amount of polymer in distilled water or PBS at room temperature. Polymer solutions containing equimolar amounts of D- and L-enantiomer of PLA₁₅-PEG12500-PLA₁₅ or PEG21800-(PLA₁₄)₈ at a concentration of 13 w/v% and 10 w/v%, respectively,

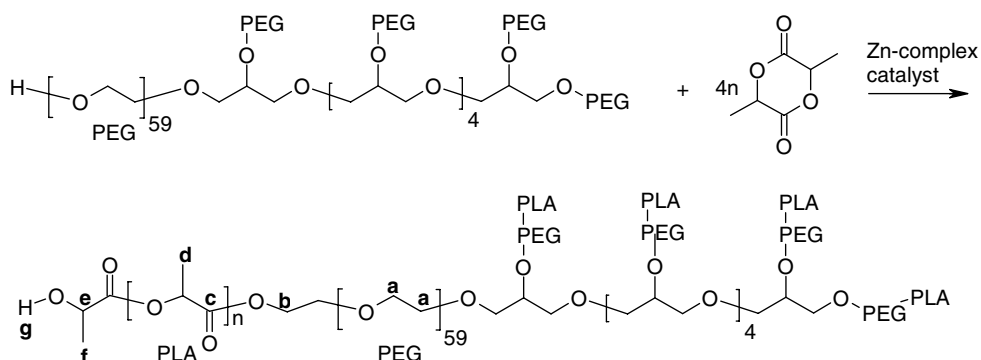
were mixed, homogenized and quickly applied to the rheometer. A flat plate measuring geometry was used (25 mm diameter, gap 0.5 mm). To prevent the evaporation of water, a layer of oil was put around the polymer sample. Gelation of the polymer solutions was monitored by measuring the shear storage modulus G' as well as the loss modulus G'' at 20 °C or 37 °C for 48 h. A frequency ω of 1 Hz and a strain γ of 1% were applied to minimize the influence of the deformation on the formation of the hydrogels. This strain is within the linear viscoelastic range. After gelation, amplitude and frequency sweeps were performed at respectively $\gamma = 0.01$ -10% ($\omega = 1$ Hz) and $\omega = 0.01$ -10 Hz ($\gamma = 1\%$). Subsequently, the temperature was increased to 60 °C at 1.4 °C/min or 1 °C/min ($\omega = 1$ Hz, $\gamma = 1\%$).

3.4 Results and discussion

3.4.1 Synthesis and characterization

A convenient way to prepare PEG-PLA block copolymers is the $\text{Sn}(\text{Oct})_2$ catalyzed ring opening polymerization of lactide initiated by hydroxyl end groups of PEG12500 in toluene at 105 °C.⁹ The ^1H NMR spectra of the synthesized PLA-PEG-PLA triblock copolymers revealed that all PEG hydroxyl groups initiated the ring opening polymerization and that the polymers have a well-defined block copolymer structure. The obtained PLA blocks lengths calculated from the ^1H NMR spectra are close to the theoretical values (Table 1).

PEG-(PLA)₈ star block copolymers were analogously prepared by ring opening polymerization of L- or D-lactide in the presence of star PEG21800 and the single site Zn-complex catalyst $\text{Zn}(\text{Et})[\text{SC}_6\text{H}_4(\text{CH}(\text{Me})\text{NC}_5\text{H}_{10})_2]$ in dichloromethane at room temperature for 4 h (Scheme 1).



Scheme 1. Ring opening polymerization of lactide initiated by eight-arm star PEG21800.

The advantage of the use of a single site Zn-complex catalyst is the prevention of gelation of the reaction mixture. The ^1H NMR spectra of the reaction mixtures revealed high monomer conversions (>97%) (Table 1). A typical ^1H NMR spectrum of purified PEG21800-(PLA₁₄)₈ is shown in Figure 1. Signals at δ 2.7 and 4.3-4.4 are assigned to hydroxyl end groups and methine end groups of PLA, respectively. The chemical shift of the hydroxyl end groups was confirmed by the addition of trifluoroacetic anhydride, since the signal at δ 2.7 disappeared completely and the methine protons were shifted to δ 5.3. A peak corresponding to methylene end groups of PEG linked to a trifluoroacetyl group was not observed, indicating that all hydroxyl groups of PEG initiated the ring opening polymerization of lactide. Furthermore, the block copolymer structure is confirmed by the presence of a quartet at δ 4.2-4.3, corresponding to the methylene protons of PEG connected to the PLA blocks. The average block length of the PLA blocks was calculated from the ^1H NMR spectra of the block copolymers by rationing the respective areas of the peaks corresponding to the methyl group of lactyl units and the methylene groups of PEG. As shown in Table 1 the obtained PLA block lengths are close to the theoretical values based on the feed composition and conversion. In conclusion, well-defined PEG-(PLA)₈ star block copolymers of desired molecular weights could be prepared by the Zn-complex catalyzed ring opening polymerization of lactide.

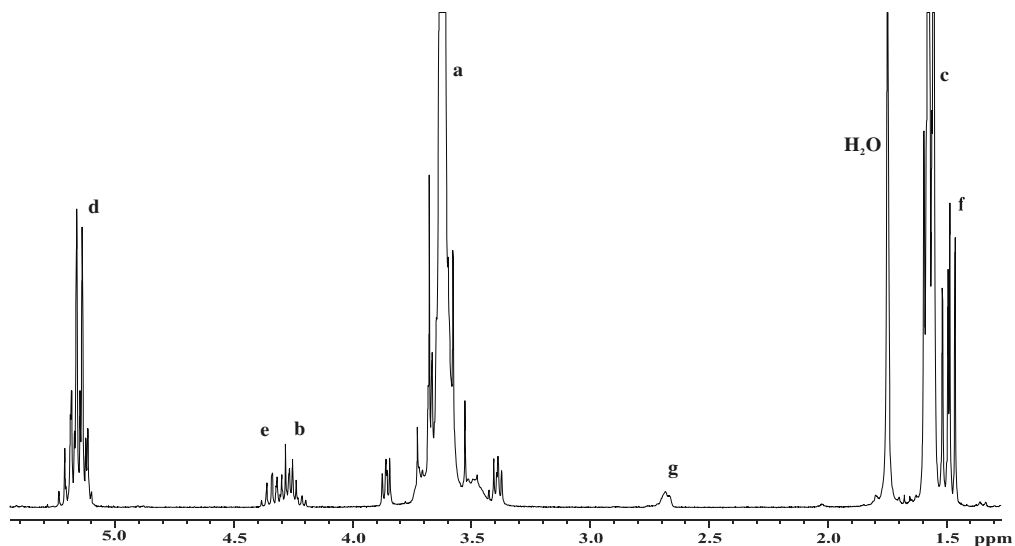


Figure 1: ^1H NMR (CDCl_3) spectrum of PEG21800-(PLA₁₄)₈ star block copolymer.

Table 1. Composition and molecular weight of PLA-PEG12500-PLA and PEG21800-(PLA)₈ block copolymers.

Polymer	Conversion (%)	$N_{\text{LA}}^{\text{a)}$		M_n	PEG content (wt%)
		Theory ^{b)}	Found ^{c)}		
PDLA-PEG12500-PDLA	83	10	10	14000	90
	89	16	15	14700	85
	88	20	19	15200	82
PLLA-PEG12500-PLLA	88	9	10	13900	90
	86	16	15	14700	85
	90	20	19	15300	82
PEG21800-(PDLA) ₈	98	14	14	29800	74
PEG21800-(PLLA) ₈	98	14	14	29500	74

^{a)} Number of lactyl units per PLA block. ^{b)} Based on feed composition and conversion. ^{c)} Calculated from ^1H NMR integral ratios.

Differential Scanning Calorimetry thermograms of both triblock and star block copolymers in the solid state showed a single melting endotherm in between 40 and 60 °C due to melting of the PEG crystals. The absence of a melting endotherm at higher temperatures revealed that the PLA blocks are in the amorphous state. This is regarded beneficial, since crystallization of PLA blocks is expected to decrease the water solubility of the PEG-PLA block copolymer and also may hamper stereocomplex formation.

3.4.2 Solubility

The solubility of PLA-PEG12500-PLA block copolymers in distilled water at room temperature was found to decrease rapidly upon increasing the PLA block length. When the number of lactyl units per PLA block was higher than 22, the copolymer was not water-soluble anymore at or above a polymer concentration of 10 w/v%. This result agrees well with that found by Vert et al. for similar PLA-PEG-PLA triblock copolymers.⁶

3.4.3 Gelation behavior

The influence of stereocomplexation on the gelation behavior of aqueous solutions containing equimolar amounts of PDLA-PEG12500-PDLA and PLLA-PEG12500-PLLA polymers was studied at room temperature. Aqueous solutions of the block copolymers with similar PLA blocks lengths were mixed and after at least 1 day of equilibration the occurrence of a gel phase was tested by the vial tilting method. All triblock copolymers studied showed gelation upon mixing of both enantiomer solutions, while the single enantiomer solutions did not form a gel at similar concentrations. The gelation upon mixing solutions of polymers of opposite chirality is illustrated for 10 w/v% solutions of PLA₁₅-PEG12500-PLA₁₅ in Figure 2. The critical gel concentration (CGC) at room temperature was found to decrease sharply upon increasing the PLA block length from 10 to 15 lactyl units, while a further increase to 19 lactyl units only caused a minor decrease in CGC (Table 2). It should be noted that enantiomeric triblock copolymers also afford hydrogels at relatively high concentrations at room temperature (Table 2). Considering biomedical applications, like the engineering of soft tissues or drug delivery systems, it is

desirable that the cells or molecules to be incorporated may be suspended into these single enantiomer solutions, which upon mixing and stereocomplexation form a hydrogel.



Figure 2. PDLA₁₅-PEG12500-PDLA₁₅ 13 w/v% solution (D) and PDLA₁₅-PEG12500-PDLA₁₅ + PLLA₁₅-PEG12500-PLLA₁₅ 13 w/v% hydrogel (D+L) at room temperature.

It is well known that upon increasing the hydrophobic block length the CGC is decreased, due to an increase in micelle number and size.^{10,11} In addition, BAB type of polymers, where B and A are hydrophobic and hydrophilic blocks, respectively, show increased intermolecular and intermicellar association upon increasing hydrophobic block length.¹²⁻¹⁴ The gelation upon mixing of aqueous solutions of PLA-PEG12500-PLA polymers of opposite chirality is driven by the stereocomplexation of the PDLA and PLLA blocks, as their precursor single enantiomer solutions stayed fluid-like. Stereocomplexation enhances interactions between the hydrophobic blocks and lowers the CGC, like when increasing PLA block length. The lowering in CGC may be due to similar changes in micelle number, size and association as observed when increasing PLA block length. The decrease in CGC may also be due to an increase in crystallinity or chain packing tendency of the hydrophobic block, as has been proposed by Jeong et al. when comparing PEG-PLLA and PEG-PDLLA diblock copolymers.¹⁵ Eleven lactyl units have been reported to be required for gelation by stereocomplexation.¹⁶ Therefore, the stereocomplexation at 10 lactyl units may not be very efficient. Due to the polydispersity of the PLA blocks, some blocks may be long enough for stereocomplexation, while shorter blocks may only interact weakly.¹⁷ The reduced stereocomplexation at 10 lactyl units may explain the sharp decrease in CGC when going from 10 to 15 lactyl units. The relatively small decrease in CGC when the number of lactyl units is increased from 15 to 19 per PLA block may be the result of a decrease in stereocomplexation efficiency, due to an increased density of the

PLA core and a decrease in water solubility as the PLA block length increases, which hamper mixing of D- and L-enantiomer blocks and stereocomplexation.

Table 2. Critical gel concentrations of PEG-PLA block copolymers in distilled water at room temperature.

Polymer	Critical gel concentration (w/v%)	
	Single enantiomer	Mixed enantiomers
PLA ₁₀ -PEG12500-PLA ₁₀	80	30
PLA ₁₅ -PEG12500-PLA ₁₅	15	10
PLA ₁₉ -PEG12500-PLA ₁₉	10	7.5
PEG21800-(PLA ₁₄) ₈	15	5

The PEG21800-(PLA₁₄)₈ star block copolymer also showed stereocomplex mediated gelation. The stereocomplexed hydrogel was formed at a relatively low CGC, which is attributed to the lower PEG content of 74 w/v% and increased stereocomplex interaction sites compared to the PLA-PEG12500-PLA polymers (Table 1).

Temperature dependent phase behavior of PLA₁₅-PEG12500-PLA₁₅ and PEG21800-(PLA₁₄)₈ block copolymer hydrogels was studied by the vial tilting method in a temperature range of 5-70 °C. Figure 3 shows that upon increasing temperature both single enantiomer and stereocomplexed hydrogels of PLA₁₅-PEG12500-PLA₁₅ and PEG21800-(PLA₁₄)₈ polymers may turn into a mobile phase, which is denoted as the sol-phase. In contrast to PLA₁₅-PEG12500-PLA₁₅ hydrogels, which formed a clear fluid phase, PEG21800-(PLA₁₄)₈ hydrogels exhibited phase separation, resulting in a clear fluid and a viscous opaque phase, caused by dehydration of the PEG chains. The different phase behavior is probably due to the lower PEG content of the PEG21800-(PLA₁₄)₈ polymer. The gel-sol transition temperatures of PLA₁₅-PEG12500-PLA₁₅ and PEG21800-(PLA₁₄)₈ single enantiomer hydrogels are very similar, which indicates that hydrogel gel to sol transition temperature depends predominantly on the PLA block length. Stereocomplexed hydrogels of PLA₁₅-PEG12500-PLA₁₅ and PEG21800-(PLA₁₄)₈ showed the same trend.

PLA₁₅-PEG12500-PLA₁₅ and PEG21800-(PLA₁₄)₈ hydrogels containing equimolar amounts of D- and L-enantiomers show gel-sol transitions that are shifted to much higher temperatures and the gel regions are expanded compared to the single enantiomer hydrogels at equal concentrations. The increased gel to sol transition temperatures of the stereocomplexed hydrogels is attributed to the stereocomplex formation and may be explained by factors that are also responsible for the lowering of the CGC.

- PLA₁₅-PEG12500-PLA₁₅ L
- PLA₁₅-PEG12500-PLA₁₅ D+L
- ▲ PEG21800-(PLA₁₄)₈ L
- △ PEG21800-(PLA₁₄)₈ D+L

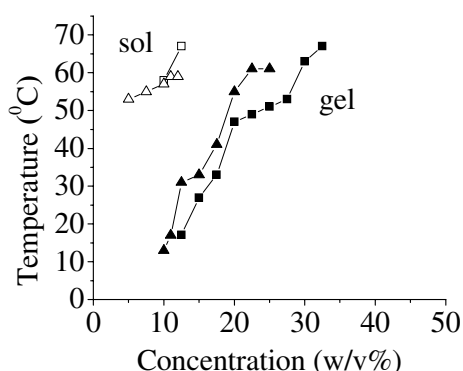


Figure 3. Gel-sol diagram of hydrogels from PLA₁₅-PEG12500-PLA₁₅ or PEG21800-(PLA₁₄)₈ block copolymers containing either single enantiomer or both D- and L-enantiomer in equimolar amounts.

The gel-sol transition which occurs upon increasing temperature of amphiphilic PEG block copolymers has been proposed to be due to the disruption of the micelle packing structure, due to a decrease in effective diameter of the micelles as a result of partial PEG dehydration.¹⁰ Li et al. have suggested for stereocomplexed PLA-PEG-PLA hydrogels that the gel-sol transition upon increasing temperature is due to a decrease in the number of stereocomplex crosslinks, caused by a shift in the equilibrium from stereocomplexation to simple D/L interactions in the amorphous state that contribute less to crosslinking.⁶

However, Fujiwara et al. have shown by WAXS measurements on stereocomplexed hydrogels that stereocomplexes are present up to at least 75 °C.⁷

3.4.4 Rheology

To confirm the stereocomplex mediated hydrogel formation and to gain insight in hydrogel properties, oscillatory rheology experiments were performed on polymer solutions containing equimolar amounts of D- and L-enantiomer of PLA₁₅-PEG12500-PLA₁₅ or PEG21800-(PLA₁₄)₈. Gel formation kinetics were studied by monitoring the storage modulus (G') and loss modulus (G'') in time (Figure 4a) for 48 h after mixing polymer solutions of opposite chirality.

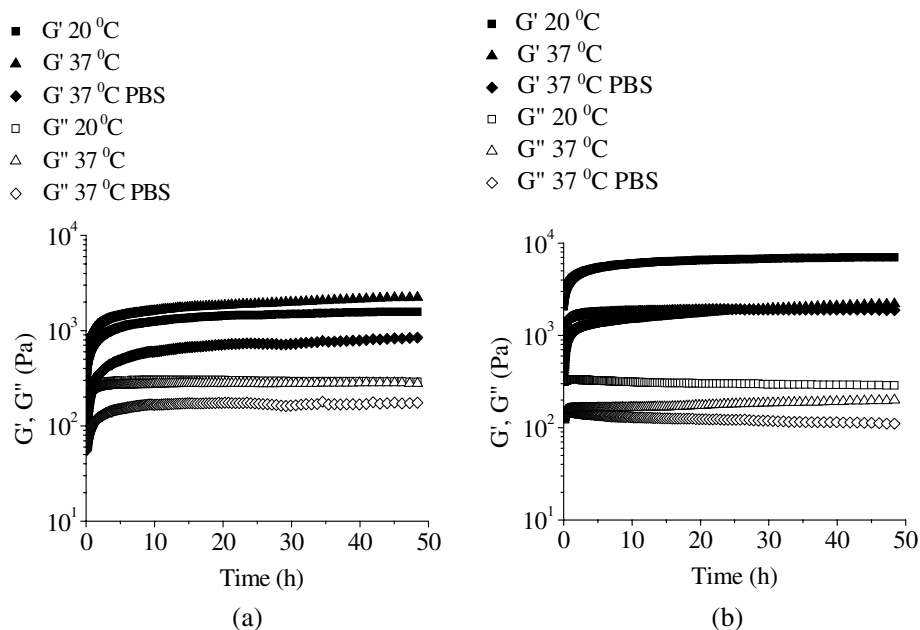


Figure 4. Storage modulus (G') and loss modulus (G'') evolutions after mixing enantiomer solutions in water or PBS at 20 °C or 37 °C containing either PLA₁₅-PEG12500-PLA₁₅ 13 w/v% (a) or PEG21800-(PLA₁₄)₈ 10 w/v% (b) as a function of time.

To study the influence of the gelation temperature and the solvent, PLA₁₅-PEG12500-PLA₁₅ and PEG21800-(PLA₁₄)₈ stereocomplexed hydrogels containing 13 w/v% and 10

w/v% of polymer, respectively, were prepared in water at 20 and 37 °C or in PBS at 37 °C. As shown in Figure 4a, the storage moduli of PLA₁₅-PEG12500-PLA₁₅ hydrogels increase rapidly during the first 10 h and finally level off at approximately 48 h, after which gelation is complete. The storage and loss moduli are listed in Table 3. The crossing of the storage and loss modulus, which is close to the gel point^{18,19}, was not observed, showing that the gel is formed almost instantaneously upon mixing of D- and L- enantiomer solutions. Interestingly, PLA₁₅-PEG12500-PLA₁₅ hydrogels showed a somewhat higher storage modulus when the hydrogel was prepared in water at 37 °C (2.2 kPa) compared to the hydrogel prepared in water at 20 °C (1.6 kPa). This may be due the increased kinetics and/or an increased aggregation tendency at 37 °C, resulting in an increase in stereocomplex interactions between PDLA and PLLA blocks. The PLA₁₅-PEG12500-PLA₁₅ hydrogel could also be formed upon mixing of polymer solutions containing equimolar amounts of D- and L-enantiomer in PBS. For biomedical applications PBS can be used as a solvent, since it has similar osmolarity as most body fluids. The storage modulus of the hydrogel prepared in PBS (0.9 kPa) is lower compared to the hydrogel in water, which is attributed to the reduction in the effective hard sphere volume of the micelles in the salt solution, which is a poorer solvent.²⁰⁻²² Storage moduli found for the PLA₁₅-PEG12500-PLA₁₅ hydrogels agree well with previously reported values on similar PLA-PEG-PLA hydrogels.^{6,7} As shown in Figure 4b the gelation of the mixed enantiomer solutions of PEG21800-(PLA₁₄)₈ reveals somewhat faster gelation kinetics as the PLA₁₅-PEG12500-PLA₁₅ hydrogels. Gelation occurred instantaneously upon mixing polymer solutions of opposite chirality and was completed within approximately 48 h. As summarized in Table 3, 10 w/v% PEG21800-(PLA₁₄)₈ hydrogels have higher storage moduli compared to the 13 w/v% PLA₁₅-PEG12500-PLA₁₅ hydrogels, which is attributed to the increased stereocomplex interaction sites of the PEG21800-(PLA₁₄)₈ polymer, causing an increase in crosslinking density. PBS has a negligible effect on the storage modulus of PEG21800-(PLA₁₄)₈ hydrogels, in contrast to PLA₁₅-PEG12500-PLA₁₅ hydrogels. The storage modulus of the PEG21800-(PLA₁₄)₈ hydrogels prepared in water at 37 °C (2.2 kPa) is considerably lowered compared to the hydrogels prepared in water at 20 °C (7.0 kPa), in contrast to the PLA₁₅-PEG12500-PLA₁₅ hydrogels. This difference may be due to the lower water solubility of the PEG21800-(PLA₁₄)₈, which is also seen by the

increased turbidity of the PEG21800-(PLA₁₄)₈ hydrogels with increasing temperature, while the PLA₁₅-PEG12500-PLA₁₅ hydrogels stayed clear. The lower solubility may cause formation of dense aggregates at 37 °C, which hamper mixing of D- and L-enantiomers and stereocomplexation. Though stereocomplexed PEG21800-(PLA₁₄)₈ hydrogels show higher storage moduli compared to PLA₁₅-PEG12500-PLA₁₅ hydrogels, the mechanical properties may be improved further to broaden the scope of biomedical applications. Stronger gels may be obtained by e.g. increasing block copolymer solubility, since higher concentrations have shown to give stronger hydrogels.²³

Table 3. Storage modulus (G') and loss modulus (G'') of PLA₁₅-PEG12500-PLA₁₅ and PEG21800-(PLA₁₄)₈ stereocomplexed hydrogels 48 h after mixing.

Polymer	Concentration (w/v%)	Preparation temperature (°C)	PBS/water	G' (Pa)	G'' (Pa)
PLA ₁₅ -PEG12500-PLA ₁₅	13	20	water	1580	290
	13	37	water	2230	230
	13	37	PBS	850	180
PEG21800-(PLA ₁₄) ₈	10	20	water	7040	290
	10	37	water	2200	200
	10	37	PBS	1880	110

3.5 Conclusions

PLA-PEG-PLA and PEG-(PLA)₈ hydrogels have been prepared by mixing aqueous polymer solutions of opposite chirality. The gel formation is driven by stereocomplexation of PLA blocks, since the single enantiomer solutions did not form a gel at similar concentrations. The stereocomplexation has been found to have a pronounced effect on the gelation behavior, as critical gel concentrations decreased and gel-sol transitions increased upon increasing temperature. Rheology measurements confirmed the gel formation upon mixing of polymer solutions of opposite chirality and showed improved mechanical

properties for the PEG-(PLA)₈ hydrogels compared to the PLA-PEG-PLA hydrogels, which is attributed to the higher number of stereocomplexation sites of the PEG-(PLA)₈ star block copolymer. Hydrogels prepared in PBS at 37 °C showed storage moduli of 0.9 and 1.9 kPa for PLA-PEG-PLA and PEG-(PLA)₈, respectively. These stereocomplexed hydrogels have potential for biomedical applications, since they can be easily prepared and bioactive moieties (e.g. proteins and cells) can be easily suspended into the single enantiomer solutions before gelation.

3.6 Acknowledgements

This study is financed by the Netherlands Organization for Scientific Research (NWO).

3.7 References

1. Yamaoka, T.; Tabata, Y.; Ikada, Y., Distribution and tissue uptake of poly(ethylene glycol) with different molecular weights after intravenous administration to mice. *J. Pharm. Sci.* 1994, 83, 601-606.
2. Jeong, B.; Bae, Y. H.; Lee, D. S.; Kim, S. W., Biodegradable block copolymers as injectable drug-delivery systems. *Nature* 1997, 388, 860-862.
3. Zhong, Z.; Dijkstra, P.; Feijen, J.; Kwon, Y.; Bae, Y.; Kim, S., Synthesis and aqueous phase behavior of thermoresponsive biodegradable poly(D,L-3-methylglycolide)-block-poly(ethylene glycol)-block-poly(D,L-3-methylglycolide) triblock copolymers. *Macromol. Chem. Phys.* 2003, 203, 1797-1803.
4. de Jong, S. J.; De Smedt, S. C.; Demeester, J.; van Nostrum, C. F.; Kettenes-van den Bosch, J. J.; Hennink, W. E., Biodegradable hydrogels based on stereocomplex formation between lactic acid oligomers grafted to dextran. *J. Controlled Release* 2001, 72, 47-56.
5. Grijpma, D. W.; Feijen, J., Hydrogels by stereo-complexation of water-soluble PLLA-PEO-PLLA and PDLA-PEO-PDLA triblock-copolymers. *J. Controlled Release* 2001, 72, 247-249.

6. Li, S.; Vert, M., Synthesis, characterization, and stereocomplexation-induced gelation of block copolymers prepared by ring-opening polymerization of L(D)-Lactide in the presence of poly(ethylene glycol). *Macromolecules* 2003, 36, 8008-8014.
7. Fujiwara, T.; Mukose, T.; Yamaoka, T.; Yamane, H.; Sakurai, S.; Kimura, Y., Novel thermo-responsive formation of a hydrogel by stereo-complexation between PLLA-PEG-PLLA and PDLA-PEG-PDLA block copolymers. *Macromol. Biosci.* 2001, 1, 204-208.
8. Mukose, T.; Fujiwara, T.; Nakano, J.; Taniguchi, I.; Miyamoto, M.; Kimura, Y.; Teraoka, I.; Lee, C. W., Hydrogel formation between enantiomeric B-A-B-type block copolymers of polylactides (PLLA or PDLA : A) and polyoxyethylene (PEG : B); PEG-PLLA-PEG and PEG-PDLA-PEG. *Macromol. Biosci.* 2004, 4, 361-367.
9. Stevels, W. M.; Ankone, M. J. K.; Dijkstra, P. J.; Feijen, J., Stereocomplex formation in ABA triblock copolymers of poly(lactide)(A) and poly(ethylene-glycol)(B). *Macromol. Chem. Phys.* 1995, 196, 3687-3694.
10. Park, S. Y.; Han, B. R.; Na, K. M.; Han, D. K.; Kim, S. C., Micellization and gelation of aqueous solutions of star-shaped PLLA-PEO block copolymers. *Macromolecules* 2003, 36, 4115-4124.
11. Jeong, B.; Kim, S. W.; Bae, Y. H., Thermosensitive sol-gel reversible hydrogels. *Adv. Drug Deliv. Rev.* 2002, 54, 37-51.
12. Zhou, Z. K.; Yang, Y. W.; Booth, C.; Chu, B., Association of a triblock ethylene oxide (E) and butylene oxide (B) copolymer (B(12)E(260)B(12)) in aqueous solution. *Macromolecules* 1996, 29, 8357-8361.
13. Yang, Y. W.; Yang, Z.; Zhou, Z. K.; Attwood, D.; Booth, C., Association of triblock copolymers of ethylene oxide and butylene oxide in aqueous solution. A study of B(n)E(m)B(n) copolymers. *Macromolecules* 1996, 29, 670-680.
14. Liu, T. B.; Zhou, Z. K.; Wu, C. H.; Chu, B.; Schneider, D. K.; Nace, V. M., Self-assembly of poly(oxybutylene)-poly(oxyethylene)-poly(oxybutylene) (B6E46B6) triblock copolymer in aqueous solution. *J. Phys. Chem. B* 1997, 101, 8808-8815.
15. Jeong, B.; Lee, D.; Shon, J.; Bae, Y. H.; Kim S. W., Thermoreversible gelation of poly(ethylene oxide) biodegradable polyester block copolymers. *J. Polym. Sci. Polym. Chem.* 1999, 37, 751-760.

16. de Jong, S. J.; De Smedt, S. C.; Wahls, M. W. C.; Demeester, J.; Kettenes-van den Bosch, J. J.; Hennink, W. E., Novel self-assembled hydrogels by stereocomplex formation in aqueous solution of enantiomeric lactic acid oligomers grafted to dextran. *Macromolecules* 2000, 33, 3680-3686.
17. Tsuji, F., Autocatalytic hydrolysis of amorphous-made polylactides: effects of L-lactide content, tacticity, and enantiomeric polymer blending. *Polymer* 2002, 43, 1789-1796.
18. Chambon, F., Linear viscoelasticity of crosslinking polymers at the gel point. Massachusetts, 1986.
19. Axelos, M. A. V.; Kolb, M., Crosslinked biopolymers - experimental-evidence for scalar percolation theory. *Phys. Rev. Lett.* 1990, 64, 1457-1460.
20. Tanodekaew, S.; Godward, J.; Heatley, F.; Booth, C., Association and surface properties of diblock copolymers of ethylene oxide and DL-lactide in aqueous solution. *Macromol. Chem. Phys.* 1997, 198, 3385-3395.
21. Malmsten, M.; Lindman, B. Self-assembly in aqueous block copolymer solutions. *Macromolecules* 1992, 25, 5440-5445.
22. Bahadur, P.; Pandya, K.; Almgren, M.; Li, P.; Stilbs, P., Effect of inorganic salts on the micellar behavior of ethylene oxide-propylene oxide block-copolymers in aqueous-solution. *Coll. Polym. Sci.* 1993, 271, 657-667.
23. Aamer, K. A.; Sardinha, H.; Bhatia, S. R.; Tew, G. N., Rheological studies of PLLA-PEO-PLLA triblock copolymer hydrogels. *Biomaterials* 2004, 25, 1087-1093.

Chapter 4

In situ formation of biodegradable hydrogels by stereocomplexation of PEG-(PLLA)₈ and PEG-(PDLA)₈ star block copolymers¹

Christine Hiemstra^a, Zhiyuan Zhong^{a*}, Liangbin Li^b, Pieter J. Dijkstra^a, and Jan Feijen^{a*}

^a Department of Polymer Chemistry and Biomaterials, Faculty of Science and Technology, Institute for Biomedical Technology, University of Twente, P. O. Box 217, 7500 AE Enschede, The Netherlands

^b National Synchrotron Radiation Laboratory, University of Science and Technology of China, Hefei, 230026, PR China

4.1 Abstract

Eight-arm poly(ethylene glycol)-poly(L-lactide), PEG-(PLLA)₈, and poly(ethylene glycol)-poly(D-lactide), PEG-(PDLA)₈, star block copolymers were synthesized by ring-opening polymerization of either L-lactide or D-lactide at room temperature in the presence of a single-site ethylzinc complex and 8-arm PEG ($M_n = 21,800$ or $43,500$) as a catalyst and initiator, respectively. High lactide conversions (>95%) and well-defined copolymers with PLLA or PDLA blocks of the desired molecular weights were obtained. Star block copolymers were water-soluble when the number of lactyl units per poly(lactide) (PLA) block did not exceed 14 and 17 for PEG21800-(PLA)₈ and PEG43500-(PLA)₈, respectively. PEG-(PLA)₈ stereocomplexed hydrogels were prepared by mixing aqueous solutions with equimolar amounts of PEG-(PLLA)₈ and PEG-(PDLA)₈ in a polymer concentration range of 5 to 25 w/v% for PEG21800-(PLA)₈ star block copolymers

¹ This chapter has been published in *Biomacromolecules*, 2006, 7, 2790-2795.

and of 6 to 8 w/v% for PEG43500-(PLA)₈ star block copolymers. The gelation is driven by stereocomplexation of the PLLA and PDLA blocks, as confirmed by wide angle X-ray scattering experiments. The stereocomplexed hydrogels were stable in a range from 10-70 °C, depending on their aqueous concentration and the PLA block length. Stereocomplexed hydrogels at 10 w/v% polymer concentration showed larger hydrophilic and hydrophobic domains compared to 10 w/v% single enantiomer solutions, as determined by cryo-TEM. Correspondingly, dynamic light scattering showed that 1 w/v% solutions containing both PEG-(PLLA)₈ and PEG-(PDLA)₈ have larger “micelles” compared to 1 w/v% single enantiomer solutions. With increasing polymer concentration and PLLA and PDLA block length the storage modulus of the stereocomplexed hydrogels increases and the gelation time decreases. Stereocomplexed hydrogels with high storage moduli (up to 14 kPa) could be obtained at 37 °C in PBS. These stereocomplexed hydrogels are promising for use in biomedical applications, including drug delivery and tissue engineering, since they are biodegradable and the in situ formation allows for easy immobilization of drugs and cells.

4.2 Introduction

Hydrogels are highly attractive materials for use in biomedical applications, such as tissue engineering and drug delivery, since they possess good biocompatibility due to their high hydrophilicity. Recently, much effort has been directed to hydrogels that can be formed in situ under physiological conditions. In situ gelation is preferred, because bioactive compounds and/or cells can be mixed homogeneously with the polymer solutions prior to gelation. Also, in situ gelation allows preparation of complex shapes and applications using minimally invasive surgery. The most common in situ formed, chemically crosslinked hydrogels are based on photo-crosslinkable, (meth)acrylate functionalized polymers.¹⁻⁴ Other groups have prepared hydrogels by disulfide bond formation⁵ and Michael addition reactions between thiols and either acrylates or vinyl sulfones.⁶ Physically crosslinked hydrogels have been prepared by self-assembly of polymers through several types of secondary interactions, such as hydrophobic and ionic interactions.⁷⁻¹⁴ Crosslinking by physical interactions has several advantages over chemical crosslinking, since it avoids the use of photo-irradiation, organic solvents, auxiliary crosslinking agents and/or other reactive molecules that may damage cells or proteins to be

incorporated. Recently, several research groups have shown that hydrogels can be prepared in-situ from water-soluble poly(L-lactide) (PLLA) and poly(D-lactide) (PDLA) based block copolymers, in which the physical crosslinks are provided by stereocomplexation between the enantiomeric PLLA and PDLA blocks.¹⁵⁻¹⁹ De Jong et al. have shown that stereocomplexed dextran-poly(lactide), dextran-PLA, graft copolymer hydrogels quantitatively release proteins over a period of one week with full preservation of the protein activity.¹⁶ Moreover, *in vivo* tests showed that these stereocomplexed hydrogels are biocompatible and effective tools for local IL-2 delivery.^{20,21} Li et al.¹⁸ have shown that proteins can be released from stereocomplexed PLA-PEG-PLA triblock copolymer hydrogels over a prolonged period of time (up to 15 days). These results show that in situ formed, stereocomplexed hydrogels are interesting materials for use in biomedical applications. Synthesis of the dextran-PLA graft copolymers however requires several steps, while the PLA-PEG-PLA triblock copolymer stereocomplexed hydrogels show low mechanical strength and slow gelation kinetics compared to the dextran-PLA graft copolymers, due to a low crosslinking density. We found previously that PEG-(PLLA)₈ and PEG-(PDLA)₈ star block copolymers gelate faster and form stereocomplexed hydrogels with improved mechanical strength as compared to PLLA-PEG-PLLA and PDLA-PEG-PDLA triblock copolymers.¹⁵ In this paper, the effect of PLA block length, PEG molecular weight and polymer concentration on the temperature dependent phase behavior, gelation kinetics and mechanical properties PEG-(PLLA)₈ and PEG-(PDLA)₈ star copolymer stereocomplexed hydrogels were studied. Furthermore, the gelation mechanism by stereocomplexation between PLLA and PDLA blocks was confirmed by wide angle X-ray scattering (WAXS) measurements.”

4.3 Materials and Methods

Materials. D-lactide and L-lactide were obtained from Purac and recrystallised from dry toluene. Star PEG's ($M_{n, NMR} = 21,800$, denoted as PEG21800 and $M_n = 43,500$, denoted as PEG43500) were supplied by Nektar and were used as received. GPC data, provided by the producer, showed that both starting PEG21800 and PEG43500 have a low polydispersity of 1.11 and 1.12, respectively. The single site Zn-complex catalyst

(Zn(Et)[SC₆H₄(CH(Me)NC₄H₈)-2]) was kindly provided by Professor G. van Koten of the University of Utrecht (The Netherlands). Dichloromethane (CH₂Cl₂) was dried over calcium hydride and distilled prior to use.

Synthesis. Eight-arm poly(ethylene glycol)-poly(L-lactide), PEG-(PLLA)₈, and poly(ethylene glycol)-poly(D-lactide), PEG-(PDLA)₈, star block copolymers were prepared at room temperature by ring-opening polymerization of L-lactide and D-lactide in CH₂Cl₂, respectively. The single site Zn-complex catalyst Zn(Et)[SC₆H₄(CH(Me)NC₄H₈)-2] and 8-arm star PEG were used as catalyst and initiator, respectively.¹⁵ Briefly, PEG21800 (0.730 g, 0.0335 mmol) and lactide (0.270 g, 1.88 mmol) were dissolved in 7.5 ml of CH₂Cl₂ ([LA]₀ = 0.25 M). To this solution a solution of single site Zn-complex catalyst (0.040 g, 0.134 mmol) was added in 1 ml of CH₂Cl₂ and the reaction mixture was stirred for 4 h. The polymerization was terminated by the addition of an excess of glacial acetic acid and the polymer was precipitated in a mixture of cold diethyl ether/methanol (20/1 v/v). Conversion: 98%, yield: 89%. ¹H NMR (CDCl₃): 1.4 (m, CH₃CHOH end group PLA), 1.5 (m, CH₃CH), 3.6 (m, CH₂O), 4.2-4.3 (m, CH₂CO, linking unit PEG), 4.3-4.4 (q, CHOH end group PLA), 5.1 (m, CHCO)

Characterization. ¹H NMR spectra (CDCl₃) were recorded on a Varian Inova Spectrometer (Varian, Palo, Alto, USA) operating at 300 MHz. The average number of lactyl units per poly(lactide) (PLA) block was calculated based on the methyl protons of lactyl units at δ 1.5 and the methylene protons of PEG at δ 3.6. Cloud point measurements were performed on a homemade light scattering set-up at 670 nm using a polymer concentration of 5 w/v% in water. The samples were heated from 20 to 60 °C at a heating rate of 1°C/min. Critical association concentrations (CAC's) were determined at 20 °C with the hydrophobic dye solubilization method using 1,6-diphenyl-1,3,5-hexatriene (DPH).²² UV/Vis absorption spectra were recorded in the 300-500 nm range using a Cary 300 Bio UV-Visible Spectrophotometer (Varian). Dynamic light scattering experiments were performed on a Zetasizer 4000 (Malvern) and the data was analyzed by the CONTIN method. Critical gel concentrations (CGC's) were determined as described before.¹⁵ Briefly, PEG21800-(PLA)₈ and PEG43500-(PLA)₈ star block copolymer solutions were prepared with concentration increments of 2.5 and 1 w/v%, respectively, by dissolving the polymers overnight. Subsequently, polymer solutions containing equimolar amounts of

PEG-(PLLA)₈ and PEG-(PDLA)₈ star block copolymers were mixed and equilibrated overnight. The critical gel concentrations were determined by inverting the vials. When the sample showed no flow within 20 s, it was regarded as a gel. The thermostability of stereocomplexed hydrogels was studied using the vial tilting method at temperatures between 5 and 70 °C with intervals of 2 °C. At each temperature, the samples were allowed to equilibrate for 10 min. X-ray diffractions were performed with a Bruker D8 Discovery equipped with a copper source (x-ray wavelength $\lambda = 0.154$ nm) and a two-dimensional detector (Hi-Star). All measurements were conducted in reflection geometry. After the measurements, the two-dimensional x-ray scattering images were integrated into one-dimensional intensity profiles with 2θ as x-axis, where θ is the scattering angle. The data were corrected with a background profile collected from pure water. Cryo-TEM was carried out with a CM12 apparatus (Philips) at 100-120 KV. Rheology experiments were performed on a US 200 Rheometer (Anton Paar), using a flat plate measuring geometry (25 mm diameter, gap 0.5 mm), a frequency of 1 Hz and a strain of 1%, as described previously.¹⁵ Polymer solutions containing equimolar amounts of PEG-(PLLA)₈ and PEG-(PDLA)₈ star block copolymers were mixed, homogenized and quickly applied to the rheometer.

4.4 Results and Discussion

4.4.1 Synthesis of water-soluble PEG-PLA star block copolymers

To prepare materials that are well soluble in water, poly(ethylene glycol)-poly(L-lactide), PEG-(PLLA)₈, and poly(ethylene glycol)-poly(D-lactide), PEG-(PDLA)₈, star block copolymers were synthesized by a Zn-complex catalyzed ring-opening polymerization of L- and D-lactide, respectively, initiated by 8-arm star PEG (Table 1). The use of the single site Zn-catalyst allowed excellent control over the degree of polymerization of the poly(lactide) (PLA) blocks, as determined by ¹H NMR. ¹H NMR showed that all hydroxyl groups of PEG had initiated the ring-opening polymerization.¹⁵ Star block copolymers of PEG with a molecular weight of 21,800 and PLA with average block lengths of 10, 12, 14 or 16 lactyl units were prepared. Also, PEG-(PLLA)₈ and PEG-

(PDLA)₈ star block copolymers with a PEG molecular weight of 43,500 and PLA with average block lengths of 13, 17 or 20 lactyl units were synthesized.

Table 1. Synthesis of PEG-(PLLA)₈ and PEG-(PDLA)₈ star block copolymers.^{a)}

Polymer	Conversion (%)	N _{LA} ^{b)}		M _n ¹ H NMR	PEG content (wt%)
		Theory ^{c)}	¹ H NMR		
PEG21800-(PLLA) ₈	97	10	9	27200	81
	98	12	12	28400	76
	98 ^{d)}	14	14	29500	74
PEG21800-(PDLA) ₈	97	10	10	27400	79
	99	12	12	28700	76
	98	14	14	29800	73
PEG43500-(PLLA) ₈	~95	14	13	50900	85
	96	18	17	53300	82
PEG43500-(PDLA) ₈	~95	14	13	50800	86
	98	18	17	53300	82

^{a)} The ring-opening polymerization of lactide was performed in CH₂Cl₂ for 4 h at RT using 8-arm PEG and the single site Zn-complex Zn(Et)[SC₆H₄(CH(Me)NC₄H₈)-2] as initiator and catalyst, respectively ([LA]₀ = 0.25 M, PEG-OH : Zn catalyst = 2 : 1). ^{b)} Number of lactyl units per PLA block. ^{c)} Based on feed composition and conversion. ^{d)} Data for these star block copolymers have been reported previously.¹⁵

The solubility of PEG21800-(PLA)₈ and PEG43500-(PLA)₈ in distilled water at room temperature decreased rapidly upon increasing the PLA block length. When the number of lactyl units per PLA block for PEG21800-(PLA)₈ was higher than 14, the copolymer was not water-soluble above polymer concentrations of ~0.1 w/v% (data not shown). PEG43500-(PLA)₈ star block copolymers were water-soluble up to 17 lactyl units per PLA block. At 17 lactyl units per PLA block, PEG43500-(PLA)₈ was only soluble at low concentrations of ~0.1 w/v% (data not shown). Moreover, with increasing PLLA block length the critical gel concentration (CGC) of the PEG-(PLA)₈ star block copolymers decreased (Table 2). For instance, PEG21800-(PLA₁₀)₈ star block copolymers showed a

CGC of 40 w/v%, while PEG21800-(PLA₁₄)₈ star block copolymers showed a CGC of 15 w/v%. Star block copolymers based on PEG43500 are much less water-soluble, possibly due to the high molecular weight of the PEG. Similar to the PEG21800-(PLA)₈ star block copolymers, the CGC of PEG43500-(PLA)₈ star block copolymers decreases rapidly at higher PLA block lengths and only the PEG43500-(PLA₁₃)₈ copolymer, which is soluble up to 9 w/v%, was used for further studies (Table 2).

Critical association concentration (CAC) values were determined at 20 °C using the hydrophobic dye 1,6-diphenyl-1,3,5-hexatriene solubilization method.²² CAC values at 20 °C for PEG21800-(PLA₁₄)₈, PEG21800-(PLA₁₂)₈ and PEG21800-(PLA₉)₈ were found to be 0.07, 0.22 and 0.44 w/v%, respectively. The decreasing CAC value with increasing PLLA block length is due to increased hydrophobic interactions and subsequent increased aggregation tendency. PEG43500-(PLA₁₃)₈ showed a CAC of 0.11 w/v%. For these star block copolymers the PEG molecular weight has little influence on the association behavior. The cloud points of 5 w/v% PEG-(PLA)₈ solutions in water increased with decreasing PLA block length and were found to be 27, 49 and 61 °C for PEG21800-(PLA)₈ star block copolymers with 14, 12 and 10 lactyl units per PLA block, respectively.

4.4.2 Critical gel concentrations and phase behavior

The influence of the PLA block length and PEG molecular weight on the gelation behavior of aqueous solutions containing equimolar amounts of PEG-(PLLA)₈ and PEG-(PDLA)₈ star block copolymers was studied at room temperature. Aqueous solutions of the star block copolymers with similar PLA blocks lengths and PEG molecular weight were mixed and after equilibration it was tested whether the sample had turned into a gel by the vial tilting method. Stereocomplexed hydrogels could be prepared in a polymer concentration range of 5 to 25 w/v% for PEG21800-(PLA)₈ star block copolymers and of 6 to 8 w/v% for PEG43500-(PLA)₈ star block copolymers. From these experiments it can be seen that the CGC decreases with increasing PLA block length and gelation is possible even at very short PLA block lengths of 10 lactyl units (Table 2).

Table 2. Critical gel concentrations (CGC) of PEG-(PLLA)₈ single enantiomers and of mixed aqueous solutions containing equimolar amounts of PEG-(PLLA)₈ and PEG-(PDLA)₈ star block copolymers in distilled water at room temperature.

Polymer	CGC single enantiomer (w/v%)	CGC mixed enantiomers (w/v%)
PEG21800-(PLA ₁₀) ₈	40	25
PEG21800-(PLA ₁₂) ₈	20	10
PEG21800-(PLA ₁₄) ₈ ^{a)}	15	5
PEG43500-(PLA ₁₃) ₈	9	6

^{a)}Data for the PEG21800-(PLA₁₄)₈ star block copolymers have been reported previously.¹⁵

It was assumed that a PEG with a higher molecular weight would increase the copolymer solubility, which would allow stereocomplexed hydrogel formation at higher polymer concentrations. However, doubling of the PEG molecular weight decreased the block copolymer solubility to a large extent (Table 2). At 17 lactyl units, the PEG43500-(PLLA)₈ copolymer was soluble only at low polymer concentrations of ~ 0.1 w/v%. At these low concentrations, no stereocomplexed hydrogel could be formed.

The thermostability of PEG21800-(PLA)₈ stereocomplexed hydrogels was studied by the vial tilting method in a temperature range of 5 to 70 °C. Upon increasing the temperature the gel phase was lost and the stereocomplexed hydrogels phase separated into a mobile phase consisting of a clear fluid and a viscous opaque phase (Figure 1). In a few cases, at relatively short PLA block lengths and low concentrations, a sol phase was obtained. The hydrogels containing only the single enantiomers, which can be formed at high polymer concentrations, showed much lower phase separation temperatures (data not shown). Therefore, stereocomplexation appears to be a key factor to maintain the gel structure. In general, the thermostability of the gels increases with increasing polymer concentration and PLA block length. However, PEG21800-(PLA₁₂)₈ stereocomplexed hydrogels showed unexpected phase behavior. A steep increase in the phase separation temperature from 35 to 67 °C occurred when increasing the polymer concentration from 7.5 w/v% to 10 w/v%. At 14 w/v% however, the phase separation temperature was found at 60 °C and it further decreased to 43 °C at 15 w/v%. In the preparation of the PEG21800-

(PLA₁₂)₈ stereocomplexed hydrogels, the stereocomplexation efficiency may be changing with the polymer concentration. It appears that at 10 w/v% polymer concentration the stereocomplexation for these star block copolymers is most efficient.

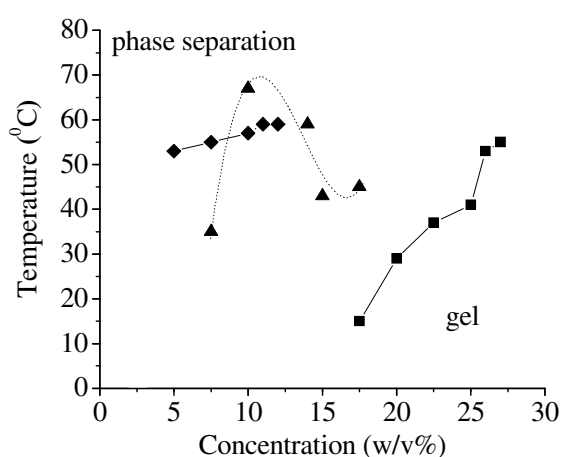


Figure 1. Thermostability of PEG-(PLA)₈ stereocomplexed hydrogels. PEG21800-(PLA₁₀)₈ (■), PEG21800-(PLA₁₂)₈ (▲), PEG21800-(PLA₁₄)₈ (◆). Data for the PEG21800-(PLA₁₄)₈ stereocomplexed hydrogel have been reported previously.¹⁵

4.4.3 Gelation mechanism and gel morphology.

To confirm the gel formation by stereocomplexation of the PLA blocks, WAXS experiments were performed on stereocomplexed hydrogels of PEG21800-(PLA₁₄)₈, PEG21800-(PLA₁₂)₈ and on a PEG21800-(PDLA₁₄)₈ single enantiomer solution as a control (Figure 2). Both PEG21800-(PLA₁₄)₈ and PEG21800-(PLA₁₂)₈ stereocomplexed hydrogels showed diffraction peaks at $2\theta = \sim 12.2, 23, 24^\circ$ (Figure 2a), which are known to correspond to the PLA stereocomplex crystal.²³ The single enantiomer solution showed no diffraction peaks, since at these short block lengths PLA is amorphous. The amorphous nature of the PLA blocks was shown previously by differential calorimetry measurements (DSC).¹⁵ The stereocomplex crystals in PEG21800-(PLA₁₂)₈ hydrogels were still present at 30 °C, but melted when the temperature was increased to 50 °C (Figure 2b). This result

agrees well with the decreasing gel strength upon increasing temperature, as was also shown by Vert et al.²⁴ for PLA-PEG-PLA triblock copolymer stereocomplexed hydrogels. The disappearance of the stereocomplex crystal peaks at 50 °C also agrees well with the phase separation temperature of 43 °C of the PEG21800-(PLA₁₂)₈ 15 w/v% stereocomplexed hydrogel, as determined by the vial tilting method.

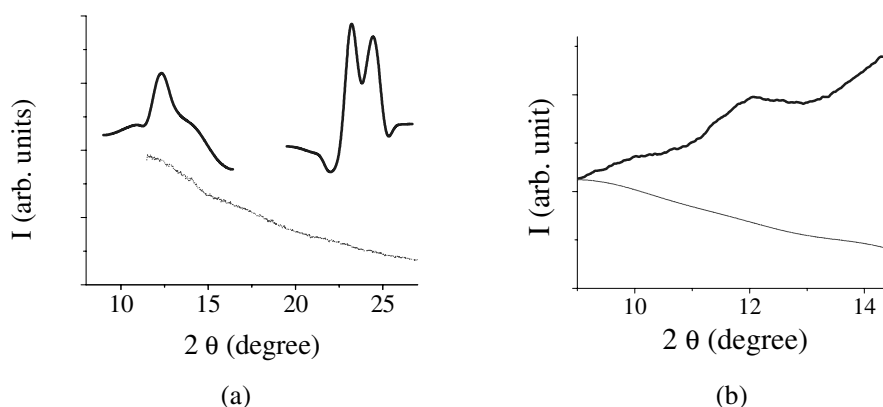


Figure 2. WAXS measurements on PEG21800-(PLA)₈ stereocomplexed hydrogels. (a) 10 w/v% PEG21800-(PLA₁₄)₈ stereocomplexed hydrogel (—) and 10 w/v% PEG21800-(PDLA₁₄)₈ single enantiomer solution (---) at 20 °C; (b) 15 w/v% PEG21800-(PLA₁₂)₈ stereocomplexed hydrogel at 30 °C (—) and 50 °C (---).

The effect of stereocomplexation on polymer aggregation in dilute solutions was also investigated. For this purpose, micellar solutions containing the single PEG21800-(PLLA₁₂)₈ or equimolar amounts of PEG21800-(PLLA₁₂)₈ and PEG21800-(PDLA₁₂)₈ were prepared. Dynamic light scattering (DLS) revealed that both the Z-average particle size (Z-av) and the photon count rate (KCT) increased in time upon mixing enantiomers of opposite chirality (Figure 3), indicating that larger aggregates are formed upon stereocomplexation. In contrast, solutions containing only the single enantiomer or a D- to L-enantiomer ratio of 75/25 showed a slight decrease in the count rate and Z-average particle size.

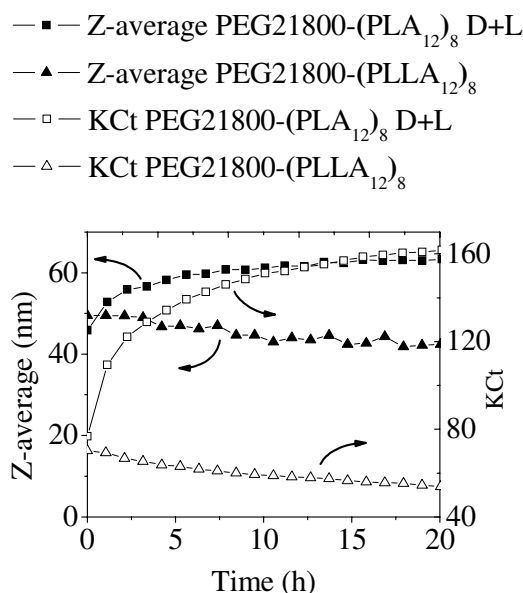


Figure 3. The Z-average particle size (Z-av) (nm) and the photon count rate (KCt) of 1 w/v% aqueous copolymer solutions as a function of time at 25 °C.

Cryo-TEM was performed to show the influence of stereocomplexation on the morphology. Cryo-TEM images of 10 w/v% PEG21800-(PDLA₁₄)₈ aqueous solutions and 10 w/v% PEG21800-(PLA₁₄)₈ stereocomplexed hydrogels both showed dark spots and grey areas, corresponding to PEG and PLA domains, respectively (Figure 4). Both the PEG21800-(PDLA₁₄)₈ aqueous solutions and PEG21800-(PLA₁₄)₈ stereocomplexed hydrogel show wormlike particles with a PEG corona and a PLA core with a core size ranging from approximately 10 to 20 nm. The cryo-TEM image of the PEG21800-(PLA₁₄)₈ stereocomplexed hydrogel (Figure 4A) shows a somewhat coarser structure compared to the PEG21800-(PDLA₁₄)₈ aqueous solution (Figure 4B). In contrast to the PEG21800-(PDLA₁₄)₈ aqueous solutions, the grey areas of the stereocomplexed hydrogel show small, darker spots, indicating more phase separation on a smaller scale upon stereocomplexation.

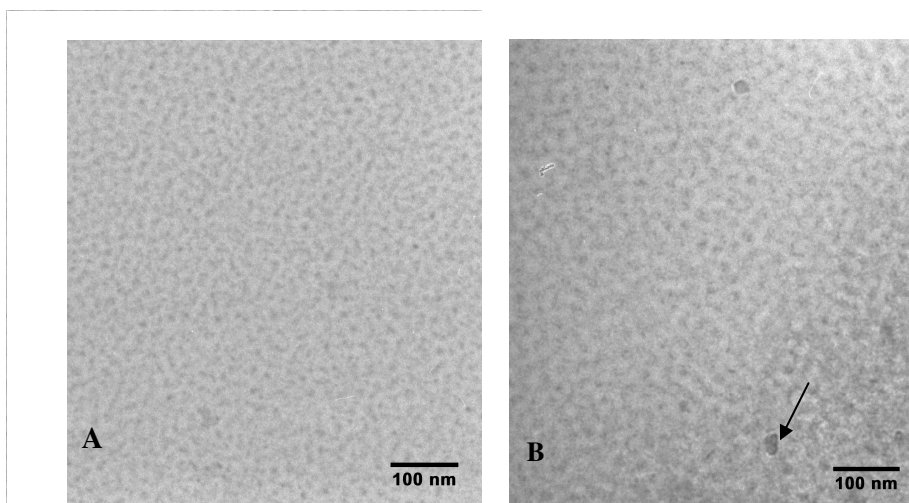


Figure 4. Cryo-TEM images of (A) a PEG21800-(PDLA₁₄)₈ aqueous solution and (B) a PEG21800-(PLA₁₄)₈ stereocomplexed hydrogel at a polymer concentration of 10 w/v%. Some ice crystals were present due to contamination during sample preparation, as indicated by the arrow.

4.4.4 Rheology

The mechanical properties of the stereocomplexed hydrogels were studied by oscillatory rheology experiments on polymer solutions containing equimolar amounts of PEG-(PLLA)₈ and PEG-(PDLA)₈ star block copolymers. Gel formation kinetics was followed by monitoring the storage modulus (G') and loss modulus (G'') in time (Figures 5 and 6). Comparing PEG21800-(PLA₁₂)₈ and PEG21800-(PLA₁₄)₈ stereocomplexed hydrogels, it can be seen from Figure 5a that increasing the PLA block length increases the storage modulus from 0.9 to 7.0 kPa at 10 w/v% polymer concentration. The gelation time, indicated by the crossing of the storage and loss modulus²⁵, increased with decreasing PLA block length. The enantiomeric mixture of PEG21800-(PLA₁₄)₈ gelled instantly, whereas the gelation time was 40 min for a similar PEG21800-(PLA₁₂)₈ mixture. To study the influence of PEG molecular weight, stereocomplexed hydrogels of PEG21800-(PLA₁₄)₈

and PEG43500-(PLA₁₃)₈ were prepared at 7.5 wt% polymer concentration at 20 °C. Figure 5b shows that the gelation time for the PEG43500-(PLA₁₃)₈ stereocomplexed hydrogel significantly increased compared to the PEG21800-(PLA₁₄)₈ stereocomplexed hydrogel (200 min vs. instant gelation). Also, after gelation the storage modulus of the PEG43500-(PLA₁₃)₈ stereocomplexed hydrogel increases slower than the storage modulus of the PEG21800-(PLA₁₄)₈ stereocomplexed hydrogel.

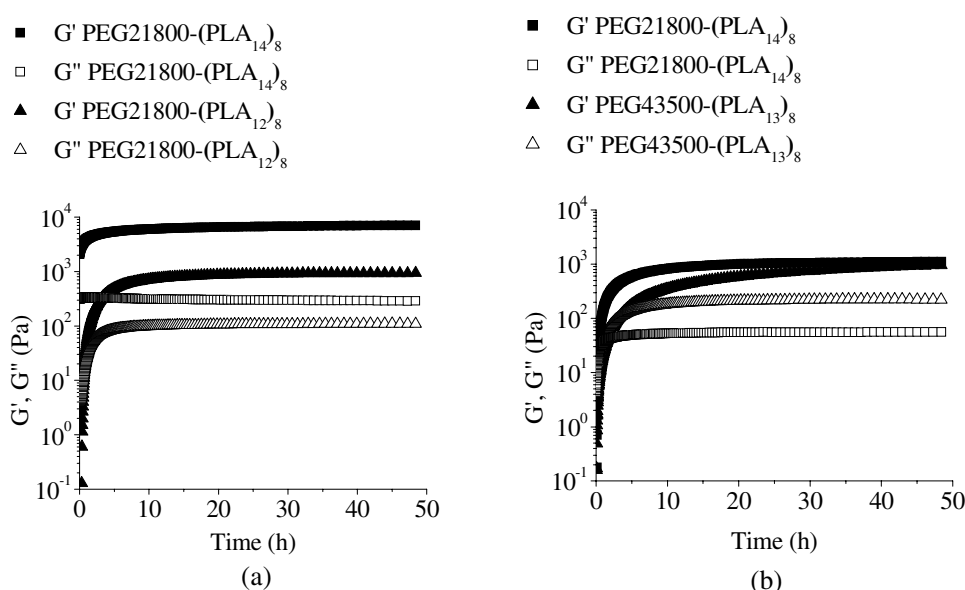


Figure 5. The storage modulus (G') and loss modulus (G'') as a function of time after mixing solutions of PEG-(PLLA)₈ and PEG-(PDLA)₈ star block copolymers in equimolar amounts in water at 20 °C. (a) PEG21800-(PLA₁₄)₈ and PEG21800-(PLA₁₂)₈ at a polymer concentration of 10 w/v%; (b) PEG21800-(PLA₁₄)₈ and PEG43500-(PLA₁₃)₈ at a polymer concentration of 7.5 w/v%. Data for stereocomplexed hydrogels containing 10 w/v% of PEG21800-(PLA₁₄)₈ star block copolymers have been reported previously.¹⁵

The longer gelation time and slower increase in storage modulus of the PEG43500-(PLA₁₃)₈ stereocomplexed hydrogel show that the gel formation kinetics are much slowed down compared to the PEG21800-(PLA₁₄)₈ stereocomplexed hydrogel, due to the high PEG molecular weight. Both stereocomplexed hydrogels have similar storage moduli of

approximately 1 kPa, although the PEG43500-(PLA₁₃)₈ stereocomplexed hydrogel contains almost twice as less PLA than the PEG21800-(PLA₁₄)₈ stereocomplexed hydrogel at the same polymer concentration. The loss modulus of the PEG43500-(PLA₁₃)₈ stereocomplexed hydrogel is however much higher compared to the PEG21800-(PLA₁₄)₈ stereocomplexed hydrogel (220 vs. 60 Pa), indicating that the PEG43500-(PLA₁₃)₈ stereocomplexed hydrogel has a less perfect network structure and contains more viscous components.²⁵ Therefore, the comparable storage moduli of the PEG43500-(PLA₁₃)₈ stereocomplexed hydrogel and the PEG21800-(PLA₁₄)₈ stereocomplexed hydrogel is attributed to the presence of more chain entanglements at the higher PEG molecular weight, which act as physical crosslinks.

In Figure 6a the storage and loss moduli of PEG21800-(PLA₁₄)₈ stereocomplexed hydrogels at polymer concentrations of 5, 7.5 and 10 w/v% are presented. The results show that at higher concentrations a significantly higher storage modulus is obtained due to the formation of a denser crosslinked network. Moreover, gelation kinetics is highly dependent on the polymer concentration. At 5 w/v% concentration the gelation time is approximately 25 min, giving a gel with a storage modulus of 0.5 kPa, but at 10 w/v% the gelation is instantaneous, affording a stereocomplexed hydrogel with a storage modulus of 7.0 kPa. The fast gelation is due to the higher probability of stereocomplex formation at higher concentrations. The highest storage moduli were obtained with stereocomplexed hydrogels of the PEG21800-(PLA₁₀)₈ copolymer at a relatively high polymer concentration of 25 w/v% (results not shown). Storage moduli of 27.2 kPa and 14.0 kPa were obtained at 20 °C in water and at 37 °C in PBS, respectively. To further confirm the gelation by stereocomplexation, PEG21800-(PLA₁₄)₈ stereocomplexed hydrogels were prepared with mismatched D- and L-enantiomer ratio's. Figure 6b shows that at a polymer concentration of 5 w/v% in water and at 20 °C the storage modulus of a 50/50 mixture is considerably higher than that of a 67/33 mixture (20 vs. 9 Pa). Also, the gelation time increases at ratios other than 50/50. Eventually, at a ratio of 84/16 no gel formation was observed anymore. The influence of temperature and the presence of salts on the rheological properties of hydrogels is important considering the envisaged in-vivo application. We have previously shown that independent of the PLA block length, enantiomeric mixtures of PEG21800-(PLA)₈ afforded strong hydrogels at 37 °C in PBS buffer at pH 7.4.¹⁵ In summary, the rheology results show that the PEG-(PLA)₈ star block copolymers provide faster gelation

kinetics, higher storage moduli and a more densely crosslinked network structure (as indicated by the high storage to loss modulus ratio), compared to the PLA-PEG-PLA triblock copolymers reported by our group and by Li et al.^{15,18} and to the dextran-PLA graft copolymer stereocomplexed hydrogels prepared by De Jong et al.²⁶ Moreover, the results show that the gelation time and mechanical properties of the star block copolymer hydrogels can be tuned by simply varying the polymer concentration and/or the PLA block length.

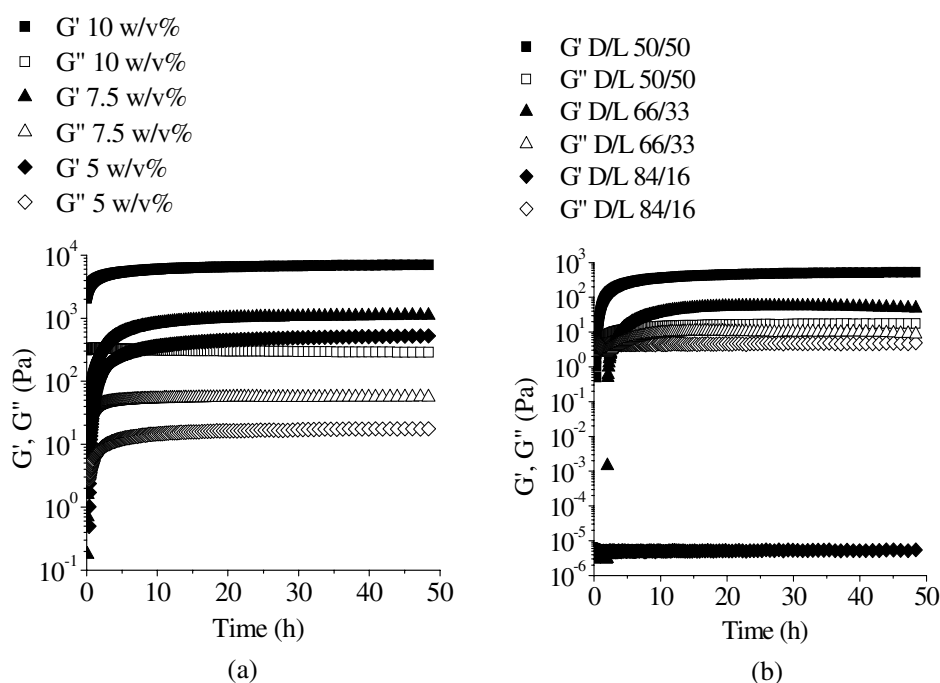


Figure 6. The storage modulus (G') and loss modulus (G'') as a function of time after mixing solutions of PEG21800-(PLLA₁₄)₈ and PEG21800-(PDLA₁₄)₈ star block copolymers (a) with a D/L ratio of 50/50 in water at 20 °C at polymer concentrations of 10 w/v%, 7.5 w/v% and 5 w/v%; (b) at a polymer concentration of 5 w/v% in water at 20 °C with D/L ratios of 50/50, 66/33 and 84/16. Data for PEG21800-(PLA₁₄)₈ star block copolymers at 10 w/v% has been reported previously.¹⁵

4.5 Conclusions

Water-soluble 8-arm PEG-PLLA and PEG-PDLA star block copolymers were synthesized by ring-opening polymerization of L-lactide and D-lactide at room temperature using a single-site ethylzinc complex and 8-arm PEG as catalyst and initiator, respectively. Stereocomplexed hydrogels were formed by mixing aqueous solutions of PEG-(PLLA)₈ and PEG-(PDLA)₈ star block copolymers. Rheology on the stereocomplexed hydrogels showed that hydrogels with a range of storage moduli (up to 14 kPa in PBS at 37 °C) and gelation times (instant gelation up to approximately 1 h) can be designed by varying the PLA block length and polymer concentration. These stereocomplexed hydrogels are promising for use in biomedical applications, since they can be formed in situ under physiological conditions with suitable mechanical properties.

4.6 Acknowledgements

This work was funded by the Netherlands Organization for Scientific Research (NWO). We thank P. Bomans (University of Maastricht, The Netherlands) for the cryo-TEM measurements.

4.7 References

1. Sawhney, A. S.; Pathak, C. P.; Hubbell, J. A., Bioerodible hydrogels based on photopolymerized poly(ethylene glycol)-co-poly(alpha-hydroxy acid) diacrylate macromers. *Macromolecules* 1993, 26, 581-587.
2. Burdick, J. A.; Mason, M. N.; Hinman, A. D.; Thorne, K.; Anseth, K. S., Delivery of osteoinductive growth factors from degradable PEG hydrogels influences osteoblast differentiation and mineralization. *J. Controlled Release* 2002, 83, 53-63.
3. West, J. L.; Hubbell, J. A., Polymeric biomaterials with degradation sites for proteases involved in cell migration. *Macromolecules* 1999, 32, 241-244.
4. Nuttelman, C. R.; Henry, S. M.; Anseth, K. S., Nuttelman, C. R.; Henry, S. M.; Anseth, K. S., Synthesis and characterization of photocrosslinkable, degradable

- poly(vinyl alcohol)-based tissue engineering scaffolds. *Biomaterials* 2002, 23, 3617-3626.
5. Goessl, A.; Tirelli, N.; Hubbell, J. A., A hydrogel system for stimulus-responsive, oxygen-sensitive in situ gelation. *J. Biomater. Sci.-Polym. Ed.* 2004, 15, 895-904.
 6. Pratt, A. B.; Weber, F. E.; Schmoekel, H. G.; Muller, R.; Hubbell, J. A., Synthetic extracellular matrices for in situ tissue engineering. *Biotechnol. Bioeng.* 2004, 86, 27-36.
 7. Jeong, B.; Bae, Y. H.; Lee, D. S.; Kim, S. W., Biodegradable block copolymers as injectable drug-delivery systems. *Nature* 1997, 388, 860-862.
 8. Zhong, Z. Y.; Dijkstra, P. J.; Feijen, J.; Kwon, Y. M.; Bae, Y. H.; Kim, S. W., Synthesis and aqueous phase behavior of thermoresponsive biodegradable poly(D,L-3-methylglycolide)-block-poly(ethylene glycol)-block-poly(D,L-3-methylglycolide) triblock copolymers. *Macromol. Chem. Phys.* 2002, 203, 1797-1803.
 9. Kim, S.; Healy, K. E., Synthesis and characterization of injectable poly(N-isopropylacrylamide-co-acrylic acid) hydrogels with proteolytically degradable cross-links. *Biomacromolecules* 2003, 4, 1214-1223.
 10. Collier, J. H.; Hu, B. -H.; Ruberti, J. W.; Zhang, J.; Shum, P.; Thompson, D. H.; Messersmith, P. B., Thermally and photochemically triggered self-assembly of peptide hydrogels. *JACS* 2001, 123, 9463-9464.
 11. Yi, J. W.; Na, K.; Bae, Y. H., Ionic strength/temperature-induced gelation of aqueous poly(N-isopropylacrylamide-co-vinylimidazole) solution. *Macromol. Symp.* 2004, 207, 131-138.
 12. Kisiday, J.; Jin, M.; Kurz, B.; H, H.; Semino, C.; Zhang, S.; Grodzinsky, A. J., Self-assembling peptide hydrogel fosters chondrocyte extracellular matrix production and cell division: Implications for cartilage tissue repair. *PNAS.* 2002, 99, 9996-10001.
 13. Li, J.; Ni, X. P.; Leong, K. W., Injectable drug-delivery systems based on supramolecular hydrogels formed by poly(ethylene oxide) and alpha-cyclodextrin. *J. Biomed. Mater. Res.* 2003, 65A, 196-202.
 14. Van Tomme, S. R.; van Steenberg, M. J.; De Smedt, S. C.; van Nostrum, C. F.; Hennink, W. E., Self-gelling hydrogels based on oppositely charged dextran microspheres. *Biomaterials* 2005, 26, 2129-2135.

15. Chapter 3, Hiemstra, C.; Zhong, Z. Y.; Dijkstra, P. J.; Feijen, J., Stereocomplex mediated gelation of PEG-(PLA)₂ and PEG-(PLA)₈ block copolymers. Published in *Macromol. Symp.* 2005, 224, 119-132.
16. de Jong, S. J.; van Eerdenbrugh, B.; van Nostrum, C. F.; Kettenes-van de Bosch, J. J.; Hennink, W. E., Physically crosslinked dextran hydrogels by stereocomplex formation of lactic acid oligomers: degradation and protein release behavior. *J. Controlled Release* 2001, 71, 261-275.
17. Grijpma, D. W.; Feijen, J., Hydrogels by stereo-complexation of water-soluble PLLA-PEO-PLLA and PDLA-PEO-PDLA triblock-copolymers. *J. Controlled Release* 2001, 72, 247-249.
18. Li, S.; El Ghzaoui, A.; Dewinck, E., Rheology and drug release properties of bioresorbable hydrogels prepared from polylactide/poly(ethylene glycol) block copolymers. *Macromol. Symp.* 2005, 222, 23-36.
19. Mukose, T.; Fujiwara, T.; Nakano, J.; Taniguchi, I.; Miyamoto, M.; Kimura, Y.; Teraoka, I.; Lee, C. W., Hydrogel formation between enantiomeric B-A-B-type block copolymers of polylactides (PLLA or PDLA : A) and polyoxyethylene (PEG : B); PEG-PLLA-PEG and PEG-PDLA-PEG. *Macromol. Biosci.* 2004, 4, 361-367.
20. Bos, G. W.; Hennink, W. E.; Brouwer, L. A.; den Otter, W.; Veldhuis, T. F. J.; van Nostrum, C. F.; van Luyn, M. J. A., Tissue reactions of in situ formed dextran hydrogels crosslinked by stereocomplex formation after subcutaneous implantation in rats. *Biomaterials* 2005, 26, 3901-3909.
21. Bos, G.; Jacobs, J.; Koten, J.; Van Tomme, S.; Veldhuis, T.; van Nostrum, C.; Den Otter, W.; Hennink, W., In situ crosslinked biodegradable hydrogels loaded with IL-2 are effective tools for local IL-2 therapy. *Eur. J. Pharm. Sci.* 2004, 21, 561-567.
22. Alexandridis, P.; Holzwarth, J. F.; Hatton, T. A., Micellization of poly(ethylene oxide)-poly(propylene oxide)-poly(ethylene oxide) triblock copolymers in aqueous-solutions - thermodynamics of copolymer association. *Macromolecules* 1994, 27, 2414-2425.
23. Sarasua, J. -R.; Prud'homme, R. E.; Wisniewski, M.; Le Borgne, A.; Spassky, N., Crystallization and melting behavior of polylactides. *Macromolecules* 1998, 31, 3895-3905.

24. Li, S.; Vert, M., Synthesis, characterization, and stereocomplexation-induced gelation of block copolymers prepared by ring-opening polymerization of L(D)-lactide in the presence of poly(ethylene glycol). *Macromolecules* 2003, 36, 8008-8014.
25. Chambon, F.; Winter, H. H., Linear viscoelasticity at the gel point of a crosslinking PDMS with imbalanced stoichiometry. *J. Rheol.* 1987, 31, 683-696.
26. De Jong, S. J.; De Smedt, S. C.; Wahls, M. W. C.; Demeester, J.; Kettenes-van den Bosch, J. J.; Hennink, W. E., Novel self-assembled hydrogels by stereocomplex formation in aqueous solution of enantiomeric lactic acid oligomers grafted to dextran. *Macromolecules* 2000, 33, 3680-3686.

Chapter 5

In vitro and in vivo protein delivery from in situ forming poly(ethylene glycol)-poly(lactide) hydrogels¹

Christine Hiemstra^a, Zhiyuan Zhong^a, Sophie R. Van Tomme^b, Mies J. van Steenbergen, John J. L. Jacobs^c, Willem Den Otter^c, Wim E. Hennink^b, and Jan Feijen^a

^a Department of Polymer Chemistry and Biomaterials, Faculty of Science and Technology, Institute for Biomedical Technology, University of Twente, P. O. Box 217, 7500 AE Enschede, The Netherlands

^b Department of Pharmaceutics, Utrecht Institute for Pharmaceutical Sciences (UIPS), Utrecht University, P. O. Box 80.082, 3508 TB Utrecht, The Netherlands

^c Department of Pathobiology, Faculty of Veterinary Medicine, Utrecht University, P. O. Box 80158, 3508 TD Utrecht, The Netherlands

5.1 Abstract

Previous studies have shown that stereocomplexed hydrogels are rapidly formed in situ by mixing aqueous solutions of eight-arm poly(ethylene glycol)-poly(L-lactide) and poly(ethylene glycol)-poly(D-lactide) star block copolymers (denoted as PEG-(PLLA)₈ and PEG-(PDLA)₈, respectively). In this study, *in vitro* and *in vivo* protein release from stereocomplexed hydrogels was investigated. These hydrogels were fully degradable under physiological conditions. Proteins could be easily loaded into the stereocomplexed hydrogels by mixing protein containing aqueous solutions of PEG-(PLLA)₈ and PEG-(PDLA)₈ copolymers. The release of the relatively small protein lysozyme (d_h is 4.1 nm)

¹ This chapter has been accepted for publication in *J. Controlled Release*, 2007.

followed first order kinetics and approximately 90% was released in 10 days. Bacteria lysis experiments showed that the released lysozyme had retained its activity. The relatively large protein IgG (d_h is 10.7 nm) could be released from stereocomplexed hydrogels with nearly zero order kinetics, wherein up to 50% was released in 16 days. The *in vitro* release of the therapeutic protein rhIL-2 from stereocomplexed hydrogels also showed nearly zero order kinetics, wherein up to 45% was released in 7 days. The therapeutic efficacy of stereocomplexed hydrogels loaded with 1×10^6 IU of rhIL-2 was studied using SL2-lymphoma bearing DBA/2 mice. The PEG-(PLLA)₈/PEG-(PDLA)₈/rhIL-2 mixture could be easily injected intratumorally. The released rhIL-2 was therapeutically effective as the tumor size was reduced and the cure rate was 30%, whereas no therapeutic effect was achieved when no rhIL-2 was given. However, the cure rate of rhIL-2 loaded stereocomplexed hydrogels was lower, though not statistically significant, compared to that of a single injection with 1×10^6 IU of free rhIL-2 at the start of the therapy (cure rate is 70%). The therapeutic effect of rhIL-2 loaded stereocomplexed hydrogels was retarded for approximately 1-2 weeks compared to free rhIL-2, most likely due to a slow, constant release of rhIL-2 from the hydrogels.

5.2 Introduction

Recombinant human IL-2 (rhIL-2) is a broadly acting T cell-derived cytokine with proven anti-tumor activity, especially after local administration, and is produced by recombinant DNA technology.¹ Local IL-2 therapy is most effective against cancer when injected intratumorally.² In a clinical phase II trial, patients with advanced nasopharyngeal carcinoma were treated with combined radiotherapy and local rhIL-2 immunotherapy. The patients received 15 injections of rhIL-2 (3 times 5 daily injections in week 2, 4 and 6). After five years 63% of the patients were tumor-free, whereas treatment with only radiotherapy resulted in 8% tumor-free patients.³ To avoid frequent and painful injections, a long acting protein delivery system is required.

Hydrogels have been used extensively as carriers for proteins, since their high water content renders them compatible with incorporated proteins and living tissue.⁴ Injectable, *in situ* forming hydrogels are particularly interesting, because they allow easy and homogeneous loading of proteins.⁵ Hydrogels can be formed by chemical and physical

crosslinking. In situ forming physically crosslinked hydrogels have been prepared by a variety of noncovalent interactions, including self-assembly through hydrophobic interactions of poly(ethylene glycol) based block copolymers⁶⁻⁸ or poly(N-isopropylacrylamide) (PNIPAAm) (co)polymers⁹⁻¹¹. Crosslinking by physical interactions proceeds under milder conditions as compared to chemical crosslinking, which requires the use of photo-irradiation, organic solvents, auxiliary crosslinking agents and/or other reactive molecules that may damage the proteins to be incorporated. Recently, hydrogels have been prepared in situ from water-soluble poly(L-lactide) (PLLA) and poly(D-lactide) (PDLA) based block copolymers, in which the physical crosslinks are provided by stereocomplexation between the enantiomeric PLLA and PDLA blocks.¹²⁻¹⁸ De Jong et al. have prepared stereocomplexed hydrogels from dextran-lactate graft copolymers¹⁴ and Li et al. have prepared stereocomplexed hydrogels based on PLA-PEG-PLA triblock copolymers¹⁵. These stereocomplexed hydrogels have many advantages, e.g. they can be formed in situ at physiological conditions (37 °C, pH 7.4) by simply mixing two aqueous enantiomer solutions, the gelation process is very mild in which both temperature and pH do not change, and they are biodegradable. Nevertheless, dextran-PLA stereocomplexed hydrogels require involved synthesis of dextran-PLA graft copolymers, and stereocomplexed hydrogels based on PLA-PEG-PLA triblock copolymers exhibit relatively slow gelation and low mechanical strength. Nevertheless, dextran-PLA stereocomplexed hydrogels require involved synthesis of dextran-PLA graft copolymers, and stereocomplexed hydrogels based on PLA-PEG-PLA triblock copolymers exhibit relatively slow gelation and low mechanical strength.

The use of hydrogels for the release of rhIL-2 has been investigated.¹⁷⁻¹⁹ Hanes et al. prepared rhIL-2 loaded microspheres by crosslinking of gelatin and chondroitin sulphate with glutaraldehyde. Release experiments *in vivo* using a brain tumor mice model showed a cure rate of 40%.¹⁹ De Groot et al. prepared rhIL-2 loaded dextran-(hydroxyethyl)methacrylate (dex-(HE)MA) hydrogels by redox initiated polymerization.¹⁷ When these hydrogels were used *in vivo* in SL2-lymphoma bearing DBA/2 mice, cure rates of 62% were obtained. Bos et al. studied release of rhIL-2 *in vivo* from stereocomplexed hydrogels based on dextran-L-lactate and dextran-D-lactate copolymers

in this SL2-DBA/2 tumor mice model.¹⁸ The therapeutic effect of rhIL-2 loaded hydrogels was at least comparable to injection of an equal dose with free rhIL-2 (cure rate of 60%).

We have previously reported on stereocomplexed hydrogels based on eight-arm PEG-PLA star block copolymers (PEG-(PLA)₈).^{13, 20} The PEG-(PLA)₈ copolymers could readily be prepared with controlled compositions. Upon mixing aqueous solutions of PEG-(PLLA)₈ and PEG-(PDLA)₈ copolymers, hydrogels with a high physical crosslinking density were rapidly formed. Rheological experiments showed that the hydrogel storage modulus increased with increasing PLA block length and polymer concentration, thus indicating a higher crosslinking density and a smaller hydrogel mesh size at higher PLA block length and higher polymer concentration. In this paper, the *in vitro* release of two model proteins with different hydrodynamic diameters, lysozyme and immunoglobulin G (IgG), were studied, as well as the release of the therapeutic protein rhIL-2. The therapeutic efficacy of rhIL-2 loaded stereocomplexed hydrogels was studied using the SL2 tumor mice model.

5.3 Materials and Methods

Materials. Eight-arm PEG-(PLLA)₈ and PEG-(PDLA)₈ star block copolymers were prepared as reported previously.¹³ Lysozyme (from hen egg white) was purchased from Fluka (Buchs, Switzerland) and bovine immunoglobulin G (IgG, fraction II) was purchased from ICN Biochemicals BV (Zoetermeer, The Netherlands). Recombinant human interleukin-2 (rhIL-2) was purchased from Chiron BV (Amsterdam, The Netherlands). When the white lyophilized powder is reconstituted with 1.2 ml of water each vial contains per ml solution: 1 mg (18×10^6 IU) of rhIL-2, 50 mg (5 w/v%) of mannitol, and 0.2 mg (0.02% w/v) of SDS, buffered with sodium phosphates to a pH of 7.5 (range 7.2-7.8).

Critical gel concentration. PEG-(PLA)₈ star block copolymer solutions were prepared with concentration increments of 2.5 w/v%, by dissolving the polymers overnight. Subsequently, solutions of equimolar amounts of PEG-(PLLA)₈ and PEG-(PDLA)₈ star block copolymers were mixed and equilibrated overnight. The critical gel concentrations were determined by inverting the vials. When the sample showed no flow within 20 s, it was regarded as a gel.

Hydrogel degradation/swelling tests. Stereocomplexed hydrogels (0.5 ml) containing equimolar amounts of PEG-(PLLA)₈ and PEG-(PDLA)₈ star block copolymers were prepared by mixing aqueous solutions of both polymers in HEPES buffered saline (pH 7.0, 100 mM, adjusted to 300 mOsm with NaCl, 0.02 wt% NaN₃) and equilibration overnight. Subsequently, 3 ml of HEPES buffered saline was applied on top of the hydrogels and the hydrogels were allowed to swell at 37 °C. The swelling experiment was performed in triplicate. The swollen hydrogels were weighed at regular time intervals after removal of excess buffer. After each weighing the buffer was refreshed. Similar degradation/swelling studies were performed at pH 5.0 using an ammonium acetate buffer (100 mM, adjusted to 300 mOsm with NaCl). The swelling ratio of the hydrogels was calculated from the initial hydrogel weight after preparation (W_0) and the swollen hydrogel weight after exposure to buffer (W_t):

$$\text{Swelling ratio} = \frac{W_t}{W_0}$$

In vitro release of model proteins. For the *in vitro* release of the model proteins lysozyme and IgG, 20 µl of a concentrated protein solution was added to both PEG-(PLLA)₈ and PEG-(PDLA)₈ solutions in HEPES buffered saline (pH 7.0) to a final protein concentration of 1 wt%. Stereocomplexed hydrogels (0.5 ml) were prepared by mixing the solutions of equimolar amounts of PEG-(PLLA)₈ and PEG-(PDLA)₈. After equilibration overnight, the hydrogels were transferred to cylindrically shaped vials with a flat bottom and a diameter of 8.8 mm, only exposing the upper surface of the hydrogel (device described in ref. ²¹). Subsequently, 3 ml of HEPES buffered saline was applied on top of the gels and the system was kept at 37 °C. Samples of 0.5 ml of the supernatant buffer were taken at regular time intervals (the first days after 30 min, 1 h, 2 h, 4 h, 8 h and 24 h, and subsequently after one to three days) and replaced by an equal volume of fresh buffer. Similar release experiments were performed at pH 5.0 using ammonium acetate buffered saline. The concentrations of lysozyme and IgG in the release samples were determined using the BCA® Protein assay.²² Standard protein solutions (concentration range 0.01-2 mg/ml) were prepared to generate calibration curves. Release samples (25 µl) were pipetted into a 96-microwells plate and 200 µl of working reagent (BCA reagent A: BCA reagent B, 50:1 v/v) was added. The plates were incubated for 30 min at 37 °C and then

cooled to room temperature. Finally, the absorbance at 550 nm was determined with a Microplate Manager ® (Bio-Rad Laboratories, Hercules, CA, USA).

The enzymatic activity of lysozyme was determined for a few release samples. The assay is based on the lysis of the outer cell membrane of *Micrococcus lysodeikticus*, resulting in solubilization of the affected bacteria and consequent decrease of light scattering.²³ The release samples were diluted to a concentration of 50-100 µg/ml and 10 µl of the sample was added to 1.3 ml of the bacteria suspension (0.2 mg/ml, HEPES buffered saline, pH 7.0). The decrease in turbidity was measured at 450 nm and the percent remaining enzymatic activity was determined by comparing the activity of the sample with that of a freshly prepared reference lysozyme solution (0.1 mg/ml).

In vitro release of rhIL-2. For the *in vitro* release of rhIL-2, 20 µl of a concentrated rhIL-2 solution was added to both PEG-(PLLA)₈ and PEG-(PDLA)₈ solutions in HEPES buffered saline (pH 7.0) to a final concentration of 12×10^6 IU of rhIL-2 per 0.5 ml of solution. Stereocomplexed hydrogels (0.5 ml) were prepared by mixing these solutions of equimolar amounts of PEG-(PLLA)₈ and PEG-(PDLA)₈. After equilibration overnight, the hydrogels were transferred to cylindrically shaped vials with a flat bottom and a diameter of 8.8 mm, only exposing the upper surface of the hydrogel. Subsequently, 3 ml of PBS (pH 7.2, 100 mM, adjusted to 300 mOsm with NaCl, 0.02 wt% NaN₃) was placed on top of the gels and the system was kept at 37 °C. PBS contained 0.01 wt% SDS to prevent precipitation of rhIL-2.²⁴ The concentration of rhIL-2 in the release samples was determined by reversed phase high-performance liquid chromatography (RP-HPLC) using a LC Module I system (Waters™) with an analytical column (Jupiter, 5 µm C4 300 A, 150 x 4.6 mm, including a SecurityGuard™ cartridge system with Widepore, C4, 4 x 3 mm). The rhIL-2 samples were centrifuged for 1 min (13,000 g) and 100 µl of the supernatant was applied on the column. A linear gradient was run from 40% A (water/acetonitrile 95:5 w/w; 100 mM sodium perchlorate (NaClO₄); 10 mM perchloric acid (HClO₄)) and 60% B (water/acetonitrile 5:95 w/w; 100 mM NaClO₄; 10 mM HClO₄) to 100% B in 10 min. The flow rate was set at 1.0 ml/min and the column oven was set at 30 °C. UV detection at a wavelength of 205 nm was applied or the fluorescent emission at 300 nm (excitation wavelength of 295 nm) was measured. Peak areas were determined with Millennium 2010V.2.15 software (Waters Associates Inc.). The total amount of oxidized and native

rhIL-2 was calculated by using a rhIL-2 calibration curve over the range of $1 \cdot 10^3$ - $92 \cdot 10^3$ IU of rhIL-2.

Animals and tumor cells. Inbred female DBA/2 mice (age 6-8 weeks) were obtained from Charles River France (Saint Aubin les Elbeuf, France) and were housed in filter-top cages. SL2 lymphosarcoma cells, originally arisen as a spontaneous tumor in DBA/2 mice, were propagated by intraperitoneal injection. After 7 days, tumor cells were harvested by peritoneal lavage with 5 ml of RPMI-1640 medium supplemented with 100 U/ml penicillin, 100 μ g/ml streptomycin and 100 μ g/ml neomycin sulphate. The cells were spun down and resuspended in medium after removal of the supernatant.

Animal model. 1×10^5 SL2 cells in 0.1 ml of medium were injected subcutaneously in DBA/2 mice and the tumors were allowed to grow for 11 days. Four different treatment groups were chosen. Two negative controls, group A (HEPES buffered saline, pH 7.0) and group B (PEG-(PLA₁₂)₈ hydrogels without rhIL-2), consisting of 10 and 4 mice, respectively, and one positive control, group C (free rhIL-2), consisting of 7 mice. The experimental group D (rhIL-2 loaded PEG-(PLA₁₂)₈ hydrogels) consisted of 10 mice. At day 0, group A was injected intratumorally with 400 μ l of HEPES buffered saline and group B with 400 μ l of empty PEG-(PLA₁₂)₈ hydrogel. Group C was injected intratumorally with 400 μ l of a rhIL-2 solution in HEPES buffered saline (1×10^6 IU/400 μ l) and group D with 400 μ l of rhIL-2 loaded hydrogel (1×10^6 IU/400 μ l). A single injection with 1×10^6 IU rhIL-2 was chosen for both the free rhIL-2 control and the rhIL-2 loaded hydrogel groups, as this dose is effective in SL2-lymphoma bearing DBA/2 mice.^{2, 35} Using this experimental setup, the therapeutic efficacies of rhIL-2 slowly released from the gel and free rhIL-2 administered by a single injection were compared. Stereocomplexed hydrogels were prepared by mixing rhIL-2 containing aqueous solutions of PEG-(PLLA₁₂)₈ and PEG-(PDLA₁₂)₈ in HEPES buffered saline. The mixture was injected intratumorally within 5 min of mixing. The therapeutic efficacy was measured by the reduction in the tumor size and the survival rate of the mice. When treated animals survived for more than 60 days without visible signs of tumors, they were considered to be cured.²

Ethics. The protocol of the animal experiments was approved by the ethics committee of the Faculty of Veterinary Sciences of the Utrecht University.

5.4 Results and Discussion

5.4.1 Star PEG-PLA stereocomplexed hydrogels.

Our previous studies showed that hydrogels were rapidly formed under physiological conditions upon mixing aqueous solutions of eight-arm poly(ethylene glycol)-poly(L-lactide) and eight-arm poly(ethylene glycol)-poly(D-lactide) star block copolymers (denoted as PEG-(PLLA)₈ and PEG-(PDLA)₈, respectively) via stereocomplexation of the PLLA and PDLA blocks.^{13, 20} In this study, PEG-(PLLA)₈ and PEG-(PDLA)₈ star block copolymers ($M_{n, PEG} = 21,800$) with 12, 14 and 15 lactyl units per PLA block were prepared. Stereocomplexed hydrogels were formed in situ by mixing aqueous solutions in HEPES buffered saline (pH 7.0) of equimolar amounts of PEG-(PLLA)₈ and PEG-(PDLA)₈ star block copolymers, when the polymer concentration was above the critical gel concentration (CGC). The CGCs for PEG-(PLA)₈ copolymers with 12, 14 and 15 lactyl units per PLA block were 7.5, 5 and 5 w/v%, respectively (as determined by vial tilting). Degradation/swelling tests, performed at 37 °C and pH 7.0, showed that the swelling of the stereocomplexed hydrogels increased over a period of 2 days (results not shown). After 2 days, the swelling could not be determined accurately, since the stereocomplexed hydrogels became too fragile to effectively remove all excess buffer and to subsequently weigh the stereocomplexed hydrogels. After 3 weeks a clear solution was obtained, showing that the stereocomplexed hydrogels fully degraded into water-soluble degradation products. In contrast, at pH 5.0 PLA degradation is substantially retarded²⁵ and the stereocomplexed hydrogels remained intact for 3 weeks, showing negligible swelling (results not shown). This indicates that the stereocomplexed hydrogels are initially physically stable and that the loss of the hydrogel integrity is associated with PLA degradation.

5.4.2 Release of model proteins *in vitro*.

The release of two model proteins, lysozyme (hydrodynamic diameter of 4.1 nm²⁶) and immunoglobulin G (IgG, hydrodynamic diameter of 10.7 nm²⁷) was studied at 37 °C and pH 7.0. Proteins could be easily loaded into the stereocomplexed hydrogels by mixing

protein containing aqueous solutions of PEG-(PLLA)₈ and PEG-(PDLA)₈ copolymers (Figure 1).

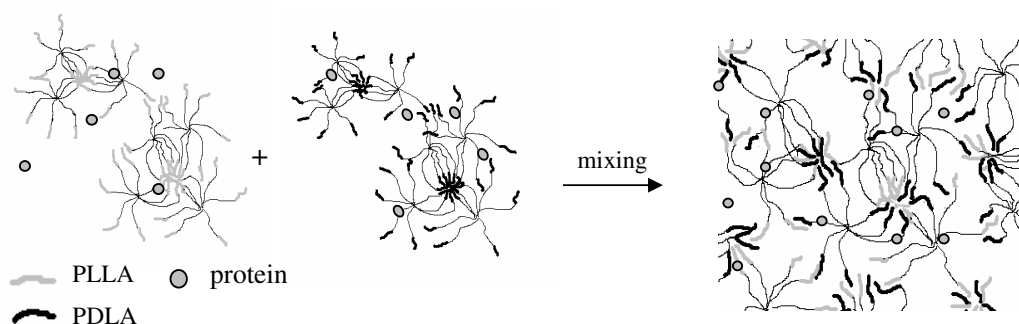


Figure 1. Preparation of protein loaded stereocomplexed hydrogels by mixing protein containing aqueous solutions of PEG-(PLLA)₈ and PEG-(PDLA)₈ star block copolymers.

In Figures 2a and 2b the release profiles of lysozyme from stereocomplexed PEG-(PLA)₈ hydrogels are shown as a function of polymer concentration and PLA block length, respectively. The release is proportional to the square root of time up to a cumulative release of approximately 80% irrespective of the polymer concentration or PLA block length, indicating that the release kinetics are first order (inserts in Figure 2a and 2b). Although this release profile suggests a typical diffusion-controlled release of a compound from a hydrogel²⁸, which has reached equilibrium swelling, the actual situation is more complex. The stereocomplexed hydrogels degrade in time, caused by removal of physical crosslinks, leading to increased swelling and final disintegration of the network. All these factors influence the release behavior of the protein. Lysozyme was released approximately 90% in 10 days. The release of lysozyme is hardly influenced by the polymer concentration and PLA block length, which indicates that the pores in the hydrogel are substantially larger than the hydrodynamic diameter of the protein (Figure 2a and 2b). Bacteria lysis experiments showed that the released lysozyme retained its activity (results not shown). This emphasizes the protein-friendly preparation process of the stereocomplexed hydrogels.

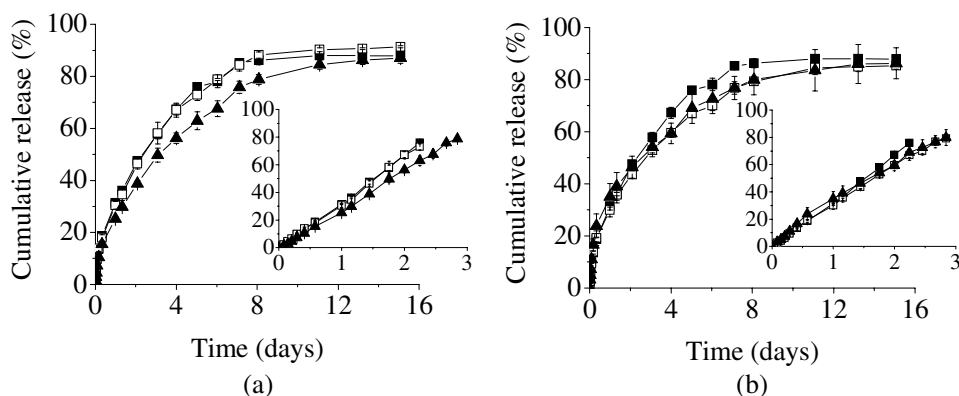


Figure 2. Cumulative release profiles of lysozyme from stereocomplexed PEG-(PLA)₈ hydrogels at 37 °C (average \pm S.D., $n = 3$). (a) PEG-(PLA₁₂)₈ hydrogels at pH 7.0 and initial polymer concentrations of 10 (■), 12.5 (□) and 15 w/v% (▲); (b), PEG-(PLA₁₂)₈ (■), PEG-(PLA₁₄)₈ (□) and PEG-(PLA₁₅)₈ (▲) hydrogels at pH 7.0 and 10 w/v% initial polymer concentration. The inserts show the cumulative release (%) as a function of the square root of time (days^{1/2}).

The release profile at pH 7.0 was similar to that at pH 5.0 (Figure 3), indicating that the release is mainly determined by diffusion rather than degradation of the hydrogel matrix. At pH 5.0 the hydrogel showed negligible swelling and degradation over the release period. In contrast, at pH 7.0 the hydrogels completely degraded over the release period. Most likely, the initial mesh size of the hydrogel is larger than the hydrodynamic diameter of lysozyme (4.1 nm) and the release at pH 5.0 is diffusion-controlled.

Figure 4a shows that stereocomplexed PEG-(PLA₁₂)₈ and PEG-(PLA₁₄)₈ hydrogels at 12.5 w/v% polymer concentration release IgG with nearly zero order release kinetics during the first 16 days. Stereocomplexed PEG-(PLA₁₄)₈ hydrogels with a polymer concentration of 7.5 w/v% show a biphasic release. The release kinetics were nearly zero order up to 5 days, whereafter the release was accelerated, and the release kinetics became close to first order. It should be noted that the acceleration in the release was observed only for hydrogels formed at a lower polymer concentration of 7.5 w/v%. The acceleration in the release is probably caused by partial disintegration and/or fragmentation of the network due to PLA degradation. The lower release rate at 12.5 w/v% polymer concentration

compared to 7.5 w/v% polymer concentration is most likely due to a smaller initial hydrogel pore size as well as a slower degradation of the hydrogel at 12.5 w/v% polymer concentration. The lower release rate at higher polymer concentration is in line with previous rheological experiments, which showed increased hydrogel storage moduli at increased polymer concentration.²⁰ The lower release rate at higher polymer concentration is in line with previous rheological experiments, which showed increased hydrogel storage moduli at increased polymer concentration,²⁰ The release of IgG, using corresponding hydrogels, was much slower than the release of lysozyme. After 16 days up to 50% and approximately 60% IgG was released from stereocomplexed hydrogels at 12.5 and 7.5 w/v% polymer concentration, respectively. The slow, constant release of IgG is most likely due to a combination of diffusion and degradation/swelling. It should be noted that after 3 weeks, IgG was not completely retrieved. This may be due to interaction with hydrophobic domains and partial denaturation during the release experiment.²⁹ At pH 5.0 a small burst effect is observed for the release of IgG, while at pH 7.0 the initial release is almost linear in time (Figure 4b). Surprisingly, a faster release of IgG is observed at pH 5.0 compared to pH 7.0, despite the fact that PLA degrades slower at pH 5.0 compared to pH 7.0. IgG is known to destabilize at pH values that deviate from neutral due to conformational changes.³⁰ Our release data suggest that at pH 5.0 smaller, more compact IgG structures are formed compared to pH 7.0. Vermeer et al. have observed the formation of small, compact IgG structures at pH 2.0.³¹

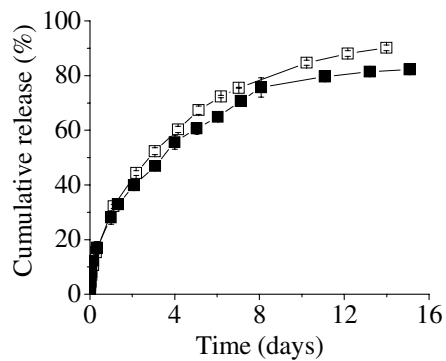


Figure 3. Cumulative release profiles of lysozyme from stereocomplexed PEG-(PLA₁₄)₈ hydrogels at 12.5 w/v% initial polymer concentration, 37 °C and pH 7.0 (■) or pH 5.0 (□) (average ± S.D., n = 3).

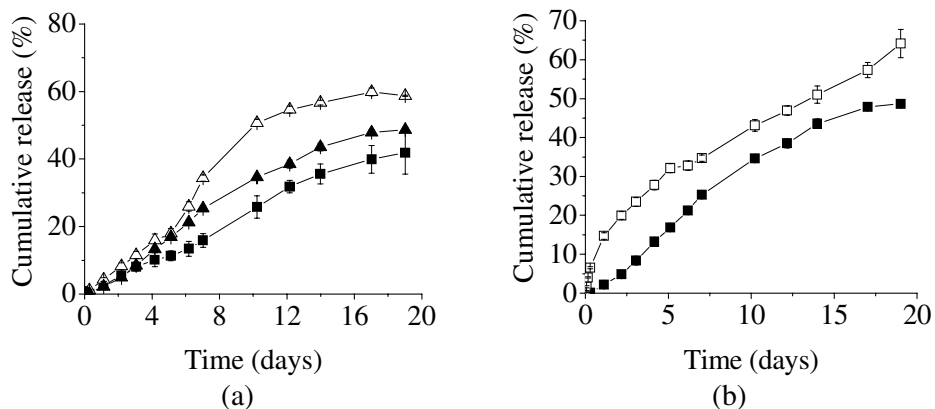


Figure 4. Cumulative release profiles of IgG from stereocomplexed PEG-(PLA)₈ hydrogels at 37 °C (average ± S.D., n = 3). (a) PEG-(PLA₁₂)₈ hydrogel at 12.5 w/v% initial polymer concentration (■) and PEG-(PLA₁₄)₈ hydrogel at initial polymer concentrations of 7.5 (△) and 12.5 w/v% (▲) at pH 7.0; (b) PEG-(PLA₁₄)₈ hydrogels at 12.5 w/v% initial polymer concentration and pH 7.0 (■) or pH 5.0 (□).

5.4.3 Release of rhIL-2 *in vitro*.

RhIL-2 was released *in vitro* from stereocomplexed PEG-(PLA₁₂)₈ and PEG-(PLA₁₄)₈ hydrogels. The amount of rhIL-2 in the release samples was determined with HPLC using both UV and fluorescence detection. Figure 5a shows that the incorporated rhIL-2 was released with almost zero order kinetics from stereocomplexed PEG-(PLA₁₂)₈ hydrogels up to 7 days, independent of the polymer concentration. Lysozyme and rhIL-2 have similar molecular weights (14.6 kDa and 15.3 kDa, respectively) and therefore similar release kinetics were expected for these proteins. The difference in release kinetics of rhIL-2 and lysozyme may be due differences in hydrophobicity as well as formation of rhIL-2 dimers and/or larger hydrodynamic size of rhIL-2 due to SDS interaction.²⁴ The release of rhIL-2 from stereocomplexed PEG-(PLA₁₂)₈ hydrogels is not influenced by the polymer concentration, which is most likely because rhIL-2, similar to lysozyme, is substantially smaller than the hydrogel mesh size. The cumulative release profiles measured with UV and fluorescence detection were similar up to 6 days. However, fluorescence detection showed approximately 5-10% higher release at later time points, due to a higher sensitivity (results not shown), resulting in a cumulative release of approximately 45 and 50% in 7 and 10 days, respectively. The cumulative release from stereocomplexed PEG-(PLA₁₄)₈ hydrogels was approximately 5-20% lower compared to stereocomplexed PEG-(PLA₁₂)₈ hydrogels and increased with decreasing polymer concentration (Figure 5b, measured with UV detection). RhIL-2 is a relatively hydrophobic protein. The longer and more hydrophobic PLA blocks may therefore have caused increased interaction with rhIL-2, especially at increased polymer concentration. Generally, the cumulative release of rhIL-2 did not reach 100% when all hydrogel material had been dissolved, which may be due interaction with hydrophobic domains and partial denaturation during the release experiment. Low retrieval of rhIL-2 was also reported by Bos et al., who obtained a cumulative release of approximately 65% for stereocomplexed dextran-lactate hydrogels.¹⁸

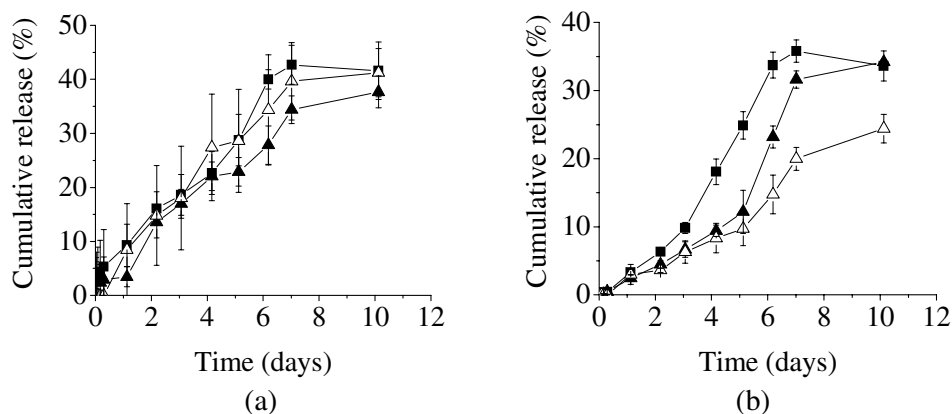


Figure 5. Cumulative release profiles of rhIL-2 from stereocomplexed PEG-(PLA)₈ hydrogels at 37 °C and pH 7.2 (average \pm S.D., $n = 3$). (a) PEG-(PLA₁₂)₈ hydrogels at initial polymer concentrations of 10 (■), 12.5 (▲) and 15 w/v% (△); (b) PEG-(PLA₁₄)₈ hydrogels at initial polymer concentrations of 7.5 (■), 10 (▲) and 12.5 w/v% (△).

5.4.4 Animal model.

DBA/2 mice were injected subcutaneously with 1×10^5 SL2 lymphosarcoma cells and the tumors were allowed to grow for 11 days before starting the experiments. At day 0, immunotherapy was started on mice bearing tumors of 44–176 mm² (average 100 mm², corresponding to 4% of the body weight). Stereocomplexed PEG-(PLA₁₂)₈ hydrogels with 10 w/v% polymer concentration were selected for the further *in vivo* release study because they showed a close to zero-order release of rhIL-2 *in vitro* and a higher cumulative release of rhIL-2 *in vitro* as compared to PEG-(PLA₁₄)₈ hydrogels. RhIL-2 loaded (1×10^6 IU) stereocomplexed hydrogels or a solution of free rhIL-2 (1×10^6 IU) in HEPES buffered saline (pH 7.0) were injected intratumorally. The stereocomplexed hydrogels were prepared by mixing rhIL-2 containing solutions of PEG-(PLLA₁₂)₈ and PEG-(PDLA₁₂)₈ in HEPES buffered saline and intratumorally injected within 5 min of mixing. This time was considered optimal, since the mixtures still had a low viscosity, which allowed easy injection, while after 5 min the injection became increasingly difficult. The therapeutic efficacy of rhIL-2 loaded stereocomplexed PEG-(PLA₁₂)₈ hydrogels was measured by the

reduction in the average tumor size (Figure 6) as well as by the survival rate of the mice (Figure 7). All *in vivo* data was analyzed by Kaplan-Meier statistics. Figure 6 shows that the tumors of the negative control groups (administered HEPES buffered saline or empty 10 w/v% PEG-(PLA₁₂)₈ hydrogel) grew rapidly compared to the positive control group (administered free rhIL-2 in HEPES buffered saline) and the experimental group (administered rhIL-2 loaded hydrogel). The size of the tumors of the free rhIL-2 treated group stabilized at day 3 and 1, 3 and 5 out of 7 mice were tumor-free after 10, 17 and 24 days of treatment, respectively (data not shown). The size of the tumors of the rhIL-2 loaded stereocomplexed hydrogels stabilized around day 17 and 2 and 3 out of 10 mice were tumor-free after 24 and 31 days of treatment, respectively (data not shown). This difference in timing and number of mice becoming tumor-free was statistically significant ($p = 0.01$, data not shown). In Figure 6 the small increase in the average tumor size between day 31 and 45 in the rhIL-2-loaded stereocomplexed hydrogels treated group is caused by a single mouse with progressive disease after a partial regression of tumor growth prior to day 31. At day 45 this mouse died, and the other mice of this group remained tumor-free.

The Kaplan-Meier survival curves show a statistically significant ($p < 0.05$) higher cure rate in the experimental group (30% cures) and positive control group (70% cures) compared to the negative controls (0% cures), wherein most mice died after 6 to 13 days (Figure 7). The hazard ratios of rhIL-2 loaded hydrogel and free rhIL-2 are 0.30 and 0.14, respectively. The difference in cure rate of the rhIL-2 loaded stereocomplexed PEG-(PLA₁₂)₈ hydrogels and free rhIL-2 is not statistically significant ($p = 0.15$). These results show that rhIL-2 loaded stereocomplexed hydrogels as well as free rhIL-2 have a therapeutic effect on SL2 tumor bearing mice. Both treatments reduce tumor size, induce tumor regression and increase the cure rate. The data on tumor size and survival (Figure 6 and Figure 7) indicate that the therapeutic effect of rhIL-2 loaded stereocomplexed hydrogels, though clearly present, is significantly retarded compared to free rhIL-2. Remarkably, rhIL-2 loaded stereocomplexed hydrogels have a similar therapeutic effect in the SL2-lymphoma bearing mice model as 5 subsequent daily injections with 1×10^5 IU of free rhIL-2 (unpublished results). The *in vitro* release experiments showed that during the first five days a similar amount of rIL-2 is released every day (Figure 5a). Therefore, the retardation of the therapeutic effect of rhIL-2 loaded stereocomplexed hydrogels compared

to free rhIL-2 is most likely due to a slow, constant release of rhIL-2 from the hydrogels. Bos et al. showed that the therapeutic efficacy of rhIL-2 loaded stereocomplexed dextran-lactate hydrogels is at least equal to free rhIL-2.¹⁸ However, *in vitro* release studies showed that these stereocomplexed dextran-lactate hydrogels released 50% of the rhIL-2 within a few hours. In the SL2 mice model the tumor grows rapidly and most of the mice of the negative control groups (no rhIL-2) had already died before the rhIL-2 released from the stereocomplexed hydrogels started to stabilize tumor growth at day 10. Fast growing tumors in humans and veterinary animals do not grow as fast as the SL2 tumor in mice. Therefore, patients may benefit from a slow release system giving a prolonged therapy compared to a single injection of free rhIL-2. The results obtained on the stereocomplexed PEG-(PLA₁₂)₈ hydrogels suggest that treatment may be improved by one injection of free rhIL-2 followed by slow release of rhIL-2 from the PEG-(PLA₁₂)₈ stereocomplexed hydrogel. Further study is needed to optimize the dose of rhIL-2 in the hydrogel.

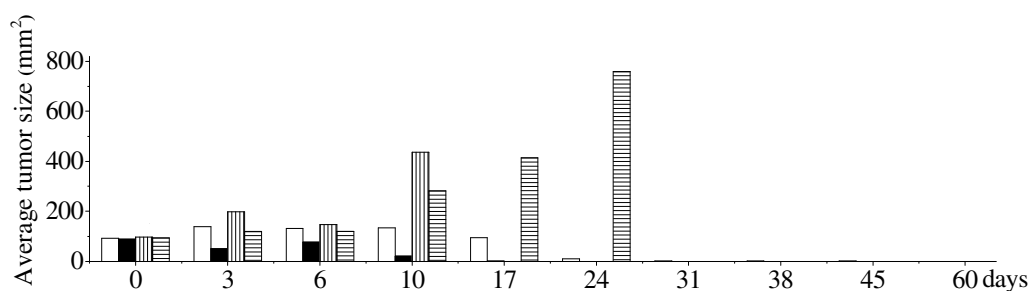


Figure 6. Average absolute tumor size by group of SL2 tumor bearing mice injected intratumorally with □, an in situ forming stereocomplexed PEG-(PLA₁₂)₈ hydrogel at 10 w/v% initial polymer concentration loaded with 1×10^6 IU of rhIL-2 (n = 10); ■, a solution of 1×10^6 IU of rhIL-2 in HEPES buffered saline (n = 7); ▨, an in situ forming, empty stereocomplexed PEG-(PLA₁₂)₈ hydrogel at 10 w/v% polymer concentration (n = 4); ▤, HEPES buffered saline (n = 10).

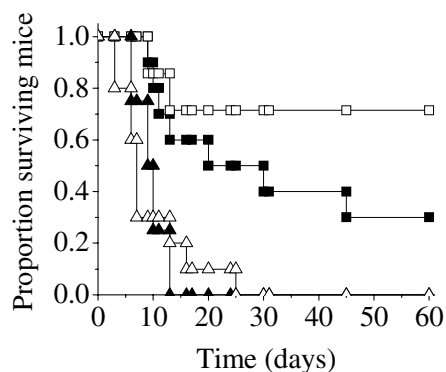


Figure 7. Kaplan-Meier survival curves of SL2 tumor bearing mice injected intratumorally with an in situ forming stereocomplexed PEG-(PLA₁₂)₈ hydrogel at 10 w/v% initial polymer concentration loaded with 1×10^6 IU of rhIL-2 (n = 10) (■); a solution of 1×10^6 IU of rhIL-2 in HEPES buffered saline (n = 7) (□); an in situ forming, empty stereocomplexed PEG-(PLA₁₂)₈ hydrogel at 10 w/v% polymer concentration (n = 4) (▲); HEPES buffered saline (n = 10) (△).

5.5 Conclusions

Stereocomplexed PEG-PLA hydrogels were rapidly formed in situ by mixing aqueous solutions of PEG-(PLLA)₈ and PEG-(PDLA)₈ star block copolymers. These hydrogels degraded under physiological conditions and the single enantiomeric solutions had a low viscosity, thus allowing easy injection. Proteins could be easily loaded into the stereocomplexed hydrogels by mixing protein containing aqueous solutions of PEG-(PLLA)₈ and PEG-(PDLA)₈ copolymers. The *in vitro* release of the relatively small protein lysozyme (d_h is 4.1 nm) followed first order kinetics, wherein a high cumulative release of approximately 90% was obtained in 10 days. Importantly, the released lysozyme retained its enzymatic activity, emphasizing the protein-friendly hydrogel preparation method. The larger protein IgG (d_h is 10.7 nm) could be released *in vitro* with nearly zero order kinetics for 16 days. The release of the therapeutic protein rhIL-2 followed almost zero order kinetics for 7 days, wherein up to 45% was released. The therapeutic efficacy of rhIL-2 loaded stereocomplexed PEG-PLA hydrogels was demonstrated using mice bearing fast growing, large malignant tumors. The PEG-(PLLA)₈/PEG-(PDLA)₈/rhIL-2 mixtures could

be easily injected intratumorally. Compared to injection with free rhIL-2, the therapeutic effect of the released protein started approximately 1-2 weeks later, indicating that the stereocomplexed PEG-PLA hydrogels act as a slow releasing depot of rhIL-2. Combining a single injection with free rhIL-2 with slow release of rhIL-2 from the stereocomplexed hydrogels may be a promising alternative for the current standard therapy wherein frequent, painful injections with free rhIL-2 are given.

5.5.1 Acknowledgements

This work was funded by the Netherlands Organization for Scientific Research (NWO).

5.6 References

1. Bernsen, M. R.; Tang, J. W.; Everse, L. A.; Koten, J. W.; Den Otter, W., Interleukin 2 (IL-2) therapy: potential advantages of locoregional versus systemic administration. *Cancer Treat. Rev.* 1999 25 73-82.
2. Jacobs, J. L. L., Sparingdam, D.; Den Otter, W., Local interleukin 2 therapy is most effective against cancer when injected intratumorally. *Cancer Immunol. Immunother.* 2005, 54, 647-654.
3. Jacobs, J. J. L.; Hordijk, G. J.; Jurgentliemk-Schulz, I. M.; Terhaard, C. H. J.; Koten, J. W.; Battermann, J. J.; Den Otter, W., Treatment of stage III-IV nasopharyngeal carcinomas by external beam irradiation and local low doses of IL-2. *Cancer Immunol. Immunother.* 2005, 54 792-798.
4. Peppas N. A., Bures, P.; Leobandung, W.; Ichikawa, H., Hydrogels in pharmaceutical formulations, *Eur. J. Pharm. Biopharm.* 2000, 50 27-46.
5. Chitkara, D.; Shikanov, A., Kumar, N.; Domb, A. J., Biodegradable injectable in situ depot-forming drug delivery systems. *Macromol. Biosci.* 2006, 6, 977-990.
6. Jeong, B.; Bae, Y. H.; Lee, D. S.; Kim, S. W., Biodegradable block copolymers as injectable drug-delivery systems. *Nature* 1997, 388, 860-862.
7. Jeong, B.; Bae, Y. H.; Kim, S. W., Thermoreversible gelation of PEG-PLGA-PEG triblock copolymer aqueous solutions. *Macromolecules* 1999, 32, 7064-7069.

8. Zhong, Z. Y.; Dijkstra, P. J.; Feijen, J.; Kwon, Y. M.; Bae, Y. H.; Kim, S. W., Synthesis and aqueous phase behavior of thermoresponsive biodegradable poly(D,L-3-methylglycolide)-block-poly(ethylene glycol)-block-poly(D,L-3-methylglycolide) triblock copolymers. *Macromol. Chem. Phys.* 2002, 203, 1797-1803.
9. Kim, S.; Healy, K. E.; Synthesis and characterization of injectable poly(N-isopropylacrylamide-co-acrylic acid) hydrogels with proteolytically degradable cross-links. *Biomacromolecules* 2003, 4, 1214-1223.
10. Lee, B. H.; West, B.; McLemore, R.; Pauken, C.; Vernon, B. L., In-situ injectable physically and chemically gelling NIPAAm-based copolymer system for embolization. *Biomacromolecules* 2006, 7, 2059-2064.
11. Liu, Y. Y.; Shao, Y. H.; Lu, J., Preparation, properties and controlled release behaviors of pH-induced thermosensitive amphiphilic gels. *Biomaterials* 2006, 27, 4016-4024.
12. Grijpma, D. W.; Feijen, J., Hydrogels by stereo-complexation of water-soluble PLLA-PEO-PLLA and PDLA-PEO-PDLA triblock-copolymers. *J. Controlled Release* 2001, 72, 247-249.
13. Chapter 3, Hiemstra, C.; Zhong, Z. Y.; Dijkstra, P. J.; Feijen, J., Stereocomplex mediated gelation of PEG-(PLA)₂ and PEG-(PLA)₈ block copolymers. Published in *Macromol. Symp.* 224, 2005, 119-132.
14. de Jong, S. J.; De Smedt, S. C.; Demeester, J.; van Nostrum, C. F.; Kettenes-van den Bosch, J. J.; Hennink, W. E., Biodegradable hydrogels based on stereocomplex formation between lactic acid oligomers grafted to dextran. *J. Controlled Release* 72, 2001, 47-56.
15. Li, S. M.; El Ghzaoui, A.; Dewinck, E., Rheology and drug release properties of bioresorbable hydrogels prepared from polylactide/poly(ethylene glycol) block copolymers. *Macromol. Symp.* 2005, 222, 23-36.
16. Mukose, T.; Fujiwara, F.; Nakano, J.; Taniguchi, I.; Miyamoto, M.; Kimura, Y.; Teraoka, I.; Lee, C. W., Hydrogel formation between enantiomeric B-A-B-type block copolymers of polylactides (PLLA or PDLA: A) and polyoxyethylene (PEG: B); PEG-PLLA-PEG and PEG-PDLA-PEG. *Macromol. Biosci.* 2004, 4, 361-367.

17. De Groot, C. J.; Cadee, J. A.; Kolen, J. W.; Hennink, W. E.; Den Otter, W., Therapeutic efficacy of IL-2-loaded hydrogels in a mouse tumor model. *Int. J. Cancer* 2002, 98, 134-140.
18. Bos, G. W.; Jacobs, J. L. L.; Kolen, J. W.; Van Tomme, S. R.; Veldhuis, T. F. J.; van Nostrum, C. F.; Den Otter, W.; Hennink, W. E., In situ crosslinked biodegradable hydrogels loaded with IL-2 are effective tools for local IL-2 therapy. *Eur. J. Pharm. Sci.* 2004, 21, 561-567.
19. Hanes, J.; Sills, A.; Zhao, Z.; Suh, K. W.; Tyler, B.; DiMeco, F.; Brat, D. J.; Choti, M. A.; Leong, K. W.; Pardoll, D. M.; Brem, H., Controlled local delivery of interleukin-2 by biodegradable polymers protects animals from experimental brain tumors and liver tumors. *Pharm. Res.* 2001, 18, 899-906.
20. Chapter 4, Hiemstra, C.; Zhong, Z. Y.; Li, L.; Dijkstra, P. J.; Feijen, J., In-situ formation of biodegradable hydrogels by stereocomplexation of PEG-(PLLA)₈ and PEG-(PDLA)₈ star block copolymers. Published in *Biomacromolecules* 2006, 7, 2790-2795.
21. Van Tomme, S. R.; de Geest, B. G.; Braeckmans, K.; De Smedt, S. C.; Siepmann, F.; Siepmann, J.; van Nostrum, C. F.; Hennink, W. E., Mobility of model proteins in hydrogels composed of oppositely charged dextran microspheres studied by protein release and fluorescent recovery after photobleaching. *J. Controlled Release* 110, 2005, 67-78.
22. Smith, P. K.; Krohn, R. I.; Hermanson, G. T.; Mallia, A. K.; Gartner, F. H.; Provenzano, M. D.; Fujimoto, E. K.; Goeke, N. M.; Olson, B. J.; Klenk, D. C.; Measurement of protein using bicinchoninic acid. *Anal. Biochem.* 1985, 150, 237-245.
23. Shih, P.; Malcolm, B. A.; Rosenberg, S.; Kirsch, J. F.; Wilsow, A. C., Reconstruction and testing of ancestral proteins. *Methods Enzymol.* 224 (1993) 576-590.
24. Cadee, J. A.; De Groot, C. J.; Jiskoot, W.; Den Otter, W.; Hennink, W. E., Release of recombinant human interleukin-2 from dextran-based hydrogels. *J. Controlled Release* 2002, 78, 1-13.
25. de Jong, S. J.; Arias, E. R.; Rijkers, D. T. S.; van Nostrum, C. F.; Kettenes-van den Bosch, J. J.; Hennink, W. E., New insights into the hydrolytic degradation of

- poly(lactic acid): participation of the alcohol terminus. *Polymer* 2001, 42, 2795-2802.
26. Merrill, E. W.; Dennison, K. A.; Sung, C., Partitioning and diffusion of solutes in hydrogels of poly(ethylene oxide). *Biomaterials* 1993, 14, 1117-1126.
 27. Burczak, K.; Fujisato, T.; Hatada, M.; Ikada, Y., Protein permeation through poly(vinyl alcohol) hydrogel membranes, *Biomaterials* 1994, 15, 231-238.
 28. Siepmann, J.; Peppas, N., Modeling of drug release from delivery systems based on hydroxypropyl methylcellulose (HPMC). *Adv. Drug Deliv. Rev.* 2001, 48, 139-157.
 29. Vermeer, A. W. P.; Norde, W.; van Amerongen, A., The unfolding/denaturation of immunoglobulin of isotype 2b and its F-ab and F-c fragments. *Biophys. J.* 79, 2000, 2150-2154.
 30. Chen, C. C.; Chang, H. M., Effect of thermal protectants on the stability of bovine milk immunoglobulin G. *J. Agr. Food Chem.* 1998, 46, 3570-3576.
 31. Vermeer, A. W. P.; Norde, W., The thermal stability of immunoglobulin: Unfolding and aggregation of a multi-domain protein. *Biophys. J.* 2000, 78, 394-404.

Chapter 6

Rapidly in situ forming biodegradable robust hydrogels by combining stereocomplexation and photocrosslinking

Christine Hiemstra^a, Zhiyuan Zhong^{a*}, Mariëlle Wouters^b, and Jan Feijen^{a*}

^a Department of Polymer Chemistry and Biomaterials, Faculty of Science and Technology, Institute for Biomedical Technology, University of Twente, P. O. Box 217, 7500 AE Enschede, The Netherlands

^b TNO Science and Industry, P. O. Box 6235, 5600 HE, Eindhoven, The Netherlands

6.1 Abstract

Our previous studies have shown that stereocomplexed hydrogels can be rapidly formed *in vitro* as well as *in vivo* upon mixing aqueous solutions of eight-arm poly(ethylene glycol)-poly(L-lactide) (PEG-PLLA) and poly(ethylene glycol)-poly(D-lactide) (PEG-PDLA) star block copolymers. In this paper, stereocomplexation and photopolymerization are combined to yield rapidly in situ forming robust hydrogels. Two types of methacrylate functionalized PEG-PLLA and PEG-PDLA star block copolymers, PEG-PLLA-MA and PEG-PDLA-MA, which have methacrylate groups at the PLA chain ends and PEG-MA/PLLA and PEG-MA/PDLA, which have methacrylate groups at the PEG chain ends, were designed and prepared. Results showed that stereocomplexed hydrogels could be rapidly formed (within 1-2 min) in a polymer concentration range of 12.5 to 17.5 w/v%, in which the methacrylate group hardly interfered with the stereocomplexation. When subsequently photopolymerized, these hydrogels showed largely increased storage moduli as compared to the corresponding hydrogels that were crosslinked by stereocomplexation or photopolymerization only. Interestingly, the storage modulus of stereocomplexed-photopolymerized PEG-PLA-MA hydrogels increased linearly with increasing stereocomplexation equilibration time prior to photopolymerization (from approximately 6

to 32 kPa), indicating that stereocomplexation aids in photopolymerization. Importantly, photopolymerization of stereocomplexed hydrogels could take place at very low initiator concentrations (0.003 wt%). Swelling/degradation studies showed that combining stereocomplexation and photopolymerization yielded hydrogels with prolonged degradation times as compared to corresponding hydrogels crosslinked by photopolymerization only (3 vs. 1.5 weeks). Stereocomplexed-photopolymerized PEG-MA/PLA hydrogels degraded much slower than corresponding PEG-PLA-MA hydrogels, with degradation times ranging from 7 to more than 16 weeks. Therefore, combining stereocomplexation and photopolymerization is a novel approach to obtain rapidly in situ forming robust hydrogels.

6.2 Introduction

Hydrogels have been widely used for biomedical applications, such as tissue engineering and drug delivery, due to their favorable characteristics.¹⁻³ Hydrogels are water-swollen networks of crosslinked hydrophilic polymers. Their high water content renders them highly biocompatible and also leads to minimal adsorption of proteins. The mechanical properties of hydrogels parallel those of soft tissues, making them particularly interesting for tissue engineering. Hydrogels may be formed in situ, thus allowing easy mixing of cells and bioactive molecules, such as proteins, with the polymer solutions prior to gelation.⁴⁻⁶ Moreover, in situ hydrogel formation enables the preparation of complex shapes and use of minimally invasive surgery. In situ forming hydrogels have been prepared by physical and chemical crosslinking methods. Physically crosslinked hydrogels include those based on hydrophobic interactions between thermosensitive block or graft polymers⁷⁻¹¹, stereocomplexation between poly(L-lactide) (PLLA) and poly(D-lactide) (PDLA) graft¹² and block copolymers¹³⁻¹⁵, inclusion complexation using α -dextrin polymers¹⁶⁻²⁰, and ionic interactions between oppositely charged microparticles²¹ or peptides²². The crosslinking conditions for these gels are generally very mild, thus allowing the entrapment of labile compounds, such as proteins. However, in general they are mechanically weak compared to chemically crosslinked hydrogels and changes in the external environment (e.g. ionic strength, pH, temperature) may give rise to disruption of the network.

Chemically crosslinked hydrogels have been formed in situ by Michael addition between thiols and acrylates or vinyl sulfones²³⁻²⁹, reaction between aldehydes and dihydrazides³⁰ or amines³¹, reaction between activated esters and amines³² and redox initiated radical chain polymerization of (meth)acrylates³³⁻³⁷. Photopolymerization of (meth)acrylates⁵ using UV-light³⁸⁻⁴¹ or visible light⁴²⁻⁴⁴ has been mostly used for in situ formation of chemically crosslinked hydrogels. Biodegradable hydrogels prepared by photocrosslinking of poly(ethylene glycol)-poly(lactide) (PEG-PLA) diacrylate derivatives were first reported by the group of Hubbell.⁴² More recently, this group has prepared degradable hydrogels by the incorporation of plasmin degradable peptide sequences.^{39, 43} When modified with cell-adhesive RGD peptide sequences, these hydrogels supported three-dimensional outgrowth of human fibroblasts embedded as a cluster within the hydrogel. Another type of degradable hydrogel was prepared by copolymerization of a hyaluronic acid methacrylate derivative and PEG diacrylate.⁴⁴ Fibroblasts adhered and proliferated when cultured on the RGD functionalized hydrogels. The group of Anseth has done much work on degradable hydrogels based on PEG-PLA dimethacrylates.⁴⁰ It was shown that by using combinations of PEG and PEG-PLA dimethacrylates and/or by changing the PLA block length, the hydrogel degradation rate, compressive modulus and crosslinking density could be tuned to provide suitable scaffolds for cartilage tissue engineering.⁴¹ The major advantage of photopolymerization is the spatial and temporal control over the polymerization. However, photopolymerization *in vivo* is hampered by the absorption of UV-light by the skin (> 99%). In clinical applications, fast gelation is desired to prevent diffusion of hydrogel precursors or bioactive molecules to the surrounding tissue. Elisseff et al. have reported on transdermal photopolymerization of a 20 wt% PEG dimethacrylate aqueous solution injected subcutaneously into nude mice by UV-irradiation for 3 min at 2 mW/cm² incident light intensity.⁴⁵ In this study, high molecular weight PEG (100,000) was used as an additive to prevent rapid diffusion of the gel precursors after injection and to increase the mechanical properties of the photopolymerized hydrogel. A drawback is that it is very difficult to excrete high molecular weight PEG by the kidneys.⁴⁶ Elisseff et al. have studied the UV-light attenuation by the skin using swine skin as a model.⁴⁷ The incident light intensity of 100 mW/cm² was attenuated by the skin to approximately 0.05 mW/cm². After 3 min of UV-irradiation of a 20 wt% PEG dimethacrylate aqueous solution with 0.04 wt% photoinitiator concentration, a conversion of approximately 10% was reached. The

remaining unsaturated bonds may cause toxicity problems and the incomplete conversion may result in hydrogels with weak mechanical properties.⁴⁸ The polymerization rate may be increased by increasing the photoinitiator concentration or the intensity of the incident light. However, due to their toxicity photoinitiators can only be used at low concentrations (approximately 0.01-0.05 wt%)⁴⁹ and the intensity of the UV-light is limited to approximately 5-10 mW/cm² to prevent cell damage. Visible light is less attenuated by the skin, but efficient initiators with less cytotoxicity are required.^{49, 50} Another problem of photopolymerization is that fast polymerization is generally accompanied by substantial heat effects.⁴⁸ The resulting temperature rise may cause local cell morbidity and tissue necrosis surrounding the implant.

In this paper, we have combined two crosslinking methods, i. e. stereocomplexation and photopolymerization, to achieve fast *in situ* forming, robust hydrogels. Stereocomplexation provides fast gelation *in vitro* and *in vivo*^{13, 51, 52}, allowing for lower photopolymerization rates, providing easier handling, limiting the local temperature rise and potentiating the use of low initiator concentrations and low light intensities. Moreover, photopolymerization provides robust hydrogels, with increased mechanical properties and prolonged degradation times compared to hydrogels crosslinked by stereocomplexation only.⁵¹ Interestingly, our results show that stereocomplexation aids in the photopolymerization of methacrylate groups, resulting in hydrogels with increased storage moduli and degradation times compared to the corresponding hydrogels that were formed by photopolymerization only.

6.3 Materials and Methods

Materials. L-lactide and D-lactide were obtained from Purac and recrystallized from dry toluene. Eight-arm star PEG ($M_{n, NMR} = 21,800$) was supplied by Nektar and used as received. The single site Zn-complex catalyst ($Zn(Et)[OC_6H_4(CH_2N(Me)_2)_2-2, Me-4]$) was kindly provided by Professor G. van Koten of the University of Utrecht (The Netherlands). Methacrylic anhydride was purchased from Merck and Irgacure 2959 from Ciba Specialty Chemicals. Both were used as received. Dichloromethane and triethylamine (TEA) were dried over calcium hydride and potassium hydroxide, respectively, and distilled prior to

use. Eight-arm poly(ethylene glycol)-poly(L-lactide) and poly(ethylene glycol)-poly(D-lactide) star block copolymers with 12 lactyl units per poly(lactide) (PLA) block (PEG-PLLA₁₂ and PEG-PDLA₁₂, respectively) were prepared as reported previously (M_n , PEG = 21,800).⁵³

Synthesis. PEG-PLLA₁₂-MA and PEG-PDLA₁₂-MA were synthesized by partial methacrylation of the hydroxyl groups of PEG-PLLA₁₂ and PEG-PDLA₁₂, respectively, according to the procedure reported by Lin-Gibson et al.⁵⁴ Typically, PEG-PLLA₁₂ (5.0 g, 0.174 mmol, dried overnight under vacuum over phosphorous pentoxide) was dissolved in 18 ml of dichloromethane. A solution of TEA (0.171 g, 1.690 mmol) in 1 ml of dichloromethane was added and the reaction mixture was cooled in an ice bath. Subsequently, a solution of methacrylic anhydride (0.244 g, 1.583 mmol) in 2 ml of dichloromethane was added dropwise. The reaction mixture was stirred for 2 days at 30 °C and the product was recovered by precipitation in a mixture of cold diethyl ether/hexane/methanol (10/1/1 v/v). Degree of methacrylation: 40%, yield: 88%. ¹H NMR (CDCl₃): δ 1.4 (m, CH(CH₃)OH end group PLA), 1.5 (m, CHCH₃), 1.9 (s, C(CH₃)=CH₂), 3.6 (m, PEG methylene protons), 4.2-4.3 (m, CH₂OCO, linking unit PEG-PLA), 4.3-4.4 (q, CH(CH₃)OH end group PLA), 5.1 (m, CHCH₃), 5.6 and 6.2 (C(CH₃)=CH₂)

PEG-MA/PLLA and PEG-MA/PDLA, in which both MA and PLA blocks are directly linked to PEG, were synthesized by ring opening polymerization of lactide using partially methacrylate functionalized eight-arm star PEG (PEG-MA). For the synthesis of PEG-MA, typically, PEG (16.0 g, 0.734 mmol) was dissolved in 33 ml of dichloromethane. A solution of TEA (0.442 g, 4.368 mmol) in 1 ml of dichloromethane was added and the reaction mixture was cooled in an ice bath. Subsequently, a solution of methacrylic anhydride (0.654 g, 4.242 mmol) in 2 ml of dichloromethane was added dropwise. The reaction mixture was stirred for 2 days at 30 °C and the product was recovered by precipitation in a mixture of cold diethyl ether/hexane/methanol (10/1/1 v/v). Degree of methacrylation: 42%, yield: 90%. ¹H NMR (CDCl₃): δ 1.9 (s, C(CH₃)=CH₂), 3.6 (m, PEG methylene protons), 4.2 (m, CH₂OCO, linking unit PEG-MA), 5.6 and 6.2 (C(CH₃)=CH₂)

PEG-MA/PLLA and PEG-MA/PDLA were synthesized by ring opening polymerization of L-lactide and D-lactide, respectively, in dichloromethane at room temperature, initiated by the remaining hydroxyl groups of PEG-MA (dried overnight under vacuum over

phosphorous pentoxide). The single site Zn-complex Zn(Et)[OC₆H₃(CH₂Me₂)-2-Me-4] was used as a catalyst. Typically, PEG-MA (3.0 g, 0.136 mmol) (degree of methacrylation 42%) and L-lactide (0.532 g, 3.694 mmol) were dissolved in 14 ml of dichloromethane ([LA]₀ = 0.25 M). A solution of single site Zn-complex catalyst (0.064 g, 0.247 mmol) was added in 1 ml of dichloromethane and the reaction mixture was stirred for 1 h. The polymerization was terminated by the addition of an excess of glacial acetic acid and the polymer was precipitated in a mixture of cold diethyl ether/methanol (20/1 v/v). Lactide conversion: 95%, yield: 85%. ¹H NMR (CDCl₃): δ 1.4 (m, CH(CH₃)OH end group PLA), 1.5 (m, CHCH₃), 1.9 (s, C(CH₃)=CH₂), 3.6 (m, PEG methylene protons), 4.2 (m, CH₂OCO, linking unit PEG-MA), 4.2-4.3 (m, CH₂OCO, linking unit PEG-PLA), 4.3-4.4 (q, CH(CH₃)OH end group PLA), 5.1 (m, CHCH₃), 5.6 and 6.2 (C(CH₃)=CH₂)

Characterization. ¹H NMR spectra (CDCl₃) were recorded on a Varian Inova Spectrometer (Varian, Palo, Alto, USA) operating at 300 MHz. The number of lactyl units per PLA block was calculated based on the methyl protons of lactyl units (δ 1.4-1.5) and the methylene protons of PEG (δ 3.6). The number of methacrylate groups per PEG molecule was determined based on the methylene protons of PEG (δ 3.6) and the methylene protons of the methacrylate group (δ 5.6 and 6.2).

Critical gel concentrations (CGCs) were determined as described before.⁵³ Briefly, polymer solutions were prepared by dissolving the polymers in deionized water overnight. Subsequently, polymer solutions of equimolar amounts of PEG-PLLA-MA and PEG-PDLA-MA, or PEG-MA/PLLA and PEG-MA/PDLA star block copolymers were mixed and equilibrated overnight. The CGCs were determined at room temperature by inverting the vials. When the sample showed no flow within 20 s, it was regarded as a gel.

Rheology experiments were performed on a US 200 Rheometer (Anton Paar), as described previously.⁵³ Briefly, a parallel plate measuring geometry (25 mm diameter, gap 0.5 mm), a frequency of 1 Hz and a strain of 1% were used. Polymer solutions in HEPES buffered saline (pH 7.0, 100 mM, adjusted to 300 mOsm with NaCl) containing equimolar amounts of PEG-PLLA-MA and PEG-PDLA-MA, or PEG-MA/PLLA and PEG-MA/PDLA star block copolymers were mixed, homogenized, quickly applied to the rheometer and measured at 37 °C.

In situ UV-irradiation and rheology experiments were performed on a US 200 Rheometer (Anton Paar) equipped with a UV-light source (Bluepoint 4, Dr. Hönle, intensity of 16 mW/cm² in the 350-400 nm range). The samples were irradiated from above. A parallel plate measuring geometry made of Quartz glass (10 mm diameter, gap 0.1 mm) was used in an oscillatory measurement with a frequency of 1 Hz and a strain of 1% or 5%. Both strains are within the linear viscoelastic region. Both PEG-PLA-MA or PEG-MA/PLA stereocomplexed hydrogels (stereo hydrogels) and solutions of PEG-PLLA-MA or PEG-MA/PLLA single enantiomers in HEPES buffered saline were UV-irradiated and at the same time measured at 37 °C. Irgacure 2959 was used as photoinitiator. The stereo hydrogels were measured 10 min after mixing the enantiomeric solutions, unless mentioned otherwise.

Hydrogels for scanning electron microscopy (SEM) experiments and swelling/degradation tests were prepared similarly in a 96 wells plate with sample volumes of 125 µl, resulting in cylinders of approximately 4 mm in height and 6 mm in diameter. PEG-PLA₁₂-MA or PEG-PLA₁₆/MA stereo-photo hydrogels were prepared by UVA-irradiation (250 mW/cm²) for 10 min of the stereo hydrogels (equilibrated for approximately 15 min after mixing of the enantiomeric solutions) with 8 mol% initiator concentration (with respect to the methacrylate groups) prepared in HEPES buffered saline. Photo hydrogels were formed similarly by UVA-irradiation of PEG-PLLA₁₂-MA or PEG-MA₁₆/PLLA single enantiomer solutions in HEPES buffered saline.

SEM experiments were performed on freeze-dried hydrogels using a LEO Gemini 1550 FEG-SEM, fitted with a field Emission Gun, and a voltage of 2 kV. Freeze-dried hydrogels were prepared by freezing in liquid nitrogen and subsequent freeze-drying at -50 °C and 5×10⁻⁷ bar overnight.

For the swelling/degradation tests, the hydrogel cylinders were placed in vials and after addition of 1 ml of HEPES buffered saline the hydrogels were allowed to swell at 37 °C. The swelling experiment was performed in duplicate or triplicate. The swollen hydrogels were weighed at regular intervals after removal of the buffer. After each weighing the buffer was refreshed. The swelling ratio of the hydrogels was calculated from the initial hydrogel weight after hydrogel preparation (W_0) and the swollen hydrogel weight after exposure to buffer (W_t):

$$\text{Swelling ratio} = \frac{W_t}{W_0}$$

6.4 Results and Discussion

6.4.1 Synthesis

Two types of methacrylate functionalized poly(ethylene glycol)-poly(lactide) (PEG-PLA) star block copolymers, PEG-poly(L-lactide)-methacrylate (PEG-PLLA-MA) and PEG-poly(D-lactide)-methacrylate (PEG-PDLA-MA) (Figure 1A), and poly(ethylene glycol)-methacrylate/poly(L-lactide) (PEG-MA/PLLA) and poly(ethylene glycol)-methacrylate/poly(D-lactide) (PEG-MA/PDLA) (Figure 1B), were designed. PEG-PLLA-MA and PEG-PDLA-MA copolymers were prepared by a two-step synthesis procedure. First, eight-arm PEG-PLLA and PEG-PDLA star block copolymers with 12 lactyl units per PLA block (PEG-PLLA₁₂ and PEG-PDLA₁₂, M_n , PEG = 21,800) were synthesized, as reported previously (Table 1, entry 1 and 2).⁵³ Subsequently, the PLA hydroxyl end groups were reacted with methacrylic anhydride using triethylamine (TEA) as a catalyst and dichloromethane as a solvent at 30 °C. The PEG-PLLA₁₂-MA and PEG-PDLA₁₂-MA copolymers were recovered by precipitation in a diethyl ether/hexane/methanol mixture (10/1/1 v/v) (Table 1, entry 3 and 4). ¹H NMR showed a degree of methacrylation of approximately 40%, determined by comparing the integrals of the peaks corresponding to the methylene protons of the methacrylate group (δ 5.6 and 6.2) and the methylene protons of PEG (δ 3.6). PEG-MA/PLA copolymers were prepared by a two-step synthesis procedure. First approximately 40% of the hydroxyl end groups of an eight-arm star PEG (M_n = 21,800) were methacrylated. Subsequently, the ring opening polymerization of L-lactide or D-lactide was initiated by the remaining hydroxyl groups of methacrylate functionalized PEG, using a single-site Zn-complex as a catalyst and dichloromethane as a solvent at room temperature. PEG-MA/PLLA and PEG-MA/PDLA copolymers were obtained by precipitation in a diethyl ether/methanol mixture (20/1 v/v). PEG-MA/PLA copolymers with 12 and 16 lactyl units per PLA block were prepared by varying the

feeding ratio of lactide to PEG (Table 1, entry 5-8). The use of the single site Zn-catalyst allowed excellent control over the degree of polymerization of the PLA blocks and the methacrylation reaction was reproducible, giving similar degrees of methacrylation (Table 1).

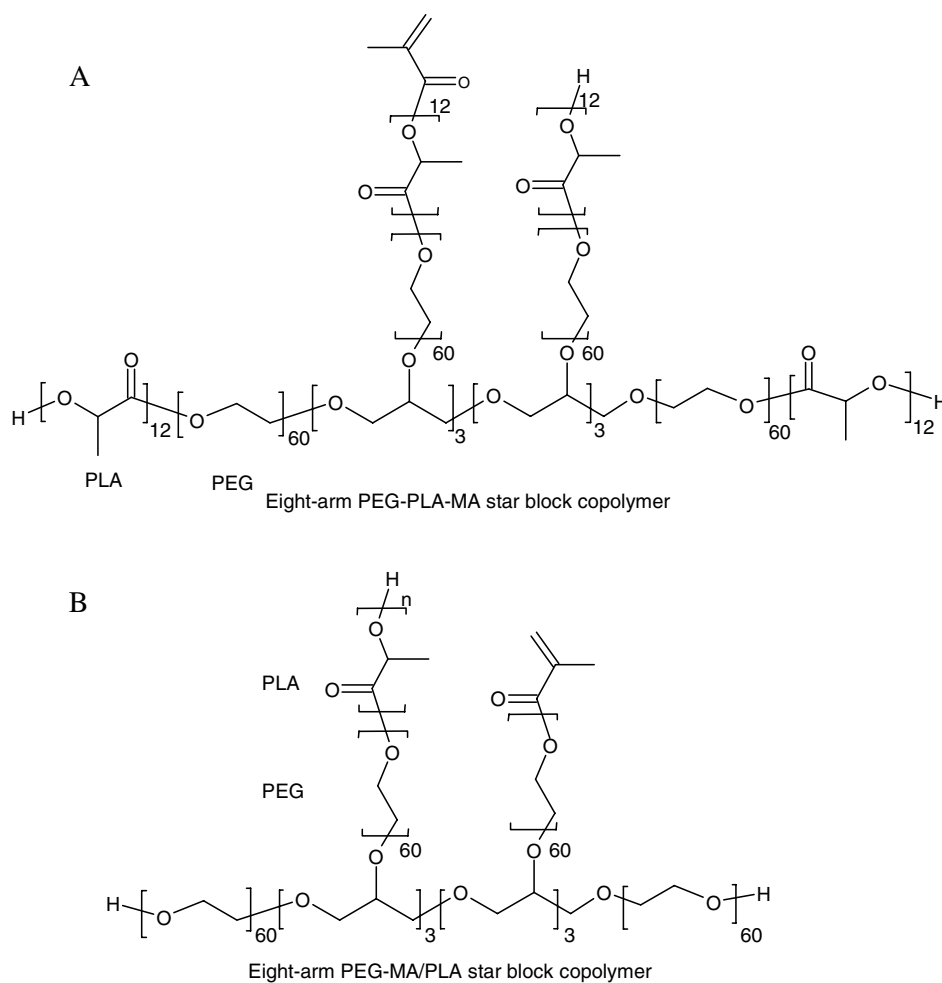


Figure 1. Molecular structures of (A) eight-arm PEG-PLA₁₂-MA star block copolymers and (B) PEG-MA/PLA_n (n = 12 or 16) star block copolymers. As an example three methacrylate groups per molecule are drawn.

Table 1. Synthesis of PEG-PLLA-MA and PEG-PDLA-MA, and PEG-MA/PLLA and PEG-MA/PDLA star block copolymers^{a)}.

Entry	Polymer	Lactide conversion (%)	$N_{LA}^{b)}$		Degree of methacrylation (%)	$M_n \times 10^{-3}$ ¹ H NMR
			Theory ^{c)}	¹ H NMR		
1	PEG-PLLA ₁₂	94	12	12	-	28.7
2	PEG-PDLA ₁₂	96	12	12	-	28.7
3	PEG-PLLA ₁₂ -MA	94	12	12	40	28.8
4	PEG-PDLA ₁₂ -MA	96	12	12	42	28.9
5	PEG-MA/PLLA ₁₂	95	12	12	46	25.6
6	PEG-MA/PDLA ₁₂	94	12	12	46	25.6
7	PEG-MA/PLLA ₁₆	99	17	16	42	27.4
8	PEG-MA/PDLA ₁₆	95	16	16	42	27.4

^{a)} The ring opening polymerization of lactide was performed in dichloromethane for 1 h at RT using PEG or partially methacrylate functionalized PEG as an initiator and the single site Zn-complex $Zn(Et)[OC_6H_3(CH_2Me_2)-2-Me-4]$ as a catalyst, ($[LA]_0 = 0.25$ M, PEG hydroxyl groups : Zn catalyst = 2 : 1). The methacrylation was performed in dichloromethane for 2 days at 30 °C ($[OH]_0 \approx 5$ mM, MA : OH: TEA = 1 : 1.5 : 1.1). ^{b)} Number of lactyl units per PLA block. ^{c)} Based on feed composition and conversion.

6.4.2 Gelation by stereocomplexation

The influence of the methacrylate groups and the PLA block length on stereocomplex hydrogel (denoted as stereo hydrogel) formation was studied at room temperature. Aqueous solutions of equimolar amounts of PEG-PLLA-MA and PEG-PDLA-MA, or PEG-MA/PLLA and PEG-MA/PDLA star block copolymers were mixed and after equilibration it was tested whether the sample had turned into a gel by the vial tilting method. Table 2 shows that the critical gel concentrations (CGCs) for stereocomplexation of PEG-PLA₁₂-MA and PEG-PLA₁₂ are equal, indicating that the methacrylate end groups do not influence the stereocomplexation. PEG-PLLA, PEG-PLLA-MA and PEG-MA/PLLA single enantiomers were also able to form gels at relatively high polymer concentrations. The CGC of PEG-PLLA₁₂-MA single enantiomer is somewhat lower

compared to PEG-PLLA₁₂ single enantiomer, which is attributed to the increased hydrophobicity of PEG-PLLA₁₂-MA. Aqueous solutions of PEG-MA/PLLA₁₂ single enantiomer could be prepared up to much higher polymer concentrations compared to PEG-PLLA₁₂-MA single enantiomer. Stereo hydrogels could also be formed from PEG-MA/PLLA₁₂ and PEG-MA/PDLA₁₂ copolymers, but at much higher polymer concentrations compared to PEG-PLLA₁₂-MA and PEG-PDLA₁₂-MA copolymers. The higher CGC for stereocomplexation of PEG-MA/PLA₁₂ compared to PEG-PLA₁₂-MA is due to the lower crosslinking functionality (i.e. number of PLA blocks per molecule) and lower hydrophobicity of PEG-MA/PLA₁₂ compared to PEG-PLA₁₂-MA. Previously we have shown that the CGC for stereocomplexation of PLA-PEG-PLA triblock copolymers are higher compared to the CGC of eight-arm PEG-PLA star block copolymers.¹³ PEG-MA/PLA₁₆ copolymers showed lower CGC values for stereocomplexation compared to PEG-MA/PLA₁₂ copolymers, due to the increased PLA block length.

Table 2. Critical gel concentrations (CGCs) of solutions containing PEG-PLLA, PEG-PLLA-MA and PEG-MA/PLLA single enantiomer star block copolymers or equimolar amounts of PEG-PLLA and PEG-PDLA, PEG-PLLA-MA and PEG-PDLA-MA, or PEG-MA/PLLA and PEG-MA/PDLA star block copolymers in deionized water at room temperature.

Polymer	CGC single enantiomer (w/v%)	CGC mixed enantiomers (w/v%)
PEG-PLA ₁₂	20	7.5
PEG-PLA ₁₂ -MA	17.5	7.5
PEG-MA/PLA ₁₂	30	22.5
PEG-MA/PLA ₁₆	20	12.5

6.4.3 Rheology

The mechanical properties of stereo hydrogels were studied by rheological experiments at 37 °C. Stereo hydrogels were prepared by mixing aqueous solutions of equimolar

amounts of PEG-PLLA₁₂ and PEG-PDLA₁₂, PEG-PLLA₁₂-MA and PEG-PDLA₁₂-MA, or PEG-MA/PLLA₁₂ and PEG-MA/PDLA₁₂ star block copolymers in HEPES buffered saline (pH 7) in a polymer concentration range of 12.5 to 17.5 w/v%. After mixing, the solutions were quickly applied to the rheometer and the evolution of the storage modulus (G') and loss modulus (G'') was recorded (Figure 2a). Due to fast gelation, the gelation point of PEG-PLA₁₂, PEG-PLA₁₂-MA and PEG-MA/PLA₁₆ in a polymer concentration range of 12.5 to 17.5 w/v% could not be determined by rheology. After application of the sample on the rheometer, approximately 1-2 min were needed to set the instrument before starting the measurement. This shows that stereo hydrogels of PEG-PLA₁₂, PEG-PLA₁₂-MA and PEG-MA/PLA₁₆ were formed within 1-2 min. The storage modulus increased in time due to the ongoing stereocomplexation, until reaching a plateau value, marking the end of the crosslinking process (Figure 2a). Figure 2a shows that the storage modulus evolutions and plateau values of PEG-PLA₁₂-MA and PEG-PLA₁₂ copolymers were similar, which agrees well with the vial tilting tests, indicating that the methacrylate groups hardly influence the stereocomplexation (Table 2). For PEG-PLA₁₂ and PEG-PLA₁₂-MA copolymers the storage modulus plateau value was reached within approximately 5 h after mixing (Figure 2a). In contrast, the storage moduli of PEG-MA/PLA₁₆ stereo hydrogels continuously increased over 48 h. The storage moduli of the stereo hydrogels increased from 2.4 to 12.5 kPa for PEG-PLA₁₂-MA and from 0.1 to 5.2 kPa for PEG-MA/PLA₁₆, upon increasing the polymer concentration from 12.5 to 15 w/v% (Figure 2b). The PEG-PLA₁₂-MA stereo hydrogels showed lower damping factors ($\tan \delta = G''/G'$) compared to the PEG-MA/PLA₁₆ stereo hydrogels (Figure 2b), indicating a higher network perfection.

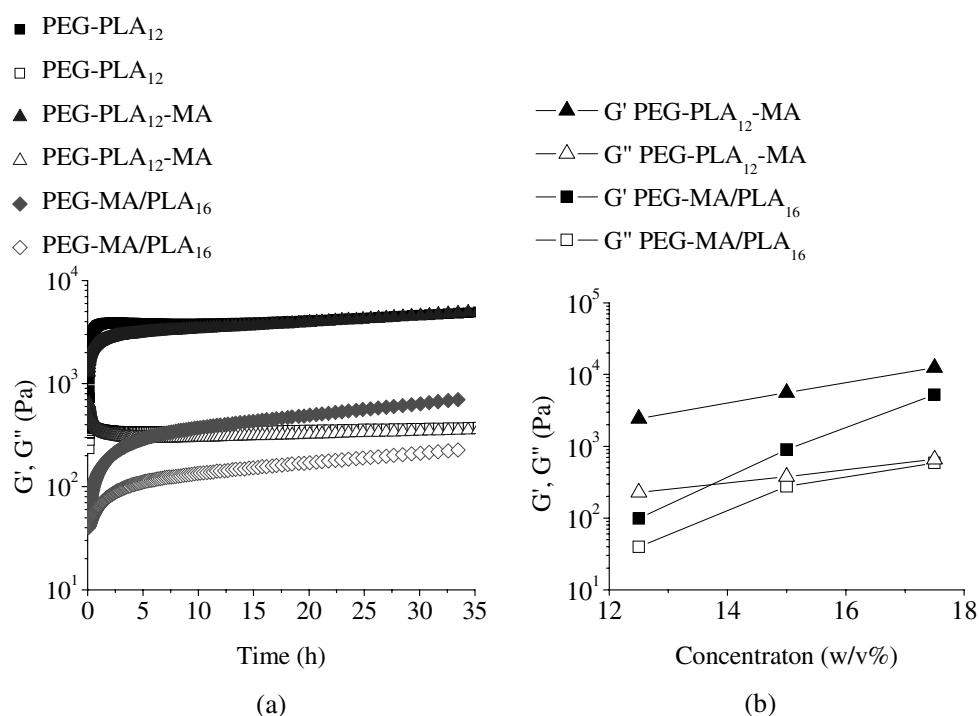


Figure 2. The storage modulus (G') and loss modulus (G'') of stereo hydrogels containing equimolar amounts of PEG-PLLA₁₂ and PEG-PDLA₁₂, PEG-PLLA₁₂-MA and PEG-PDLA₁₂-MA, or PEG-MA/PLLA₁₂ and PEG-MA/PDLA₁₂ star block copolymers in HEPES buffered saline (pH 7) at 37 °C. (a) PEG-PLA₁₂, PEG-PLA₁₂-MA and PEG-MA/PLA₁₆ at 15 w/v% polymer concentration as a function of time; (b) PEG-PLA₁₂-MA and PEG-MA/PLA₁₆, 48 h after mixing as a function of the polymer concentration.

6.4.4 In situ monitoring of mechanical properties during photopolymerization

The mechanical properties of photopolymerized hydrogels were determined by in situ rheology and UV-irradiation (350-400 nm, 16 mW/cm²) of PEG-PLA₁₂-MA or PEG-

MA/PLA₁₆ stereo hydrogels (yielding stereo-photo hydrogels) or solutions of PEG-PLLA₁₂-MA or PEG-MA/PLLA₁₆ single enantiomers (yielding photo hydrogels) in HEPES buffered saline (pH 7) at 37 °C (Figure 3 and 4).

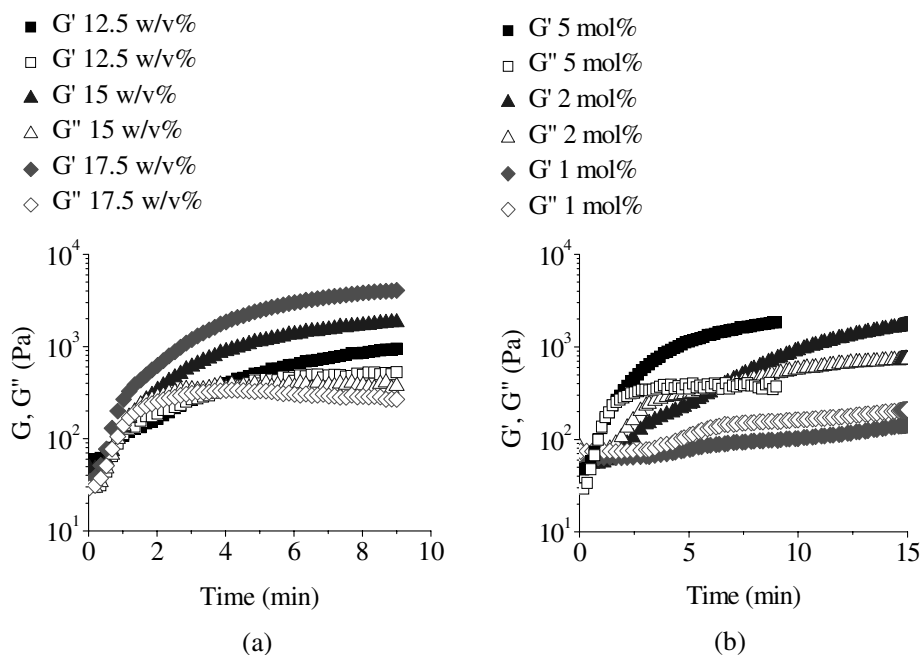


Figure 3. The storage modulus (G') and loss modulus (G'') as a function of UV-irradiation time (350-400 nm, 16 mW/cm²) of PEG-PLLA₁₂-MA solutions in HEPES buffered saline (pH 7) at 37 °C. (a) 12.5, 15 and 17.5 w/v% polymer concentration and 5 mol% initiator concentration (with respect to the methacrylate groups); (b) 1, 2 and 5 mol% initiator concentration and 15 w/v% polymer concentration.

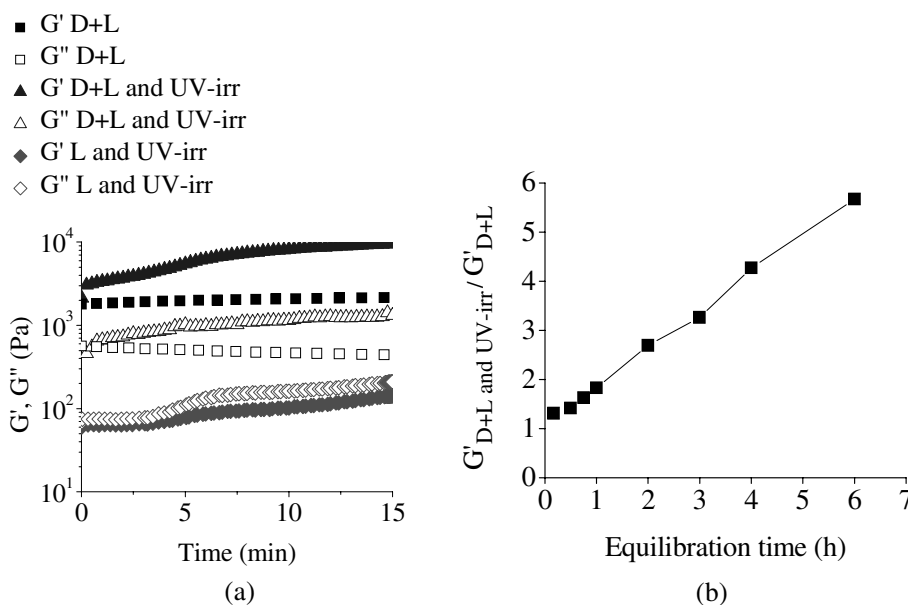


Figure 4. Rheology of UV-irradiated (350-400 nm, 16 mW/cm²) PEG-PLA₁₂-MA in HEPES buffered saline (pH 7) at 15 w/v% polymer concentration and 37 °C. (a) Storage modulus (G') and loss modulus (G'') as a function of time of a stereo hydrogel (D+L) and a stereo-photo hydrogel (D+L and UV-irr) after 10 min of stereocomplex equilibration, and a UV-irradiated PEG-PLLA₁₂-MA solution (L) at 1 mol% initiator concentration (with respect to the methacrylate groups); (b) ratio of the storage modulus plateau value of a stereo-photo hydrogel ($G'_{D+L \text{ and UV-irr}}$) and the storage moduli plateau value of a stereo hydrogel (G'_{D+L}) after 8 min of UV-irradiation as a function of the stereocomplexation equilibration time.

Figure 3a shows that the gelation time of PEG-PLLA₁₂-MA single enantiomer decreased from approximately 3 to 0.5 min upon increasing the polymer concentration from 12.5 to 17.5 w/v% at 5 mol% initiator concentration (with respect to the methacrylate groups). The storage modulus plateau value was reached within approximately 8 min and increased from 0.9 to 4.1 kPa upon increasing the polymer concentration from 12.5 to 17.5 w/v%

(Figure 3a). Figure 3b shows that the gelation time of PEG-PLLA₁₂-MA single enantiomer at 15 w/v% polymer concentration decreased rapidly with increasing initiator concentration. At initiator concentrations of 2 and 5 mol% (with respect to the methacrylate groups) the gelation times of PEG-PLLA₁₂-MA single enantiomer were 6.5 and 1.7 min, respectively. At 1 mol% initiator concentration the 15 w/v% PEG-PLLA₁₂-MA single enantiomer solution did not gelate within 15 min (Figure 3b). As shown earlier, a stereo hydrogel was formed within 1-2 min after mixing aqueous solutions of equimolar amounts of PEG-PLLA₁₂-MA and PEG-PDLA₁₂-MA copolymers. UV-irradiation of the stereo hydrogel at 1 mol% initiator and 15 w/v% polymer concentration 10 min after mixing increased the storage modulus from 5.6 to 9.6 kPa within 15 min due to photocrosslinking (Figure 4a). Here, an initiator concentration of 1 mol% (with respect to the methacrylate groups) corresponds to 0.003 wt%, which is very low compared to the commonly used concentration of 0.05 wt%.⁴⁹ Low initiator concentrations are preferred, due to toxicity of the initiator. The photocrosslinking at this low initiator concentration implies in turn that low light intensities may be used to obtain stereo-photo hydrogels.

The storage modulus of the stereo-photo hydrogel is highly dependent on the stereocomplex equilibration time before UV-irradiation. Figure 4b shows a plot of the ratio of the storage modulus of a PEG-PLA₁₂-MA stereo-photo hydrogel and the storage modulus plateau value of the corresponding stereo hydrogel (reached after approximately 5h, Figure 2a) as a function of the stereocomplex equilibration time. The storage modulus plateau value of the stereo-photo hydrogel (after 8 min of UV-irradiation) increased linearly with increasing the stereocomplex equilibration time at 15 w/v% polymer concentration and 5 mol% initiator concentration (corresponding to 0.015 wt%). This initiator concentration is low compared to the generally used concentration of 0.05 wt%.⁴⁹ UV-irradiation after 6 h of equilibration resulted in an almost 6-fold increase in the storage modulus of the PEG-PLA₁₂-MA stereo-photo hydrogel compared to the corresponding PEG-PLA₁₂-MA stereo hydrogel (31.6 vs. 5.6 kPa) and a 17-fold increase compared to the corresponding PEG-PLLA₁₂-MA photo hydrogel and (31.6 vs. 1.8 kPa). Since the hydrophobic methacrylate groups are at the PLA chain ends, the chemical crosslinks are most probably formed in the PLA domains. A schematic representation of the stereo and stereo-photo hydrogel preparation for PEG-PLA-MA and PEG-MA/PLA copolymers is shown in Figure 5. Furthermore, the photoinitiator used, Irgacure 2959, is rather

hydrophobic (maximum concentration in water is 0.7 wt%⁴⁹), and may therefore preferably partition into the hydrophobic PLA domains, thereby increasing the local initiator concentration and thus photopolymerization rate in these domains. Therefore, the increased storage modulus upon increased stereocomplex equilibration time may be due to the formation of more PLA domains, resulting in a more densely crosslinked network and increased photopolymerization conversion. PEG-MA/PLA₁₆ stereo-photo hydrogels also showed much higher storage moduli compared to the corresponding PEG-MA/PLLA₁₆ stereo or photo hydrogels (results not shown). Therefore, combining stereocomplexation and photocrosslinking may provide fast gelation *in vitro* and *in vivo*⁵⁵, yielding hydrogels with good mechanical properties.

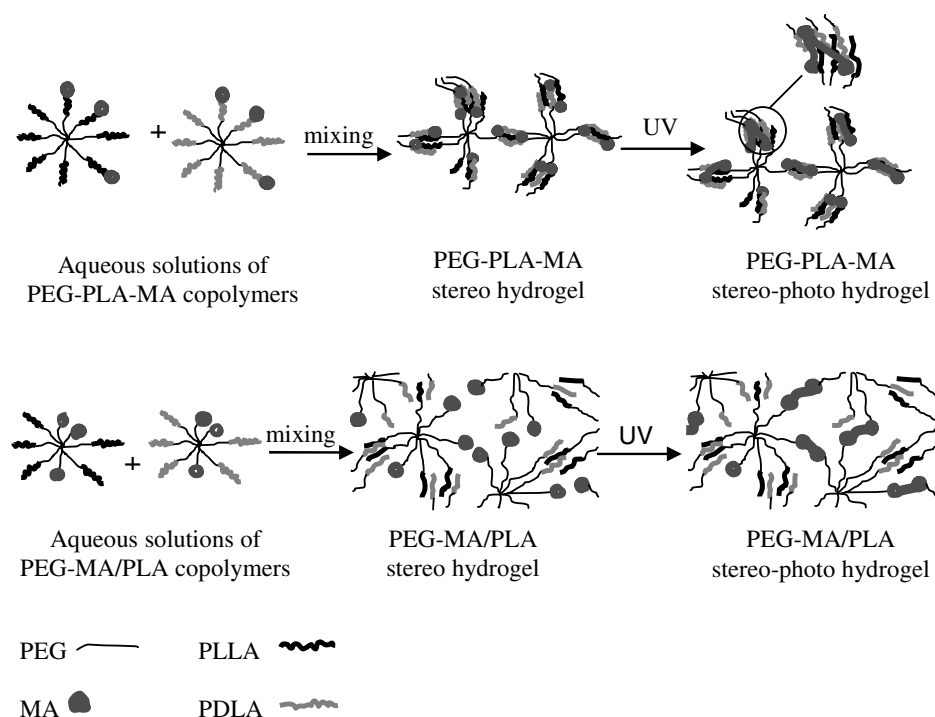


Figure 5. Schematic representation of the preparation of stereo and stereo-photo hydrogels based on PEG-PLA-MA or PEG-MA/PLA star block copolymers.

6.4.5 Morphology of photopolymerized hydrogels

To study the influence of stereocomplexation on the morphology of photopolymerized hydrogels scanning electron microscopy (SEM) measurements were performed on freeze-dried PEG-PLA₁₂-MA and PEG-MA/PLA₁₆ stereo-photo and photo hydrogels (Figures 6A and 6B).

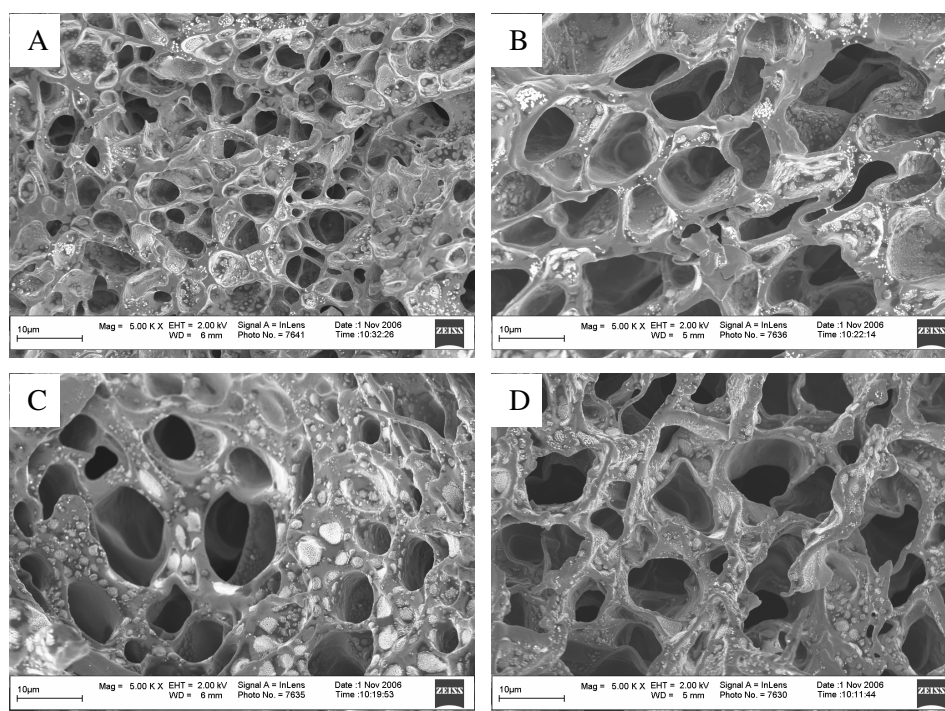


Figure 6. SEM photos of freeze-dried photopolymerized hydrogels prepared in HEPES buffered saline (pH 7) at 15 w/v% polymer concentration and 8 mol% initiator concentration (with respect to the methacrylate groups) by UVA-irradiation for 10 min (stereo hydrogels were equilibrated for approximately 15 min after mixing of the enantiomeric solutions). (A) PEG-PLA₁₂-MA stereo-photo hydrogel; (B) PEG-PLLA₁₂-MA photo hydrogel; (C) PEG-MA/PLA₁₆ stereo-photo hydrogel; (D) PEG-MA/PLLA₁₆ photo hydrogel.

The stereo-photo and photo hydrogels were prepared by UVA-irradiation (250 mW/cm²) of PEG-PLA₁₂-MA or PEG-MA/PLA₁₆ stereo hydrogels (equilibrated for approximately 15 min after mixing the enantiomeric solutions) and solutions of PEG-PLLA₁₂-MA or PEG-MA/PLLA₁₆ single enantiomers, respectively, in HEPES buffered saline (pH 7) at 8 mol% initiator and 15 w/v% polymer concentration. Figures 6A and 6B show that PEG-PLA₁₂-MA stereo-photo hydrogels have pore sizes of approximately 5 μm, while PEG-PLLA₁₂-MA photo hydrogels have pore sizes of approximately 10 μm, indicating that stereocomplexation has a significant influence on the pore size of the freeze-dried PEG-PLA-MA hydrogels. In contrast, PEG-MA/PLA₁₆ stereo-photo hydrogels and PEG-MA/PLLA₁₆ photo hydrogels showed similar pore sizes (approximately 10 μm, Figure 6C and 6D). Apparently, the position of the crosslinking group has much influence on the pore size of freeze-dried stereo-photo hydrogels.

6.4.6 Hydrogel swelling and degradation

Hydrogels based on PEG-PLA-MA or PEG-MA/PLA copolymers were degradable under physiological conditions. To study the rate of degradation, stereo-photo and photo hydrogels were prepared by UVA-irradiation (250 mW/cm²) of PEG-PLA₁₂-MA or PEG-MA/PLA₁₆ stereo hydrogels (equilibrated for approximately 15 min after mixing the enantiomeric solutions) and solutions containing PEG-PLLA₁₂-MA or PEG-MA/PLLA₁₆ single enantiomer, respectively, in HEPES buffered saline (pH 7) at 8 mol% initiator concentration. After the hydrogels were formed, HEPES buffered saline was applied on top and the gels were allowed to swell at 37 °C. At regular time intervals, the swelling ratio was calculated by rationing the swollen hydrogel weight after exposure to buffer with the initial hydrogel weight after preparation (W_t/W_0). Figure 7a shows that the PEG-PLA₁₂-MA stereo-photo hydrogels swelled to approximately twice their initial weight within 1 day, independent of the polymer concentration. The swelling ratio of PEG-PLLA₁₂-MA photo hydrogels also doubled after 1 day at 15 w/v% polymer concentration (Figure 7a). After the initial swelling, the swelling ratio remained constant for the PEG-PLA₁₂-MA stereo-photo hydrogels, while the swelling ratio of PEG-PLLA₁₂-MA photo hydrogels continued to increase. In time, both hydrogels disintegrated, as shown by the decreasing swelling ratio, until they finally dissolved completely. The degradation time is defined as

the time required to completely dissolve at least one of the two or three hydrogels used for testing one type of hydrogel. Figure 7a shows that the PEG-PLA₁₂-MA stereo-photo hydrogels were completely degraded after approximately 3 weeks and increasing the polymer concentration from 12.5 to 17.5 w/v% hardly affected the degradation time. Interestingly, the degradation time of the PEG-PLA₁₂-MA stereo hydrogels was twice as high as compared to the PEG-PLLA₁₂-MA photo hydrogels (approximately 3 vs. 1.5 weeks, Figure 7a). This may be due to a higher crosslinking density of PEG-PLA₁₂-MA stereo-photo hydrogels compared to PEG-PLLA₁₂-MA photo hydrogels, as was also shown by the rheology measurements.

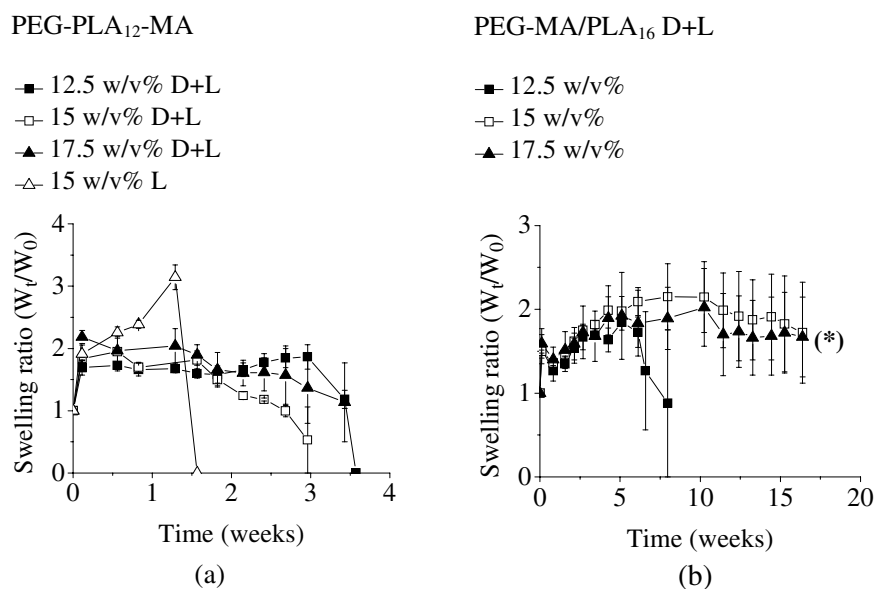


Figure 7. Swelling ratio (W_t/W_0) profiles of photopolymerized hydrogels prepared in HEPES buffered saline (pH 7) at 8 mol% initiator concentration (with respect to the methacrylate groups) and 37 °C by UVA-irradiation for 10 min (stereo hydrogels were equilibrated for approximately 15 min after mixing of the enantiomeric solutions). (a) PEG-PLA₁₂-MA stereo-photo hydrogels at 12.5, 15 and 17.5 w/v% polymer concentration and PEG-PLLA₁₂-MA photo hydrogels at 15 w/v% polymer concentration; (b) PEG-MA/PLA₁₆ stereo-photo hydrogels at 12.5, 15 and 17.5 w/v% polymer concentration. (*) PEG-MA/PLA₁₆ stereo-photo hydrogels at 15 and 17.5 w/v% polymer concentration retained their integrity after 16 weeks.

The PEG-MA/PLA₁₆ stereo-photo hydrogels swelled over a period of approximately 5 weeks until reaching approximately twice their initial weight, independent of the polymer concentration (Figure 7b). The ongoing swelling is most likely due to PLA degradation, upon which the physical crosslinks are lost, resulting in a less densely crosslinked network held together by only chemical crosslinks (Figure 8). PEG-MA/PLA₁₆ stereo-photo hydrogels with 12.5 w/v% polymer concentration completely degraded after 7 weeks, while at 15 and 17.5 w/v% polymer concentration the stereo-photo hydrogels retained their integrity after 16 weeks. The much slower degradation of the PEG-MA/PLA₁₆ stereo-photo hydrogels compared to the PEG-PLA₁₂-MA stereo-photo hydrogels is attributed to the slower hydrolysis of ester bonds of the polymerized methacrylate groups compared to the ester bonds of the PLA blocks, which correlates well with the results obtained by Bryant et al. for photopolymerized PEG dimethacrylate and PEG-PLA dimethacrylate hydrogels.⁵⁶ PEG-PLA-MA stereo-photo hydrogels degrade mainly through hydrolysis of the ester bonds in the PLA block, upon which both physical and chemical crosslinks are lost (Figure 8). In contrast, PLA degradation in the PEG-MA/PLA stereo-photo hydrogels leads to the formation of a less densely, chemically crosslinked network with increased swelling (Figure 8). The swollen PEG-MA/PLA stereo-photo hydrogels finally degrade through hydrolysis of the ester bonds of the polymerized methacrylate groups. It is possible to combine PEG-PLA-MA and PEG-MA/PLA copolymers to vary the degradation time.

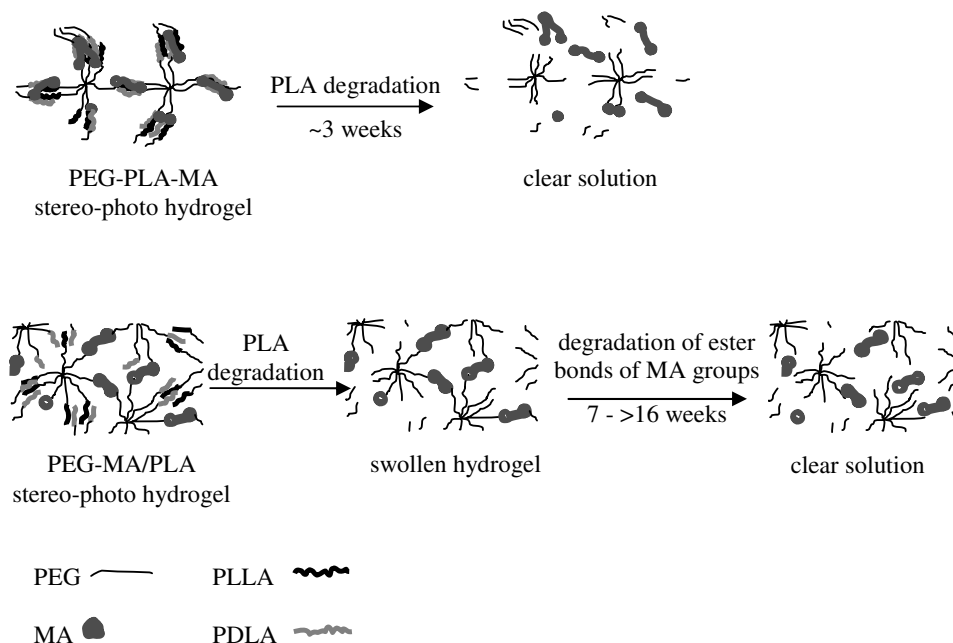


Figure 8. Schematic representation of the degradation of stereo-photo hydrogels based on PEG-PLA-MA or PEG-MA/PLA star block copolymers.

6.5 Conclusions

PEG-PLA-MA copolymers were prepared by methacrylation of approximately 40% of the PLA hydroxyl end groups of eight-arm PEG-PLA star block copolymers. PEG-MA/PLA copolymers were prepared by ring opening polymerization of lactide initiated by eight-arm star PEG with 40% of its hydroxyl end groups methacrylated. PEG-PLA-MA and PEG-MA/PLA stereocomplexed hydrogels could be rapidly formed in situ upon mixing aqueous solutions containing equimolar amounts of PEG-PLLA-MA and PEG-PDLA-MA, or PEG-MA/PLLA and PEG-MA/PDLA copolymers. Interestingly, stereocomplexation aided in the photopolymerization of the methacrylate groups. Photocrosslinking of stereo hydrogels, yielding stereo-photo hydrogels, resulted in increased hydrogel storage moduli, compared to the hydrogels crosslinked by only stereocomplexation (stereo hydrogels) or only photocrosslinking (photo hydrogels).

Moreover, photocrosslinking of stereo hydrogels already took place at very low initiator concentrations. The degradation time of PEG-PLA-MA stereo-photo hydrogels was doubled compared to PEG-PLLA-MA photo hydrogels (approximately 3 vs. 1.5 weeks). PEG-MA/PLA stereo-photo hydrogels degraded within approximately 7 to over 16 weeks, depending on the polymer concentration. In principle, PEG-PLA-MA and PEG-MA/PLA may be combined to vary the hydrogel degradation rate. To our knowledge, this is a first report on fast in situ forming hydrogels by combined crosslinking via photopolymerization and physical interactions. The fast gelation *in vitro* and *in vivo* due to stereocomplexation circumvents the need for fast photopolymerization, thus preventing substantial heat effects due to the photopolymerization and potentiating the use of low initiator concentrations and low light intensities. Moreover, the fast gelation allows for easy handling. The combination of stereocomplexation and photopolymerization is a novel approach to obtain fast in situ forming and robust hydrogels, which have a high potential for *in vivo* applications, including tissue engineering and drug delivery.

6.6 Acknowledgements

This work was funded by the Netherlands Organization for Scientific Research (NWO). We thank M. A. Smithers (University of Twente, Enschede, The Netherlands) for the SEM measurements.

6.7 References

1. Peppas, N. A.; Bures, P.; Leobandung, W.; Ichikawa, H., Hydrogels in pharmaceutical formulations. *Eur. J. Pharm. Biopharm.* 2000, 50, 27-46.
2. Peppas, N. A.; Hilt, J. Z.; Khademhosseini, A.; Langer, R., Hydrogels in biology and medicine: From molecular principles to bionanotechnology. *Adv. Mater.* 2006, 18, 1345-1360.
3. Qiu, Y.; Park, K., Environment-sensitive hydrogels for drug delivery. *Adv. Drug Deliv. Rev.* 2001, 53, 321-339.

Chapter 6

4. Ruel-Gariepy, E.; Leroux, J. C., In situ-forming hydrogels-review of temperature sensitive systems. *Eur. J. Pharm. Biopharm.* 2004, 58, 409-426.
5. Nguyen, K. T.; West, J. L., Photopolymerizable hydrogels for tissue engineering applications. *Biomaterials* 2002, 23, 4307-4314.
6. Temenoff, J. S.; Mikos, A. G., Injectable biodegradable materials for orthopedic tissue engineering. *Biomaterials* 2000, 21, 2405-2412.
7. Jeong, B.; Bae, Y. H.; Kim, S. W., Thermoreversible gelation of PEG-PLGA-PEG triblock copolymer aqueous solutions. *Macromolecules* 1999, 32, 7064-7069.
8. Zhong, Z. Y.; Dijkstra, P. J.; Feijen, J.; Kwon, Y. M.; Bae, Y. H.; Kim, S. W., Synthesis and aqueous phase behavior of thermoresponsive biodegradable poly(D,L-3-methylglycolide)-block-poly(ethylene glycol)-block-poly(D,L-3-methylglycolide) triblock copolymers. *Macromol. Chem. Phys.* 2002, 203, 1797-1803.
9. Shim, W. S.; Kim, J. H.; Park, H.; Kim, K.; Kwon, I. C.; Lee, D. S., Biodegradability and biocompatibility of a pH- and thermo-sensitive hydrogel formed from a sulfonamide-modified poly(epsilon-caprolactone-co-lactide)-poly(ethylene glycol)-poly(epsilon-caprolactone-co-lactide) block copolymer. *Biomaterials* 2006, 27, 5178-5185.
10. Kang, G. D.; Cheon, S. H.; Khang, G.; Song, S. C., Thermosensitive poly(organophosphazene) hydrogels for a controlled drug delivery. *Eur. J. Pharm. Biopharm.* 2006, 63, 340-346.
11. Seong, J. Y.; Jun, Y. J.; Jeong, B.; Sohn, Y. S., New thermogelling poly(organophosphazenes) with methoxypoly(ethylene glycol) and oligopeptide as side groups. *Polymer* 2005, 46, 5075-5081.
12. de Jong, S. J.; van Eerdenbrugh, B.; van Nostrum, C. F.; Kettenes-van de Bosch, J. J.; Hennink, W. E., Physically crosslinked dextran hydrogels by stereocomplex formation of lactic acid oligomers: degradation and protein release behavior. *J. Controlled Release* 2001, 71, 261-275.
13. Chapter 4, Hiemstra, C.; Zhong, Z. Y.; Li, L. B.; Dijkstra, P. J.; Feijen, J., In-situ formation of biodegradable hydrogels by stereocomplexation of PEG-(PLLA)₈ and PEG-(PDLA)₈ star block copolymers. Published in *Biomacromolecules* 2006, 7, 2790-2795.

14. Mukose, T.; Fujiwara, T.; Nakano, J.; Taniguchi, I.; Miyamoto, M.; Kimura, Y.; Teraoka, I.; Lee, C. W., Hydrogel formation between enantiomeric B-A-B-type block copolymers of polylactides (PLLA or PDLA : A) and polyoxyethylene (PEG : B); PEG-PLLA-PEG and PEG-PDLA-PEG. *Macromol. Biosci.* 2004, 4, 361-367.
15. Li, S. M.; El Ghzaoui, A.; Dewinck, E., Rheology and drug release properties of bioresorbable hydrogels prepared from polylactide/poly(ethylene glycol) block copolymers. *Macromol. Symp.* 2005, 222, 23-35.
16. Li, J.; Ni, X. P.; Leong, K. W., Injectable drug-delivery systems based on supramolecular hydrogels formed by poly(ethylene oxide) and alpha-cyclodextrin. *J. Biomed. Mater. Res.* 2003, 65A, 196-202.
17. Li, J.; Li, X.; Ni, X. P.; Wang, X.; Li, H. Z.; Leong, K. W., Self-assembled supramolecular hydrogels formed by biodegradable PEO-PHB-PEO triblock copolymers and alpha-cyclodextrin for controlled drug delivery. *Biomaterials* 2006, 27, 4132-4140.
18. Zhao, S. P.; Zhang, L. M.; Ma, D., Supramolecular hydrogels induced rapidly by inclusion complexation of Poly(epsilon-caprolactone)-poly(ethylene glycol)-poly(epsilon-caprolactone) block copolymers with alpha-cyclodextrin in aqueous solutions. *J. Phys. Chem. B* 2006, 110, 12225-12229.
19. Huh, K. M.; Cho, Y. W.; Chung, H.; Kwon, I. C.; Jeong, S. Y.; Ooya, T.; Lee, W. K.; Sasaki, S.; Yui, N., Supramolecular hydrogel formation based on inclusion complexation between poly(ethylene glycol)-modified chitosan and alpha-cyclodextrin. *Macromol. Biosci.* 2004, 4, 92-99.
20. Sabadini, E.; Cosgrove, T., Inclusion complex formed between star-poly(ethylene glycol) and cyclodextrins. *Langmuir* 2003, 19, 9680-9683.
21. Van Tomme, S. R.; van Steenberg M. J.; De Smedt, S. C.; van Nostrum, C. F.; Hennink, W. E., Self-gelling hydrogels based on oppositely charged dextran microspheres. *Biomaterials* 2005, 26, 2129-2135.
22. Ramachandran, S.; Tseng, Y.; Yu, Y. B., Repeated rapid shear-responsiveness of peptide hydrogels with tunable shear modulus. *Biomacromolecules* 2005, 6, 1316-1321.

Chapter 6

23. Elbert, D. L.; Pratt, A. B.; Lutolf, M. P.; Halstenberg, S.; Hubbell, J. A., Protein delivery from materials formed by self-selective conjugate addition reactions. *J. Controlled Release* 2001, 76, 11-25.
24. Lutolf, M. P.; Hubbell, J. A., Synthesis and physicochemical characterization of end-linked poly(ethylene glycol)-co-peptide hydrogels formed by Michael- type addition. *Biomacromolecules* 2003, 4, 713-722.
25. Lutolf, M. P.; Raeber, G. P.; Zisch, A. H.; Tirelli, N.; Hubbell, J. A., Cell-responsive synthetic hydrogels. *Adv. Mater.* 2003, 15, 888-892.
26. Shu, X. Z.; Liu, Y. C.; Palumbo, F. S.; Lu, Y.; Prestwich, G. D., Attachment and spreading of fibroblasts on an RGD peptide-modified injectable hyaluronan hydrogel. *Biomaterials* 2004, 25, 1339-1348.
27. Peattie, R. A.; Rieke, E. R.; Hewett, E. M.; Fisher, R. J.; Shu, X. Z.; Prestwich, G. D., Dual growth factor-induced angiogenesis in vivo using hyaluronan hydrogel implants. *Biomaterials* 2006, 27, 1868-1875.
28. Ghosh, K.; Ren, X. D.; Shu, X. Z.; Prestwich, G. D.; Clark, R. A. F., Fibronectin functional domains coupled to hyaluronan stimulate adult human dermal fibroblast responses critical for wound healing. *Tissue Eng.* 2006, 12, 601-613.
29. Chapter 7, Hiemstra, C.; van der Aa, L. J.; Zhong, Z. Y.; Dijkstra, P. J.; Feijen, J., Novel in situ forming, degradable dextran hydrogels by Michael addition chemistry: Synthesis, rheology and degradation. Published in *Macromolecules* 2007, 40, 1165-1173.
30. Maia, J.; Ferreira, L.; Carvalho, R.; Ramos, M. A.; Gil, M. H., Synthesis and characterization of new injectable and degradable dextran-based hydrogels. *Polymer* 2005, 46, 9604-9614.
31. Balakrishnan, B.; Jayakrishnan, A., Self-cross-linking biopolymers as injectable in situ forming biodegradable scaffolds. *Biomaterials* 2005, 26, 3941-3951.
32. Yoshida, T.; Aoyagi, T.; Kokufuta, E.; Okano, T., Newly designed hydrogel with both sensitive thermoresponse and biodegradability. *J. Polym. Sci. Polym. Chem.* 2003, 41, 779-787.
33. Cadee, J. A.; De Kerf, M.; De Groot, C. J.; Den Otter, W.; Hennink, W. E., Synthesis, characterization of 2-(methacryloyloxy)ethyl-(di-) -lactate and their application in dextran-based hydrogels. *Polymer* 1999, 40, 6877-6881.

34. Kasper, F. K.; Seidlits, S. K.; Tang, A.; Crowther, R. S.; Carney, D. H.; Barry, M. A.; Mikos, A. G., In vitro release of plasmid DNA from oligo(poly(ethylene glycol) fumarate) hydrogels. *J. Controlled Release* 2005, 104, 521-539.
35. Oudshoorn, M. H. M.; Rissmann, R.; Bouwstra, J. A.; Hennink, W. E., Synthesis and characterization of hyperbranched polyglycerol hydrogels. *Biomaterials* 2006, 27, 5471-5479.
36. Temenoff, J. S.; Park, H.; Jabbari, E.; Conway, D. E.; Sheffield, T. L.; Ambrose, C. G.; Mikos, A. G., Thermally cross-linked oligo(poly(ethylene glycol) fumarate) hydrogels support osteogenic differentiation of encapsulated marrow stromal cells in vitro. *Biomacromolecules* 2004, 5, 5-10.
37. Kim, S.; Chung, E. H.; Gilbert, M.; Healy, K. E., Synthetic MMP-13 degradable ECMs based on poly(N-isopropylacrylamide-co-acrylic acid) semi-interpenetrating polymer networks. I. Degradation and cell migration. *J. Biomed. Mater. Res.* 2005, 75A, 73-88.
38. Baroli, B., Photopolymerization of biomaterials: issues and potentialities in drug delivery, tissue engineering, and cell encapsulation applications. *J. Chem. Tech. Biotechnol.* 2006, 81, 491-499.
39. West, J. L.; Hubbell, J. A., Polymeric biomaterials with degradation sites for proteases involved in cell migration. *Macromolecules* 1999, 32, 241-244.
40. Bryant, S. J.; Anseth, K. S., Hydrogel properties influence ECM production by chondrocytes photoencapsulated in poly(ethylene glycol) hydrogels. *J. Biomed. Mater. Res.* 2002, 59, 63-72.
41. Bryant, S. J.; Bender, R. J.; Durand, K. L.; Anseth, K. S., Encapsulating chondrocytes in degrading PEG hydrogels with high modulus: Engineering gel structural changes to facilitate cartilaginous tissue production. *Biotechnol. Bioeng.* 2004, 86, 747-755.
42. Sawhney, A. S.; Pathak, C. P.; Hubbell, J. A., Bioerodible hydrogels based on photopolymerized poly(ethylene glycol)-co-poly(alpha-hydroxy acid) diacrylate macromers. *Macromolecules* 1993, 26, 581-587.
43. Halstenberg, S.; Panitch, A.; Rizzi, S.; Hall, H.; Hubbell, J. A., Biologically engineered protein-graft-poly(ethylene glycol) hydrogels: A cell adhesive and plasm

Chapter 6

- in-degradable biosynthetic material for tissue repair. *Biomacromolecules* 2002, 3, 710-723.
44. Park, Y. D.; Tirelli, N.; Hubbell, J. A., *Biomaterials* 2003, 24, 893-900.
 45. Elisseeff, J.; Anseth, K.; Sims, D.; McIntosh, W.; Randolph, M.; Yaremchuk, M.; Langer, R., Transdermal photopolymerization of poly(ethylene oxide)-based injectable hydrogels for tissue-engineered cartilage. *Plast. Reconstr. Surg.* 1999, 104, 1014-1022.
 46. Yamaoka, T.; Tabata, Y.; Ikada, Y., distribution and tissue uptake of poly(ethylene glycol) with different molecular weights after intravenous administration to mice. *J. Pharm. Sci.* 1994, 83, 601-606.
 47. Elisseeff, J.; Anseth, K.; Sims, D.; McIntosh, W.; Randolph, M.; Langer, R., Transdermal photopolymerization for minimally invasive implantation. *PNAS* 1999, 96, 3104-3107.
 48. Burdick, J. A.; Peterson, A. J.; Anseth, K. S., Conversion and temperature profiles during the photoinitiated polymerization of thick orthopaedic biomaterials. *Biomaterials* 2001, 22, 1779-1786.
 49. Bryant, S. J.; Nuttelman, C. R.; Anseth, K. S., Cytocompatibility of UV and visible light photoinitiating systems on cultured NIH/3T3 fibroblasts *in vitro*. *J. Biomater. Sci. Polymer Edn.* 2000, 11, 439-457.
 50. Muggli, D. S.; Burkoth, A. K.; Keyser, S. A.; Lee, H. R.; Anseth, K. S., Reaction behavior of biodegradable, photo-cross-linkable polyanhydrides. *Macromolecules* 1998, 31, 4120-4125.
 51. Chapter 5, Hiemstra, C.; Zhong, Z. Y.; Van Tomme, S. R.; Jacobs, J. J. L.; Den Otter, W.; Hennink, W. E.; Feijen, J., In vitro and in vivo protein delivery from in situ forming poly(ethylene glycol)-poly(lactide) hydrogels. Published in *J. Controlled Release* 2007, *accepted*.
 52. Bos, G. W.; Jacobs, J. J. L.; Koten, J. W.; Van Tomme, S. R.; Veldhuis, T. F. J.; van Nostrum, C. F.; Den Otter, W.; Hennink, W. E., In situ crosslinked biodegradable hydrogels loaded with IL-2 are effective tools for local IL-2 therapy. *Eur. J. Pharm. Sci.* 2004, 21, 561-567.

53. Chapter 3, Hiemstra, C.; Zhong, Z. Y.; Dijkstra, P. J.; Feijen, J., Stereocomplex mediated gelation of PEG-(PLA)₂ and PEG-(PLA)₈ block copolymers. Published in *Macromol. Symp.* 2005, 224, 119-131.
54. Lin-Gibson, S.; Bencherif, S.; Cooper, J. A.; Wetzel, S. J.; Antonucci, J. M.; Vogel, B. M.; Horkay, F.; Washburn, N. R., Synthesis and Characterization of PEG Dimethacrylates and Their Hydrogels. *Biomacromolecules* 2004, 5, 1280-1287.
55. Bos, G. W.; Hennink, W. E. Brouwer, L. A.; den Otter, W.; Veldhuis, T. F. J.; van Nostrum, C. F.; van Luyn, M. J. A., Tissue reactions of in situ formed dextran hydrogels crosslinked by stereocomplex formation after subcutaneous implantation in rats. *Biomaterials* 2005, 26, 3901-3909.
56. Bryant, S. J.; Anseth, K. S., Controlling the spatial distribution of ECM components in degradable PEG hydrogels for tissue engineering cartilage. *J. Biomed. Mater. Res.* 2002, 64A, 70-79.

Chapter 7

Novel in situ forming, degradable dextran hydrogels by Michael addition chemistry: Synthesis, rheology and degradation¹

Christine Hiemstra, Leonardus J. van der Aa, Zhiyuan Zhong, Pieter J. Dijkstra, and Jan Feijen**

Department of Polymer Chemistry and Biomaterials, Faculty of Science and Technology, Institute for Biomedical Technology, University of Twente, P. O. Box 217, 7500 AE Enschede, The Netherlands

7.1 Abstract

Various vinyl sulfone functionalized dextrans (dex-VS) ($M_{n, \text{dextran}} = 14\text{K}$ or 31K) with degrees of substitution (DS) ranging from 2 to 22 were conveniently prepared by a one-pot synthesis procedure at room temperature. This procedure involved reaction of a mercapto alkanic acid with an excess amount of divinyl sulfone yielding vinyl sulfone alkanic acid, followed by conjugation to dextran using N,N'-dicyclohexylcarbodiimide (DCC)/4-(dimethylamino)pyridinium 4-toluenesulfonate (DPTS) as a catalyst system. By using two different mercapto alkanic acids, 3-mercaptopropionic acid (**1a**) and 4-mercaptopbutyric acid (**1b**), dex-VS conjugates with either an ethyl spacer (denoted as dex-Et-VS) or a propyl spacer (denoted as dex-Pr-VS) between the thioether and ester groups were obtained. Linear and four-arm mercapto poly(ethylene glycol) ($M_n = 2.1 \text{ K}$) with two or four thiol groups (denoted as PEG-2-SH and PEG-4-SH, respectively) were also prepared.

¹ This chapter has been published in *Macromolecules*, 2007, 40, 1165-1173.

Hydrogels were rapidly formed in situ under physiological conditions by Michael type addition upon mixing aqueous solutions of dex-VS and multi-functional PEG-SH at a concentration of 10 to 20 w/v%. The gelation time ranged from 0.5 to 7.5 min, depending on the DS, concentration, dextran molecular weight and PEG-SH functionality. Rheological studies showed that these dextran hydrogels are highly elastic. The storage modulus increased with increasing DS, concentration and dextran molecular weight and hydrogels with a broad range of storage moduli from 3 to 46 kPa were obtained. Swelling/degradation studies revealed that these dextran hydrogels have a low initial swelling and are degradable under physiological conditions. The degradation time varied from 3 to 21 days depending on the DS, concentration, dextran molecular weight and PEG-SH functionality. Interestingly, dex-Pr-VS hydrogels showed prolonged degradation times, but otherwise similar properties compared to dex-Et-VS hydrogels. The hydrolysis of the linker ester bonds of the dex-VS conjugates under physiological conditions was confirmed by ¹H NMR. The results showed that the hydrolysis kinetics were independent of the DS and the dextran molecular weight. Therefore the degradation rate of these hydrogels can be precisely controlled.

7.2 Introduction

Hydrogels are three-dimensional, hydrated networks of crosslinked hydrophilic polymers. They have been studied extensively for biomedical applications, such as drug delivery^{1, 2} and tissue engineering³, due to their excellent biocompatibility. Hydrogels that can be formed in situ under physiological conditions have received much attention recently, due to their many favorable characteristics. Bioactive compounds and/or cells can be mixed homogeneously with the polymer solutions prior to gelation and the in situ gelation allows preparation of complex shapes and applications using minimally invasive surgery. In situ formed, physically crosslinked hydrogels have been prepared by stimuli responsive block copolymers^{4, 6}, stereocomplexation between poly(L-lactide) and poly(D-lactide) blocks of poly(ethylene glycol)-poly(lactide) (PEG-PLA) or dextran-PLA copolymers⁷⁻¹⁰, β -sheet or coiled-coil formation of peptides^{11, 12}, inclusion complexation

In situ forming degradable dextran vinyl sulfone hydrogels

between α -cyclodextrins and PEG¹³ and ionic interactions between microparticles of dextran-(2-hydroxyethyl methacrylate) (dextran-HEMA) copolymerized with methacrylic acid (MAA) or dimethylaminoethyl methacrylate (DMAEMA)¹⁴. The crosslinking conditions for these types of hydrogels are generally mild, thus allowing for the entrapment of labile compounds, such as proteins. The main drawback of physically crosslinked hydrogels is however that they are generally mechanically weak. Chemically crosslinked hydrogels are generally stronger compared to physically crosslinked hydrogels. The most common in situ formed, chemically crosslinked hydrogels are based on UV-irradiation of (meth)acrylate functionalized polymers.¹⁵⁻²⁰ Their in situ formation in vivo is however limited by the low penetration depth of the UV light due to the absorption by the skin.²¹ Hydrogels prepared by Michael type addition reaction between thiols and either acrylates or vinyl sulfones may overcome this problem, since they can be rapidly formed under physiological conditions without the aid of UV-irradiation. Hubbell and Metters et al. have prepared hydrogels by Michael type addition between small molecules bearing several thiol groups and multi-arm star PEG acrylates or vinyl sulfones.²²⁻²⁷ PEG acrylate hydrogels released human growth hormone in vitro for up to a few months with preservation of the protein integrity. PEG vinyl sulfone hydrogels containing cell-binding and protease-cleavable sites allowed the ingrowth of cells due to cellular activity in vitro. Prestwich et al. have prepared hydrogels by Michael type addition between thiol-modified hyaluronic acid (HA) or chondroitin sulfate (CS) and PEG diacrylate.^{28, 29} These hydrogels quantitatively released basic fibroblast growth factor in vitro for up to 28 days with 55% of its original biological activity. Furthermore, when modified with cell adhesion peptides, they supported attachment and spreading of fibroblasts in vitro.

Dextran based materials are highly hydrophilic, biocompatible and show low protein adsorption. Water-soluble dextran with molecular weights of $< \sim 30,000$ can be excreted through the kidneys.³⁰ Dextran has many hydroxyl groups, allowing for a broad range of substitution with functional groups, in contrast to the limited number of functional groups of PEG. Cadee et al. have prepared degradable dextran hydrogels based on dextran-lactate-HEMA derivatives crosslinked by redox initiated polymerization of the double bonds.³¹ These hydrogels were biocompatible when implanted subcutaneously into rats.³² Maia et al. prepared injectable, degradable dextran hydrogels by crosslinking oxidized dextran with adipic acid dihydrazide (AAD).³³ The gels, formed within 2-4 min, had good mechanical

properties and degraded within 3 w. In this paper, we report a novel degradable hydrogel that is rapidly formed under physiological conditions by Michael type addition between dextran vinyl sulfones and multi-functional mercapto PEG. Our results show that the gelation time, mechanical properties, as well as the degradation time of the dextran vinyl sulfone hydrogels can be well-controlled by the DS, concentration and dextran molecular weight.

7.3 Materials and Methods

Materials. Dextrans ($M_{n, GPC} = 14K$ with $M_w/M_n = 1.45$, denoted as dex14K, and $M_{n, GPC} = 31K$ with $M_w/M_n = 1.38$, denoted as dex31K), linear poly(ethylene glycol) (PEG) ($M_{n, MALDI-TOF MS} = 2.1K$ with $M_w/M_n = 1.02$), calcium hydride, divinyl sulfone and 2,2'-Azobisisobutyronitrile (AIBN) were purchased from Fluka. Four-arm PEG ($M_{n, MALDI-TOF MS} = 2.1K$, $M_w/M_n = 1.01$) was obtained from Nektar. Dextran and PEG were dried by azeotropic distillation with toluene. AIBN was recrystallized from ethanol. 3-Mercaptopropionic acid (3-MPA), sodium hydride, allylbromide and dithioerythritol (DTE) were obtained from Aldrich. *N,N'*-dicyclohexylcarbodiimide (DCC), thioacetic acid (TAA) and sodium thiomethoxide (STM) were supplied by Acros. These chemicals were used as received. 4-Mercaptobutyric acid (4-MBA) was prepared by reduction of 4,4'-dithiodibutyric acid (Acros) by tripropylphosphine (Aldrich) and water in dioxane and subsequent evaporation of the solvents. 4-(Dimethylamino)pyridinium 4-toluenesulfonate (DPTS) was synthesized from 4-(dimethylamino)pyridine (DMAP, Merck) and hydrated *p*-toluenesulfonic acid (PTSA, Fluka) and recrystallized from toluene. Dimethylsulfoxide (DMSO), dichloromethane, ethanol and dioxane were dried over calcium hydride. Toluene was dried over sodium wire. All solvents were distilled prior to use.

Synthesis.

Dex-Et-VS. Dextran vinyl sulfone esters with an ethyl spacer between the thioether and the ester groups (denoted as dex-Et-VS) were synthesized by a one-pot synthesis procedure at room temperature from dextran, DVS and 3-MPA. Typically, DVS (32.85 g, 278 mmol, molar ratio of DVS to 3-MPA is 20) was dissolved in DMSO (90 ml) and 3-MPA (1.476 g,

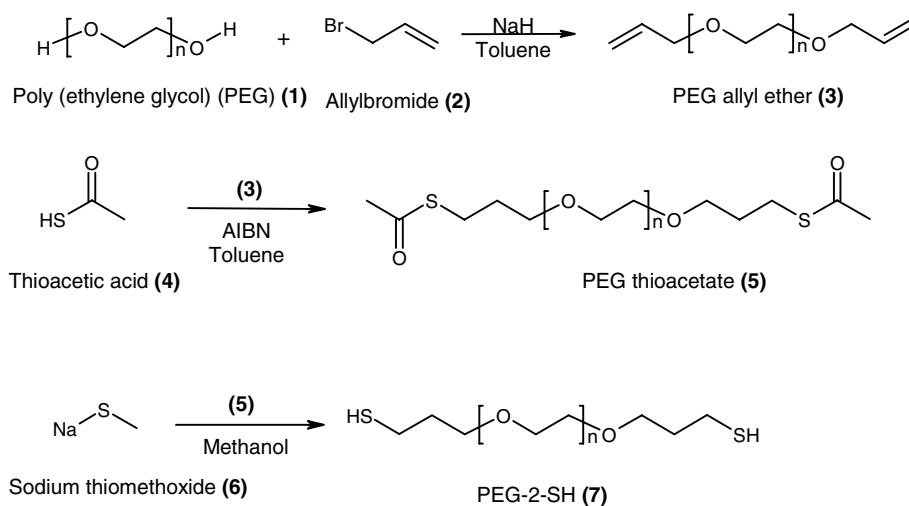
In situ forming degradable dextran vinyl sulfone hydrogels

13.9 mmol, molar ratio of 3-MPA to anhydroglucosidic rings (AHG) of dextran is 0.45) was added dropwise and the reaction was stirred for 4 h. Dextran (5.0 g, 30.9 mmol AHG, 3.3 w/v% concentration), DPTS (0.62 g, 2.1 mmol, molar ratio of DPTS to 3-MPA is 0.15) and DCC (4.346 g, 21.1 mmol, molar ratio of DCC to 3-MPA is 1.5) were dissolved in DMSO (60 ml) and added to the DVS/3-MPA mixture and the reaction was stirred for another 24 h. Subsequently, the formed N,N-dicyclohexylurea (DCU) salt was removed by filtration and the product was recovered by precipitation in cold ethanol. The precipitate was washed with ethanol, dissolved in water (pH 8) and purified by ultrafiltration (MWCO 5,000). The final product was obtained by lyophilization. DS ($^1\text{H NMR}$): 4. Yield: 4.75 g, 95%. $^1\text{H NMR}$ (D_2O): δ 2.8–3.0 (m, $-\text{CH}_2-\text{CH}_2-\text{S}-\text{CH}_2-\text{CH}_2-$), 3.4–4.1 (m, dextran glucosidic protons), 5.0 (s, dextran anomeric proton), 5.2 and 5.4 (m, glucosidic protons linked to vinyl sulfone substituents), 6.5 (m, $-\text{SO}_2\text{CH}=\text{CH}_2$), 6.9 (m, $-\text{SO}_2\text{CH}=\text{CH}_2$).

Different degrees of substitution (DS) were obtained by using different molar ratios of 3-MPA to AHG of dextran (ratios were 0.30; 0.45; 0.53; 0.60 and 0.90, Table 1).

Dex-Pr-VS. Dextran vinyl sulfone esters with a propyl spacer between the thioether and the ester groups (denoted as dex-Pr-VS) were synthesized similarly to dex-Et-VS with the exception that 4-MBA was used instead of 3-MPA. Typically, DVS (65.64 g, 556 mmol, molar ratio of DVS to 4-MBA is 20) was dissolved in DMSO (90 ml), a 4-MBA/triisopropylphosphine mixture (10.007 g, 27.8 mmol, molar ratio of 4-MBA to AHG is 0.90) was added dropwise and the reaction was stirred for 4 h. Dextran (5.0 g, 31 mmol AHG, 3.3 w/v% concentration), DPTS (1.239 g, 4.2 mmol, molar ratio of DPTS to 4-MBA is 0.15) and DCC (8.684 g, 42.1 mmol, molar ratio of DCC to 4-MBA is 1.5) were dissolved in DMSO (60 ml) and were added to the DVS/4-MBA mixture and the reaction was stirred for another 24 h. Subsequently, the formed DCU salt was removed by filtration and the product was recovered by precipitation in cold ethanol. The precipitate was washed with ethanol, dissolved in water (pH 8) and purified by ultrafiltration (MWCO 5,000). The final product was obtained by lyophilization. DS ($^1\text{H NMR}$): 10. Yield: 3.77 g, 75%. $^1\text{H NMR}$ (D_2O): δ 2.0 (m, $-\text{CH}_2-\text{CH}_2-\text{CH}_2-\text{S}-$), 2.5–2.7 (m, $-\text{CH}_2-\text{CH}_2-\text{CH}_2-\text{S}-$ and $-\text{S}-\text{CH}_2-\text{CH}_2-\text{SO}_2-$), 2.9 (t, $-\text{S}-\text{CH}_2-\text{CH}_2-\text{SO}_2-$), 3.4–4.1 (m, dextran glucosidic protons), 5.0 (s, dextran anomeric proton), 5.2 and 5.4 (m, dextran glucosidic protons linked to vinyl sulfone substituents), 6.5 (m, $-\text{SO}_2\text{CH}=\text{CH}_2$), 6.9 (m, $-\text{SO}_2\text{CH}=\text{CH}_2$).

Mercapto PEG. Linear and four-arm mercapto poly(ethylene glycol) (denoted as PEG-2-SH and PEG-4-SH, respectively) were obtained by a three-step synthesis procedure as reported previously by Goessl et al.³⁴ (Scheme 1).



Scheme 1. Schematic representation of the three-step synthesis of mercapto PEG, shown for PEG-2-SH.

First, the hydroxyl groups were converted to allyl groups, which were subsequently reacted with thioacetic acid to yield thioacetate groups. The thioacetate groups were removed by reaction with a base. To convert the hydroxyl groups of PEG into allyl groups, typically linear PEG (**1**, 40 g) was dissolved in toluene (432 ml, hydroxyl group concentration is 93 mM) at 25 °C. Sodium hydride (2.88 g, 120 mmol, 3 times molar excess to hydroxyl groups) was suspended in a small volume of toluene and was added to the solution. After hydrogen evolution, allyl bromide (**2**, 17.4 ml, 200 mmol, 5 times molar excess to hydroxyl groups) was added dropwise to the solution and the reaction was stirred overnight. Subsequently, the sodium salts were removed by filtration and toluene was evaporated. The product was dissolved in dichloromethane, extracted four times with water and subsequently the organic phase was dried over anhydrous sodium sulphate. The PEG allyl ether (**3**) was recovered by two times precipitation in cold hexane and dried in vacuo.

In situ forming degradable dextran vinyl sulfone hydrogels

Conversion ($^1\text{H NMR}$): 92%. Yield: 33.37 g, 83%. $^1\text{H NMR}$ (CDCl_3): δ 3.5-3.7 (m, PEG main chain protons), 4.0 (m, $-\text{O}-\text{CH}_2-\text{CH}=\text{CH}_2$), 5.2-5.3 (m, $-\text{O}-\text{CH}_2-\text{CH}=\text{CH}_2$), 5.8-6.0 (m, $-\text{O}-\text{CH}_2-\text{CH}=\text{CH}_2$).

To obtain the PEG thioacetate (PEG-TA), typically linear PEG allyl ether (**3**, 20 g) was dissolved in toluene (120 ml, allyl group concentration is 160 mM) and the mixture was degassed for 30 min by argon bubbling. Subsequently, AIBN (30.58 g, 192 mmol, 10 mol equivalents to allyl groups) and TAA (**4**, 10.9 ml, 154 mmol, 10 mol equivalents to allyl groups) were added to the solution. TAA was added in five equal aliquots during an hour and the reaction proceeded for 24 h at 65°C . The PEG-TA (**5**) was recovered by three times precipitation in cold diethyl ether and dried in vacuo. Conversion: 100%. Yield: 19.16 g, 96%. $^1\text{H NMR}$ (CDCl_3): δ 1.8-1.9 (q, $-\text{O}-\text{CH}_2-\text{CH}_2-\text{CH}_2-\text{S}-$), 2.3 (s, $-\text{CH}_2-\text{S}-\text{CO}-\text{CH}_3$), 2.9-3.0 (t, $-\text{O}-\text{CH}_2-\text{CH}_2-\text{CH}_2-\text{S}-$), 3.5 (t, $-\text{O}-\text{CH}_2-\text{CH}_2-\text{CH}_2-\text{S}-$), 3.6-3.8 (m, PEG main chain protons).

To remove the thioacetate groups and obtain the PEG-2-SH, linear PEG-TA (**5**, 10.25 g) was dissolved in methanol (5 ml, TA concentration is 100 mM). STM (**6**) was dissolved in methanol (92 ml, 1 M) and added to the PEG-TA solution. After 30 min of reaction, the solution was added to 0.1 M HCl (10 ml) and extracted four times with dichloromethane. The organic layer was subsequently washed with brine and dried over anhydrous magnesium sulphate. The solvents were removed under vacuum and after dissolution in deionized water a small amount of DTE was added to reduce possibly formed disulfide bonds. Finally, PEG-2-SH (**7**) was purified by ultrafiltration against deionized water under a nitrogen atmosphere (MWCO 1,000) and obtained by lyophilization. Yield: 5.72 g, 56%. The Ellman test showed a thiol functionality of 85%. $^1\text{H NMR}$ (CDCl_3): δ 1.80-1.90 (m, $-\text{O}-\text{CH}_2-\text{CH}_2-\text{CH}_2-\text{SH}$), 2.52 – 2.60 (q, $-\text{O}-\text{CH}_2-\text{CH}_2-\text{CH}_2-\text{SH}$), 3.47-3.53 (t, $-\text{O}-\text{CH}_2-\text{CH}_2-\text{CH}_2-\text{SH}$), 3.53-3.80 (m, PEG main chain protons).

PEG-4-SH was synthesized similarly to PEG-2-SH. The Ellman test showed a thiol functionality of 89%.

Characterization. Molecular weights of dextran were determined by gel permeation chromatography (GPC) using a Viscotek GPCmax with Viscotek 302 Triple Detection Array. As eluent 0.1 M NaNO_3 was used with a flow of 1 ml/min. Molecular weights of PEG were determined by MALDI-TOF mass spectrometry (MS) performed on a Voyager

(Applied Biosystems) in the reflector mode using ditranol as matrix. ^1H NMR spectra were recorded on a Varian Inova Spectrometer (Varian, Palo, Alto, USA) operating at 300 MHz. The DS of dex-VS is defined as the amount of substituents per 100 AHG. The DS was calculated from the ^1H NMR spectra (D_2O) based on the glucosidic protons of dextran (δ 3.4-4.1, 5.2 and 5.4) and the protons of the vinyl sulfone group (δ 6.5 and 6.9). The conversion of the PEG derivatives was calculated from the PEG main chain protons at δ 3.5-3.7 and protons from the characteristic functional end groups. For PEG allyl ether the protons of the allyl group at δ 5.1-5.3 and 5.8-6.0 were used and for PEG-TA the protons of the thioacetate group at δ 2.3 were used. The number of free thiol groups of PEG-SH was determined by the Ellman test.³⁵ Absorption of diluted PEG-SH solutions (PBS buffer, pH 7, 100 mM) was recorded at 412 nm on a Cary 300 Bio UV-Visible Spectrophotometer (Varian). The concentration of free thiol groups was calculated using a calibration curve derived from mercaptoethanol standard solutions.

Gelation time and swelling tests. To determine the gelation time, solutions of dex-VS with various degrees of substitution and concentrations, and PEG-SH (molar ratio of thiol to vinyl sulfone groups is kept at 1.1) in 250 μl of HEPES buffered saline (pH 7, 100 mM, adjusted to 300 mOsm with NaCl) were mixed at 37 $^\circ\text{C}$ by vortexing. The gelation time was determined by the vial tilting method. When the sample showed no flow within 20 s, it was regarded as a gel. Subsequently, 3 ml of buffer solution was put on top of the hydrogels and the hydrogels were allowed to swell at 37 $^\circ\text{C}$. The swollen hydrogels were weighed at regular time intervals after removal of the buffer. After each weighing the buffer was refreshed. The swelling ratio of the hydrogels was calculated from the initial hydrogel weight after preparation (W_0) and the swollen hydrogel weight after exposure to buffer (W_t):

$$\text{Swelling ratio} = \frac{W_t}{W_0}$$

Degradation of dex-VS materials. The kinetics of the ester bond hydrolysis of the dex-Et-VS and dex-Pr-VS materials at 37 $^\circ\text{C}$ in PBS (pH 7, 100 mM, adjusted to 300 mOsm with NaCl) were followed. Dex-VS solutions were placed in dialysis bags (MWCO 3,000), which allows complete removal of the vinyl sulfone alkanolic acid degradation byproduct.

In situ forming degradable dextran vinyl sulfone hydrogels

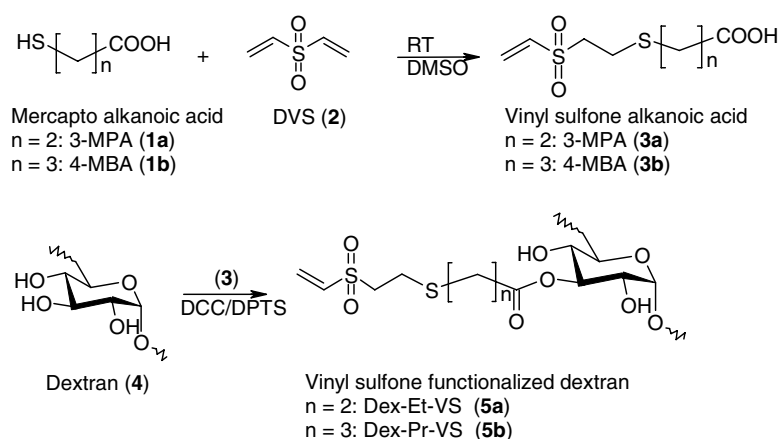
At regular time intervals samples were taken and after lyophilization the DS of the dex-VS conjugates was determined by ^1H NMR (D_2O).

Rheology. Rheology experiments were performed at $37\text{ }^\circ\text{C}$ on a US 200 rheometer (Anton Paar). Solutions of dex-VS and PEG-SH in HEPES buffered saline were mixed (molar ratio of thiol groups to vinyl sulfone groups is kept at 1.1) and quickly applied to the rheometer using a double barreled syringe with a mixing chamber (Mixpac). To prevent evaporation, a thin layer of oil was applied. Parallel plates (25 mm in diameter) with an adjustable gap were used to have a normal force of maximal 0.1 N and a frequency of 1 Hz was applied. The strain was adjusted to the torque limits of the machine and was 1% or 0.1%. Both strains are within the linear viscoelastic region.

7.4 Results and Discussion

7.4.1 Synthesis of dextran vinyl sulfone conjugates and mercapto poly(ethylene glycol)s.

Dextran vinyl sulfone derivatives were prepared by a one-pot synthesis procedure at room temperature using dimethylsulfoxide (DMSO) as a solvent (Scheme 2).



Scheme 2. Schematic representation of the one-pot synthesis procedure of dextran vinyl sulfone conjugates with an ethyl spacer (dex-Et-VS) or a propyl spacer (dex-Pr-VS) between the thioether and ester groups.

3-Mercaptoproionic acid (3-MPA, **1a**) was first reacted with 20 times excess of divinyl sulfone (DVS) (**2**) for 4 h. Test reactions, using ^1H NMR, showed 100% conversion of **1a**, yielding the corresponding vinyl sulfone propionic acid (**3a**). The formed **3a**, without isolation, was subsequently coupled to dextran (**4**) using *N,N'*-dicyclohexylcarbodiimide (DCC)/4-(dimethylamino)pyridinium 4-toluenesulfonate (DPTS) as a catalyst system. The reaction was allowed to proceed for 24 h and the resulting dextran vinyl sulfone conjugates (**5a**) were isolated by filtering off the DCU salt, precipitation in cold ethanol, ultrafiltration against water and lyophilization. Yields of 68-98% were obtained.

The vinyl sulfone derivatization of dextran was confirmed by ^1H NMR. Figure 1b shows, besides signals attributed to dextran, new peaks at δ 6.5 and 6.9 (peaks **e'** and **f'**) due to the vinyl sulfone protons (Figure 1b). The vinyl sulfone derivatization was further confirmed by the presence of small peaks at δ 5.2 and 5.4 (peaks **c'**), due to the peak shift of glucosidic protons of the anhydroglucose unit upon reaction with the vinyl sulfone acid (Figure 1b). We did not study in detail the position at which the substitution took place. The degree of substitution (DS) was determined by comparing the peak areas corresponding to the vinyl sulfone protons at δ 6.5 and 6.9 and the dextran glucosidic protons at δ 3.4-4.1, 5.2 and 5.4. The DS is defined as the number of substituents per 100 anhydroglucosidic rings (AHG). Dextrans with two different molecular weights, 14K and 31K, were used to study the effect of the molecular weight on the hydrogel formation. The DS of dex14K-Et-VS ranged from 2 to 22 when varying the molar ratio of 3-MPA to the AHG of dextran from 0.3 to 0.9 (Table 1, entry 1-5). Likewise, dex31K-Et-VS materials with DS 2 to 14 were obtained by varying the molar ratio 3-MPA to the AHG of dextran from 0.3 to 0.6 (Table 1, entry 6-9). The DS is proportional to the molar feeding ratio of 3-MPA and AHG of dextran, using the same reaction conditions. At higher dextran concentrations, but otherwise same conditions, higher DSs could be obtained (Table 1, entry 4). Dextran vinyl sulfone derivatives with a propyl spacer between the thioether and the ester groups (dex-Pr-VS) were also prepared in a similar way (Scheme 2). 4-Mercapto butyric acid (4-MBA, Scheme 2, **1b**) was obtained by reduction of 4,4'-dithiodibutyric acid using tripropylphosphine and was used without further purification. From literature it is known that with increased spacing between the thioether and the ester bond the hydrolytic

susceptibility of the ester bond decreases.³⁶ Therefore, the hydrogels derived from dex-Pr-VS are expected to degrade slower compared to the dex-Et-VS hydrogels. The ¹H NMR spectrum (Figure 1c) of dex-Pr-VS also showed peaks at δ 6.5 and 6.9 (peaks e'' and f'') due to the presence of the vinyl sulfone substituents and at δ 5.2 and 5.4 (peaks c'') due to the glucosidic protons linked to the vinyl sulfone substituents. Dex14K-Pr-VS with DS 8 and dex31K-Pr-VS with DS 10 were synthesized using molar feeding ratio's of 4-MBA to the AHG of dextran of 0.53 and 0.90, respectively (Table 1, entry 10 and 11). This one-pot synthesis procedure is a convenient method to prepare vinyl sulfone functionalized dextrans with a broad range of substitution degrees.

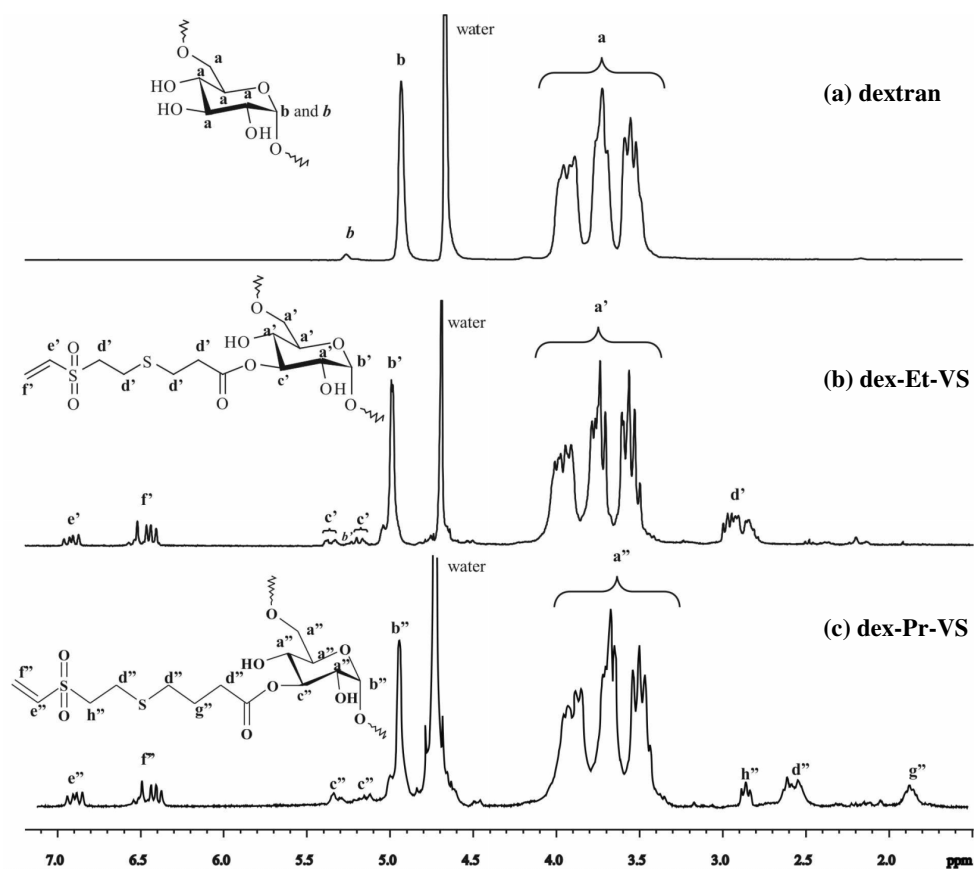


Figure 1. ¹H NMR spectra (D₂O) of (a) dextran, (b) dex-Et-VS (Table 1, entry 3) and (c) dex-Pr-VS (Table 1, entry 10). The substitution at position C-3 is given as an example.

Chapter 7

Mercapto poly(ethylene glycol)s were synthesized in three steps as reported previously by Goessl et al.³⁴ In order to investigate the influence of the thiol functionality on the hydrogel formation, two mercapto poly(ethylene glycol)s with two and four thiol groups (denoted as PEG-2-SH and PEG-4-SH, respectively) were prepared. Both the linear and four-arm PEG have a molecular weight of 2.1K, as determined by MALDI-TOF MS. Ellman tests³⁵ showed a thiol functionality of 85 and 89% for PEG-2-SH and PEG-4-SH, respectively.

Table 1. Synthesis of dextran vinyl sulfone derivatives, dex-Et-VS and dex-Pr-VS.

Entry	Dextran derivative	$M_{n, GPC}$ dextran $\times 10^{-3}$	Molar feeding ratio of mercapto alkanic acid to AHG of dextran ^{a)}	DS ^{e)}
1			0.30	2
2			0.45	4
3	Dex-Et-VS	14	0.60	8
4			0.60 ^{b)}	13
5			0.90	22
6			0.30	2
7	Dex-Et-VS	31	0.45	4
8			0.53 ^{c)}	9
9			0.60 ^{d)}	13
10	Dex-Pr-VS	14	0.53	10
11		31	0.90	8

^{a)} Dextran concentration is 3.3 w/v%. ^{b)} Dextran concentration is 4.7 w/v%. ^{c)} Dextran concentration is 3.7 w/v%. ^{d)} Dextran concentration is 4.3 w/v%. ^{e)} Degree of substitution (DS), defined as the number of vinyl sulfone groups per 100 AHG of dextran, was determined by ¹H NMR by comparing the peak areas corresponding to the dextran glucosidic protons (δ 3.4-4.1, 5.2 and 5.4) and the protons of the vinyl sulfone group (δ 6.5 and 6.9).

7.4.2 In situ hydrogel formation.

Dextran hydrogels were formed in situ via Michael type addition between dex-VS and PEG-SH in HEPES buffered saline at pH 7 and 37 °C (Figure 2). The molar ratio of thiol to vinyl sulfone groups was kept at 1.1, since thiol groups may form some disulfide bonds due to exposure to air, thus lowering the effective concentration of free thiol groups. In the concentration range studied (10 to 20 w/v%) these hydrogels were transparent.

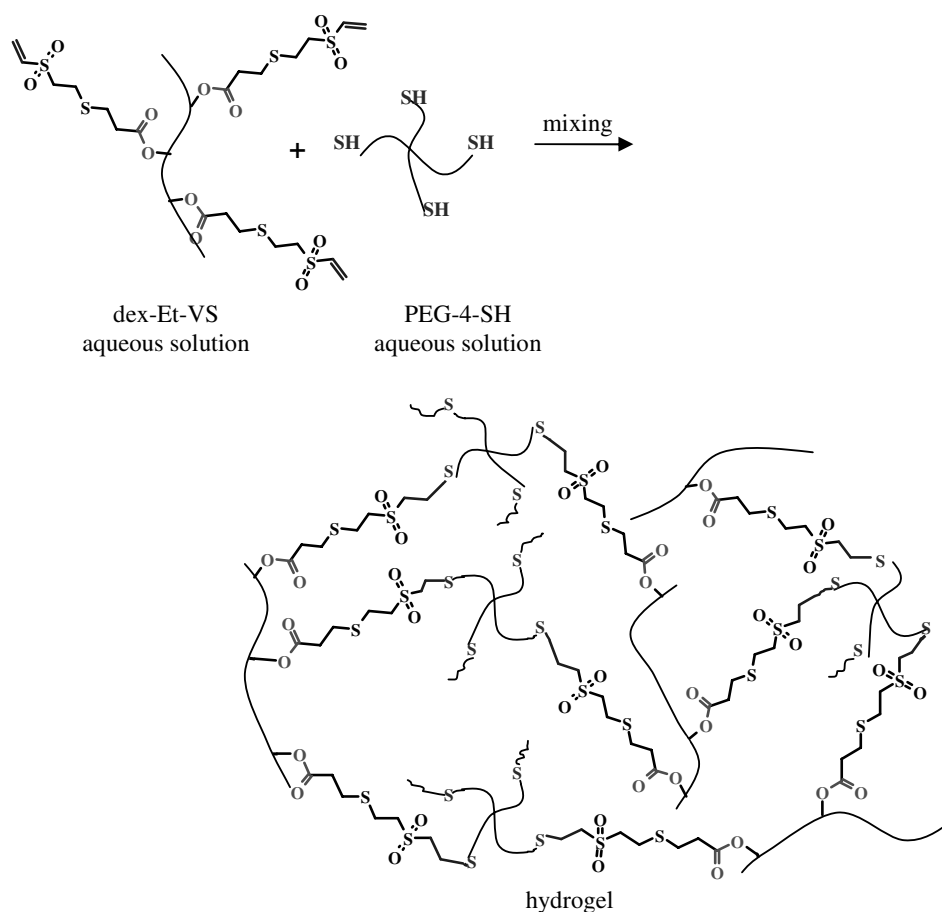


Figure 2. Schematic representation of the Michael type addition between dex-VS and PEG-SH, shown for dex-Et-VS and PEG-4-SH.

The gelation time was determined by the vial tilting method. The concentration is defined as the total dry weight of both PEG and dextran per volume of buffer. Figure 3a

shows the gelation time as a function of the DS for dex14K-Et-VS and dex31K-Et-VS crosslinked with PEG-4-SH at a constant concentration of 15 w/v%. The gelation time decreased with increasing DS and was 7 min for dex14K-Et-VS with DS 4 and 0.5 min for dex14K-Et-VS with DS 13. A further increase in DS did not alter the gelation time. In Figure 3b the gelation time is shown as a function of the concentration for dex14K-Et-VS DS 8 and dex31K-Et-VS with a comparable DS, crosslinked with PEG-4-SH. The gelation time for dex14K-Et-VS DS 8 decreased from approximately 7.5 to 1.5 min by increasing the concentration from 10 to 20 w/v%. Similarly, the gelation time for dex31K-Et-VS DS 9 decreased from 1.5 to 0.5 min when increasing the concentration from 10 to 20 w/v% (Figure 3b). In Figure 3c the gelation times are shown of dex14K-Pr-VS DS 10, dex31K-Pr-VS DS 8 crosslinked with PEG-4-SH and of dex31K-Pr-VS DS 8 crosslinked with PEG-2-SH as a function of the concentration. Similar to dex-Et-VS the gelation time of dex-Pr-VS decreased by increasing the concentration from 10 to 20 w/v% and by increasing the dextran molecular weight from 14K to 31K. Increasing the PEG thiol functionality from two to four somewhat decreased the gelation time (from approximately 3 to 2 min) at 10 w/v% concentration, while the gelation times were comparable at 15 and 20 w/v% concentrations (Figure 3c). Dex31K-Et-VS DS 9 and dex31K-Pr-VS DS 8 showed comparable gelation times at the same concentration (Figure 3b and Figure 3c), indicating that the spacer between the thioether and the ester groups has little influence on the gelation process. In general, the gelation times of these dex-VS materials are short compared those (approximately 15 min or longer) reported by Lutolf et al. for four-arm PEG vinyl sulfones crosslinked with dithiol peptides at similar conditions (pH 7, 10 w/v% solutions).³⁷ This is most likely due to the generally higher crosslinking functionality of the dex-VS as compared to the PEG vinyl sulfones. Dex-VS hydrogels could also be formed by using dithioerythritol (DTE) in stead of PEG-4-SH or PEG-2-SH. Gelation times ranged from 0.5 to 7 min in a concentration range of 10 to 20 w/v%. In order to be able to compare the influence of different thiol functionalities only PEG-2-SH and PEG-4-SH were used for further studies. Hydrogels could not be formed at DS 2 at 15 w/v% concentration for dex14K-Et-VS and dex31K-Et-VS crosslinked with PEG-4-SH. Apparently, at these conditions the number of reacted groups is lower than the critical crosslinking density at which the three-dimensional network can be formed. For dex-VS

with DS 4 or higher, gelation occurred on a time scale of 0.5 to 7.5 min, which is particularly appealing for application as injectable hydrogels.

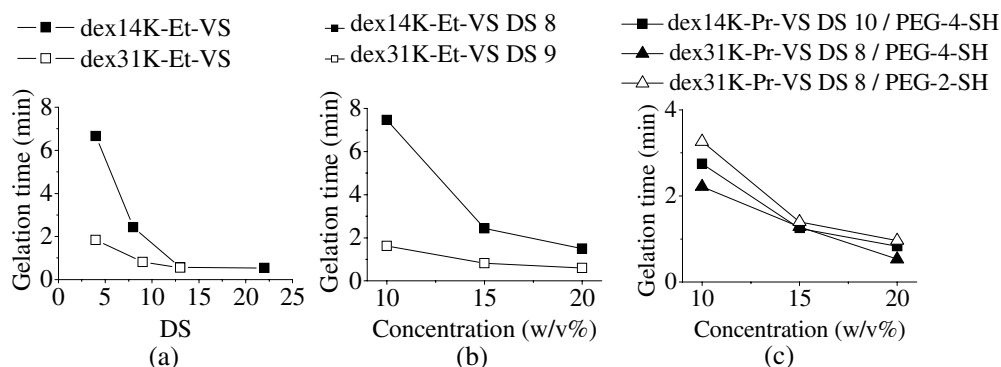


Figure 3. Gelation times (± 5 s) determined by the vial tilting method after mixing solutions of dex-VS and PEG-SH (molar ratio of SH to VS is kept at 1.1) in HEPES buffered saline at pH 7 and 37 °C. (a) dex14K-Et-VS and dex31K-Et-VS with PEG-4-SH as a function of the DS at 15 w/v% concentration; (b) dex14K-Et-VS DS 8 and dex31K-Et-VS DS 9 with PEG-4-SH as a function of the concentration; (c) dex14K-Pr-VS DS 10 with PEG-4-SH and dex31K-Pr-VS DS 8 with PEG-4-SH or PEG-2-SH as a function of the concentration.

7.4.3 Rheology.

The mechanical properties of the dextran hydrogels were studied by oscillatory rheology experiments on solutions in HEPES buffered saline at pH 7 and 37 °C. Dex-VS and PEG-SH solutions (molar ratio of thiol groups to vinyl sulfone groups is kept at 1.1) were mixed by a double barreled syringe with a mixing chamber and quickly applied to the rheometer. Subsequently, the kinetics of the gelation were followed by monitoring the storage modulus (G') and loss modulus (G'') in time. Figure 4a shows that the storage modulus sharply increases after mixing of dex14K-Et-VS DS 4 and PEG-4-SH at 15 w/v% concentration. The gelation point is reached 4 min after mixing as indicated by the crossing of the storage and loss modulus. The vial tilting method showed a somewhat longer

gelation time of 7 min (Figure 3a). This is attributed to the fact that a certain yield stress is needed to have zero flow at vial tilting. Li et al. found for PEG-poly(butylene oxide) diblock copolymer hydrogels that a yield stress of at least approximately 65 Pa is needed to have zero flow at vial tilting.³⁸ Dex31K-Et-VS DS 4 crosslinked with PEG-4-SH at 15 w/v% concentration showed faster gelation compared to the corresponding dex14K-Et-VS DS 4 mixture, due to the higher number of vinyl sulfone groups per dextran molecule (Figure 4a). The higher number of vinyl sulfone groups per molecule of dex31K-Et-VS also yields higher storage moduli compared to dex14K-Et-VS at the same DS and concentration. Dex31K-Et-VS DS 4 showed a storage modulus of 4.5 kPa, while dex14-Et-VS DS 4 showed a storage modulus of 8 kPa when crosslinked with PEG-4-SH at 15 w/v% concentration. A plot of the storage modulus vs. the DS (Figure 5a) showed that this effect leveled off at higher DS. Figure 4b shows that both the gelation rate and the storage moduli of dex31K-Pr-VS DS 8 and dex31K-Et-VS DS 9 crosslinked with PEG-4-SH at 10 w/v% concentration are similar, indicating that the nature of the spacer between the thioether and the ester groups does not affect the mechanical properties. Dex31K-Pr-VS DS 8 crosslinked with PEG-4-SH gelled faster compared to when PEG-2-SH is used as a crosslinker (Figure 4b).

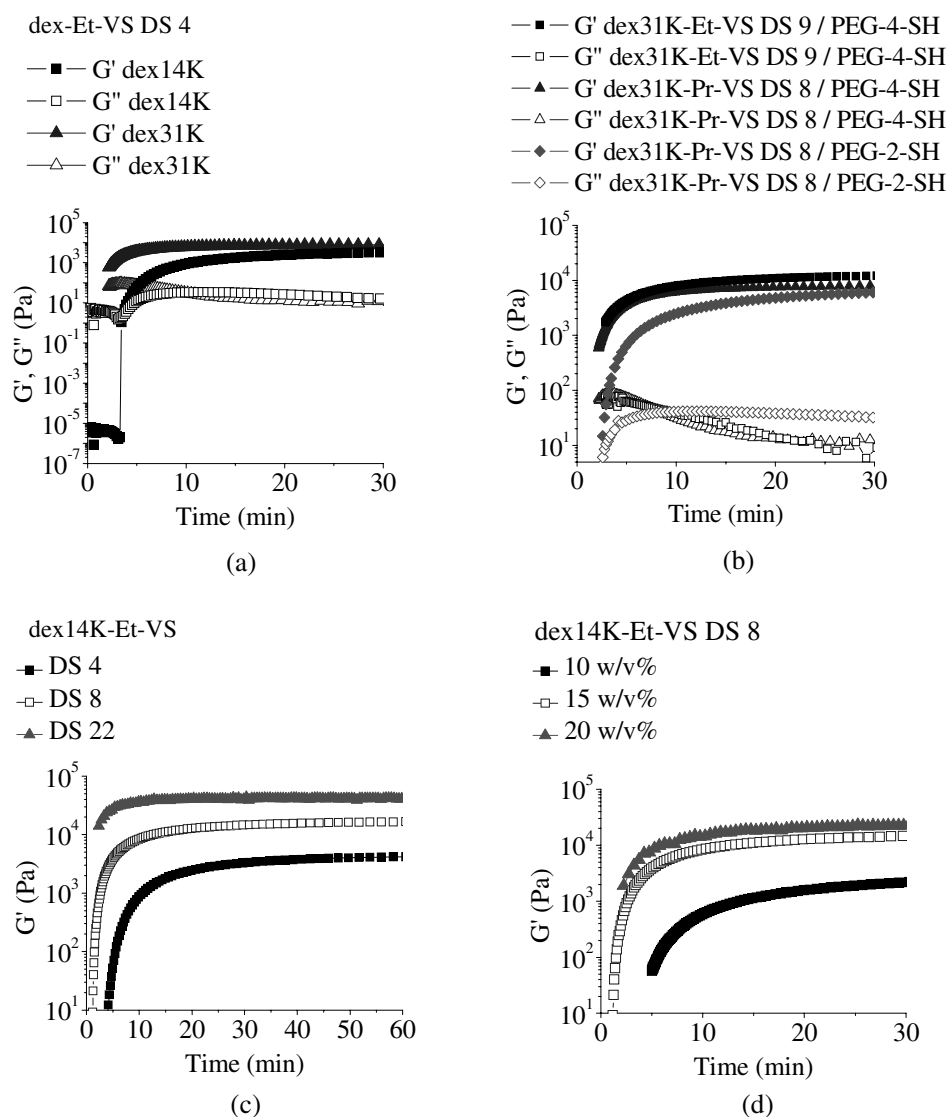


Figure 4. The storage modulus (G') and the loss modulus (G'') as a function of time of dex-VS / PEG-SH mixtures in HEPES buffered saline at pH 7 and 37 °C. (a) dex14K-Et-VS DS 4 and dex31K-Et-VS DS 4 with PEG-4-SH at 15 w/v% concentration; (b) dex31K-Et-VS DS 9 with PEG-4-SH and dex31K-Pr-VS DS 8 with PEG-4-SH or PEG-2-SH at 10 w/v% concentration; (c) dex14K-Et-VS at DS 4, 8 and 22 at 15 w/v% concentration; (d) dex14K-Et-VS DS 8 at 10, 15 and 20 w/v% concentration.

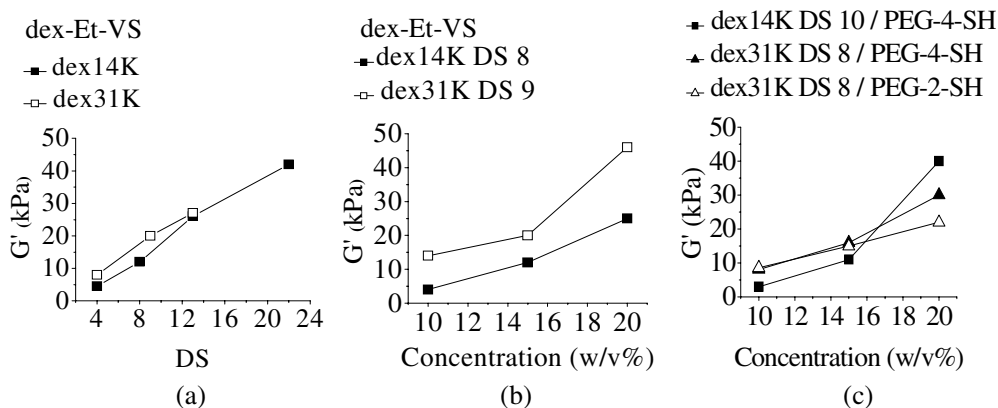


Figure 5. The storage modulus plateau values of dex-Et-VS and dex-Pr-VS hydrogels in HEPES buffered saline at pH 7 and 37 °C. (a) dex14K-Et-VS and dex31K-Et-VS with PEG-4-SH as a function of the degree of substitution (DS); (b) dex14K-Et-VS and dex31K-Et-VS with PEG-4-SH as a function of the concentration; (c) dex14K-Pr-VS DS 10 with PEG-4-SH and dex31K-Pr-VS DS 8 with PEG-4-SH or PEG-2-SH as a function of the concentration.

A plot of the storage modulus vs. the concentration (Figure 5c) shows that the storage moduli of dex31K-Pr-VS DS 8 crosslinked with PEG-4-SH or PEG-2-SH are similar at 10 and 15 w/v% concentration (approximately 8 and 15 kPa, respectively), and at 20 w/v% the storage modulus is somewhat higher for the PEG-4-SH hydrogel (30 vs. 22 kPa). The similar storage modulus values may be due to the high vinyl functionality of the dextran, wherein increasing the number of thiol groups from two to four per PEG molecule hardly influences the gel storage modulus. Generally, the damping factors ($\tan \delta = G''/G'$) of these dex-VS hydrogels were lower than 0.01, indicating that these hydrogels are highly elastic. The loss moduli of dex-VS hydrogels with DS higher than 4 either at 15 or at 20 w/v% concentrations were too low to be accurately measured and therefore only the evolutions of the storage modulus of these hydrogels are shown. Figure 4c shows that the gelation rate increases considerably with increasing DS for dex14K-Et-VS hydrogels at 15 w/v% concentration. At DS 22 the storage modulus plateau value is reached within a few min, while at DS 4 this takes approximately 20 min. Dex31K-Et-VS hydrogels showed a similar increase in gelation rate with increasing DS. A plot of the storage modulus vs. the DS

(Figure 5a) shows that the storage moduli of both dex31K-Et-VS and dex14K-Et-VS hydrogels increase almost linearly with increasing DS. At DS 4 dex14K-Et-VS hydrogels have a storage modulus of 4.5 kPa, while at DS 22 the storage modulus is 42 kPa. As shown in Figure 4d the gelation rate of dex14K-Et-VS crosslinked with PEG-4-SH increases by increasing the concentration from 10 to 20 w/v%. Plot of the storage modulus vs. the polymer concentration (Figure 5b and Figure 5c) show that the storage modulus of dex-Et-VS and dex-Pr-VS hydrogels increases with increasing concentration. For example, at 10 w/v% dex14K-Et-VS DS 8 hydrogels have a storage modulus of 4 kPa, while at 20 w/v% the storage modulus is 25 kPa (Figure 5b). In summary, dex-VS hydrogels with storage moduli ranging from 3 to 46 kPa could be obtained by varying the DS, concentration and dextran molecular weight.

7.4.4 Hydrogel swelling and degradation.

The dex-VS hydrogels were degradable under physiological conditions. To study the rate of degradation of these hydrogels, solutions of dex-VS and PEG-SH were mixed in HEPES buffered saline at pH 7 and 37 °C (molar ratio of thiol groups to vinyl sulfone groups is kept at 1.1). After the hydrogels were formed, HEPES buffer was applied on top and the gels were allowed to swell at 37 °C. At regular time intervals, the swelling ratio was calculated by rationing the swollen hydrogel weight with the initial hydrogel weight (W_t/W_0). Figure 6 shows that in general the initial swelling ratio of the dex-VS hydrogels is low. All hydrogels displayed gradual swelling in time, until they rapidly dissolved. This is caused by the hydrolytic cleavage of the ester bonds between the dextran backbone and the thioether group. The degradation time is defined as the time after which the hydrogel is almost or completely dissolved.

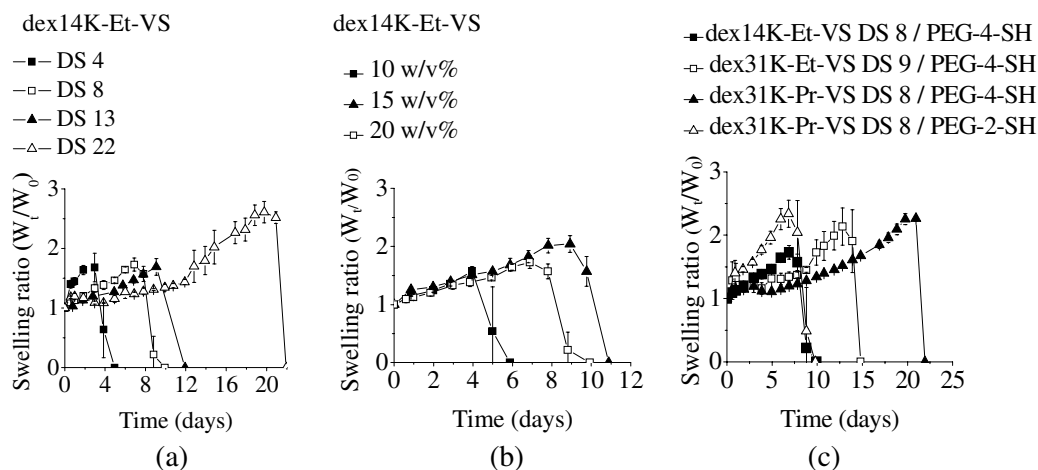


Figure 6. Swelling ratio (W_t/W_0) profiles of dex-VS hydrogels in HEPES buffered saline at pH 7 and 37 °C ($n = 3$); (a) dex14K-Et-VS with PEG-4-SH at DS 4, DS 8, DS 13 and DS 22 at 15 w/v% concentration; (b) dex14K-Et-VS DS 8 with PEG-4-SH at concentrations of 10, 15 and 20 w/v%; (c) dex14K-Et-VS DS 8 and dex31K-Et-VS DS 9 with PEG-4-SH and dex31K-Pr-VS DS 8 with PEG-4-SH or PEG-2-SH at 15 w/v% concentration.

A plot of the degradation time vs. the DS (Figure 7a) revealed that the hydrogel degradation time increased with increasing DS. The corresponding dex31K-Et-VS hydrogels follow the same trend and showed degradation times of 5 and 16 days at DS 4 and DS 13, respectively (Figure 6a). In Figure 6b the swelling ratio profiles are shown of dex14K-Et-VS DS 8 hydrogels crosslinked with PEG-4-SH at 10, 15 and 20 w/v% concentrations. Increasing the concentration from 10 to 20 w/v% increased the hydrogel degradation time from 3 to 9 days. For the corresponding dex31K-Et-VS DS 9 hydrogels the degradation time increased from 9 to 14 days when increasing the concentration from 10 to 15 w/v%, while the effect leveled off at 20 w/v% (Figure 7b).

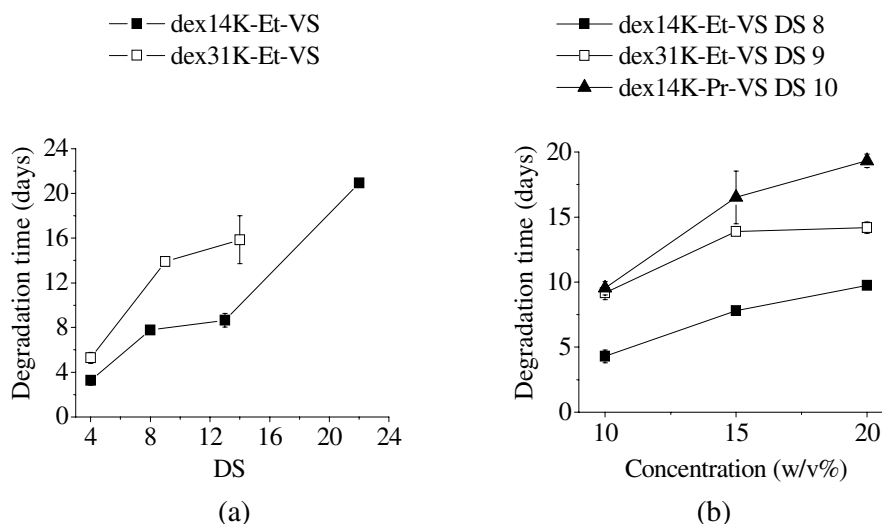


Figure 7. Plots of degradation times vs. DS or concentration of dex-Et-VS hydrogels crosslinked with PEG-4-SH in HEPES buffered saline at pH 7 and 37 °C (n = 3). (a) dex14K-Et-VS and dex31K-Et-VS as a function of the DS at 15 w/v% concentration; (b) dex14K-Et-VS DS 8, dex31K-Et-VS DS 9 and dex14K-Pr-VS DS 10 as a function of the concentration.

Figure 7b shows that by increasing the dextran molecular weight from 14K to 31K the hydrogel degradation time almost doubles, due to the higher number of vinyl sulfone groups per dextran molecule. Interestingly, as shown in Figure 6c, the use of a propyl spacer in stead of an ethyl spacer between the thioether and ester groups considerably increases the hydrogel degradation time. The hydrogel degradation times are 14 and 21 days for dex31K-Et-VS DS 9 and dex31K-Pr-VS DS 8 crosslinked with PEG-4-SH at 15 w/v% concentration, respectively. This is due to the lower positive charge on the carbonyl carbon when more methylene groups are spaced between the thioether and the ester linkage, rendering the ester linkage less susceptible to hydrolysis.³⁶ Figure 7b shows that, similar to dex-Et-VS hydrogels, the degradation time of the dex-Pr-VS hydrogels increases with increasing concentration from 10 to 20 w/v%. The degradation times were 10 and 19 days at 10 and 20 w/v%, respectively. As shown in Figure 6c the degradation time decreases with decreasing the number of thiol groups per PEG molecule (8 vs. 21 days).

The degradation of dex-VS conjugates in PBS at pH 7 and 37 °C was followed by ^1H NMR. A dialysis bag (MWCO 3,000) was used and at regular time intervals samples were removed, lyophilized and the remaining DS was determined by rationing the peak areas of the dextran glucosidic protons and protons of the vinyl sulfone group. Figure 8 shows that degradation rates for dex14K-Et-VS conjugates with DS 4, 8, 13 and 22 and of dex31K-Et-VS DS 13 are similar, indicating that the hydrolysis kinetics are independent of the DS and the dextran molecular weight. On the other hand, dex14K-Pr-VS DS 10 and dex31K-Pr-VS DS 8 degrade somewhat slower than dex-Et-VS conjugates. This agrees well with the slower degradation of the dex-Pr-VS hydrogels compared to the corresponding dex-Et-VS hydrogels. In summary, the degradation rate of dex-VS hydrogels can be readily controlled by the DS, concentration, dextran molecular weight, PEG-SH functionality and the length of the spacer between the thioether and ester groups.

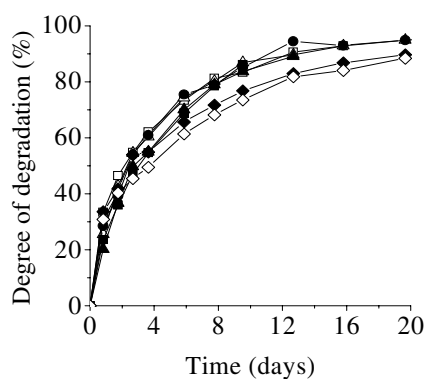


Figure 8. Degree of degradation of dex-VS conjugates in PBS at pH 7 and 37 °C as determined by ^1H NMR. Dex14K-Et-VS DS 4 (■), DS 8 (□), DS 13 (▲) and DS 22 (△), dex31K-Et-VS DS 13 (●), dex14K-Pr-VS DS 10 (◆) and dex31K-Pr-VS DS 8 (◇).

7.5 Conclusions

Dextrans with pendant vinyl sulfone groups linked by a hydrolytically susceptible ester bond were synthesized by a one-pot synthesis procedure to a broad range of degrees of substitution. Hydrogels were rapidly formed in situ under physiological conditions by mixing aqueous solutions of vinyl sulfone functionalized dextrans and multi-functional mercapto PEG. Their mechanical and degradation properties are readily controlled by the degree of vinyl sulfone substitution, concentration, dextran molecular weight and PEG thiol functionality. The hydrogels showed storage moduli ranging from 3 to 46 kPa and degraded within 3 to 21 days. Furthermore, hydrogels with similar mechanical properties, but decreased degradation rates could be prepared by increasing the spacer length between the thioether and the ester groups. These hydrogels are very promising for use in biomedical applications, since they can be rapidly formed in situ in the body by co-injection of aqueous solutions of vinyl sulfone dextran and multi-functional mercapto PEG. Also, they offer a broad range of degradation and mechanical properties. Furthermore, in principle bioactive molecules, such as proteins and peptides, can readily be incorporated by using thiol-containing biomolecules to give biomimetic scaffolds.

7.6 Acknowledgements

This work was funded by the Netherlands Organization for Scientific Research (NWO).

7.7 References

1. Kashyap, N.; Kumar, N.; Kumar, M. N. V. R., Hydrogels for pharmaceutical and biomedical applications. *Crit. Rev. Ther. Drug Carrier Syst.* 2005, 22, 107-149.
2. Peppas, N.; Bures, P.; Ichikawa, H., Hydrogels in pharmaceutical formulations. *Eur. J. Pharm. Biopharm.* 2000, 50, 27-46.
3. Hubbell, J. A., Materials as morphogenetic guides in tissue engineering. *Curr. Opin. Biotech.* 2003, 14, 551-558.

4. Kim, S.; Healy, K. E., Synthesis and characterization of injectable poly(N-isopropylacrylamide-co-acrylic acid) hydrogels with proteolytically degradable cross-links. *Biomacromolecules* 2003, 4, 1214-1223.
5. Zhong, Z. Y.; Dijkstra, P. J.; Feijen, J.; Kwon, Y. M.; Bae, Y. H.; Kim, S. W., Synthesis and aqueous phase behavior of thermoresponsive biodegradable poly(D,L-3-methylglycolide)-block-poly(ethylene glycol)-block-poly(D,L-3-methylglycolide) triblock copolymers. *Macromol. Chem. Phys.* 2002, 203, 1797-1803.
6. Jeong, B.; Bae, Y. H.; Lee, D. S.; Kim, S. W., Biodegradable block copolymers as injectable drug-delivery systems. *Nature* 1997, 388, 860-862.
7. Chapter 3, Hiemstra, C.; Zhong, Z. Y.; Dijkstra, P. J.; Feijen, J., Stereocomplex mediated gelation of PEG-(PLA)₂ and PEG-(PLA)₈ block copolymers. Published in *Macromol. Symp.* 2005, 224, 119-131.
8. Mukose, T.; Fujiwara, T.; Nakano, J.; Taniguchi, I.; Miyamoto, M.; Kimura, Y.; Teraoka, I.; Lee, C. W., Hydrogel formation between enantiomeric B-A-B-type block copolymers of polylactides (PLLA or PDLA : A) and polyoxyethylene (PEG : B); PEG-PLLA-PEG and PEG-PDLA-PEG. *Macromol. Biosci.* 2004, 4, 361-367.
9. Li, S. M.; El Ghzaoui, A.; Dewinck, E., Rheology and drug release properties of bioresorbable hydrogels prepared from polylactide/poly(ethylene glycol) block copolymers. *Macromol. Symp.* 2005, 222, 23-35.
10. de Jong, S. J.; van Eerdenbrugh, B.; van Nostrum, C. F.; Kettenes-van de Bosch, J. J.; Hennink, W. E., Physically crosslinked dextran hydrogels by stereocomplex formation of lactic acid oligomers: degradation and protein release behavior. *J. Controlled Release* 2001, 71, 261-275.
11. Collier, J. H.; Hu, B.-H.; Ruberti, J. W.; Zhang, J.; Shum, P.; Thompson, D. H.; Messersmith, P. B., Thermally and photochemically triggered self-assembly of peptide hydrogels. *JACS* 2001, 123, 9463-9464.
12. Nowak, A. P.; Breedveld, V.; Pakstis, L.; Ozbas, B.; Pine, D. J.; Pochan, D.; Deming, T. J., Rapidly recovering hydrogel scaffolds from self-assembling diblock copolypeptide amphiphiles. *Nature* 2002, 417, 424-428.
13. Li, J.; Li, X.; Ni, X. P.; Wang, X.; Li, H. Z.; Leong, K. W., Self-assembled supramolecular hydrogels formed by biodegradable PEO-PHB-PEO triblock

- copolymers and alpha-cyclodextrin for controlled drug delivery. *Biomaterials* 2006, 27, 4132-4140.
14. Van Tomme, S. R.; van Steenberg, M. J.; De Smedt, S. C.; van Nostrum, C. F.; Hennink, W. E., Self-gelling hydrogels based on oppositely charged dextran microspheres. *Biomaterials* 2005, 26, 2129-2135.
 15. Park, Y. D.; Tirelli, N.; Hubbell, J. A., Photopolymerized hyaluronic acid-based hydrogels and interpenetrating networks. *Biomaterials* 2003, 24, 893-900.
 16. Halstenberg, S.; Panitch, A.; Rizzi, S.; Hall, H.; Hubbell, J. A., Biologically engineered protein-graft-poly(ethylene glycol) hydrogels: A cell adhesive and plasmin-degradable biosynthetic material for tissue repair. *Biomacromolecules* 2002, 3, 710-723.
 17. Davis, K. A.; Burdick, J. A.; Anseth, K. S., Photoinitiated crosslinked degradable copolymer networks for tissue engineering applications. *Biomaterials* 2003, 24, 2485-2495.
 18. Quick, D. J.; Anseth, K. S., Gene delivery in tissue engineering: A photopolymer platform to coencapsulate cells and plasmid DNA. *Pharm. Res.* 2003, 20, 1730-1737.
 19. Nguyen, K. T.; West, J. L., Photopolymerizable hydrogels for tissue engineering applications. *Biomaterials* 2002, 23, 4307-4314.
 20. Zhu, J. M.; Beamish, J. A.; Tang, C.; Kottke-Marchant, K.; Marcant, R. E., Extracellular matrix-like cell-adhesive hydrogels from RGD-containing poly(ethylene glycol) diacrylate. *Macromolecules* 2006, 39, 1305-1307.
 21. Elisseeff, J.; Anseth, K.; Sims, D.; McIntosh, W.; Randolph, M.; Langer, R., Transdermal photopolymerization for minimally invasive implantation. *PNAS* 1999, 96, 3104-3107.
 22. Metters, A.; Hubbell, J., Network formation and degradation behavior of hydrogels formed by Michael-type addition reactions. *Biomacromolecules* 2005, 6, 290-301.
 23. van de Wetering, P.; Metters, A. T.; Schoenmakers, R. G.; Hubbell, J. A., Poly(ethylene glycol) hydrogels formed by conjugate addition with controllable swelling, degradation, and release of pharmaceutically active proteins. *J. Controlled Release* 2005, 102, 619-627.

Chapter 7

24. Rizzi, S. C.; Hubbell, J. A., Recombinant protein-co-PEG networks as cell-adhesive and proteolytically degradable hydrogel matrixes. Part 1: Development and physicochemical characteristics. *Biomacromolecules* 2005, 6, 1226-1238.
25. Seliktar, D.; Zisch, A. H.; Lutolf, M. P.; Wrana, J. L.; Hubbell, J. A., MMP-2 sensitive, VEGF-bearing bioactive hydrogels for promotion of vascular healing. *J. Biomed. Mater. Res.* 2004, 68A, 704-716.
26. Raeber, G. P.; Lutolf, M. P.; Hubbell, J. A., Molecularly engineered PEG hydrogels: A novel model system for proteolytically mediated cell migration. *Biophys. J.* 2005, 89, 1374-1388.
27. DuBose, J. W.; Cutshall, C.; Metters, A. T. J., Controlled release of tethered molecules via engineered hydrogel degradation: Model development and validation. *Biomed. Mater. Res.* 2005, 74A, 104-116.
28. Cai, S. S.; Liu, Y. C.; Shu, X. Z.; Prestwich, G. D., Injectable glycosaminoglycan hydrogels for controlled release of human basic fibroblast growth factor. *Biomaterials* 2005, 26, 6054-6067.
29. Shu, X. Z.; Ghosh, K.; Liu, Y. C.; Palumbo, F. S.; Luo, Y.; Clark, R. A.; Prestwich, G. D., Attachment and spreading of fibroblasts on an RGD peptide-modified injectable hyaluronan hydrogel. *J. Biomed. Mater. Res.* 2004, 68A, 365-375.
30. Yamaoka, T.; Tabata, Y.; Ikada, Y., Comparison of body distribution of poly(vinyl alcohol) with other water-soluble polymers after intravenous administration. *J. Pharm. Pharmacol.* 1995, 47 79-486.
31. Cadee, J. A.; De Kerf, M.; De Groot, C. J.; Den Otter, W.; Hennink, W. E., Synthesis, characterization of 2-(methacryloyloxy)ethyl-(di-)-lactate and their application in dextran-based hydrogels. *Polymer* 1999, 40, 6877-6881.
32. Cadee, J. A.; van Luyn, M. J. A.; Brouwer, L. A.; Plantinga, J. A.; van Wachem, P. B.; de Groot, C. J.; den Otter, W.; Hennink, W. E., In vivo biocompatibility of dextran-based hydrogels. *J. Biomed. Mater. Res.* 2000, 50, 397-404.
33. Maia, J.; Ferreira, L.; Carvalho, R.; Ramos, M. A.; Gil, M. H., Synthesis and characterization of new injectable and degradable dextran-based hydrogels. *Polymer* 2005, 46, 9604-9614.
34. Goessl, A.; Tirelli, N.; Hubbell, J. A., A hydrogel system for stimulus-responsive, oxygen-sensitive in situ gelation. *J. Biomater. Sci.-Polymer Ed.* 2004, 15, 895-904.

In situ forming degradable dextran vinyl sulfone hydrogels

35. Ellman, G. A colorimetric method for determining low concentrations of mercaptans. *Arch. Biochem. Biophys.*, 1958, 74, 443-450.
36. Schoenmakers, R. G.; van de Wetering, P.; Elbert, D. L.; Hubbell, J. A., The effect of the linker on the hydrolysis rate of drug-linked ester bonds. *J. Controlled Release* 2004, 95, 291-300.
37. Lutolf, M. P.; Hubbell, J. A., Synthesis and physicochemical characterization of end-linked poly(ethylene glycol)-co-peptide hydrogels formed by Michael- type addition. *Biomacromolecules* 2003, 4, 713-722.
38. Li, H.; Yu, G. E.; Price, C.; Booth, C., Hecht, E., Hoffmann, H., Concentrated aqueous micellar solutions of diblock copoly(oxyethylene/oxybutylene) E(41)B(8): A study of phase behavior. *Macromolecules* 1997, 30, 1347-1354.

Chapter 8

Rapidly in situ forming degradable hydrogels from dextran thiols through Michael addition¹

Christine Hiemstra, Leonardus J. van der Aa, Zhiyuan Zhong, and Jan Feijen**

Department of Polymer Chemistry and Biomaterials, Faculty of Science and Technology, Institute for Biomedical Technology, University of Twente, P. O. Box 217, 7500 AE Enschede, The Netherlands

8.1 Abstract

Thiol functionalized dextrans (dex-SH) ($M_{n, \text{dextran}} = 14\text{K}$ or 31K) with degrees of substitution (DS) ranging from 12 to 25 were synthesized and investigated for in situ hydrogel formation via Michael type addition using poly(ethylene glycol) tetra-acrylate (PEG-4-Acr) or a dextran vinyl sulfone conjugate with DS 10 (dex-VS DS 10). Dex-SH was prepared by activation of the hydroxyl groups of dextran with 4-nitrophenyl chloroformate and subsequent reaction with cysteamine. Hydrogels were rapidly formed in situ under physiological conditions upon mixing aqueous solutions of dex-SH and either PEG-4-Acr or dex-VS DS 10 at polymer concentrations of 10 to 20 w/v%. Rheological studies showed that these hydrogels are highly elastic. By varying the DS, concentration, dextran molecular weight and type of crosslinker, hydrogels with a broad range of storage moduli of 9 to 100 kPa could be obtained. Varying the ratio of thiol to vinyl sulfone groups from 0.9 to 1.1 did not alter the storage modulus of the hydrogels, whereas larger deviations from equimolarity (thiol to vinyl sulfone ratio's of 0.75 and 1.5) considerably decreased the storage modulus. The plateau value of hydrogel storage modulus was reached much faster at pH 7.4 compared to pH 7, due to a higher concentration of the

¹ This chapter has been accepted for publication in *Biomacromolecules*, 2007.

thiolate anion at higher pH. These hydrogels were degradable under physiological conditions. Degradation times were 3 to 7 weeks for dex-SH/dex-VS DS 10 hydrogels and 7 to over 21 weeks for dex-SH/PEG-4-Acr hydrogels, depending on the DS, concentration and dextran molecular weight.

8.2 Introduction

Dextran is highly hydrophilic and biocompatible, hardly shows interactions with proteins and can be excreted through the kidneys up to molecular weights of approximately 30,000.¹ Dextran hydrogels have been studied extensively for biomedical applications, in particular for drug delivery and tissue engineering.²⁻¹³ The group of Chu has prepared degradable dextran hydrogels by copolymerization of dextran modified with allyl groups and poly(D,L-lactide) diacrylate. These hydrogels released indomethacin, a low molecular weight drug, with biphasic release kinetics (an initial burst effect followed by a slower sustained release), wherein 100% was released in approximately 1 month.^{2, 3} Logeart-Avrarmoglou et al. have formed hydrogels by crosslinking dextran carboxylate, sulfate and benzylamide derivatives with sodium trimetaphosphate.^{4, 5} Hydrogels loaded with bone morphogenetic protein (BMP) were shown to be osteoinductive when implanted in rats. Shoichet et al. prepared cell-adhesive dextran hydrogels, by copolymerization of dextran-methacrylate (dex-MA) with aminoethyl methacrylate (AEMA) followed by coupling of cell-adhesive peptide sequences.⁶ Sawicka et al. prepared glucose-responsive hydrogels by copolymerization of dextran acrylate and concanavalin A acrylate for self-regulated insulin delivery.⁷

Recently, hydrogels formed in situ under physiological conditions have received much attention, due to their many favorable characteristics. For instance, bioactive compounds and/or cells can be mixed homogeneously with the polymer solutions prior to gelation. Furthermore, in situ gelation allows preparation of complex shapes and applications using minimally invasive surgery. Hennink et al. prepared in situ forming, degradable dextran hydrogels by stereocomplexation of dextran-poly(L-lactide) and dextran-poly(D-lactide) graft copolymers.^{8, 9} When loaded with the protein interleukin-2 (IL-2) these hydrogels were shown to be effective tools for immunotherapy of SL2 lymphoma in mice.¹⁰

Hydrogels were also formed in situ by ionic interactions between oppositely charged microspheres of dextran-HEMA copolymerized with methacrylic acid (MA) or dimethylaminoethyl methacrylate (DMAEMA).¹¹ These hydrogels showed a primarily diffusion controlled released of lysozyme up to 25 days, wherein the enzymatic activity of lysozyme was preserved.¹² Gil et al. have synthesized in situ formed, degradable dextran hydrogels by crosslinking oxidized dextran with adipic acid dihydrazide (AAD).¹³ The hydrogels formed rapidly at pH 8, 37 °C with good mechanical properties and degraded within 3 weeks.

Michael addition between thiols and either acrylates or vinyl sulfones has recently been used for in situ formation of hydrogels.¹⁴⁻¹⁹ The reaction is highly selective versus biological amines¹⁴ and can be carried out under physiological conditions. Moreover, biomimetic scaffolds can be easily obtained by incorporation of thiol-bearing molecules. Hubbell et al. prepared in situ forming hydrogels by Michael addition of multifunctional poly(ethylene glycol) (PEG) vinyl sulfones or acrylates and multifunctional thiol compounds.¹⁴⁻¹⁶ These hydrogels released bovine serum albumin (BSA) with zero-order kinetics for approximately 4 days.¹⁴ Cell-responsive hydrogels were prepared by Michael addition between four-arm PEG vinyl sulfone and a bis-cysteine, protease-cleavable peptide sequence, in the presence of a mono-cysteine cell-adhesion peptide sequence.¹⁶ Fibroblasts adhered to these hydrogels and were able to migrate into the hydrogel. Prestwich et al. prepared hydrogels by Michael type addition between thiol-modified hyaluronic acid (HA) and PEG diacrylate.¹⁷ These hydrogels were shown to induce angiogenesis in vivo by the dual release of vascular endothelial growth factor (VEGF) and keratinocyte growth factor (KGF).¹⁷ Hydrogels that recruited fibroblasts in vivo were also prepared by Michael addition of HA and PEG diacrylate in the presence of a mono-cysteine fibronectin functional domain.¹⁸ We have previously reported on degradable hydrogels that rapidly formed in situ by Michael addition of dextran vinyl sulfone conjugates and multi-functional mercapto PEG.¹⁹ The gelation time, hydrogel degradation time and storage moduli were well-controlled by the degree of substitution (DS), concentration and dextran molecular weight. However, the hydrogels degraded within 3 to 21 days, which is too fast for certain applications, such as tissue engineering of cartilage. In this paper we report on dextran hydrogels prepared by a different approach, in which dextran thiols (dex-SH) are crosslinked with PEG tetra-acrylate (PEG-4-Acr) or a dextran

vinyl sulfone conjugate (dex-VS DS 10). These hydrogels degrade much slower compared to the previously reported dex-VS/PEG-SH hydrogels, with degradation times ranging from 3 to over 21 weeks. Furthermore, the dex-SH/PEG-4-Acr hydrogels can be obtained with high storage moduli up to 100 kPa.

8.3 Materials and Methods

Materials. Calcium hydride and cysteamine were purchased from Fluka. Dithioerythritol (DTE) was obtained from Aldrich. 4-Nitrophenyl chloroformate (4-NC) and pyridine were supplied by Acros. These chemicals were used as received. Dextran ($M_{n, GPC} = 14K$, $M_w/M_n = 1.45$, denoted as dex14K, and $M_{n, GPC} = 31K$, $M_w/M_n = 1.38$, denoted as dex31K) (Fluka) and 4-arm poly(ethylene glycol) (PEG) (Nektar) were dried by azeotropic distillation of toluene. Toluene was previously dried over sodium wire followed by distillation. Dimethyl formamide (DMF) and dichloromethane were dried over calcium hydride and molecular sieves 4 Å, respectively, and distilled before use. Triethylamine (TEA) (Aldrich) was dried over calcium hydride and distilled prior to use. Lithium chloride was obtained from J.T. Baker and dried in vacuo at 80 °C. Vinyl sulfone functionalized dextran ($M_{n, dextran} = 14K$) with DS 10 (denoted as dex-VS DS 10) was prepared as reported previously.¹⁹

Synthesis.

Dex-SH. To obtain thiol functionalized dextran (dex-SH), the hydroxyl groups were first activated with 4-NC, as reported previously by Ramirez et al.²⁰, and subsequently reacted with cysteamine. Typically, dextran (7.5 g, 46 mmol anhydroglucosidic rings, AHG) was dissolved in DMF (225 ml) containing 2 w/v% of lithium chloride at 90°C. The reaction mixture was cooled to 0 °C and pyridine (2.1 ml, 26 mmol, molar ratio of pyridine to AHG is 0.56) was added to the dextran solution followed by 4-NC (5.25 g, 26 mmol, molar ratio of 4-NC to AHG is 0.56). The reaction mixture was stirred for 2 h at 0 °C and finally the 4-NC activated dextran was obtained by twice precipitation in cold ethanol, washed with diethyl ether and dried in vacuo over phosphorus pentoxide. DS (¹H NMR): 15. Yield: 7.38 g, 98%. ¹H NMR (DMSO-d₆): δ 3.1-4.0 (m, dextran glucosidic protons), 4.7 (s, dextran

anomeric proton), 4.5, 4.9 and 5.1 (s, dextran hydroxyl protons), 5.3 and 5.5 (s, dextran glucosidic protons at positions which have nitrophenyl substituents), 7.5 and 8.3 (dd, aromatic protons).

In the second step, typically 4-NC activated dextran (7.0 g, 37 mmol AHG) was dissolved in DMF (56 ml, concentration of nitrophenyl groups is 0.10 M) containing 1 w/v% of lithium chloride. Cysteamine (3.49 g, 45 mmol, molar ratio of cysteamine to nitrophenyl groups is 8) was dissolved in DMF (56 ml) and added to the dextran solution. The reaction was stirred for 24 h at room temperature. Subsequently, the product was recovered by precipitation in cold ethanol and washed several times with ethanol to remove *p*-nitrophenol. A small amount of DTE was added to a solution of dex-SH in water to reduce any disulfide bonds. This solution was ultrafiltrated (MWCO 5,000) against deionized water under a nitrogen atmosphere and the product was finally obtained by lyophilization. DS: 12. Yield: 4.50 g, 64%. ¹H NMR (D₂O): δ 2.7 (t, -NH-CH₂-), 3.3 (d, -CH₂-SH), 3.4-4.1 (m, dextran glucosidic protons), 5.2 and 5.3 (s, dextran glucosidic protons at positions which have thiol group containing substituents).

PEG-4-Acr. PEG tetra-acrylate (PEG-4-Acr) was synthesized from 4-arm PEG and acryloyl chloride according to the procedure reported by Hubbell et al.¹⁴ Typically, PEG (7.0 g, 3.3 mmol) was dissolved in dichloromethane (260 ml, hydroxyl group concentration is 54 mM). After dissolution of the PEG, TEA (2.83 g, 28 mmol, molar ratio of TEA to hydroxyl groups is 2) was added and the solution was cooled to 0 °C. Subsequently, acryloyl chloride (1.9 g, 21 mmol, 1.5 equivalents to hydroxyl groups) was added dropwise and the reaction was stirred overnight at room temperature. The solution was filtered over Celite and the filtrate was stirred with sodium carbonate for 1.5 h. After filtration and concentration, the modified PEG was precipitated by adding cold diethyl ether in an ice bath. The precipitate was further purified by ultrafiltration (MWCO 1,000) against deionized water and finally recovered by lyophilization. Conversion (¹H NMR): 91%. Yield: 1.85 g, 26%. ¹H NMR (CDCl₃): δ 3.5-3.7 (m, PEG main chain protons), 4.3 (t, -CH₂-O-CO), 5.9 (d, -CH=CH₂), 6.2 and 6.4 (dd, -CH=CH₂).

Characterization. Molecular weights of dextran were determined by gel permeation chromatography (GPC) using a Viscotek GPCmax with Viscotek 302 Triple Detection Array. As eluent 0.1 M NaNO₃ was used with a flow of 1 ml/min. The molecular weight of PEG was determined by MALDI-TOF mass spectrometry performed on a Voyager mass

specrometer (Applied Biosystems) in the reflector mode using ditranol as a matrix. ¹H NMR spectra were recorded on a Varian Inova Spectrometer (Varian, Palo, Alto, USA) operating at 300 MHz. The degree of substitution (DS) of dextran is defined as the number of substituents per 100 AHG. The DS of the nitrophenyl activated dextrans was calculated from the ¹H NMR spectra (DMSO-d₆) based on the glucosidic protons of dextran (δ 3.1-4.0, 5.3 and 5.5) and the protons of the nitrophenyl groups (δ 7.5 and 8.3). The number of free thiol groups of the dex-SH was determined by the Ellman test.²¹ The absorption at 412 nm of diluted dex-SH solutions (PBS buffer, pH 7.4, 100 mM) was recorded on a Cary 300 Bio UV-Visible Spectrophotometer (Varian) and the free thiol concentration was calculated using a calibration curve derived from mercaptoethanol standard solutions. The conversion of PEG acrylate was calculated from ¹H NMR spectra (CDCl₃) based on the PEG main chain protons (δ 3.5-3.7) and the protons of the acrylate groups (δ 5.9, 6.2 and 6.4).

Gelation time and swelling tests. To determine the gelation time, 250 μl solutions of dex-SH and PEG-4-Acr or dex-VS DS 10 (molar ratio of thiol to unsaturated groups was kept at 1.1) in HEPES buffered saline (pH 7, 100 mM, adjusted to 300 mOsm with NaCl) were mixed at 37 °C by vortexing. The gelation time was determined by the vial tilting method. When the sample showed no flow within 5 s, it was regarded as a gel. For the swelling test, hydrogels were allowed to swell at 37 °C after applying 3 ml of HEPES buffered saline. The swelling experiment was performed in triplicate. The swollen hydrogels were weighed at regular time intervals after removal of the buffer and after each weighing the buffer was refreshed. The swelling ratio of the hydrogels was calculated from the initial hydrogel weight after preparation (W_0) and the swollen hydrogel weight after exposure to buffer (W_t):

$$\text{Swelling ratio: } = \frac{W_t}{W_0}$$

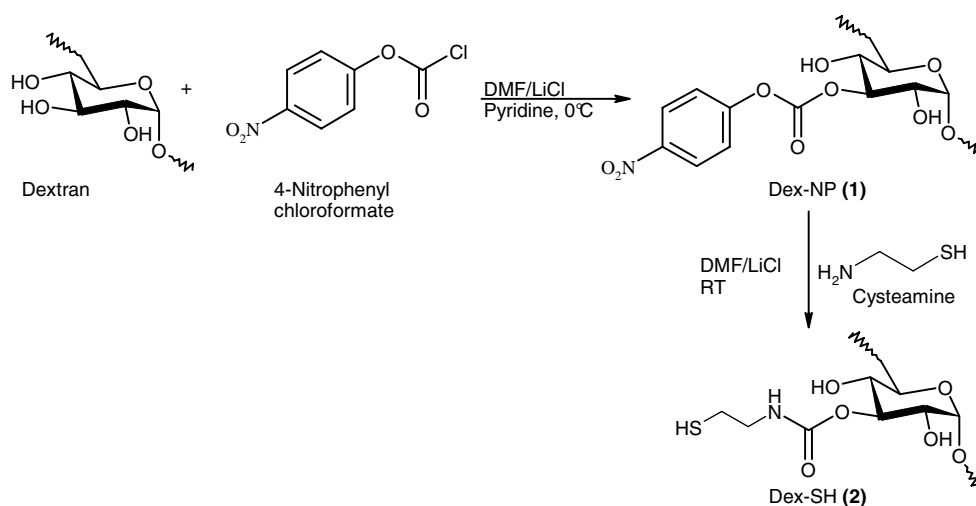
Rheology. Rheology experiments were performed at 37 °C on a US 200 rheometer (Anton Paar). The dex-SH and the PEG-4-Acr or dex-VS DS 10 solutions in HEPES buffered saline were mixed (molar ratio of thiol groups to unsaturated groups was kept at 1.1, unless mentioned otherwise) and quickly applied to the rheometer using a double barreled syringe with a mixing chamber (Mixpac). To prevent evaporation, a thin layer of

oil was applied. Parallel plates (25 mm in diameter) were used with an adjustable gap width to keep the normal force close to 0 N (maximal normal force is 0.1 N). The storage and loss modulus were measured at a strain of 0.1% and a frequency of 1 Hz.

8.4 Results and Discussion

8.4.1 Synthesis of dextran-thiol conjugates and poly(ethylene glycol) acrylate

Thiol functionalized dextrans (dex-SH) were synthesized by a two-step reaction using dimethyl formamide (DMF)/LiCl as a solvent (Scheme 1).



Scheme 1. Schematic representation of the two-step synthesis of thiol functionalized dextran (dex-SH). The substitution at position C-3 is given as an example.

Dextrans with molecular weights of 14K (denoted as dex14K) and 31K (denoted as dex31K) were used. First, the hydroxyl groups of dextran were activated with 4-nitrophenyl chloroformate (4-NC) using pyridine as a catalyst at 0 °C for 2 h to yield nitrophenyl substituted dextran (dex-NP) (1).²⁰ Dex-NP was purified by precipitation in

cold ethanol. Then dex-NP was reacted with an excess amount of cysteamine at room temperature for 24 h. Interestingly, under the used conditions (room temperature and DMF/LiCl as a solvent) the amine group of cysteamine was much more reactive than the thiol group leading to the exclusive formation of dex-SH. The resulting dex-SH (**2**) was recovered by precipitation in cold ethanol. After reduction of possibly formed disulfide bonds with dithioerythritol (DTE), the dex-SH was purified by ultrafiltration (MWCO 5,000) against deionized water and finally obtained by lyophilization. Overall yields of 50-80% were obtained. The nitrophenyl derivatization of dextran was confirmed by ¹H NMR (DMSO-d₆). Figure 1a shows, besides signals of dextran, peaks due to the protons of the nitrophenyl aromatic ring (δ 7.5 and 8.3, peaks **e** and **f**). The derivatization was further confirmed by the presence of small peaks due to the shift of the glucosidic protons upon reaction with 4-NC (δ 5.3 and 5.5, peaks **d**). We did not study in detail the position at which the substitution took place. The degrees of substitution (DS, defined as the number of substituents per 100 anhydroglucosic rings, AHG, of dextran) was determined by comparing the peak areas corresponding to the aromatic protons of the nitrophenyl group (δ 7.5 and 8.3) and the dextran glucosidic protons (δ 3.1-4.0, 5.3 and 5.5). Molar feeding ratio's of 4-NC to AHG of dextran of 0.56, 0.75 and 1.13 resulted in dex31K-NP with DS 15, 21 and 25, respectively (Table 1, entry 1-3). Dex14K-NP with DS 15 was prepared by using a molar feeding ratio of 4-NC to AHG of dextran of 0.56 (Table 1, entry 4). Therefore, dex-NP with different DS could be obtained by varying the molar feeding ratio of 4-NC to the AHG of dextran.

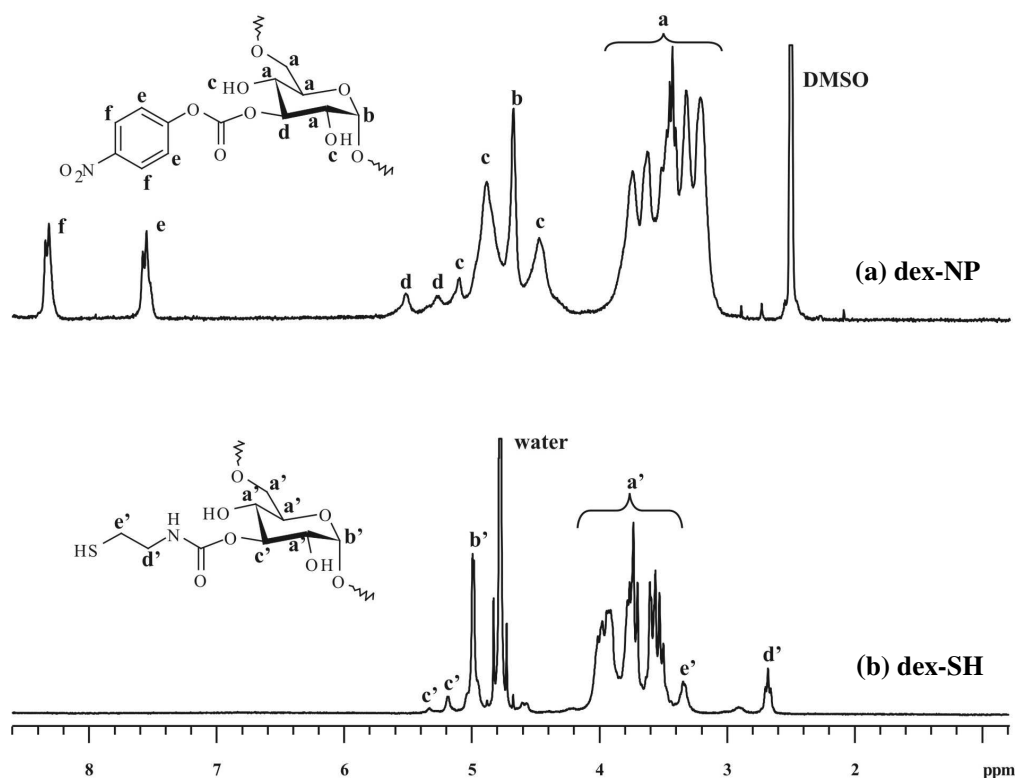


Figure 1. ¹H-NMR spectra of (a) dex-NP (DMSO-d₆, Table 1, Entry 4) and (b) dex-SH (D₂O, Table 1, Entry 4). The substitution at position C-3 is given as an example.

Table 1. Synthesis of dextran nitrophenyl (dex-NP) and dextran thiol (dex-SH) derivatives.

Entry	Dextran	Dex-NP		Dex-SH DS ^{b)}
		Molar feeding ratio of 4-NC to AHG of dextran	DS ^{a)}	
1		0.56	15	16
2	31K	0.75	21	22
3		1.13	25	25
4	14K	0.56	15	12

^{a)} The degree of substitution (DS), defined as the number of substituents per 100 AHG of dextran, was determined by ¹H NMR (DMSO-d₆) by comparing the peak areas corresponding to the dextran glucosidic protons (δ 3.1-4.0, 5.3 and 5.5) and the protons of the nitrophenyl group (δ 7.5 and 8.3).

^{b)} The DS was determined by Ellman tests.²¹

The complete reaction of dex-NP with cysteamine was confirmed by ¹H NMR (D₂O). Figure 1b shows that signals attributable to the nitrophenyl aromatic ring protons have

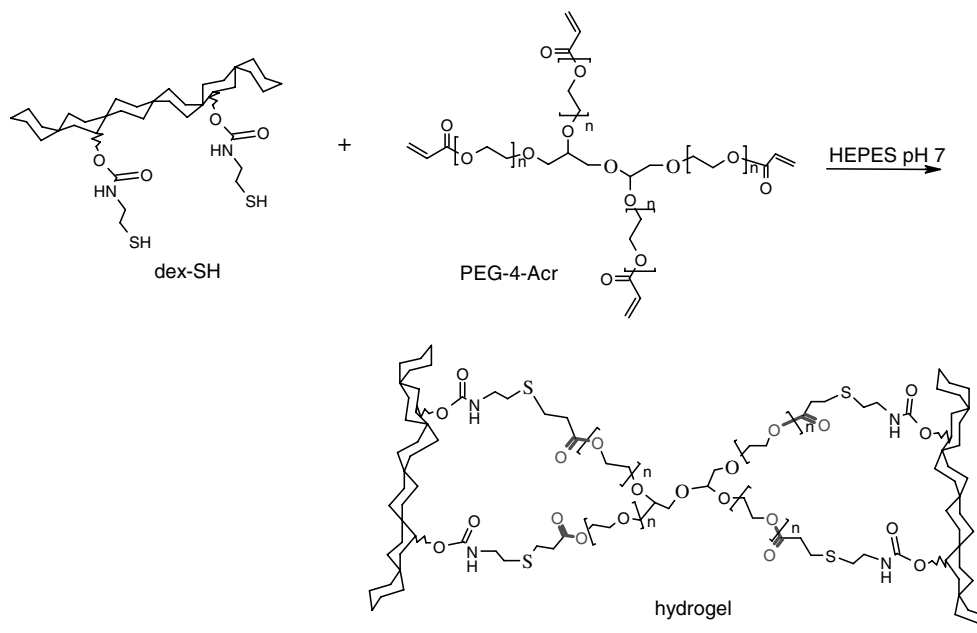
completely disappeared, whereas signals due to the methylene protons of the cysteamine residue (δ 2.7 and 3.3, peaks **d'** and **e'**) and signals due to the peak shift of the glucosidic protons after conjugation with cysteamine (δ 5.2 and 5.3, peaks **c'**) are clearly detected. Ellman tests²¹ showed that dex31K-SH DS 16, 22 and 25 were obtained by using dex31K-NP DS 15, 21 and 25, respectively (Table 1, entry 1-3). Dex14K-SH DS 12 was obtained by using dex14K-NP DS 15 (Table 1, entry 4). The DS could also be determined using ¹H NMR by comparing the peak areas corresponding to the methylene protons of the cysteamine residue (δ 2.7) and the dextran glucosidic protons (δ 3.4-4.1, 5.2 and 5.3) (results not shown). The values obtained from ¹H NMR were in good agreement with those from the Ellman tests. These results indicate that quantitative aminolysis of dex-NP took place upon reaction with cysteamine. Therefore, this two-step synthesis procedure provides a convenient method to prepare thiol functionalized dextrans with different DS.

To study the influence of the crosslinker on the dex-SH hydrogel formation, poly(ethylene glycol) tetra-acrylate (denoted as PEG-4-Acr) and a dextran vinyl sulfone conjugate with DS 10 (denoted as dex-VS DS 10, $M_{n, \text{dextran}} = 14\text{K}$) were used. PEG-4-Acr ($M_{n, \text{MALDI-TOF MS}} = 2.1 \text{ K}$) was prepared as reported.¹⁴ The conversion of the PEG hydroxyl groups to acrylate groups was 91%, as determined by ¹H NMR. Dex-VS DS 10 was synthesized as reported previously.¹⁹

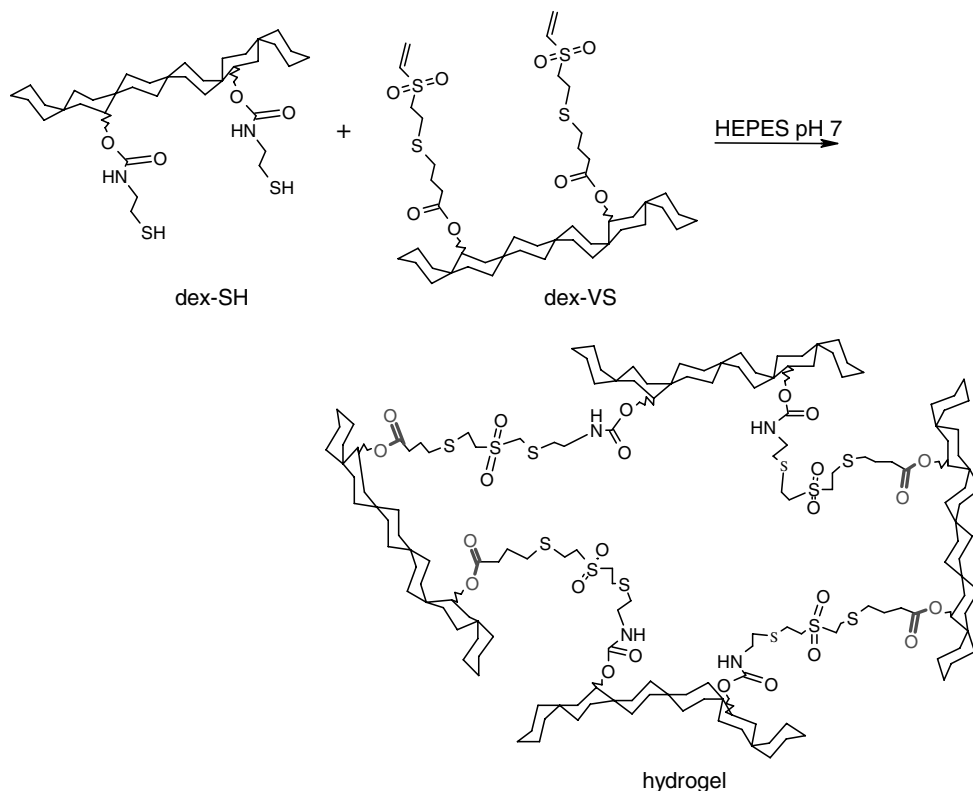
8.4.2 In situ hydrogel formation

Dextran hydrogels were formed in situ via Michael type addition between dex-SH and PEG-4-Acr (Scheme 2) or dex-VS DS 10 (Scheme 3) in HEPES buffered saline at pH 7 and 37 ° C. The molar ratio of thiol to unsaturated groups was kept at 1.1, since thiol groups may form some disulfide bonds upon exposure to air, thus lowering the effective concentration of free thiol groups. The gelation time was determined by the vial tilting method. The concentration is defined as the total dry weight of both dextran and PEG per volume of buffer.

In situ forming degradable dextran thiol hydrogels



Scheme 2. Hydrogel formation upon mixing aqueous solutions of dextran thiol (dex-SH) and PEG tetra-acrylate (PEG-4-Acr).



Scheme 3. Hydrogel formation upon mixing aqueous solutions of dextran thiol (dex-SH) and a dextran vinyl sulfone conjugate (dex-VS).

Figure 2a shows the gelation time of dex31K-SH crosslinked with PEG-4-Acr at 15 w/v% concentration as a function of the DS. The gelation time decreased from approximately 55 to 20 s when increasing the DS from 16 to 22, while a further increase to DS 25 had little influence on the gelation time. As shown in Figure 2b, the gelation times decreased from approximately 5 to 1 min for dex31K-SH DS 16/PEG-4-Acr and from approximately 90 to 40 s for dex14K-SH DS 12/PEG-4-Acr when increasing the polymer concentration from 10 to 20 w/v%. Under the same conditions, dex-VS DS 10 gave much faster gelation compared to PEG-4-Acr, which may be due to the higher crosslink functionality of the dex-VS DS 10 as compared to PEG-4-Acr as well as a higher reactivity of the vinyl sulfone group towards Michael type addition compared to the acrylate group (Figure 2b). The faster gelation of the previously reported vinyl sulfone functionalized

dextran crosslinked with tetra-functional mercapto PEG (PEG-4-SH) compared to dex-SH crosslinked with PEG-4-Acr also indicate a higher reactivity of the vinyl sulfone group compared to the acrylate group.¹⁹ For example, dex14K-SH DS 12 crosslinked with PEG-4-Acr gelled in approximately 90 s at 15 w/v% concentration, while dex14K-VS DS 13 crosslinked with PEG-4-SH gelled in approximately 30 s. The reactivity of the thiol group towards Michael addition depends on the pKa of the thiol group, since the thiolate anion is the actual reactive species in the Michael addition reaction. It has been reported previously that the pKa value of the thiol group is influenced by the electron withdrawing ability of the neighboring group.²² Both dex-SH and PEG-4-SH are non-charged and in both cases, thiol groups are linked by ethylene units. Therefore, the pKa values of dex-SH and PEG-4-SH should be similar.

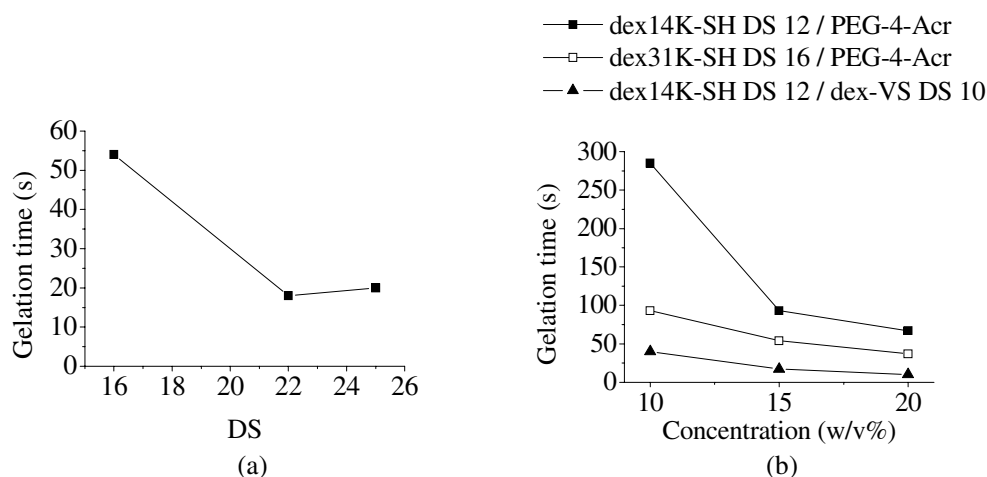


Figure 2. Gelation time (± 5 s) after mixing dex-SH and PEG-4-Acr or dex-VS DS 10 solutions in HEPES buffered saline at pH 7 and 37 °C. (a) Dex31K-SH crosslinked with PEG-4-Acr at 15 w/v% concentration as a function of the degree of substitution (DS); (b) dex14K-SH DS 12 crosslinked with and with PEG-4-Acr or dex-VS DS 10 and dex31K-SH DS 16 crosslinked with PEG-4-Acr as a function of the concentration.

8.4.3 Rheology

The mechanical properties of the dextran hydrogels were studied by oscillatory rheology experiments at 37 °C. Dex-SH and PEG-4-Acr or dex-VS DS 10 solutions in HEPES buffered saline (pH 7, molar ratio of thiol groups to unsaturated groups was kept at 1.1, unless mentioned otherwise) were mixed by a double barreled syringe with a mixing chamber and quickly applied to the rheometer. The storage modulus (G') of the hydrogels was followed in time to establish when the crosslinking reaction was completed (Figure 3).

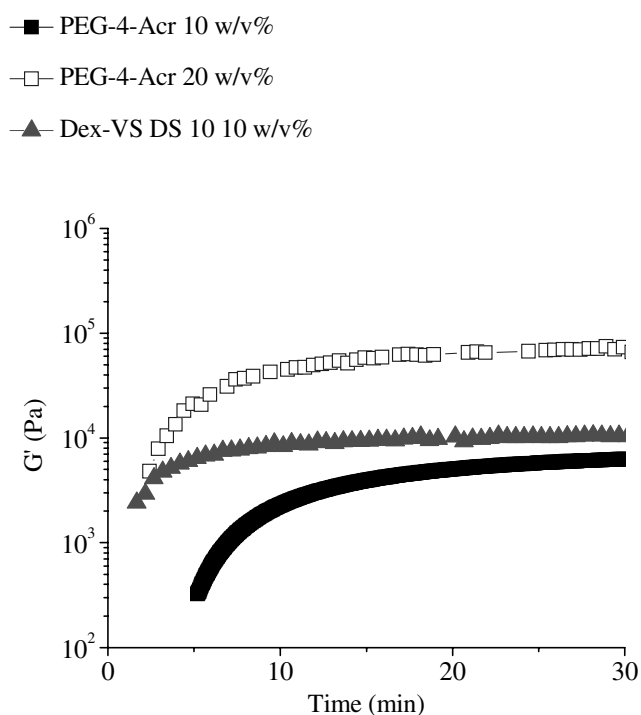


Figure 3. The evolution of the storage modulus (G') at 37 °C of dex14K-SH DS 12 crosslinked with PEG-4-Acr at 10 and 20 w/v% concentration or crosslinked with dex-VS DS 10 at 10 w/v% concentration prepared in HEPES buffered saline at pH 7. After application of the sample on the rheometer ($t = 0$ min), 1 to 5 min were needed to set the instrument before starting the measurement.

Generally, after mixing the reactants the storage modulus increased in time due to the Michael addition reaction, until reaching its plateau value, marking the end of the crosslinking process. The loss modulus (G'') of the dex-SH/PEG-4-Acr and dex-SH/dex-VS DS 10 hydrogels was too low to be accurately measured and is therefore not shown. The low loss modulus indicates that the hydrogels are highly elastic. Due to a fast gelation the gelation time could not be determined by rheology. Figure 3 shows that the increase in the storage modulus is faster at higher concentrations. For instance, after 10 min, dex14K-SH DS 12/PEG-4-Acr hydrogels reached 25 and 59% of their storage modulus plateau value at 10 and 20 w/v% concentration, respectively. The storage modulus of dex14K-SH DS 12/dex-VS DS 10 hydrogels increased faster compared to dex14K-SH DS 12/PEG-4-Acr hydrogels (Figure 3). After 10 min dex14K-SH DS 12/dex-VS DS 10 hydrogels and dex14K-SH DS 12/PEG-4-Acr hydrogels reached 76% and 59% of their storage modulus plateau value, respectively, at 10 w/v% concentration. This may be due to the higher crosslinking functionality per molecule for dex-VS DS 10 compared to PEG-4-Acr as well as a higher reactivity of the vinyl sulfone group towards Michael type addition compared to the acrylate group. Figure 4a shows that the storage modulus plateau value increases from 9 to 83 kPa for dex14K-SH DS 12/PEG-4-Acr hydrogels and from 15 to 100 kPa for dex31K-SH DS 16/PEG-4-Acr hydrogels, when increasing the concentration from 10 to 20 w/v%. Similarly, the storage modulus plateau value of dex14K-SH DS 12/dex-VS DS 10 hydrogels increased from 11 to 51 kPa, when increasing the concentration from 10 to 20 w/v% (Figure 4a). Figure 4b shows that the storage modulus increases upon increasing the DS of dex31K-SH from 16 to 22 at 15 w/v% concentration (39 vs. 70 kPa). A further increase to DS 25 did not increase the storage modulus. The storage moduli of the dex14K-SH DS 12/PEG-4-Acr hydrogels are comparable to those of the dex14K-VS DS 13/PEG-4-SH hydrogels.¹⁹

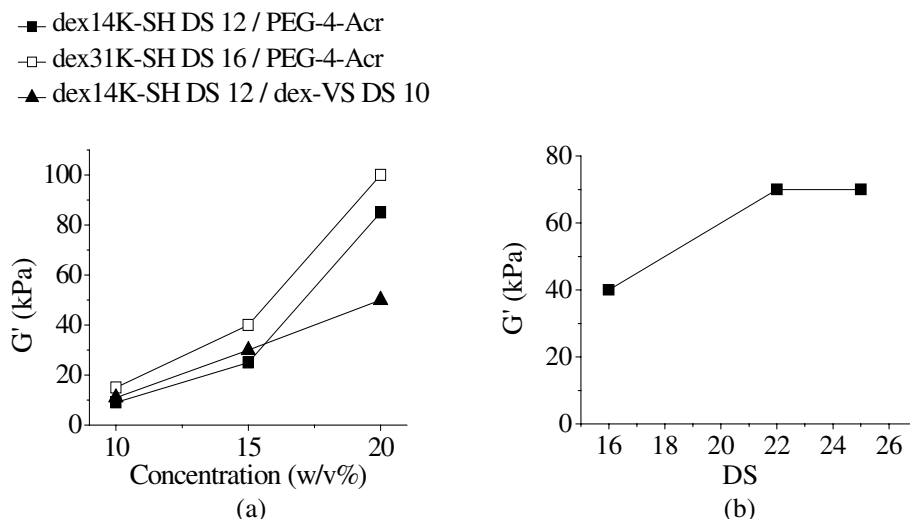


Figure 4. The storage modulus (G') plateau value of hydrogels prepared in HEPES buffered saline at pH 7 and 37 °C. (a) Dex14K-SH DS 12 crosslinked PEG-4-Acr or dex-VS DS 10 and dex31K-SH DS 16 crosslinked with PEG-4-Acr as a function of the concentration; (b) dex31K-SH crosslinked with PEG-4-Acr at 15 w/v% concentration as a function of the degree of substitution (DS).

To study the influence of the molar ratio of thiol to vinyl sulfone groups (SH:VS), dex14K-SH DS 12 was crosslinked with dex-VS DS 10 at 10 w/v% concentration and varying SH:VS ratio's of 0.75, 0.9, 1, 1.1 and 1.5 (Figure 5a). All samples had already formed a gel at the start of the measurement. The loss moduli of hydrogels formed at SH:VS ratio's of 0.9-1.1 were too low to be accurately measured. At SH:VS ratio's of 0.75 and 1.5 hydrogels showed $\tan \delta$ (G''/G') values of 0.01 and 0.03, respectively, indicating that these gels are still highly elastic.

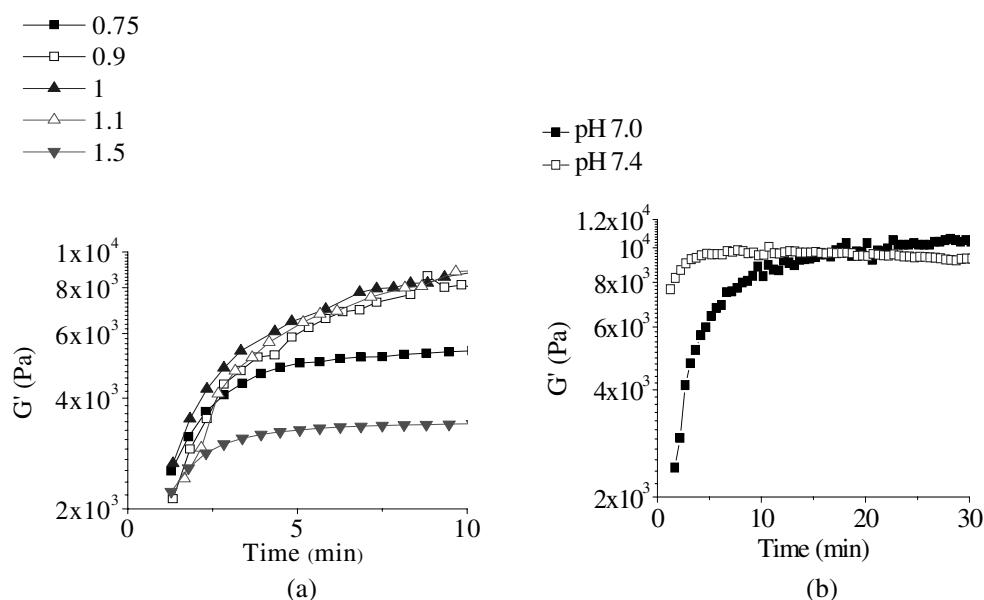


Figure 5. The storage modulus (G') as a function of time of dex14K-SH DS 12 crosslinked with dex-VS DS 10 in HEPES buffered saline at 37 °C. (a) pH 7, 10 w/v% concentration and SH:VS molar ratio's of 0.75, 0.9, 1, 1.1 and 1.5; (b) 10 w/v% concentration at pH 7 and 7.4.

The storage moduli were similar at SH:VS ratio's of 0.9-1.1, while at SH:VS ratio's of 0.75 and 1.5 the storage modulus was considerably lower (4-5 kPa vs 12 kPa). These results show that small deviations ($\leq 10\%$) from equimolarity do not alter the gel formation. This indicates that a small amount of unreacted thiol or vinyl sulfone groups has little influence on the gel formation. The influence of the pH of the HEPES buffered saline was studied for dex14K-SH DS 12 crosslinked with dex-VS DS 10 at 10 w/v% concentration. Figure 5b shows that at pH 7.4 a few min are needed to reach the storage modulus plateau value, while at pH 7 approximately 30 min were required, indicating that the crosslinking reaction is much faster at pH 7.4 compared to pH 7. The faster reaction at higher pH is due to the fact that increasing the pH increases the concentration of the thiolate anion, which is the actual reactive species for the Michael addition.²²

8.4.4 Swelling and degradation

The dex-SH/PEG-4-Acr and dex-SH/dex-VS DS 10 hydrogels were degradable under physiological conditions. Dex-SH/PEG-4-Acr hydrogels degrade through hydrolysis of the ester bond between the thioether and PEG. Dex-SH/dex-VS DS 10 hydrogels degrade through hydrolysis of the ester bond between the sulfone group and dextran. To study the rate of degradation of these hydrogels, solutions of dex-SH and PEG-4-Acr or dex-VS DS 10 were mixed in HEPES buffered saline at pH 7 and 37 °C (molar ratio of thiol groups to unsaturated groups was kept at 1.1). After the hydrogels were formed, HEPES buffered saline was applied on top and the gels were allowed to swell at 37 °C. At regular time intervals, the swelling ratio was calculated by rationing the swollen hydrogel weight after exposure to buffer with the initial hydrogel weight after preparation (W_t/W_0). Figure 6 shows the swelling profiles of dex31K-SH hydrogels crosslinked with PEG-4-Acr. In general, the hydrogels hardly swelled for the first 4 weeks while in time the swelling gradually increased, caused by the hydrolytic cleavage of the ester bonds. At a certain point, the swelling ratios decreased due to disintegration of the hydrogel network, resulting in partial dissolution of the hydrogels. The hydrogel degradation time is defined as the time required to completely dissolve at least one of the three hydrogels. Figure 6 shows that both the concentration and DS hardly affected the initial swelling ratio. For dex31K-SH DS 16/PEG-4-Acr hydrogels the degradation time increased from approximately 7 to 10 weeks by increasing the concentration from 10 to 20 w/v% (Figure 6a). Similarly, the degradation time of dex14K-SH DS 12/PEG-4-Acr hydrogels increased from approximately 16 to 24 weeks when increasing the concentration from 10 to 20 w/v% (results not shown). Dex31K-SH DS 16/PEG-4-Acr hydrogels degraded much faster than the corresponding dex14K-SH DS 12/PEG-4-Acr hydrogels. This may be due to a lower Michael addition conversion for dex31K-SH DS 16 compared to dex14K-SH DS 12. Figure 6b shows that the degradation time increased with increasing DS. At DS 16 and DS 22 the dex31K-SH/PEG-4-Acr hydrogels had degradation times of approximately 9 and 17 weeks at 15 w/v% concentration, respectively, while at DS 25 the hydrogel retained its integrity even after 21 weeks.

Figure 7 shows that the swelling profiles of dex14K-SH DS 12/dex-VS DS 10 hydrogels are similar to those of dex-SH/PEG-4-Acr hydrogels, with low initial swelling followed by

gradual swelling and final dissolution of the hydrogel. The degradation times of dex14K-SH DS 12/dex-VS DS 10 hydrogels were approximately 3 and 7 weeks at 10 and 20 w/v% concentration, respectively. Dex14K-SH DS 12/dex-VS DS 10 hydrogels degraded much faster than the dex14K-SH/PEG-4-Acr hydrogels. This could be due to a higher susceptibility to hydrolysis of the ester bond between the sulfone group and dextran in dex-VS DS 10 conjugates compared to the ester bond between the thioether and PEG in PEG-4-Acr.

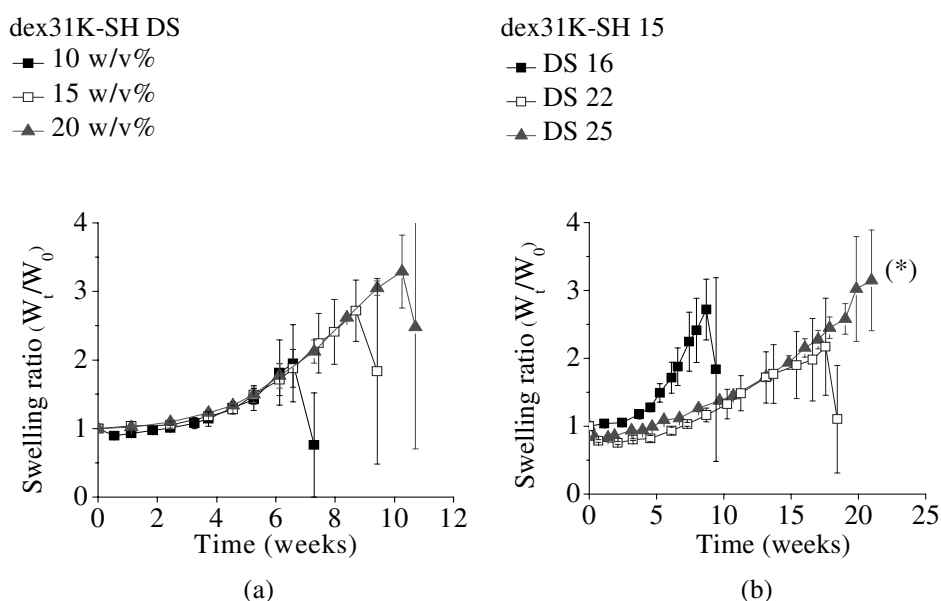


Figure 6. Swelling ratio (W_t/W_0) profiles of dex31K-SH/PEG-4-Acr hydrogels prepared in HEPES buffered saline, at pH 7 and 37 °C (average \pm S.D., $n = 3$). (a) Dex31K-SH DS 16 at 10, 15 and 20 w/v% concentration; (b) dex31K-SH DS 16, DS 22 and DS 25 at 15 w/v% concentration. (*) Dex31K-SH DS 25/PEG-4-Acr hydrogels retained their integrity after 21 weeks.

In summary, slowly degrading hydrogels could be obtained by Michael addition between dextran thiols and PEG-4-Acr or dex-VS DS 10. Hydrogel degradation times ranged from 3 to more than 21 weeks, which can be varied by the DS, polymer concentration, dextran molecular weight and type of crosslinker (PEG-4-Acr or dex-VS DS 10). The degradation is much slower compared to previously reported hydrogels prepared by reaction of dextran

vinyl sulfone conjugates with tetrafunctional mercapto PEG, which degraded within 3 weeks.¹⁹ The slow degradation is advantageous for biomedical applications, such as tissue engineering of cartilage or release of proteins over an extended period of time.

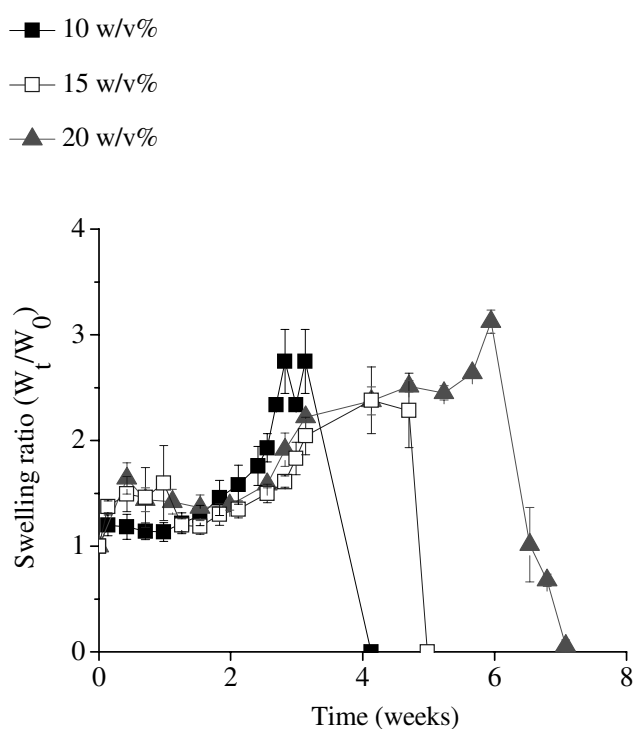


Figure 7. Swelling ratio (W_t/W_0) profiles of a dex14K-SH DS 12/dex-VS DS 10 hydrogels prepared in HEPES buffered saline, at pH 7 and 37 °C at 10, 15 and 20 w/v% concentration (average \pm S.D., $n = 3$).

8.5 Conclusions

Dextrans with pendant thiol groups (dex-SH) were conveniently synthesized by a two-step synthesis procedure with degrees of substitution (DS) ranging from 12 to 25. Hydrogels were rapidly formed in situ under physiological conditions by mixing aqueous

solutions of dex-SH and PEG tetra-acrylate (PEG-4-Acr) or a dextran vinyl sulfone conjugate (dex-VS DS 10). Their mechanical and degradation properties could be adjusted by the DS, concentration, dextran molecular weight and type of crosslinker (PEG-4-Acr or dex-VS DS 10). Storage moduli in a range of 9 to 100 kPa could be obtained. Degradation times of dex-SH/PEG-4-Acr ranged from 7 to more than 21 weeks and degradation times of dex14K-SH DS 12/dex-VS DS 10 hydrogels ranged from 3 to 7 weeks. These hydrogels are very promising for use in biomedical applications, since they can be rapidly formed in situ and are biodegradable with adjustable degradation times to match a particular application. Furthermore, in principle biomimetic scaffolds can easily be obtained by incorporation of thiol-containing bioactive molecules, such as proteins and peptides.

8.6 Acknowledgements

This work was funded by the Netherlands Organization for Scientific Research (NWO). We thank M. J. van Steenberg (University of Utrecht, The Netherlands) for the GPC measurements.

8.7 References

1. Yamaoka, T.; Tabata, Y.; Ikada, Y., Comparison of body distribution of poly(vinyl alcohol) with other water-soluble polymers after intravenous administration. *J. Pharm. Pharmacol.* 1995, 47, 479-486.
2. Zhang, Y. L.; Won, C. Y.; Chu, C. C., Synthesis and characterization of biodegradable hydrophobic-hydrophilic hydrogel networks with a controlled swelling property. *J. Polymer Sci. Polymer Chem.* 2000, 38, 2392-2404.
3. Zhang, Y. L.; Chu, C. C., Biodegradable dextran-poly lactide hydrogel networks: Their swelling, morphology and the controlled release of indomethacin. *J. Biomed. Mater. Res.* 2002, 59, 318-328.
4. MaigaRevel, O.; Chaubet, F.; Jozefonvicz, J., New investigations on heparin-like derivatized dextrans: CMDBS, synergistic role of benzylamide and sulfate substituents in anticoagulant activity. *Carbohydr. Polymers* 1997, 32, 89-93.

Chapter 8

5. Maire, M.; Chaubet, F.; Mary, P.; Blanchat, C.; Meunier, A.; Logeart-Avramoglou, D., Bovine BMP osteoinductive potential enhanced by functionalized dextran-derived hydrogels. *Biomaterials* 2005, 26, 5085-5092.
6. Levesque, S. G.; Shoichet, M. S., Synthesis of cell-adhesive dextran hydrogels and macroporous scaffolds. *Biomaterials* 2006, 27, 5277-5285.
7. Tanna, S.; Taylor, M. J.; Sahota, T. S.; Sawicka, K., Glucose-responsive UV polymerised dextran-concanavalin A acrylic derivatised mixtures for closed-loop insulin delivery. *Biomaterials* 2006, 27, 1586-1597.
8. de Jong, S. J.; De Smedt, S. C.; Wahls, M. W. C.; Demeester, J.; Kettenes-van den Bosch, J. J.; Hennink, W. E., Novel self-assembled hydrogels by stereocomplex formation in aqueous solution of enantiomeric lactic acid oligomers grafted to dextran. *Macromolecules* 2000, 33, 3680-3686.
9. de Jong, S. J.; van Eerdenbrugh, B.; van Nostrum, C. F.; Kettenes-van de Bosch, J. J.; Hennink, W. E., Physically crosslinked dextran hydrogels by stereocomplex formation of lactic acid oligomers: degradation and protein release behavior. *J. Controlled Release* 2001, 71, 261-275.
10. Bos, G. W.; Jacobs, J. J. L.; Koten, J. W.; Van Tomme, S. R.; Veldhuis, T. F. J.; van Nostrum, C. F.; Den Otter, W.; Hennink, W. E., In situ crosslinked biodegradable hydrogels loaded with IL-2 are effective tools for local IL-2 therapy. *Eur. J. Pharm. Sci.* 2004, 21, 561-567.
11. Van Tomme, S. R.; van Steenberg, M. J.; De Smedt, S. C.; van Nostrum, C. F.; Hennink, W. E., Self-gelling hydrogels based on oppositely charged dextran microspheres. *Biomaterials* 2005, 26, 2129-2135.
12. Van Tomme, S. R.; van Nostrum, C. F.; de Smedt, S. C.; Hennink, W. E., Degradation behavior of dextran hydrogels composed of positively and negatively charged microspheres. *Biomaterials* 2006, 27, 4141-4148.
13. Maia, J.; Ferreira, L.; Carvalho, R.; Ramos, M. A.; Gil, M. H., Synthesis and characterization of new injectable and degradable dextran-based hydrogels. *Polymer* 2005, 46, 9604-9614.
14. Elbert, D. L.; Pratt, A. B.; Lutolf, M. P.; Halstenberg, S.; Hubbell, J. A., Protein delivery from materials formed by self-selective conjugate addition reactions. *J. Controlled Release* 2001, 76, 11-25.

15. Lutolf, M. P.; Hubbell, J. A., Synthesis and physicochemical characterization of end-linked poly(ethylene glycol)-co-peptide hydrogels formed by Michael- type addition. *Biomacromolecules* 2003, 4, 713-722.
16. Lutolf, M. P.; Raeber, G. P.; Zisch, A. H.; Tirelli, N.; Hubbell, J. A., Cell-responsive synthetic hydrogels. *Adv. Mater.* 2003, 15, 888-892.
17. Peattie, R. A.; Rieke, E. R.; Hewett, E. M.; Fisher, R. J.; Shu, X. Z.; Prestwich, G. D., Dual growth factor-induced angiogenesis in vivo using hyaluronan hydrogel implants. *Biomaterials* 2006, 27, 1868-1875.
18. Ghosh, K.; Ren, X. D.; Shu, X. Z.; Prestwich, G. D.; Clark, R. A. F., Fibronectin functional domains coupled to hyaluronan stimulate adult human dermal fibroblast responses critical for wound healing. *Tissue Eng.* 2006, 12, 601-613.
19. Chapter 7, Hiemstra, C.; van der Aa, L. J.; Zhong, Z. Y.; Dijkstra, P. J.; Feijen, J., Novel in situ forming, degradable dextran hydrogels by Michael addition chemistry: Synthesis, rheology and degradation. Published in *Macromolecules* 2006, 40, 1165-1173.
20. Ramirez, J.; Sanchez-Chaves, M.; Arranz, F., Dextran functionalized by 4-nitrophenyl carbonate groups. *Appl. Macromol. Chem. Phys. Angew. Makromol. Chem.* 1995, 225, 123-130.
21. Ellman, G., A colorimetric method for determining low concentrations of mercaptans. *Arch. Biochem. Biophys.* 1958, 74, 443-450.
22. Lutolf, M. P.; Tirelli, N.; Cerritelli, S.; Cavalli, L.; Hubbell, J. A., Systematic modulation of Michael-type reactivity of thiols through the use of charged amino acids. *Bioconjugate Chem.* 2001, 12, 1051-1056.

Chapter 9

Release of model proteins and basic fibroblast growth factor from in situ forming degradable dextran hydrogels

Christine Hiemstra^a, Zhiyuan Zhong^{a}, Mies J. van Steenbergen^b, Wim E. Hennink^b, and Jan Feijen^{a*}*

^a Department of Polymer Chemistry and Biomaterials, Faculty of Science and Technology, Institute for Biomedical Technology, University of Twente, P. O. Box 217, 7500 AE Enschede, The Netherlands

^b Department of Pharmaceutics, Utrecht Institute for Pharmaceutical Sciences (UIPS), Utrecht University, P. O. Box 80.082, 3508 TB Utrecht, The Netherlands

9.1 Abstract

Our previous studies showed that degradable dextran hydrogels are rapidly formed in situ upon mixing aqueous solutions of dextran vinyl sulfone (dex-VS) conjugates and tetrafunctional mercapto poly(ethylene glycol) (PEG-4-SH) by Michael addition. The hydrogel degradation time and storage modulus could be controlled by the degree of vinyl sulfone substitution (DS) and dextran molecular weight. The degradation time could further be adjusted by the spacer between the thioether and the ester bond of the dex-VS conjugates (ethyl vs. propyl, denoted as dex-Et-VS and dex-Pr-VS, respectively). In this paper, the release of three model proteins, i.e. immunoglobulin G (d_h is 10.7 nm, IgG), bovine serum albumin (BSA, d_h is 7.2 nm) and lysozyme (d_h is 4.1 nm), as well as basic fibroblast growth factor (bFGF) from these in situ forming dextran hydrogels is studied. Proteins could be easily loaded into the hydrogels by mixing protein containing solutions of dex-VS and PEG-4-SH. The release of IgG from dex-Et-VS hydrogels followed biphasic release kinetics, with a slow, close to first order release for the first 9 days

followed by an accelerated release due to progressive degradation of the hydrogel. The release rate increased with decreasing DS and dextran molecular weight and over 80% of IgG was released in 12 to 25 days. Interestingly, the release of IgG from dex-Pr-VS hydrogels followed close to zero order kinetics, wherein approximately 95% was released in 21 days. The nearly constant release rate of IgG from dex-Pr-VS DS hydrogels appeared to be due to a combination of diffusion and hydrogel degradation/swelling. BSA was released much faster compared to IgG from both dex-Et-VS and dex-Pr-VS hydrogels, due to its smaller size. The release of BSA from dex-Pr-VS hydrogels followed biphasic kinetics, with almost first order release followed by close to zero order release. The acceleration in release indicates that the initial hydrogel mesh size is equal to or smaller than the hydrodynamic diameter of BSA. Approximately 75% of the entrapped BSA could be released from dex-Pr-VS hydrogels in 16 days. Dex-Pr-VS hydrogels released 40% of lysozyme in 14 days, with full preservation of the enzymatic activity of the released lysozyme, as determined by bacteria lysis experiments. The cumulative release of lysozyme was lower compared to IgG and BSA, due to precipitation of the protein in the hydrogel network. The release of basic fibroblast growth factor (bFGF) from dex-Pr-VS hydrogels showed first order kinetics, with quantitative release in 28 days. These results show that the in situ forming degradable dextran hydrogels can be used for the controlled release of proteins.

9.2 Introduction

Nowadays, many pharmaceutically active proteins can be produced on a large scale by biotechnology. Unfortunately, parental administration of proteins is hampered by rapid clearance, whereas oral administration is generally not successful due to degradation in the gastro-intestinal tract. Also, the intestinal epithelium forms a major barrier towards protein absorption. Moreover, since the delivery is not localized, relatively high doses are needed to have a therapeutic effect. The administration of proteins may be greatly improved by the use of controlled delivery systems that allow for sustained and localized release, thereby decreasing the number of administrations, and enhancing the therapeutic efficacy. It is

important that delivery systems allow modulation of the release of entrapped proteins and that their structural integrity of the proteins is preserved after being released.

Hydrogels have been widely applied for controlled drug delivery, in particular for protein delivery. Many hydrogels have been shown to be compatible with proteins and living tissue. Hydrogels may be formed *in situ* upon mixing aqueous polymer solutions, thus allowing for the preparation of complex shapes and minimally invasive surgery. Moreover, bioactive compounds can be easily dissolved or suspended in the polymer solutions prior to gelation. Hydrogels are formed by either physical or chemical crosslinking of hydrophilic polymers.¹ Physical crosslinking generally occurs under mild conditions, thus allowing for the entrapment of labile compounds, such as proteins. However, physically crosslinked hydrogels are generally mechanically weak and may be disrupted by changes in the environment (e.g. pH, temperature and ionic strength). Chemically crosslinked hydrogels are generally stronger and more stable. Chemically crosslinked hydrogels have been prepared *in situ* by several methods. Photopolymerization of poly(ethylene glycol) (PEG) (meth)acrylates has been mostly used.²⁻⁴ More recently, *in situ* forming chemically crosslinked hydrogels have been prepared by reaction of aldehyde modified dextran with adipic acid dihydrazide compounds⁵, reaction of amine groups of gelatin with aldehyde-modified alginate in the presence of small amounts of sodium tetraborate⁶ and reaction of poly(N-isopropylacrylamide (PNIPAAm) derivatives modified with activated ester groups and amine terminated poly(amino acid)s.⁷ Chemically crosslinked hydrogels have also been prepared *in situ* by Michael type addition of vinyl sulfones or acrylates with thiols.⁸⁻¹⁸ Michael type addition is selective towards thiols under physiological conditions, thus preventing reaction with e.g. lysine residues of proteins present in the body and does not produce any side products. Hubbell et al. prepared hydrogels by Michael addition between multifunctional PEG acrylate and PEG dithiol or dithioerythritol (DTT). These hydrogels released albumin *in vitro* with zero order kinetics over a period of 4 days.¹⁹ The *in vitro* release of human growth hormone (hGH, precipitated with Zn²⁺ to prevent reaction with the gel precursors) followed zero order kinetics, wherein hGH was quantitatively released for up to a few months with preservation of the protein integrity.¹¹ Cell-adhesive, enzyme degradable hydrogels with covalently incorporated VEGF were prepared by first performing a Michael addition

between RGDC peptides and VEGF-cysteine derivatives and excess of tetrafunctional PEG vinyl sulfone and subsequent gel formation by Michael addition with a matrix metalloproteinase (MMP) degradable bis-cysteine peptide.¹⁰ When implanted subcutaneously in rats, these hydrogels were completely remodeled into native, vascularized tissue. Prestwich et al. prepared hydrogels by Michael addition between thiol-modified hyaluronic acid or chondroitin sulfate containing a small amount of thiol modified heparin, and PEG diacrylate.²⁰⁻²² These hydrogels were degraded by the enzyme hyaluronase and were shown to quantitatively release basic fibroblast growth factor (bFGF) *in vitro* for 28 days, wherein bFGF retained 55% of its original biological activity.¹⁴ Moreover, bFGF loaded hydrogels dramatically increased neovascularization, when they were implanted into subcutaneous pockets in Balb/c mice.

We have previously reported on rapidly in situ forming degradable hydrogels by Michael addition between dextran vinyl sulfones and multifunctional mercapto PEG. These hydrogels showed good mechanical properties and their degradation time (ranging from 3 to 21 days) could be well-controlled by the degree of substitution (DS), polymer concentration, dextran molecular weight and length of the spacer between the ester bonds and the thioether. In this paper, the release of model proteins with different sizes, immunoglobulin G (IgG), bovine serum albumin (BSA) and lysozyme, as well as the release of basic fibroblast growth factor (bFGF) from these hydrogels is studied.

9.3 Materials and Methods

Materials. Tetrafunctional mercapto poly(ethylene glycol) with $M_n = 2,100$ (denoted as PEG-4-SH) and dextran vinyl sulfone conjugates (denoted as dex-VS) with different degree of substitution (DS, defined as the number of vinyl sulfone groups per 100 anhydroglucosidic rings, AHG, of dextran) and dextran molecular weights of 14K and 31K (denoted as dex14K and dex31K, respectively) were synthesized as reported previously.¹⁷ Lysozyme (from hen egg white, MW = 14 kDa) and dextran sulfate sodium salt (from *Leuconostoc* spp.) were purchased from Fluka. Bovine serum albumin (BSA, fraction V, MW = 67 kDa), bovine immunoglobulin G (IgG, MW = 150 kDa), ethylenediaminetetraacetic acid (EDTA), heparin sodium salt (from porcine intestinal

mucosa) and human recombinant basic fibroblast growth factor (bFGF, expressed in *E. Coli*, MW = 17.2 kDa) were obtained from Sigma.

Model protein release. For the release of the model proteins, IgG, BSA and lysozyme, hydrogels were prepared in HEPES buffered saline (pH 7, 100 mM, adjusted to 300 mOsm with NaCl) by mixing solutions of dex-VS (250 μ l) and PEG-4-SH (250 μ l) both containing 1 wt% of protein with a double barreled syringe to a final total polymer concentration of 15 w/v%. The protein containing polymer solutions were prepared by adding 20 μ l of concentrated protein solution to 230 μ l of both the dex-VS and PEG-4-SH solutions just before preparation of the hydrogel, to minimize possible reaction of the protein with the gel precursors. The molar ratio of vinyl sulfone to thiol groups was kept at 1.1, since thiol groups may form some disulfide bonds due to exposure to air, thus lowering the effective concentration of free thiol groups. The hydrogels were formed in cylindrically shaped vials with a flat bottom and a diameter of 8.8 mm, only exposing the upper surface of the hydrogel (device described in ref. ²³). Subsequently, 3 ml of HEPES buffer was applied on top of the gels and the gels were gently shaken at 37 °C. Each hydrogel formulation was prepared in duplicate or triplicate. Samples of 500 μ l were taken at regular time intervals (the first day after 30 min, 1 h, 2 h, 4 h, 8 h and 24 h, and subsequently after one or three days) and replaced by an equal volume of fresh buffer. Samples were analyzed using reversed phase high-performance liquid chromatography (RP-HPLC), as described below.

bFGF release. For the release of bFGF, hydrogels were prepared in PBS (pH 7.4, 10.5 mM, 300 mOsm) containing 0.1 wt% of BSA, 5 wt% of sucrose, 0.01 wt% of EDTA and 0.15 w/v% of dextran sulfate ($M_r \approx 500,000$) and as release buffer PBS supplemented with 10 μ g/ml heparin, 1 wt% of BSA and 1 mM of EDTA was used to retain bFGF activity and to prevent surface adsorption.¹⁴ Hydrogels with a total polymer concentration of 15 w/v% were prepared by mixing solutions of dex-VS (125 μ l) and PEG-4-SH (125 μ l) with a double barreled syringe. Each gel contained 250 pg of bFGF. Release medium (3 ml of PBS release buffer) was added to the gels and they were gently shaken at 37 °C. The release experiment was performed in quadruplicate. Samples of 500 μ l were taken at 12 and 36 h, and at 3, 6, 10, 14, 21 and 28 days, and replaced by an equal volume of fresh

buffer. The samples were stored at -30 °C until measurement. Samples were analyzed using a bFGF ELISA kit as described below.

Analysis of lysozyme release samples by RP-HPLC. A 600E Multisolvant Delivery System with a 717plus Autosampler, two concentration detectors: a 2487 Dual Wavelength Absorbance and a 2475 Multi λ Fluorescence Detector, were used (Waters Associates Inc.). An analytical column (Prosphere, 5 μ m C18 300 A) was used for separation. Standard protein solutions (concentration range 0.75-37.5 μ g/ml) were prepared to generate calibration curves. All samples were centrifuged for 1 min (10,000 g) and 10 or 50 μ l of the supernatant was injected onto the column. A linear gradient was run from 70% A (water/acetonitrile/TFAA 95/5/0.1 w/w) and 30% B (water/acetonitrile/TFAA 95/5/0.1 w/w) to 45% B in 15 min. The flow rate was set to 1.0 ml/min and the column oven was set at 4 °C. The fluorescent emission at 300 nm (excitation wavelength of 295 nm) was measured. Instruments were controlled by and peak areas were determined with Empower 2 Chromatography Data Software (Waters Associates Inc.).

Analysis of BSA and IgG release samples by RP-HPLC. A 600E Multisolvant Delivery System with a 717plus Autosampler, two concentration detectors: a 2487 Dual Wavelength Absorbance and a 2475 Multi λ Fluorescence Detector, were used (Waters Associates Inc.). An analytical column (Tosoh Biosciences TSKgelG3000SWXL, 7.6x300mm, 5 μ m) was used for separation. Standard protein solutions (concentration range 0.1-50 μ g/ml) were prepared to generate calibration curves. All samples were centrifuged for 1 min (10,000 g) and 50 μ l of the supernatant was injected onto the column. PBS (pH 7.4, 10.5 mM, 300 mOsm) was used as the mobile phase. The flow rate was set to 1.0 ml/min and the column oven was set at 4 °C. The fluorescent emission at 300 nm (excitation wavelength of 295 nm) was measured. Instruments were controlled by and peak areas were determined with Empower 2 Chromatography Data Software (Waters Associates Inc.).

Determination of the enzymatic activity of lysozyme. The enzymatic activity of released lysozyme was determined for a few samples. The assay is based on the lysis of the outer cell membrane of *Micrococcus lysodeikticus*, resulting in solubilization of the affected bacteria and consequent decrease of light scattering.²⁴ The release samples were diluted to a concentration of 50-100 μ g/ml and 10 μ l of the sample was added to 1.3 ml of the bacteria suspension (0.2 mg/ml, HEPES buffered saline, pH 7.0). The decrease in

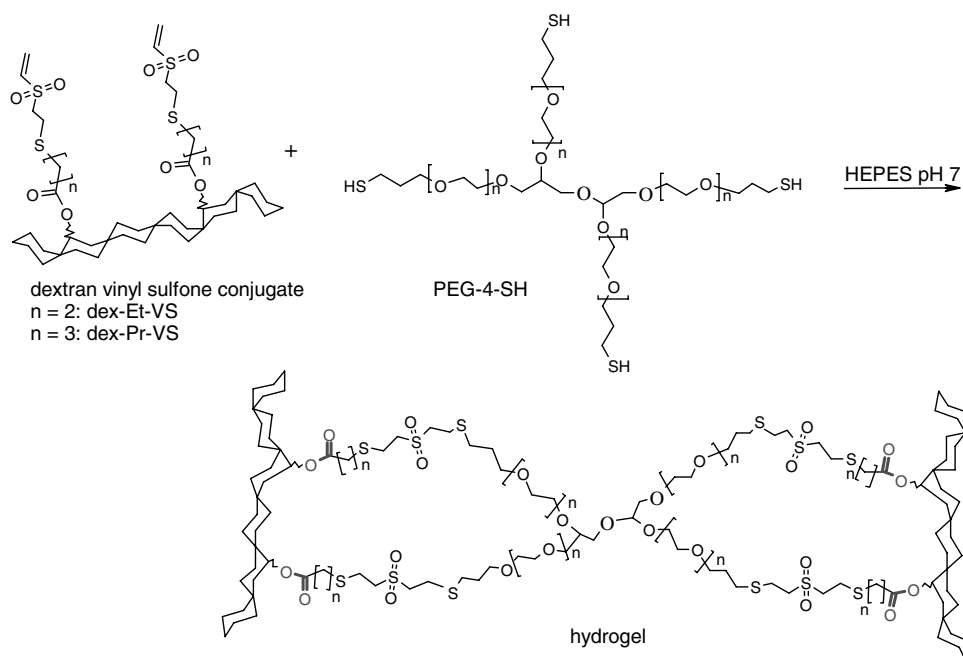
turbidity was measured at 450 nm and the percent enzymatic activity was determined by comparing the activity of the sample with that of a freshly prepared reference lysozyme solution (0.1 mg/ml).

Analysis of bFGF release samples. bFGF release samples were analyzed using a bFGF ELISA kit. 100 μ l of sample was added to each well of a 96-wells plate coated with human bFGF specific antibody. After incubation for 2.5 h at room temperature the solutions were discarded and the wells were washed 4 times. Subsequently, 100 μ l of biotinylated antibody solution was added to each well and incubated for 1 h at room temperature. The solutions were discarded after incubation and the wells were washed 4 times. Next, to each well 100 μ l of horseradish peroxidase-streptavidin solution was added and incubated for 45 min at room temperature. Subsequently, the solutions were discarded and each well was washed 5 times. In the next step 100 μ l of 3,3'-5,5'-tetramethylbenzidine (TMB) solution was added to each well and after 30 min incubation at room temperature in the dark, 50 μ l of 2 M sulfuric acid was added. The absorbance was read at 450 nm with a plate reader (SLT 340 ATC).

9.4 Results and Discussion

9.4.1 Hydrogel formation and degradation

Our previous studies showed that hydrogels are rapidly formed by mixing aqueous solutions of dextran vinyl sulfone conjugates (dex-VS) and tetrafunctional mercapto poly(ethylene glycol) (PEG-4-SH).¹⁷ The crosslinks are formed by Michael addition between the vinyl sulfone and thiol groups (Scheme 1).



Scheme 1. In situ hydrogel formation by Michael addition of dextran vinyl sulfone conjugates (dex-Et-VS or dex-Pr-VS) with tetrafunctional mercapto PEG (PEG-4-SH).¹⁷

The dex-VS conjugates used in this study are listed in Table 1. Different degrees of substitution (DS, defined as the number of vinyl sulfone groups per 100 anhydroglucosidic rings, AHG, of dextran) ranging from 8 to 22, and dextran molecular weights of 14K or 31K (denoted as dex14K and dex31K, respectively) were used. The hydrogel degradation time increases with increasing DS and dextran molecular weight, as was determined previously by swelling tests (Figure 1).¹⁷ The degradation time is defined as the time required to completely dissolve at least one of the three hydrogels used for testing one type of hydrogel. Furthermore, two types of dex-VS, having either an ethyl or a propyl spacer between the thioether and the ester bond (denoted as dex-Et-VS and dex-Pr-VS, respectively, Scheme 1), were used. Dex-Pr-VS hydrogels have prolonged degradation times but otherwise similar properties compared to the corresponding dex-Et-VS hydrogels.¹⁷

Table 1. Characteristics of dex-VS conjugates used in this study.

Dex-VS conjugates	MW dextran ^{a)}	DS ^{b)}	Type of spacer ^{c)}	Degradation time (days) ^{d)}
dex14K-Et-VS DS 13	14K	13	ethyl	9
dex14K-Et-VS DS 22		22	ethyl	21
dex14K-Pr-VS DS 10		10	propyl	17
dex31K-Et-VS DS 9	31K	9	ethyl	14
dex31K-Et-VS DS 13		13	ethyl	16
dex31K-Pr-VS DS 8		8	propyl	21

^{a)} Determined by GPC. ^{b)} Degree of substitution (DS), defined as the number of vinyl sulfone groups per 100 anhydroglucosidic rings, AHG, of dextran, determined by ¹H NMR. ^{c)} Spacer between the thioether and the ester bond. ^{d)} The degradation time of hydrogels with 15 w/v% total polymer concentration was determined by swelling tests.¹⁷ The degradation time is defined as the time required to completely dissolve at least one of the three hydrogels used for testing one type of hydrogel.

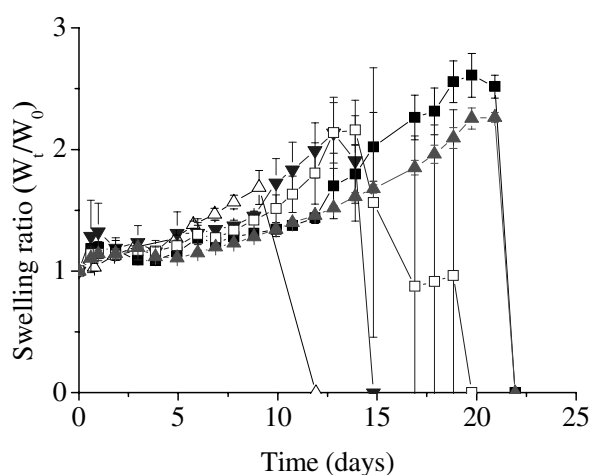


Figure 1. Swelling ratio (W_t/W_0) profiles of dex-VS hydrogels in HEPES buffered saline at pH 7.0 and 37 °C ($n = 3$).¹⁷ (a) Dex14K-Et-VS DS 13 (Δ), dex14K-Et DS 22 (\blacksquare), dex31K-Et-VS DS 9 (\blacktriangledown), dex31K-Et-VS DS 13 (\square) and dex31K-Pr-VS DS 8 (\blacktriangle).

9.4.2 Release of model proteins

The release of three model proteins with different hydrodynamic diameters (d_h), i.e. immunoglobulin G (IgG, d_h is 10.7 nm²⁵), bovine serum albumin (BSA, d_h is 7.2 nm²⁶) and lysozyme (d_h is 4.1 nm²⁶) from dex-VS hydrogels was studied, using a polymer concentration of 15 w/v% (defined as the total dry weight of both PEG and dextran per volume of buffer) in HEPES buffered saline (pH 7.0, 100 mM, 300 mOsm) at 37 °C. Proteins could be easily loaded into the dex-VS hydrogels by mixing protein containing aqueous solutions of dex-VS and PEG-4-SH. Protein containing polymer solutions were prepared by mixing concentrated protein solutions with the polymer solutions just before hydrogel preparation, to minimize reaction of the proteins with the gel precursors.

Figure 2 shows the cumulative release of IgG. All dex-Et-VS hydrogels showed a biphasic release profile of IgG (Figure 2a), with slow release for the first 9 days, which was close to first order kinetics (as the release scaled almost linearly with the square root of time, insert Figure 2a), followed by an accelerated release. This acceleration in the release is attributed to progressive degradation of the hydrogel network and indicates that the initial hydrogel mesh size is at least equal to or smaller than the hydrodynamic diameter of IgG. After sufficient degradation, the hydrogel mesh size becomes large enough to allow easy diffusion of IgG from the hydrogels. Importantly, no burst-release was observed.

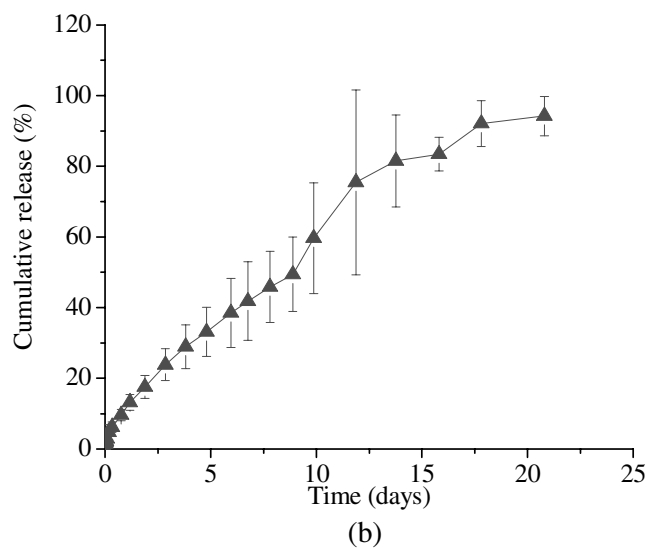
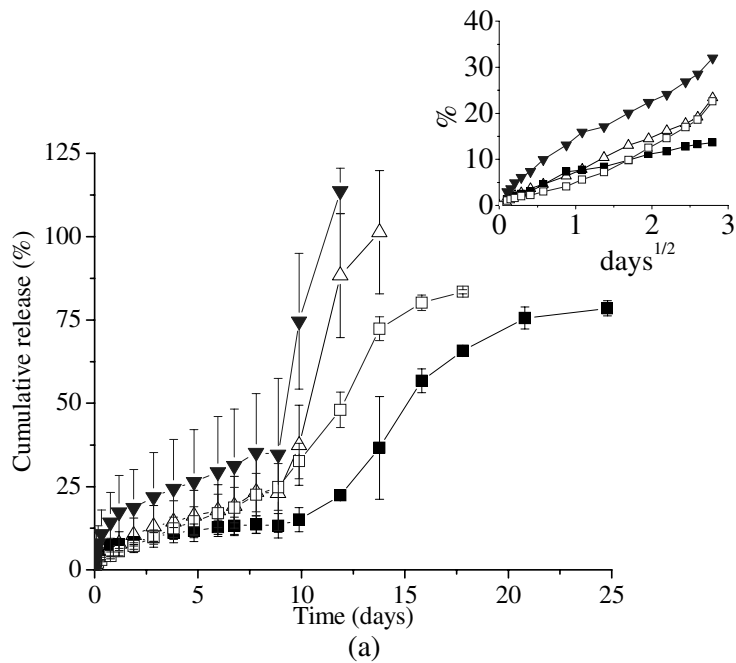


Figure 2. Cumulative release profiles of IgG from dex-VS hydrogels in HEPES buffered saline (pH 7.0) at 37 °C (average \pm S.D.). (a) Dex14K-Et-VS DS 13 (Δ , n = 3), dex14K-Et-VS DS 22 (\blacksquare , n = 2), dex31K-Et-VS DS 9 (\blacktriangledown) (n = 2) and dex31K-Et-VS DS 13 (\square , n = 2); insert shows the cumulative release as a function of the square root of time, for the sake of

clarity error bars are not shown in the insert. (b) Dex31K-Pr-VS DS 8 (n = 3).

Dex14K-Et-VS DS 13 and dex31K-Et-VS DS 9 hydrogels quantitatively released IgG in 12 to 14 days, while dex14K-Et-VS DS 22 and dex31K-Et-VS DS 13 released up to approximately 80% of IgG in 18 and 25 days, respectively. Previous studies showed that the hydrogel degradation time as well as the storage modulus increase with increasing DS and dextran molecular weight¹⁷ A higher storage modulus indicates a higher crosslinking density and thus a smaller hydrogel mesh size. It should be noted that the release of IgG continued after the degradation time as determined by swelling tests. This is most likely due to some damaging of the hydrogel during the swelling tests when removing the buffer prior to weighing, thereby underestimating the degradation time. The faster release of IgG from dex14K-Et-VS DS 13 hydrogels as compared to dex14K-Et-VS DS 22 and dex31K-Et-VS DS 13 hydrogels, having either a higher DS or a higher dextran molecular weight, respectively, may be due to a faster degradation as well as a larger initial hydrogel mesh size.

The incomplete retrieval of IgG for dex14K-Et-VS DS 22 and dex31K-Et-VS DS 13 hydrogels is due to partial precipitation of the protein, as the release media contained a small amount of precipitate at the end of the release experiment (after 30 days). HPLC chromatograms showed an extra peak at shorter retention time, which corresponds to a compound with a higher molecular weight than IgG, indicating the presence of water-soluble IgG aggregates. Possibly, denaturation, aggregation and subsequent precipitation may have occurred in time, due to reaction of the reactive groups of IgG (ϵ -amines of the lysine amino acids or the terminal α -amines or disulfide bonds) with the reactive groups of the gel precursors (vinyl sulfone and thiol groups). Hubbell et al. found that 80% of the added VEGF was covalently linked to the hydrogel matrices, which were prepared by first mixing aqueous solutions of VEGF and a large stoichiometric excess of tetrafunctional PEG vinyl sulfone for 60 min and subsequent addition of an aqueous solution of bis-cysteine MMP peptide to induce gelation at pH 8.0 and 37 °C¹⁰ They suggested that the incorporation of VEGF was due to reaction of ϵ -amines or the α -amine of VEGF with vinyl sulfone groups of the tetrafunctional PEG vinyl sulfone. Kim et al. showed that all amine groups of polyethylenimine (PEI) reacted with bifunctional vinyl sulfone-PEG-(N-hydroxysuccinimidyl) (VS-PEG-NHS) within 2 h at pH 7.0 and room temperature.²⁷ The

difference in percentage of retrieved IgG from the different dex-VS hydrogels may be due to the differences in hydrogel degradation time, as most IgG is retrieved from the most rapidly degrading hydrogels (dex14K-Et-VS DS 13 and dex31K-Et-VS DS 8).

Release of IgG from dex31K-Pr-VS DS 8 hydrogels followed almost zero order release kinetics, wherein approximately 95% of IgG was released in 21 days (Figure 2b). The difference in release profiles of dex31K-Pr-VS DS 8 hydrogels and similar dex31K-Et-VS DS 9 hydrogels is attributed to slower hydrogel degradation (Table 1). The difference in release profile of dex31K-Pr-VS DS 8 hydrogels compared to dex14K-Et-VS DS 22 hydrogels with similar degradation time, is attributed to the larger initial pore size of the dex31K-Pr-VS DS 8 hydrogels due to the lower DS. Furthermore, swelling tests showed that the swelling ratio of dex31K-Pr-VS hydrogels increased smoothly in time compared to dex14K-Et-VS DS 22 hydrogels, which showed accelerated swelling after 12 days (Figure 1). The smooth increase in swelling indicates a gradual degradation of the dex31K-Pr-VS hydrogels. Therefore, the close to zero order release of IgG from dex31K-Pr-VS DS 8 hydrogels is most likely due to a combination of degradation/swelling and diffusion.

The release of BSA from dex-Et-VS and dex-Pr-VS hydrogels was biphasic, with first close to first order kinetics (insert Figure 3), followed by a (slightly) accelerated release after 9 days (Figure 3). The release did not show a burst-effect. BSA was released much faster compared to IgG from these hydrogels, due to its smaller size. For instance, approximately 10% of IgG vs. approximately 40% of BSA was released from dex14K-Et-VS DS 22 hydrogels after 10 days. This is most likely because the initial hydrogel mesh size is much smaller than the hydrodynamic diameter of IgG, but equal to or somewhat larger than the hydrodynamic diameter of BSA. While BSA may diffuse out of the hydrogel without significant hydrogel degradation, further degradation is needed to facilitate the diffusion of IgG. The observed acceleration in release rate for both proteins indicates that the hydrogel mesh size becomes larger than the size of the proteins after approximately 9 days. The acceleration is less pronounced for BSA compared to IgG, since the cumulative release of BSA was higher compared to IgG before the acceleration. Dex14K-Et-VS DS 22 and dex31K-Et-VS DS 13 hydrogels released approximately 55 and 65% of BSA in 18 days, respectively, while dex31K-Pr-VS DS 8 hydrogels released approximately 75% of BSA in 16 days. The incomplete retrieval of BSA is due to

precipitation of the protein, as the release media contained small precipitates after the release experiment (after 30 days). The precipitation may be due to denaturation caused by reaction with the gel precursors, similar to IgG.

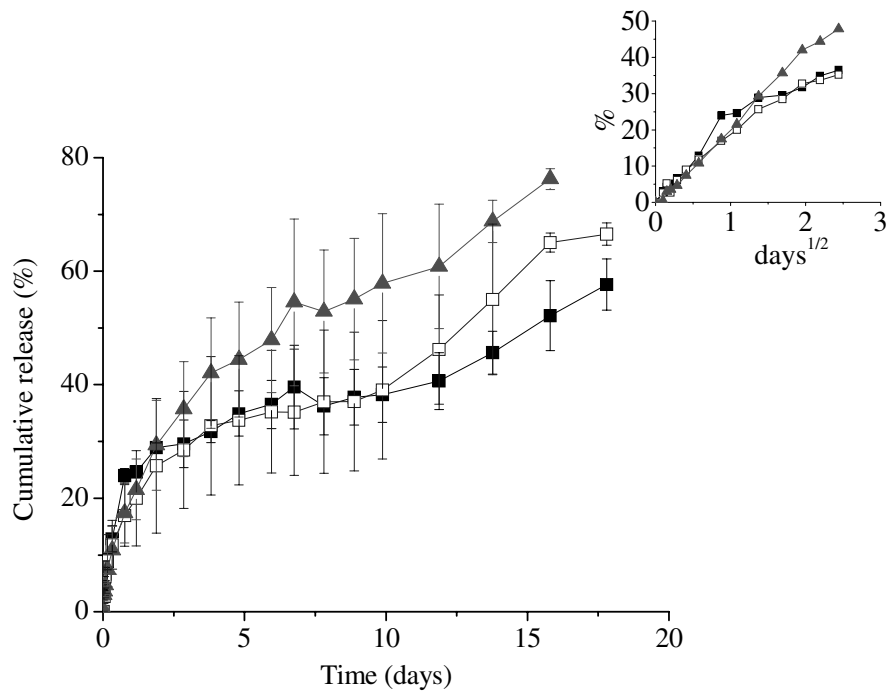


Figure 3. Cumulative release profiles of BSA from dex-VS hydrogels in HEPES buffered saline (pH 7.0) at 37 °C (average \pm S.D., n = 3). Dex14K-Et-VS DS 22 (■), dex31K-Et-VS DS 13 (□) and dex31K-Pr-VS DS 8 (▲). Insert shows the cumulative release as a function of the square root of time, for the sake of clarity error bars are not shown.

Dex31K-Pr-VS DS 8 hydrogels released approximately 40 % of lysozyme in approximately 10 days, wherein the release followed first order kinetics for the first 3 days, followed by an almost constant release (Figure 4). Dex14K-Et-VS DS 22 and dex31K-Et-VS DS 13 hydrogels released 10 and 20% of lysozyme in 10 days, respectively (results not shown). The cumulative release of lysozyme was low compared to IgG and BSA. This is due to precipitation of lysozyme, as the release media contained quite some precipitates after the release experiment (after 30 days). Similar to BSA en IgG the precipitation may be due to denaturation of lysozyme caused by reaction with the gel precursors. The underlying reasons for the increased precipitation of lysozyme as compared to IgG and BSA need to be studied further. Lysozyme released after 1 week from dex31K-Et-VS DS 13 and dex31K-Pr-VS DS 8 hydrogels fully retained its enzymatic activity after 7 days, as was shown by bacteria lysis experiments (results not shown). Lysozyme released after 1 week from dex14K-Et-VS DS 22 retained 50% of its enzymatic activity. The lower activity of released lysozyme and the lower cumulative release for dex14K-Et-VS DS 22 hydrogels (having the highest concentration of reactive groups prior to gelation) compared to the dex31K-Et-VS DS 13 and dex31K-Pr-VS DS 8 hydrogels agrees well with the view that lysozyme may react with the gel precursors. Proteins can be protected from reaction with the gel precursors by appropriate formulations. For instance, Hubbell et al. incorporated human growth hormone (hGH) by first precipitation of dissolved hGH with Zn^{2+} ions and subsequent hydrogel formation by Michael reaction upon addition of aqueous solutions of eight-arm PEG acrylate and dithiothreitol (DTT).¹¹ SDS-PAGE experiments showed that hGH retained its integrity after the Michael reaction.

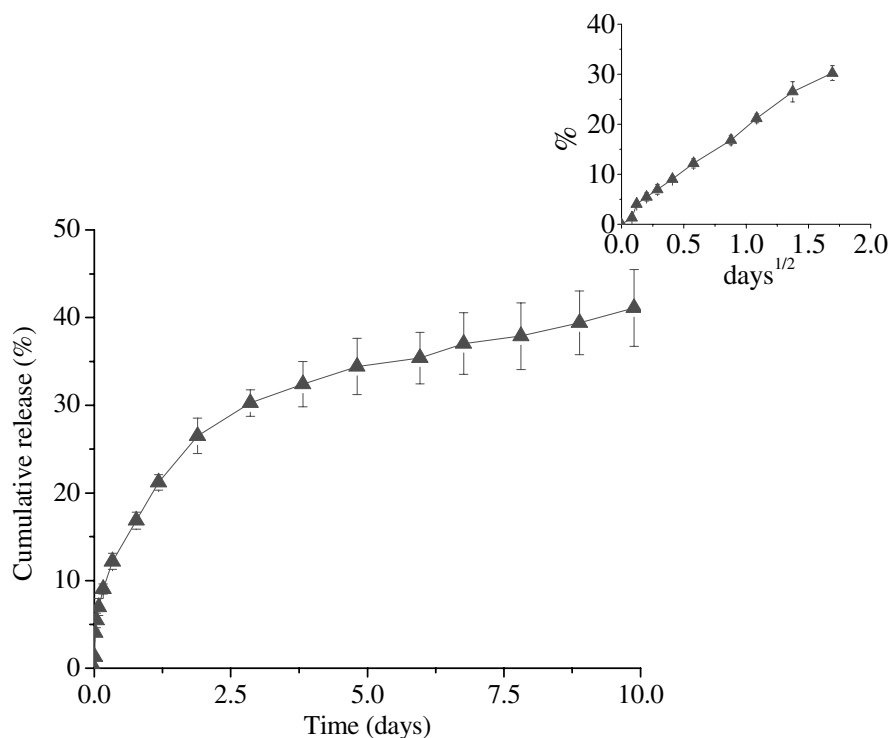


Figure 4. Cumulative release profiles of lysozyme from dex31K-Pr-VS DS 8 hydrogels in HEPES buffered saline (pH 7.0) at 37 °C (average \pm S.D., $n = 3$). Insert shows the cumulative release as a function of the square root of time.

9.4.3 Release of bFGF

The release of basic fibroblast growth factor (bFGF) from dex14K-Pr-VS DS 10 hydrogels was studied, using supplemented PBS release buffer (pH 7.4) at 37 °C (Figure 5). In the hydrogels, 0.01 wt% EDTA was used to prevent trace metal-induced disulfide exchange between the hydrogels and bFGF, 5 wt% sucrose was added to maintain the bFGF conformation, 0.1 wt% BSA was added to prevent bFGF adsorption to plastic surfaces and 0.15 w/v% dextran sulfate was added to maintain bFGF activity.^{14, 28} In the release medium 10 μ g/ml heparin was added to maintain and sequester bFGF activity after it is released, 1 wt% BSA was added to prevent adsorption and 1 mM EDTA was added as

a chelator. The concentration of bFGF in the release samples was determined by a bFGF ELISA assay.

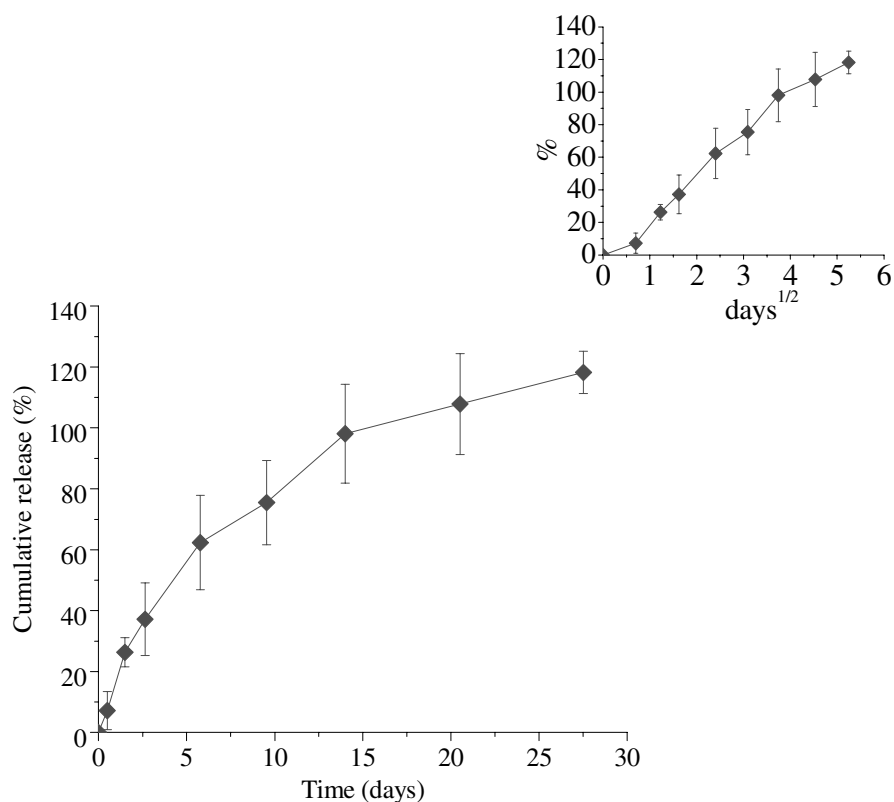


Figure 5. Cumulative release profile of bFGF from dex14K-Pr-VS DS 10 hydrogels in PBS (pH 7.4) at 37 °C (n = 4, average \pm S.D.). Insert shows the cumulative release as a function of the square root of time.

The bFGF release scaled almost linearly with the square root of time, according to first order release (insert Figure 5), wherein bFGF was quantitatively released in 28 days. Importantly, the release of bFGF from these hydrogels did not show a burst-effect. In general, bFGF was released much faster than BSA and IgG, due to a smaller hydrodynamic diameter of bFGF compared to BSA and IgG. The hydrodynamic diameter of bFGF is similar to that of lysozyme (d_h is 4.1 nm), since both have similar molecular weights (17.2 and 14, kDa respectively). The potential of released bFGF to stimulate tissue regeneration will be subject of future study. Prestwich. et al showed that bFGF releasing

hydrogels formed by Michael addition induced neovascularization when implanted subcutaneously in Balb/c mice.¹⁴ Hubbell et al. showed that hydrogels containing covalently incorporated vascular endothelial growth factor (VEGF) formed by Michael type addition completely remodeled into native, vascularized tissue when implanted subcutaneously in rats.¹⁰

9.5 Conclusions

Dex-VS hydrogels were rapidly formed in situ upon mixing aqueous solutions of dex-VS and tetrafunctional mercapto poly(ethylene glycol) (PEG-4-SH). Dex-VS conjugates with either an ethyl or a propyl spacer between the thioether and the ester bonds (dex-Et-VS and dex-Pr-VS, respectively) were used. Proteins could be easily loaded into the hydrogels by mixing protein containing aqueous polymer solutions. The release profile of the relatively large protein immunoglobulin G (IgG, d_h is 10.7 nm) was dependent on the type of hydrogel. Biphasic kinetics were observed for dex-Et-VS hydrogels and almost zero order kinetics for the slower degrading dex-Pr-VS hydrogels, wherein dex-Pr-VS hydrogels released approximately 95% of IgG in 21 days. The release rate of IgG from dex-Et-VS hydrogels was dependent on the DS and dextran molecular weight and over 80% of IgG was released in 12 to 25 days. Lysozyme was released up to 40% from dex-Pr-VS hydrogels in 14 days, with full preservation of its enzymatic activity. Basic fibroblast growth factor (bFGF) was released quantitatively from dex-Pr-VS hydrogels with close to first order kinetics in 28 days. Importantly, the release of proteins from these dextran hydrogels did not show a burst-effect. In conclusion, these rapidly in situ forming, degradable dex-VS hydrogels are very promising for the controlled release of proteins.

9.6 Acknowledgements

This work was funded by the Netherlands Organization for Scientific Research (NWO).

9.7 References

1. W. E. Hennink, C. F. van Nostrum, Novel crosslinking methods to design hydrogels. *Adv. Drug Deliv. Rev.* 2002, 54 13-36.
2. A. S. Sawhney, C. P. Pathak, J. A. Hubbell, Bioerodible hydrogels based on photopolymerized poly(ethylene glycol)-co-poly(alpha-hydroxy acid) diacrylate macromers. *Macromolecules* 1993, 26 581-587.
3. S. X. Lu, K.S. Anseth, Release behavior of high molecular weight solutes from poly(ethylene glycol)-based degradable networks. *Macromolecules* 2000, 33, 2509-2515.
4. J. Elisseeff, K. Anseth, D. Sims, W. Mcintosh, M. Randolph, M. Yaremchuk, R. Langer, Transdermal photopolymerization of poly(ethylene oxide)-based injectable hydrogels for tissue-engineered cartilage. *Plast. Reconstr. Surg.* 1999, 104, 1014-1022.
5. J. Maia, L. Ferreira, R. Carvalho, M. A. Ramos, M. H. Gil, Synthesis and characterization of new injectable and degradable dextran-based hydrogels. *Polymer* 2005, 46, 9604-9614.
6. B. Balakrishnan, A. Jayakrishnan, Self-cross-linking biopolymers as injectable in situ forming biodegradable scaffolds. *Biomaterials* 2005, 26, 3941-3951.
7. T. Yoshida, T. Aoyagi, E. Kokufuta, T. Okano, Newly designed hydrogel with both sensitive thermoresponse and biodegradability. *J. Polymer Sci. Polymer Chem.* 2003, 41 779-787.
8. D. L. Elbert, J. A. Hubbell, Conjugate addition reactions combined with free-radical cross-linking for the design of materials for tissue engineering. *Biomacromolecules* 2001, 2, 430-441.
9. M. P. Lutolf, G. P. Raeber, A. H. Zisch, N. Tirelli, J. A. Hubbell, Cell-responsive synthetic hydrogels. *Adv. Mater.* 2003, 15, 888-892.
10. A. H. Zisch, M. P. Lutolf, M. Ehrbar, G. P. Raeber, S. C. Rizzi, N. Davies, H. Schmokel, D. Bezuidenhout, V. Djonov, P. Zilla, J. A. Hubbell, Cell-demanded release of VEGF from synthetic, biointeractive cell-ingrowth matrices for vascularized tissue growth. *Faseb J.* 2003, 17, U374-U398.

11. P. van de Wetering, A. T. Metters, R. G. Schoenmakers, J. A. Hubbell, Poly(ethylene glycol) hydrogels formed by conjugate addition with controllable swelling, degradation, and release of pharmaceutically active proteins. *J. Controlled Release* 2005, 102 619-627.
12. A. Metters, J. Hubbell, Network formation and degradation behavior of hydrogels formed by Michael-type addition reactions. *Biomacromolecules*, 2005, 6 290-301.
13. K. R. Kirker, Y. Luo, J. H. Nielson, J. Shelby, G. D. Prestwich, Glycosaminoglycan hydrogel films as bio-interactive dressings for wound healing. *Biomaterials* 2002, 23, 3661-3671.
14. S. S. Cai, Y. C. Liu, X. Z. Shu, G. D. Prestwich, Injectable glycosaminoglycan hydrogels for controlled release of human basic fibroblast growth factor. *Biomaterials* 2005, 26, 6054-6067.
15. R. A. Peattie, E. R. Rieke, E. M. Hewett, R. J. Fisher, X. Z. Shu, G. D. Prestwich, Dual growth factor-induced angiogenesis in vivo using hyaluronan hydrogel implants. *Biomaterials* 2006, 27, 1868-1875.
16. K. Ghosh, X. D. Ren, X. Z. Shu, G. D. Prestwich, R. A. F. Clark. Fibronectin functional domains coupled to hyaluronan stimulate adult human dermal fibroblast responses critical for wound healing. *Tissue Eng.* 2006, 12, 601-613.
17. Chapter 7, C. Hiemstra, L. J. van der Aa, Z. Y. Zhong, P. J. Dijkstra, J. Feijen, Novel in situ forming, degradable dextran hydrogels by Michael addition chemistry. Synthesis, rheology and degradation. Published in *Macromolecules* 2007, 40, 1165-1173.
18. Chapter 8, C. Hiemstra, L. J. van der Aa, Z. Y. Zhong, J. Feijen, Rapidly in situ forming degradable hydrogels from dextran thiols through Michael addition. *Biomacromolecules* 2007, *accepted*.
19. D. L. Elbert, A. B. Pratt, M. P. Lutolf, S. Halstenberg, J. A. Hubbell, Protein delivery from materials formed by self-selective conjugate addition reactions. *J. Controlled Release* 2001, 76, 11-25.
20. H. Li, Y. C. Liu, X. Z. Shu, S. D. Gray, G. D. Prestwich, Synthesis and biological evaluation of a cross-linked hyaluronan-mitomycin C hydrogel. *Biomacromolecules* 2004, 5, 895-902.

21. X. Z. Shu, K. Ghosh, Y. C. Liu, F. S. Palumbo, Y. Luo, R. A. Clark, G. D. Prestwich, Attachment and spreading of fibroblasts on an RGD peptide-modified injectable hyaluronan hydrogel. *J. Biomed. Mater. Res.* 2004, 68A, 365-375.
22. X. Z. Shu, Y. C. Liu, F. S. Palumbo, Y. Lu, G. D. Prestwich, In situ crosslinkable hyaluronan hydrogels for tissue engineering. *Biomaterials* 2004, 25, 1339-1348.
23. P. Shih, B. A. Malcolm, S. Rosenberg, J. F. Kirch, A. C. Wilson, Reconstruction and testing of ancestral proteins. *Methods Enzymol.* 1993, 224, 576-590.
24. K. Burczak, T. Fujisato, M. Hatada, Y. Ikada, Protein permeation through poly(vinyl alcohol) hydrogel membranes. *Biomaterials* 1994, 15, 231-238.
25. E. W. Merrill, K. A. Dennison, C. Sung, Partitioning and diffusion of solutes in hydrogels of poly(ethylene oxide). *Biomaterials* 1993, 14, 1117-1126.
26. K. Sagara, S. W. Kim, A new synthesis of galactose-poly(ethylene glycol)-polyethylenimine for gene delivery to hepatocytes. *J. Controlled Release* 2002, 79, 271-281.
27. T. Kajio, K. Kawahara, K. Kato, Stabilization of basic fibroblast growth-factor with dextran sulfate. *Febs Lett.* 1992, 306, 243-246.

Appendix 1

PEG-PLLA and PEG-PDLA multiblock copolymers: Synthesis and in situ hydrogel formation by stereocomplexation¹

*Christine Hiemstra^a, Zhiyuan Zhong^a, Xulin Jiang^b, Wim E. Hennink^b, Pieter J. Dijkstra^a,
and Jan Feijen^a*

^aDepartment of Polymer Chemistry and Biomaterials, Faculty of Science and Technology,
Institute for Biomedical Technology, University of Twente, P. O. Box 217, 7500 AE
Enschede, The Netherlands

^bDepartment of Pharmaceutics, Utrecht Institute for Pharmaceutical Sciences (UIPS),
Utrecht University, P. O. Box 80.082, 3508 TB Utrecht, The Netherlands

1.1 Abstract

Water-soluble PEG-PLLA and PEG-PDLA multiblock copolymers were synthesized and investigated for in situ hydrogel formation by stereocomplexation between the PLLA and PDLA blocks. The critical gel concentration measurements showed that these multiblock copolymers are able to form stereocomplexed hydrogels at a much lower concentration in water than the parent triblock copolymers. Furthermore, rheology studies showed significantly improved mechanical properties of the multiblock copolymer stereocomplexed hydrogels compared to the triblock copolymer hydrogels, obtained under otherwise same conditions.

¹ This appendix has been published in *J. Controlled Release* 2006, 116, e17-e19.

1.2 Introduction

Biodegradable, injectable hydrogels have received much attention, due to their wide application in drug delivery and tissue engineering. Recently, we and others have shown that hydrogels can be prepared in situ from water-soluble PDLA and PLLA based block copolymers, in which the physical crosslinks are provided by stereocomplexation between the enantiomeric PDLA and PLLA blocks.¹⁻³ De Jong et al. have shown that stereocomplexed dextran-PLA graft copolymer hydrogels quantitatively released proteins over a period of one week with full preservation of the protein activity.³ Synthesis of the dextran-PLA graft copolymers however requires several steps, while the PLA-PEG-PLA triblock copolymer stereocomplexed hydrogels show low mechanical strength and slow gelation kinetics compared to the dextran-PLA graft copolymers. Previously we have shown that PEG-PLA star block copolymers provide fast gelation and high storage moduli. In this study PEG-PLA multiblock copolymers with multiple crosslinking functionality were designed, synthesized and investigated for in situ hydrogel formation through stereocomplexation.

1.3 Materials and methods

PLLA-PEG-PLLA and PDLA-PEG-PDLA triblock copolymers were prepared at 90 °C in toluene for 4 h using stannous octoate as a catalyst and PEG diol ($M_{n, NMR} 12 \times 10^3$) as an initiator. PEG-PLLA and PEG-PDLA multiblock copolymers ((PEG-PLLA)_n and (PEG-PDLA)_n) were prepared by coupling of the chain ends of PLA-PEG-PLA with diisocyanatobutane (DIB) for 20 h. Subsequently, previously distilled ethanol was added to terminate the isocyanate end groups and the reaction mixture was stirred at 70 °C for 6 h. The copolymers were isolated by precipitation in diethyl ether. ¹H NMR spectra (CDCl₃) were recorded on a Varian Inova Spectrometer (Varian, Palo, Alto, USA) operating at 300 MHz. The number of lactyl units per PLA block was calculated based on the methyl protons of lactyl units at δ 1.5 and the methylene protons of PEG at δ 3.6. A Waters (Milford, MA, USA) 2695 Alliance liquid-chromatography system was used to perform

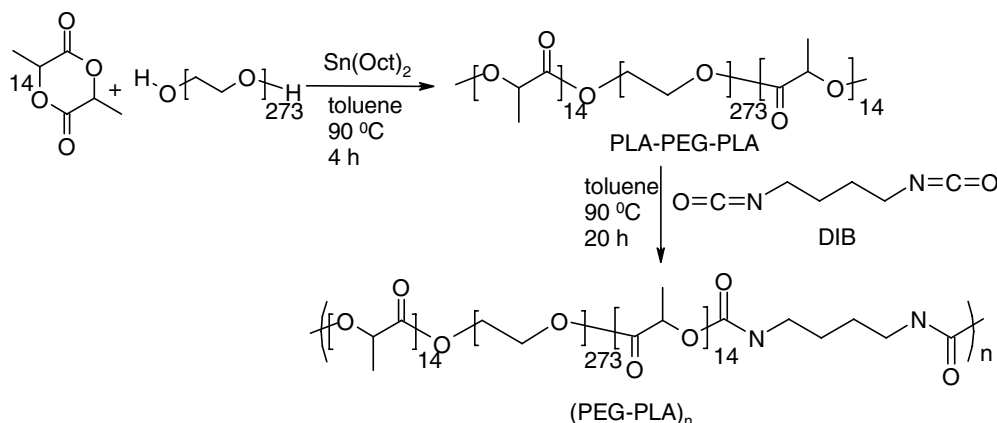
the GPC experiments. This instrument contained a built-in auto-injector and a Waters 2414 refractive-index detector (RI). A set of two linear columns (PLgel Mixed-D, 5 μm , 300x7.5mm, Polymer Labs) was thermostated at 30 °C. The eluent was DMF with 20 mM LiCl. The eluent was filtrated through a 0.2 μm HPLC filter (Nylon, Alltech) and degassed prior to use by simultaneous application of ultrasound and vacuum. The flow rate was 0.5 ml/min. The calibration curve was prepared with PEG standards. The data collection and the data analysis were done with Waters Empower software. Critical gel concentration and rheology measurements were performed as described previously.¹

1.4 Results and discussion

PEG-PLA multiblock copolymers were synthesized in a two-step procedure (Scheme 1). In the first step, the ring-opening polymerization of lactide in the presence of PEG ($M_{n, \text{NMR}} = 12,000$) and a catalytic amount of stannous octoate in toluene at 90 °C yielded PLA-PEG-PLA triblock copolymers. The ^1H NMR spectra showed that these triblock copolymers have the desired compositions (Table 1). Gel permeation chromatography (GPC) revealed a low polydispersity (PDI = 1.06). In the second step, these triblock copolymers were coupled with an equimolar amount of diisocyanatobutane (DIB), which resulted in PEG-PLA multiblock copolymers. The unreacted isocyanate groups were consumed by treatment with ethanol. GPC measurements showed that these multiblock copolymers have M_n values 4-5 times higher than the parent triblock copolymers. It should be noted that these multiblock copolymers contain a small percentage of triblock copolymer. These two PEG-PLLA and PEG-PDLA multiblock copolymers are soluble in water up to a concentration of 7.5 w/v%. The critical gel concentration (CGC) measurements showed that hydrogels are formed in situ upon mixing the aqueous solutions of PEG-PLLA and PEG-PDLA multiblock copolymers at or above a concentration of 4 w/v%. In contrast, no gel could be obtained from the mixture of the parent triblock copolymers when their aqueous concentration was lower than 15 w/v%. These triblock copolymers are soluble in water up to 22.5 w/v% concentration. Figure 2a shows that upon mixing 5 w/v% aqueous solutions of PEG-PLLA and PEG-PDLA multiblock copolymers

Appendix I

at 20 °C a gel is formed instantaneously. The resulting hydrogel has a storage modulus (G') of 590 Pa. The temperature sweep showed that these PEG-PLA multiblock copolymer stereocomplexed hydrogels are stable up to 60 °C (Figure 2b).



Scheme 1. Synthesis of PEG-PLA multiblock copolymers.

Table 1. Synthesis of PEG-PLA triblock and multiblock copolymers.^{a)}

Polymer	Conversion lactide (%) ¹ H NMR	$N_{\text{LA}}^{\text{b)}$		$M_n \times 10^{-3}$ NMR	PEG content (wt%)	$M_n \times 10^{-3}$ GPC	M_w/M_n GPC
		Theory ^{c)}	¹ H NMR				
PLLA-PEG-PLLA	94	14	14	14	86	10.9	1.06
PDLA-PEG-PDLA	92	14	14	14	86	10.9	1.06
(PEG-PLLA) _n	92	13	14	-	84	52.5 ^{d)}	1.57
(PEG-PDLA) _n	91	13	13	-	85	39.1 ^{d)}	1.36

^{a)} $M_{n,\text{GPC}} \text{ PEG} = 10,100$, $\text{PDI} = 1.05$. ^{b)} Number of lactyl units per PLA block. ^{c)} Based on feed composition and conversion. ^{d)} Contains a small percentage of parent triblock copolymer.

Interestingly, the aqueous solubility of PEG-PLLA and PEG-PDLA multiblock copolymers as well as their in situ hydrogel formation ability are highly dependent on the buffer strength. For example, the solubility of PEG-PLLA and PEG-PDLA multiblock copolymers increased to 20 w/v% in 100 mM HEPES buffer. The CGC for the in situ

hydrogel formation via stereocomplexation also increased to 15 w/v%. In contrast, this buffer strength effect was not observed for the parent triblock copolymers. Dynamic light scattering (DLS) studies showed that PEG-PLLA multiblock copolymers form smaller aggregates in 20 mM HEPES buffer than in water (100 vs.300 nm), whereas the aggregate sizes for PLLA-PEG-PLLA triblock copolymer are similar in both media (200 nm). These results indicate that the effect of the buffer strength on the solubility and gelation behavior of PEG-PLA multiblock copolymers is most likely due to the decreased hydrogen bonding between the urethane groups by the buffer.

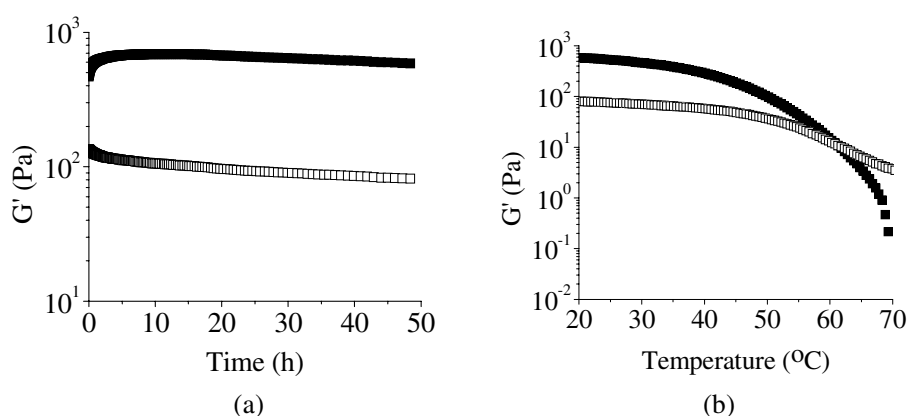


Figure 2. The storage modulus (G') (■) and loss modulus (G'') (□) after mixing 5 w/v% aqueous solutions of PEG-PLLA and PEG-PDLA multiblock copolymers in equimolar amounts in water (a) as a function of time at 20 °C, (b) as a function of temperature.

Figure 3 shows the storage and loss moduli of stereocomplexed multiblock and triblock hydrogels at 37 °C after mixing of the D- and L-enantiomer solutions at 15 w/v% concentration in 20 mM HEPES buffer (pH 7, 150 mM NaCl). Again instant hydrogel formation was observed for the multiblock copolymer. However, for the triblock copolymer the stereocomplexed hydrogel was only obtained 30 min after mixing the enantiomeric copolymer solutions. The slower kinetics is also shown by the fact that the storage modulus of the triblock copolymer hydrogel still slowly increases over a period of two days. Furthermore, the multiblock hydrogel showed a much higher storage modulus

than the triblock hydrogel at 37 °C and 15 w/v% polymer (2200 vs 54 Pa). This is attributed to the higher number of crosslinking sites of the multiblock copolymer. The in situ hydrogel formation of the PEG-PLLA multiblock/PDLA-PEG-PDLA triblock mixture with equal amounts of PLLA and PDLA blocks was also tested (Figure 3). The storage modulus of the mixture was found to be considerably higher than for the triblock copolymer alone (430 vs. 54 Pa). This further confirms that the multiblock copolymers increase the crosslinking density.

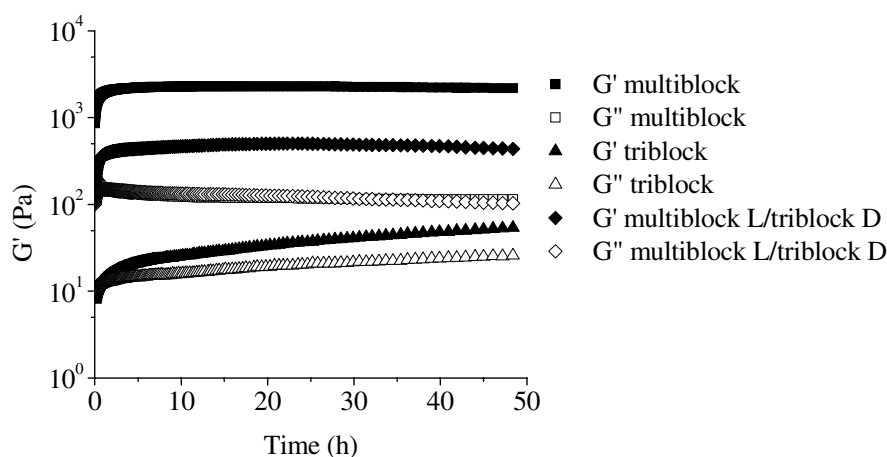


Figure 3. The storage modulus (G') and loss modulus (G'') of 15 w/v% stereocomplexed hydrogels in 20 mM HEPES (150 mM NaCl) at 37 °C after mixing PEG-PLLA and PEG-PDLA solutions.

1.5 Conclusions

We have shown that PEG-PDLA and PEG-PLLA multiblock copolymers can be prepared by a one-pot two-step synthesis procedure. A stereocomplexed hydrogel could be formed in situ by mixing aqueous solutions of PEG-PLLA and PEG-PDLA multiblock copolymers. These multiblock copolymers formed hydrogels at much lower concentrations than the parent triblock copolymer. Also, the multiblock copolymers provided fast gelation and high storage moduli compared to the parent triblock copolymers. These results show

that the multiple crosslinking sites of the multiblock copolymers effectively increase the crosslinking density. These multiblock copolymers are promising for use as in situ formed, injectable hydrogels for biomedical applications, since they can be easily synthesized and are biodegradable.

1.6 Acknowledgements

This work was funded by the Netherlands Organization for Scientific Research (NWO).

1.7 References

1. Chapter 3, Hiemstra, C.; Zhong, Z.; Dijkstra, P.; Feijen, J., Stereocomplex mediated gelation of PEG-(PLA)₂ and PEG-(PLA)₈ block copolymers. Published in *Macromol. Symp.* 2005, 224,119-131.
2. Li, S.; Vert, M., Synthesis, characterization, and stereocomplexation-Induced gelation of block copolymers prepared by ring-opening polymerization of L(D)-lactide in the presence of poly(ethylene glycol). *Macromolecules* 2003, 36, 8008-8014.
3. de Jong, S. J.; van Eerdenbrugh, B.; van Nostrum, C. F.; Kettenes-van de Bosch, J. J.; Hennink, W. E., Physically crosslinked dextran hydrogels by stereocomplex formation of lactic acid oligomers: degradation and protein release behavior. *J. Controlled Release* 2001, 71, 261-275.

Appendix 2

Computational modeling of aqueous solutions of poly(ethylene glycol)-poly(lactide) star block copolymers

Christine Hiemstra^a, Johan T. Padding^b, Menno Bokdam^b, Wim J. Briels^b, and Jan Feijen^a

^a Department of Polymer Chemistry and Biomaterials, Faculty of Science and Technology, Institute for Biomedical Technology, University of Twente, P. O. Box 217, 7500 AE Enschede, The Netherlands

^b Department of Computational Biophysics, Faculty of Science and Technology, University of Twente, P. O. Box 217, 7500 AE Enschede, The Netherlands

2.1 Introduction

Previous studies have shown that stereocomplexed hydrogels are rapidly formed in situ by mixing aqueous solutions of eight-arm poly(ethylene glycol)-poly(L-lactide) and poly(ethylene glycol)-poly(D-lactide) star block copolymers (denoted as PEG-(PLLA)₈ and PEG-(PDLA)₈, respectively).¹ The gelation is due to stereocomplexation of the PLLA and PDLA blocks. At relatively low polymer concentrations, single enantiomer solutions of these polymers were shown to form aggregates.² The PEG-(PLA)₈ stereocomplexed hydrogels are biodegradable due to degradation of the PLA blocks. The in situ formation allows easy loading of cells and bioactive compounds such as drugs, by mixing with the polymer solutions prior to gelation and enables minimally invasive surgery. Therefore, these PEG-(PLA)₈ stereocomplexed hydrogels are very promising for biomedical applications, such as drug delivery and tissue engineering. PEG-PLA star block copolymers are amphiphilic block copolymers, containing both hydrophilic PEG blocks and hydrophobic PLA blocks. Due to the hydrophobic interactions between PLA and water, self-assembled structures (e.g. micelles) form in water with hydrophilic and hydrophobic domains, wherein PLA is shielded from the water by PEG. The PEG-PLA

Appendix 2

star block copolymers are expected to show interesting phase behavior in water, since the PLA blocks are positioned at the end of the PEG chains, thus complicating shielding of the PLA blocks from the water by the PEG chains. Moreover, in aqueous solutions containing both PEG-(PLLA)₈ and PEG-(PDLA)₈ copolymers, stereocomplexation forms an additional driving force for PLA aggregation, besides hydrophobic interactions. To our knowledge, the phase behavior of these ‘frustrated’ eight-arm PEG-PLA star block copolymers and the effect of stereocomplexation on the phase behavior of amphiphilic PLA block copolymers has not been reported before in literature. Moreover, insight in the phase behavior of such PEG-PLA star copolymers is important for the rational design of hydrogels or other biomedical materials based on these polymers. In this report, a first approach is made to study the phase behavior of PEG-PLA star block copolymers by computational modeling as well as small angle neutron scattering (SANS) experiments.

2.2 Materials and methods

Computational modeling. The eight-arm PEG-PLA star block copolymer is modeled by a bead-spring model, with per molecule 1 central bead and 8 arms. One arm contains 9 PEG beads (light grey) and 3 PLA beads (dark grey) (Figure 1).

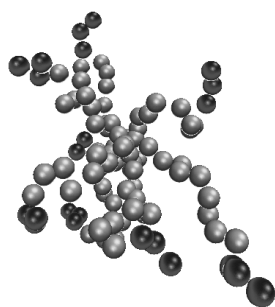


Figure 1. Bead-spring model of an eight-arm PEG-PLA star block copolymer (PEG is light grey, PLA is dark grey).

For the monomer-monomer interactions in this off-lattice simulation a common model that has been introduced by Grest et al.³ is used. All monomers are assumed to interact by means of the purely repulsive truncated and shifted Lennard-Jones (LJ) potential, $V_0(r)$, given by:

$$V_0(r) = \begin{cases} 4\varepsilon \left[\left(\frac{r}{\sigma_{LJ}} \right)^{-12} - \left(\frac{r}{\sigma_{LJ}} \right)^{-6} + \frac{1}{4} \right] & \text{if } r < 2^{1/6} \sigma_{LJ} \\ 0 & \text{if } r > 2^{1/6} \sigma_{LJ} \end{cases} \quad (1)$$

where ε sets an energy and σ_{LJ} a length scale. The LJ-potential is short ranged and vanishes beyond a distance $2^{1/6} \sigma_{LJ}$. The connectivity of the chains is modeled by an additional interaction between monomers on the same chain, which is given by the so-called finite extensible nonlinear elastic (FENE) potential $V_{FENE}(r)$:

$$V_{FENE}(r) = \begin{cases} -15\varepsilon \left(\frac{R_0}{\sigma_{LJ}} \right)^2 \ln \left[1 - \left(\frac{r}{R_0} \right)^2 \right] & \text{if } r < R_0 \\ \infty & \text{if } r > R_0 \end{cases} \quad (2)$$

with $R_0 = 1.5 \sigma_{LJ}$.

The interaction with the solvent is not explicitly simulated, but is taken into account by adding a frictional force on the beads³:

$$m \frac{d^2 r_i}{dt^2} = -\nabla U_i - \Gamma \frac{dr}{dt} + W_i(t) \quad (3)$$

where Γ is the bead friction, $W_i(t)$ describes the random force of the solvent acting on each monomer and U_i is the potential. The random force amplitude is set by

$$\{W_i(t) \cdot W_j(t')\} = \delta_{ij} \delta(t-t') 6k_B T \Gamma / m \quad (4)$$

where m is the mass of a bead. The time step Δt was set at 0.001τ , where $\tau = \sigma_{LJ}(m/\varepsilon)^{1/2}$. $k_B T$, which is a measure for the energy of the system, was set at 1 (k_B is the Boltzmann constant $1,38.10^{-23}$ J/K). The bead friction Γ acts as a coupling to the viscous background

Appendix 2

and was chosen to be τ^{-1} . The average bond length was $0.97\sigma_{LJ}$. These parameters ensure that the bonds do not cut each other.

PLA blocks are attracted to each other, and PLA blocks and water are repelled by each other, due to hydrophobic interactions. The attractive force between PLA blocks was modeled by the potential $V_{PLA}(r)$:

$$V_{PLA}(r) = \begin{cases} \varepsilon \left[\cos^2\left(\pi \frac{r - \sigma_{LJ}}{w_c}\right) - 1 \right] & \text{if } \sigma_{LJ} < r < \sigma_{LJ} + w_c \\ 0 & \text{if } \sigma_{LJ} > r > \sigma_{LJ} + w_c \end{cases} \quad (5)$$

where w_c is the maximum range of PLA-PLA interaction, which was set at $2\sigma_{LJ}$. The interaction energy ε was varied with respect to $k_B T$ and was different for pure hydrophobic interactions between PLLA and PLLA blocks (or PDLA and PDLA blocks) and additional stereocomplex interactions between PLLA and PDLA blocks. ε_{DL} was set at $1.1 \times \varepsilon_{LL}$ ($= 1.1 \times \varepsilon_{DD}$). Since the solvent is not explicitly simulated, the repulsive force between PLA and water cannot be directly simulated. Therefore, an additional attractive force between PLA chains and other polymer chains, both PLA and PEG, was added. The force on a PLA bead j , F_j , is given by:

$$\vec{F}_j = \alpha \sum_i m(r_{ij}) \frac{(\vec{r}_i - \vec{r}_j)}{|\vec{r}_i - \vec{r}_j|} \quad (6)$$

where α is a measure for the attraction and i runs over all PLA and PEG beads in the simulation. $m(r_{ij})$ measures the total mass of PLA and PEG beads at a certain distance r_{ij} from the PLA bead j . It is a weight function defined by:

$$m(r_{ij}) = \begin{cases} \cos^2\left(\frac{\pi r}{2r_c}\right) & \text{if } r < r_c \\ 0 & \text{if } r \geq r_c \end{cases} \quad (7)$$

where r_c was set at $3\sigma_{LJ}$.

The length scale in the simulation was estimated by equaling the end-to-end distance as determined by simulation to the end-to-end distance of one PEG arm. The end-to-end distance in the simulation experiments was found to be approximately 5 beads. The eight-arm PEG used for the experiments has M_n of 21,800. The end-to-end distance, $\langle r_0^2 \rangle^{1/2}$, of one PEG arm with M_n of 2725 is approximately 32.5 Å, as calculated by the following formula⁴:

$$\sqrt{\bar{r}_0^2} = l \cdot \sqrt{2C_n \frac{M_c}{M_n}} \quad (8)$$

where C_n is the characteristic ratio, l the weighted average of the bond lengths and M_r the molecular weight per repeating unit. For PEG $C_n = 4.0$, $l = 0.147$ nm, the weighted average of the bond lengths of C-C bonds (0.154 nm) and C-O bonds (0.143 nm) and $M_r = 44$ g/mol.⁵ Therefore one PEG bead has a length of approximately 6.5 Å. The polymer concentration was derived from this length scale. One eight-arm PEG-PLA molecule has M_n of approximately 29 kg/mol. 1000 kg of water (≈ 1 m³) contains:

$$\Phi(1000/29)N_{AV} = \Phi 2.1 \times 10^{25} \quad (9)$$

molecules, where Φ is the weight percentage of polymer and N_{AV} is Avogadro's number. Since N and V are known, the polymer concentration can be calculated by:

$$\Phi = 4.8 \times 10^{-26} N/V \quad (10)$$

where N is the number of PEG-PLA molecules and V is the volume of the box used in the simulation.

Small angle neutron scattering. Small angle neutron scattering (SANS) experiments were performed at the ISIS Facility of the Rutherford Appleton Laboratory (Chilton, Didcot, Oxfordshire) using a fixed geometry instrument with a spallation neutron source. The scattering vector Q describes the relationship between the incident, k_i , and scattered, k_s , wavevectors as illustrated in Figure 2.

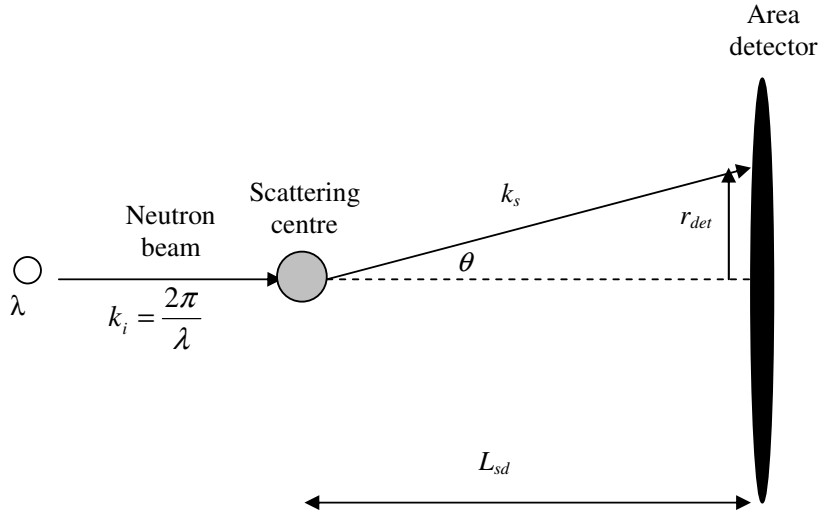


Figure 2. The geometry of a SANS experiment. Neutrons with a wavelength λ are spherically symmetrically scattered by nuclei in the sample. A fraction of the neutrons scattered through an angle θ are then recorded on a two-dimensional detector at a distance L_{sd} from the sample at a radial distance r_{det} . k_i and k_s are the wavevectors of the incident and scattered neutrons, respectively.

The modulus of Q , q , quantifies length scales in reciprocal space and is the independent variable in a SANS experiment. Its magnitude is given by:

$$q = |Q| = |k_s - k_i| = \frac{4\pi n}{\lambda} \sin(\theta/2) \approx \frac{4\pi r_{det}}{\lambda L_{sd}} \quad (11)$$

when θ is small. To a very good approximation the neutron refractive index, n , may be taken as unity. By substituting equation (11) into the Bragg law of diffraction:

$$\lambda = 2d \sin(\theta/2) \quad (12)$$

one obtains the expression:

$$d = \frac{2\pi}{q} \quad (13)$$

Here d is the molecular-level length scale by virtue of the q -range accessible in a SANS experiment.

The differential scattering cross-section, $(d\Sigma/d\Omega)(q)$, is the dependent variable measured in a SANS experiment and has dimensions of $(\text{length})^{-1}$. The intensity of scattering $I(q)$ may be expressed as:

$$I(q) = I_0(\lambda)\Delta\Omega\eta(\lambda)T(\lambda)V_s \frac{\partial\Sigma}{\partial\Omega}(q) \quad (14)$$

Where I_0 is the incident flux of neutrons, $\Delta\Omega$ is the solid angle element defined by the size of a detector pixel, η is the detector efficiency, T is the neutron transmission of the sample, and V_s is the volume of the sample illuminated by the neutron beam. The significance of $(d\Sigma/d\Omega)(q)$ is that it contains all the information on the size, shape, and interactions between the scattering centre in the sample. A generalized expression for SANS may be written as follows:

$$\frac{\partial\Sigma}{\partial\Omega}(q) = NV^2(\Delta\rho)^2 P(q)S(q) + B \quad (15)$$

Where N is the number concentration of scattering centers, V is the volume of one scattering centre, $(\Delta\rho)^2$ is the contrast in neutron scattering and B is the background signal. The term $P(q)$ is known as the form or shape factor. It is a dimensionless function that describes how $(d\Sigma/d\Omega)(q)$ is modulated by interference effects between neutrons scattered by different parts of the same scattering centre. Consequently it is dependent on both the size and shape of the scattering centre. The term $S(q)$ is called the structure factor. It is another dimensionless function, but this time describes how $(d\Sigma/d\Omega)(q)$ is modulated by interference effects between neutrons scattered by different scattering centers in the sample. Consequently it is dependent on the degree of local order in the sample and on the interaction potential between scattering centers. $S(q)$ is given by:

$$S(q) = 1 + \frac{4\pi N}{qV_s} \int_0^\infty [g(r) - 1] r \sin(qr) dr \quad (16)$$

Appendix 2

where $g(r)$ is a density distribution function related to the radial distribution function in statistical mechanics. It is typically a damped oscillatory function whose maxima correspond to the distance, r , of each nearest-neighbor coordination shell. $S(q)$ tends to unity at high- q as the concentration of scattering centers becomes more dilute. Thus the neutron scattering of materials in dilute solution is mainly determined by the form factor $P(q)$.

Calculation of SANS profiles using the computational model. For the calculation of SANS profiles from the computational model, the contrast in neutron scattering between PLA and PEG, and PLA or PEG and the solvent (either water or deuterium oxide) needs to be determined. The contrast, $(\Delta\rho)^2$, is simply the square of the difference in neutron scattering length density between the solute and the surrounding medium or matrix, ρ_m :

$$(\Delta\rho)^2 = (\rho - \rho_m)^2 \quad (17)$$

When $(\Delta\rho)^2$ is zero the scattering centers are said to be at contrast match. The scattering length density, ρ of a molecule with i atoms may be calculated from the expression:

$$\rho = N \sum_i b_i = \frac{\delta N_A}{M} \sum_i b_i \quad (18)$$

where δ is the bulk density of the molecule, M is its molecular weight and b_i is the coherent neutron scattering length of nucleus i . ρ has dimensions of $(\text{length})^{-2}$. Only coherently scattered neutrons, where phase is conserved, carry any structural information about the sample. All nuclei with non-zero spin also scatter neutrons incoherently. The coherent scattering lengths b of ^1H , ^2D , C and O nuclei are listed in Table 1.

Table 1. Coherent neutron scattering lengths (b).

Nucleus	b (10^{-14} m)
^1H	-0.3741
^2D	0.6671
C	0.6646
O	0.5803

The average b per PLA or PEG monomers and water or deuterium oxide can be calculated by adding the b values of the constituting atoms of the monomers or molecules, respectively (Table 2).

Table 2. Average coherent neutron scattering lengths per monomer or molecule ($b_{average}$), monomer or molecular weight (M_n) and bulk density (ξ).

Monomer or molecule	$b_{average}$ (10^{-14} m)	M_n (g/mol)	ξ (g/cm ³)	v (cm ³ /mol)
PLA	1.659	72	1.16	62.1
PEG	-0.334	44	1.13	38.9
H ₂ O	-0.168	18	1	18.0
D ₂ O	1.914	29	1.1	18.2

Since the solvent is not simulated explicitly, the effective b is obtained by taking b per effective volume of the monomers or molecules. The difference in coherent neutron scattering length per volume between the monomers and the solvent molecules, $\Delta b_{bead}/v$, can be calculated by using the following formulas ($\bar{b} = b_{average}$):

$$\frac{\Delta b_{bead}}{v} = \frac{\bar{b}_{bead}}{v_{monomer}} - \frac{\bar{b}_{solvent}}{v_{solvent}} \quad (19)$$

$$\bar{b}_{bead} = n\bar{b}_{monomer} \quad (20)$$

Appendix 2

$$v = \frac{M_n}{\xi} \quad (21)$$

where n is the number of equivalent monomer units per bead in the model. Since PLA is modeled by three beads, $n = 4$ and 4.67 for PEG-(PLA₁₂)₈ and PEG-(PLA₁₄)₈ copolymers, having 12 and 14 lactyl units per PLA block, respectively. One PEG arm of M_n 2725 is modeled by 9 beads, and therefore $n = 6.88$. In Table 3 $\Delta b_{bead}/v$ of PEG, PLA₁₂ and PEG-PLA₁₄ with the solvent, i.e. water or deuterium oxide, are listed.

Table 3. Effective differences in coherent neutron scattering lengths per bead ($\Delta b_{bead}/v$).

Nucleus	$\Delta b_{bead}/v$ (10^{-14} m)
PLA ₁₂ -H ₂ O	8.95
PLA ₁₄ -H ₂ O	10.45
PEG-H ₂ O	0.2
PLA ₁₂ -D ₂ O	-19.5
PLA ₁₄ -D ₂ O	-22.7
PEG-D ₂ O	-30.4

Importantly, the neutron scattering profile in water is predominantly determined by the PLA domains, since $\Delta b_{bead}/v$ of PEG-H₂O is close to zero. In deuterium oxide the scattering profile is determined by both PEG and PLA domains.

2.3 Results and discussion

PEG-(PLA)₈ star block copolymers with $M_{n,PEG}$ of 21,800 and PLA blocks containing 12 or 14 lactyl units (denoted as PEG-(PLA₁₂)₈ and PEG-(PLA₁₄)₈) were synthesized as described previously.¹ The phase behavior of these polymers in aqueous solutions was

studied by computational modeling and small angle neutron scattering (SANS) experiments. Following sections show preliminary results.

Computational modeling. The eight-arm PEG-PLA star block copolymer is modeled by a bead-spring model, with per molecule 1 central bead and 8 arms. One arm contains 9 PEG beads and 3 PLA beads (Figure 1). All modeling experiments were performed on aqueous solutions containing equimolar amounts of PEG-poly(L-lactide) (PEG-(PLLA)₈) and PEG-poly(D-lactide) (PEG-(PDLA)₈) star block copolymers. At low polymer concentration of 0.3 wt% each polymer lives individually (Figure 3).

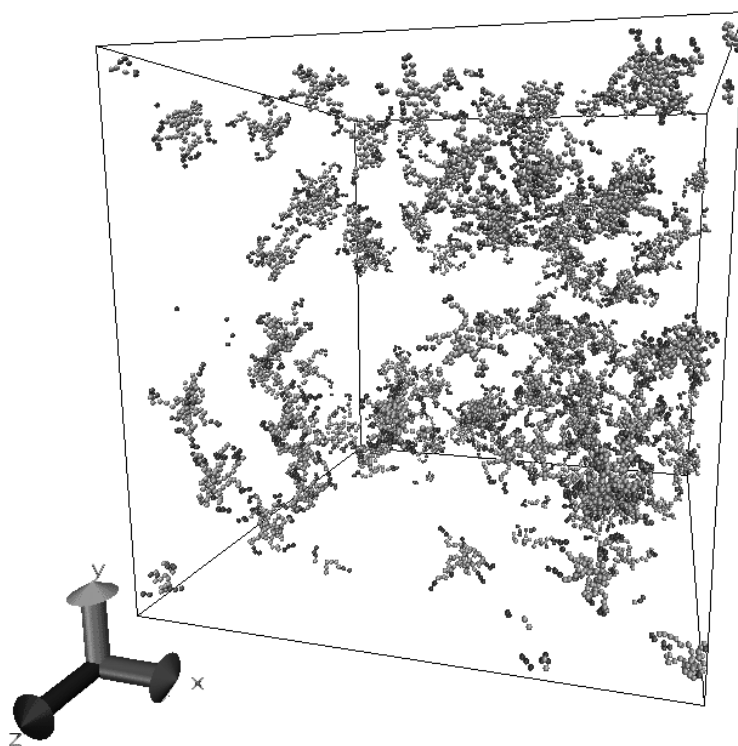


Figure 3. Snap-shot of an aqueous solution containing equimolar amounts of PEG-(PLLA)₈ and PEG-(PDLA)₈ star block copolymers at 0.3 wt% polymer concentration (PEG is light grey, PLLA and PDLA are dark grey).

Appendix 2

At a higher polymer concentration of 5 wt% the polymer molecules in this solution start to interact, as is shown by the presence PEG and PLA clusters in Figure 4.

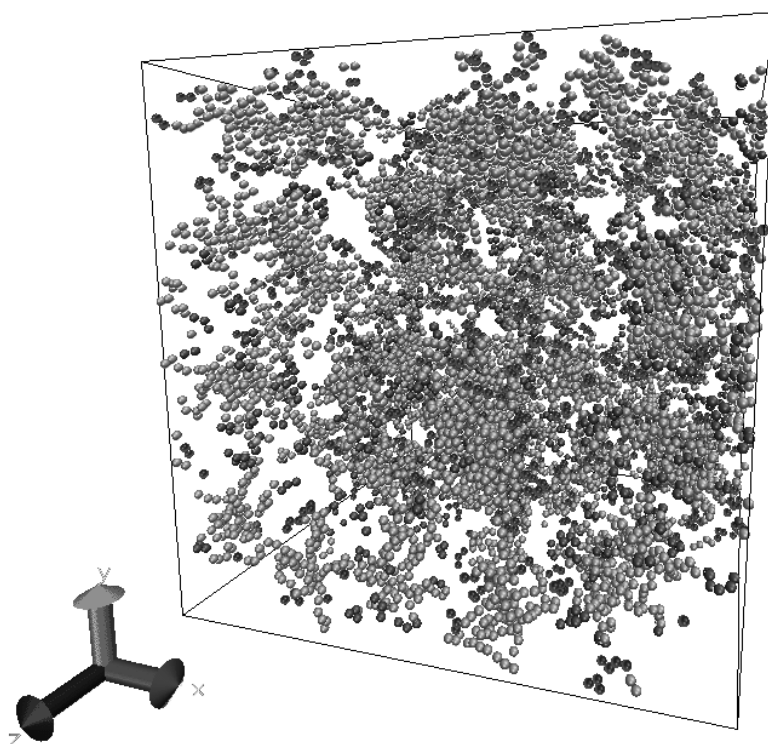


Figure 4. Snap-shot of an aqueous solution containing equimolar amounts of PEG-(PLLA)₈ and PEG-(PDLA)₈ star block copolymers at 5 wt% polymer (PEG is light grey, PLLA and PDLA are dark grey).

The radial density distribution of the PEG and PLA chains from the central monomer was calculated at 2 wt% concentration, wherein the measure for the repulsive force α between PLA and water was set at zero (Figure 5). The peak of the PEG distribution at small distance r is due to the strong attachment of the arms to the central bead. PLA is positioned around the central monomer with an almost Gaussian distribution. This shows that PEG acts as an entropic spring, wherein the chance to find a PLA chain at a distance r scales with $e^{C(r-r_0)^2}$ (C is a constant). PLA is mainly positioned at the outside, which is most probably due to the absence of a repulsive interaction between PLA and water. The

distribution of PLA hardly changes by increasing the polymer concentration from 0.3 to 3.5 wt% (Figure 6). From these experiments it seems that the entropic spring of PEG is hardly influenced by the presence of other polymer molecules. The introduction of a repulsive force α between PLA and water profoundly changes the form of the PLA distribution and gives a more realistic picture (Figure 7). At a low polymer concentration of 0.3 wt% (where the polymer molecules live individually) increasing repulsive force leads to an increasing tendency of PLA to be positioned at a smaller distance from the central monomer. Moreover, the radial distribution of PLA changes with varying polymer concentration when the repulsive force between PLA and water is taken into account, in contrast to when such a force is absent (Figure 8).

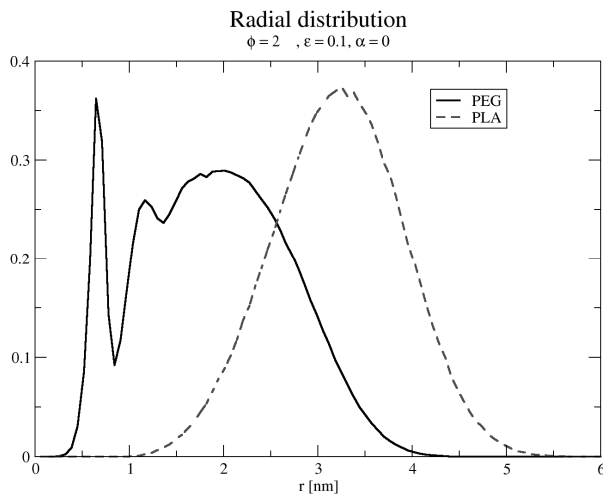


Figure 5. Radial distribution of PEG and PLA chains from the central monomer at a polymer concentration Φ of 2 wt% (the measure for the repulsive force α between PLA and water was set at zero and the interaction energy ϵ between PLA chains was set at $0.1 k_B T$).

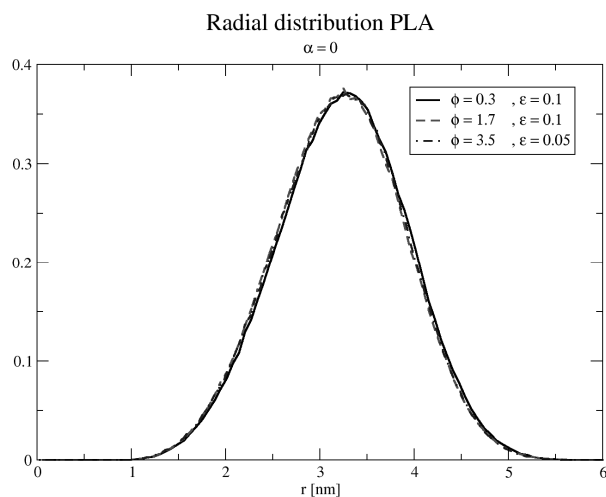


Figure 6. Radial distribution of PLA chains from the central monomer at different polymer concentrations Φ (wt%) and interaction energies ϵ ($k_B T$) (the measure for the repulsive force α between PLA and water was set at zero).

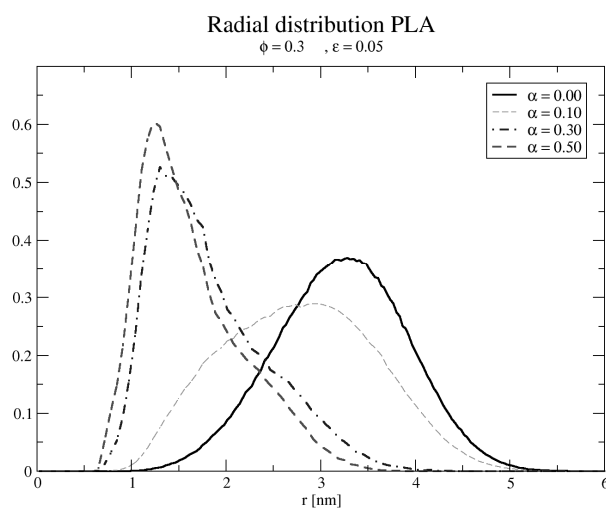


Figure 7. Radial distribution of PLA chains from the central monomer at different measures of repulsion α between PLA and water (the PLA interaction energy ϵ was set at $0.05 k_B T$ and the polymer concentration Φ was set at 0.3 wt%).

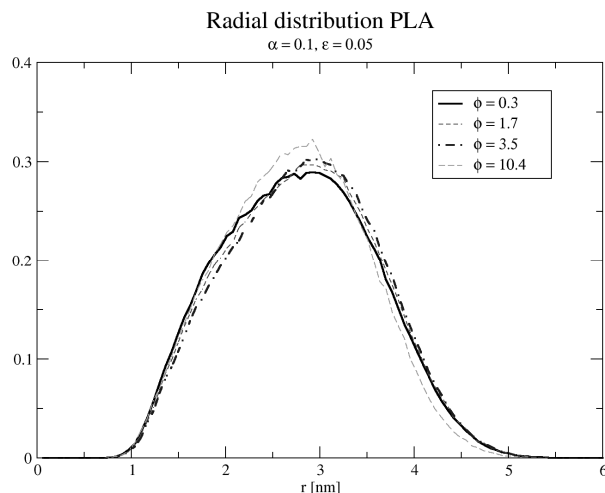


Figure 8. Radial distribution of PLA chains from the central monomer at different polymer concentrations Φ (wt%) (the PLA interaction energy ϵ was set at $0.05 k_B T$ and the measure for the repulsive force between PLA and water α was set at 0.1).

The differential scattering cross-section $d\Sigma/d\Omega$ was calculated as a function of the neutron scattering angle q for 0.3 wt% PEG-(PLA)₈ solutions at different measures of repulsive force α between PLA and solvent (either water or deuterium oxide) (Figure 9 and Figure 10). The calculated SANS profiles in water and in deuterium oxide are very similar. The scattering intensity is however much higher in deuterium oxide, which is due to the higher contrast between PEG and deuterium oxide as compared to PEG and water. The contrast between PEG and water is close to zero and hence the scattering in water is predominantly determined by PLA. The higher scattering intensity in deuterium oxide as compared to water was also observed for experimentally determined SANS profiles of 5 w/v% solutions of equimolar amounts of PEG-(PLA₁₂)₈ copolymers in water and in deuterium oxide (Figure 11). At α of 0.5 the scattering profiles show a decrease in the slope $(d\Sigma/d\Omega)/(dq)$ at $q \approx 0.06 \text{ \AA}^{-1}$ for water as well as deuterium oxide (Figure 9 and Figure 10). Similarly, at α of 0.1 the change in slope is seen at $q \approx 0.05 \text{ \AA}^{-1}$, though this change in slope is less pronounced. The change in slope points to a characteristic length d in the model system of approximately 10 nm ($d = 2\pi/q$). A similar change in slope was seen

Appendix 2

in experimentally determined neutron scattering profiles (Figure 11). The change in slope of the experimental profiles occurred at lower q values ($q \approx 0.03 \text{ \AA}^{-1}$) as compared to the calculated SANS profiles, corresponding to a characteristic length of approximately 20 nm. This could be due to an error in the calculated PEG arm length, which was used to set the length scale in the computational model. The scaling of $d\Sigma/d\Omega$ with q after the change in slope is between q^{-3} and q^{-4} , wherein q^{-4} scaling corresponds to more compact structures as compared to q^{-3} scaling³ (Figure 9 and Figure 10). Similar scaling was found for experimentally determined SANS profiles (Figure 11). The slope becomes steeper (i.e. tends more to q^{-4} scaling) with increasing α (Figure 9 and Figure 10). This result agrees well with the calculated radial distribution profiles of PLA, where the PLA chains are increasingly positioned closer to the central monomer with increasing α , thus leading to more compact structures (Figure 7).

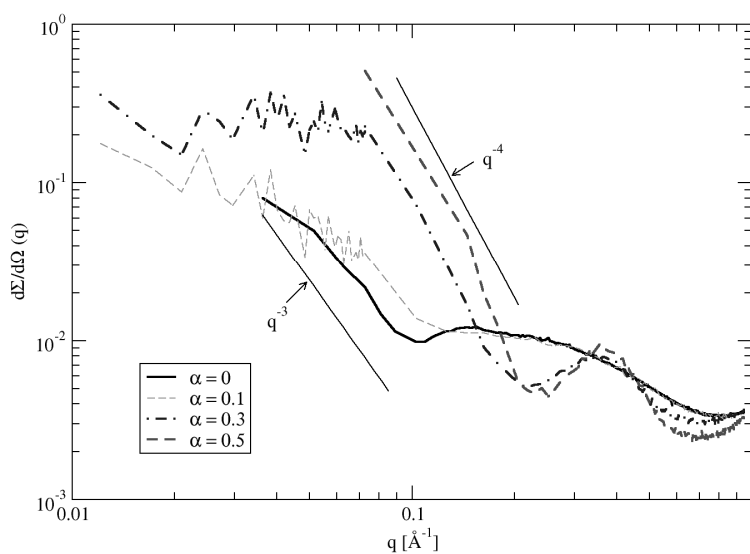


Figure 9. Differential scattering cross-section $d\Sigma/d\Omega$ as a function of the scattering angle q (\AA^{-1}) of an aqueous solution containing equimolar amounts of PEG-(PLLA)₈ and PEG-(PDLA)₈ copolymers at a concentration Φ of 0.3 wt% and different measures of repulsive interaction α between PLA and water (log-log scale).

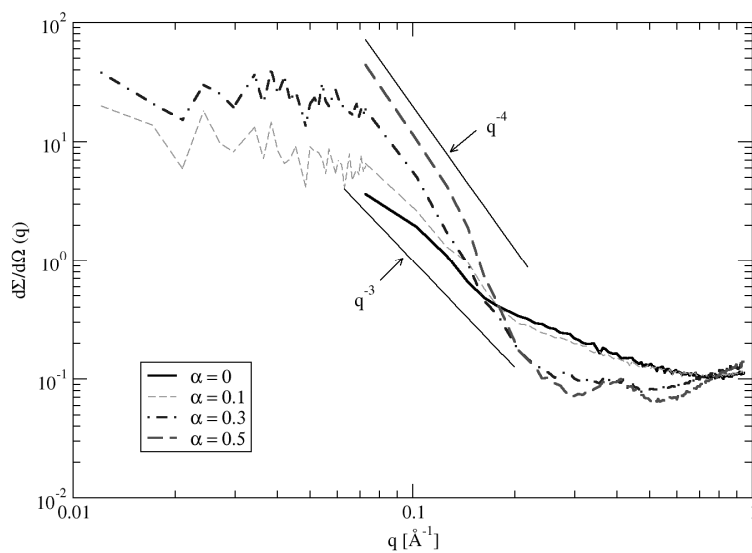


Figure 10. Differential scattering cross-section $d\Sigma/d\Omega$ as a function of the scattering angle (q) of equimolar amounts of PEG-(PLLA)₈ and PEG-(PDLA)₈ copolymers dissolved in deuterium oxide at a concentration Φ of 0.3 wt% and different measures of repulsive interaction α between PLA and water (log-log scale).

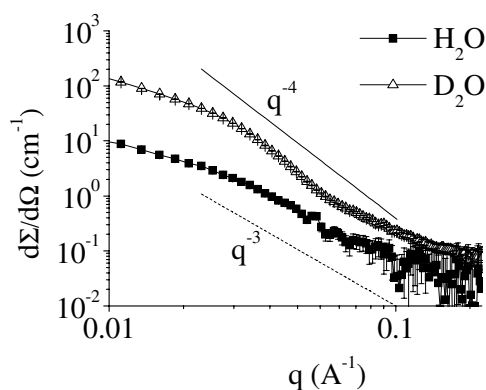


Figure 11. Experimentally determined SANS profiles of 5 w/v% solutions of equimolar amounts of PEG-(PLA₁₂)₈ copolymers in water or deuterium oxide at 40 °C (log-log scale).

2.4 Conclusions and recommendations

A computational model was developed to simulate the phase behavior of eight-arm PEG-PLA star block copolymers in water. The PEG-PLA molecule is modeled by a bead-spring model, with per molecule 1 central bead and 8 arms. One arm contains 9 PEG beads and 3 PLA beads. In the model the polymer concentration, attraction between the PLA blocks and the repulsion between PLA blocks and water can be varied. Radial density distributions of PLA show that the model becomes more realistic when the repulsion between PLA and water is taken into account. The calculated SANS profiles show a similar change in slope of the differential scattering cross-section at a similar scattering angle as the experimental SANS profiles. The change in slope points to a characteristic length in the order of 10 nm. Furthermore, the calculated SANS profiles and radial density distribution of PLA around the central monomer both show the formation of more compact PEG-PLA molecules with increasing repulsion between the PLA and water. Though promising results have been obtained, further study is needed to improve the model. To this end, experimentally determined data, such as critical aggregation concentration, storage modulus, critical gel concentration and neutron scattering may be compared with calculated data to fine tune the parameters of the model (hydrophobic and stereocomplex interactions of PLA, repulsion of PLA and water and length scale). Furthermore,

experimental SANS data on dilute polymer solutions would be useful to obtain information on the behavior of individually living PEG-PLA molecules.

2.5 Acknowledgements

This work was funded by the Netherlands Organization for Scientific Research (NWO). We thank R. K. Heenan, A. E. Terry (Rutherford Appleton Laboratory, ISIS Facility) and D. Visser (NWO) for help with the SANS experiments.

2.6 References

1. Chapter 3, Hiemstra, C.; Zhong, Z. Y.; Dijkstra, P. J.; Feijen, J., Stereocomplex mediated gelation of PEG-(PLA)₂ and PEG-(PLA)₈ block copolymers. Published in *Macromol. Symp.* 2005, 224, 119-131.
2. Chapter 4, Hiemstra, C.; Zhong, Z. Y.; Li, L.; Dijkstra, P. J.; Feijen, J., In-situ formation of biodegradable hydrogels by stereocomplexation of PEG-(PLLA)₈ and PEG-(PDLA)₈ star block copolymers. Published in *Biomacromolecules* 2006, 7, 2790-2795.
3. Grest, G. S.; Kremer, K.; Witten, T. A., Structure of many arm star polymers: a molecular simulation. *Macromolecules* 1987, 20, 1376-1383.
4. Peppas, N.; Bures, P.; Ichikawa, H., Hydrogels in pharmaceutical formulations. *Eur. J. Pharm. Biopharm.* 2000, 50, 27-46.
5. Temenoff, J. S.; Athanasiou, K. A.; LeBaron, R. G.; Mikos, A. G., Effect of poly(ethylene glycol) molecular weight on tensile and swelling properties of oligo(poly(ethylene glycol) fumarate) hydrogels for cartilage tissue engineering. *J. Biomed. Mater. Res.* 2002, 59, 429-437.

Summary

Hydrogels have been widely applied for biomedical applications, such as protein delivery and tissue engineering, due to their similarity with the extracellular matrix. Hydrogels are water-swollen, insoluble polymer networks. Their high water content renders them compatible with living tissue and proteins and their rubbery nature minimizes damage to the surrounding tissue. Conventionally, hydrogels are preformed and implanted in the body. More recently, hydrogels have been formed in situ under physiological conditions by mixing liquid precursors. These hydrogels are preferred over preformed hydrogels, since cells and bioactive compounds may be easily mixed with the precursor solutions prior to gelation. Moreover, in situ gelation allows for minimally invasive surgery and for the preparation of complex shapes.

Hydrogels are formed by physical or chemical crosslinking. Physical crosslinks are formed by noncovalent interactions, such as hydrophobic and ionic interactions and stereocomplexation. Physical crosslinking generally proceeds under mild conditions, thus enabling in situ hydrogel formation and allowing the entrapment of labile compounds. The integrity of physically crosslinked hydrogels may however be lost upon a change in physical conditions. Chemically crosslinked hydrogels are formed by covalent bonds by reaction between functional groups. Most commonly, these hydrogels have been formed by radical chain polymerization of (meth)acrylate derived polymers initiated by photoirradiation. Chemically crosslinked hydrogels are generally more stable than physically crosslinked hydrogels. Chemically crosslinked hydrogels may also be formed in situ. However, care has to be taken that the reactants, products and/or auxiliary compounds are non-toxic.

In **Chapter 2** polymers and crosslinking methods used for hydrogel preparation are reviewed, as well as application of hydrogels for drug delivery and tissue engineering. Nowadays, many biodegradable polymers are available for the preparation of hydrogels. Hydrogels are increasingly designed with additional functionality to mimic the natural extracellular matrix. To this end, polymers with proteolytically degradable and/or cell-adhesive peptide sequences have been reported. Recently, several crosslinking methods, physical as well as chemical, have been proposed for in situ formation of hydrogels. Of the

Summary

physical crosslinking methods, stereocomplexation, i.e. co-crystallization of poly(L-lactide) (PLLA) and poly(D-lactide) (PDLA), of water-soluble poly(lactide) (PLA) block copolymers is a promising approach. The gelation via stereocomplexation proceeds rapidly under physiological conditions and proteins can be easily incorporated without damaging the protein. Moreover, these hydrogels are biodegradable by hydrolysis of the PLA blocks. Photopolymerization is a common method to prepare chemically crosslinked hydrogels, which are robust and may have a wide range of degradation rates. However, hydrogel formation *in vivo* is hampered due to significant absorption of the UV-light by the skin. This crosslinking method may be improved by combining photopolymerization with a fast in situ crosslinking method. Michael type addition between thiols and acrylates or vinyl sulfones is a promising chemical crosslinking method for in situ hydrogel formation. This reaction proceeds rapidly and is selective towards thiols under physiological conditions. Biomimetic hydrogels can be easily obtained by reaction of the unsaturated groups with thiol-bearing bioactive compounds prior to gelation. In **Chapter 3** hydrogels based on poly(ethylene glycol)-PLA (PEG-PLA) block copolymers that are rapidly formed in situ under physiological conditions by mixing aqueous solutions of equimolar amounts of PEG-PLLA and PEG-PDLA copolymers via stereocomplexation between the PLLA and PDLA blocks are described. Rheology measurements showed that stereocomplexed hydrogels based on eight-arm PEG-PLA star block copolymers showed improved mechanical properties as compared to the hydrogels based on PLA-PEG-PLA triblock copolymers, due to the higher crosslinking functionality of the eight-arm PEG-PLA star block copolymers. In **Chapter 4** the gelation rate and the mechanical properties of stereocomplexed hydrogels based on eight-arm PEG-PLA star block copolymers are studied in detail as well as the gelation mechanism. The gelation time decreased and the hydrogel storage modulus increased with increasing PLA block length or polymer concentration, as determined by rheology measurements. WAXS measurements on stereocomplexed hydrogels confirmed the presence of stereocomplex crystals. Cryo-TEM showed somewhat larger “micelles” for stereocomplexed hydrogels compared to the corresponding aqueous solutions of the single enantiomer. Correspondingly, dynamic light scattering measurements showed that solutions containing equimolar amounts of PEG-PLLA and PEG-PDLA have larger “micelles” compared to the corresponding single enantiomer solutions. In **Chapter 5** the release of model proteins with different sizes as

well as the pharmaceutically active protein recombinant human interleukin-2 (rhIL-2) from stereocomplexed hydrogels based on eight-arm PEG-PLA star block copolymers is studied. Protein loaded hydrogels were easily obtained by mixing protein containing aqueous solutions of PEG-PLLA and PEG-PDLA copolymers. The *in vitro* release of the relatively small protein lysozyme (d_h is 4.1 nm) followed first order kinetics, wherein a high cumulative release of approximately 90% was obtained in 10 days. Importantly, the released lysozyme retained its enzymatic activity, emphasizing the protein-friendly hydrogel preparation method. The larger protein immunoglobulin G (IgG, d_h is 10.7 nm) could be released *in vitro* with nearly zero order kinetics for 16 days. An almost constant release of rhIL-2 over a period of a week could be achieved *in vitro*. After the release experiments, the hydrogels were completely degraded, leaving a clear solution. The therapeutic efficacy of rhIL-2 loaded stereocomplexed hydrogels was demonstrated using mice bearing fast growing, large malignant tumors. However, the cure rate of rhIL-2 loaded stereocomplexed hydrogels was lower, though not statistically significant, compared to the cure rate of a single injection with free rhIL-2 at the start of the therapy (cure rates were 30 and 70%, respectively). The treatment may be improved by combining the slow release of rhIL-2 from the stereocomplexed hydrogels with one injection of free rhIL-2 at the start of the therapy. Further study is needed to optimize the dose of rhIL-2 in the hydrogel. Hydrogels based on eight-arm methacrylate functionalized PEG-PLA star block copolymers are described in **Chapter 6**. The methacrylate group was positioned either at the PLA chain end or at the PEG chain end, yielding PEG-PLA-MA, and PEG-PLA/MA copolymers, respectively. These hydrogels form rapidly in situ under physiological conditions due to stereocomplexation and may be subsequently slowly photopolymerized at low initiator concentrations or light intensities, thus preventing an excessive local temperature rise. Interestingly, stereocomplexation aided in photopolymerization, yielding hydrogels with increased storage modulus and degradation time. Swelling tests showed that the degradation time of PEG-PLA-MA stereo-photo hydrogels (crosslinked by combined stereocomplexation and photopolymerization) was doubled compared to PEG-PLLA-MA hydrogels that were crosslinked by photopolymerization only (approximately 3 vs. 1.5 weeks). PEG-MA/PLA stereo-photo hydrogels degraded within approximately 7 to over 16 weeks, depending on the polymer concentration. In **Chapter 7** hydrogels that are rapidly formed in situ under physiological

Summary

conditions via Michael addition by mixing aqueous solutions of vinyl sulfone functionalized dextrans (dex-VS) and multi-functional mercapto PEG (PEG-SH) are described. Dextrans with pendant vinyl sulfone groups linked by a hydrolytically susceptible ester bond were synthesized by a one-pot synthesis procedure to a broad range of degrees of substitution. The hydrogel mechanical and degradation properties were readily controlled by the degree of vinyl sulfone substitution, concentration, dextran molecular weight and PEG thiol functionality. Furthermore, hydrogels with similar mechanical properties, but decreased degradation rates could be prepared by increasing the spacer length between the thioether and the ester groups. Rheology and swelling tests showed that hydrogels with storage moduli ranging from 3 to 46 kPa and degradation times ranging from 3 to 21 days, respectively, could be obtained. Degradable hydrogels that are rapidly formed in situ under physiological conditions via Michael addition upon mixing aqueous solutions of dextran thiol conjugates (dex-SH) and PEG tetra-acrylate (PEG-4-Acr) or a dex-VS conjugate are described in **Chapter 8**. Dextran thiol conjugates were conveniently synthesized by a two-step synthesis procedure with degrees of substitution ranging from 12 to 25. The hydrogel mechanical and degradation properties could be adjusted by the degree of thiol substitution, concentration, dextran molecular weight and type of crosslinker (PEG-4-Acr or dex-VS). Rheology measurements showed that hydrogels with storage moduli ranging from 9 to 100 kPa could be obtained. Degradation times of dex-SH/PEG-4-Acr hydrogels ranged from 7 to more than 21 weeks and degradation times of dex14K-SH DS 12/dex-VS DS 10 hydrogels ranged from 3 to 7 weeks, as determined by swelling tests. In **Chapter 9** the release of model proteins with different sizes, as well as basic fibroblast growth factor (bFGF) from dextran hydrogels, is described. Protein loaded hydrogels were rapidly formed in situ upon mixing protein containing aqueous solutions of dex-VS and tetrafunctional mercapto PEG. The relatively large protein IgG could be released with almost zero order kinetics from the dextran hydrogels, wherein approximately 95% of IgG was released in 21 days. Dextran hydrogels released the relatively small protein lysozyme for up to 40% in 14 days, with full preservation of the enzymatic activity. Importantly, bFGF was quantitatively released in 28 days without a burst-effect. In **Appendix 1** stereocomplexed hydrogels based on PEG-PLA multi-block copolymers are described. Rheology measurements showed that these hydrogels have improved mechanical properties compared to hydrogels based on PLA-

PEG-PLA triblock copolymers, due to the higher crosslinking functionality of the PEG-PLA multiblock copolymers. In **Appendix 2** the results are given of small angle neutron scattering (SANS) of eight-arm PEG-PLA star block copolymers in water. The shape of the experimental scattering profiles and the apparent characteristic length could be approximated with computational model. In the model the PEG-PLA molecule was simulated by a bead-spring model, wherein attraction between PLA blocks and repulsion between PLA blocks and water could be varied.

Samenvatting

Hydrogelen worden veel gebruikt voor biomedische toepassingen, zoals eiwitafgifte en tissue engineering, omdat ze erg op de natuurlijke extracellulaire matrix lijken. Hydrogelen zijn watergezwollen, niet oplosbare polymeer netwerken. Doordat ze veel water bevatten, zijn ze compatibel met levend weefsel en eiwitten. Ook wordt weefselschade geminimaliseerd door hun rubberachtige eigenschappen. Hydrogelen worden conventioneel eerst gevormd en dan geïmplanteerd in het lichaam. Meer recentelijk zijn hydrogelen in situ gevormd door het mengen van precursor oplossingen. Deze hydrogelen hebben voorkeur boven de van tevoren gevormde hydrogelen, omdat cellen en bioactieve stoffen nu eenvoudig gemengd kunnen worden met de precursor oplossingen voordat gelvorming plaatsvindt. Bovendien maakt in situ vorming van de gel minimaal invasieve operaties en de bereiding van complexe vormen mogelijk.

Hydrogelen worden gevormd door fysische of chemische crosslinking. Fysische crosslinks worden gevormd door noncovalente interacties, zoals hydrofobe en ionische interacties en stereocomplexatie. Fysische crosslinking verloopt in het algemeen onder milde condities, waardoor het mogelijk is om de gel in situ te vormen en te beladen met labiele stoffen. Fysisch gecrosslinkte hydrogelen kunnen echter hun integriteit verliezen door veranderingen in fysische condities. Chemisch gecrosslinkte hydrogelen worden gevormd door reacties tussen functionele groepen. Doorgaans worden deze gellen gemaakt door radicaal keten polymerisatie van (meth)acrylaat gefunctionaliseerde polymeren geïnitieerd door bestraling met licht. Chemisch gecrosslinkte hydrogelen zijn over het algemeen stabiel dan fysisch gecrosslinkte hydrogelen. Chemisch gecrosslinkte hydrogelen kunnen ook in situ gevormd worden, maar er moet zorg gedragen worden dat de reactanten, producten en/of hulpstoffen niet-toxisch zijn.

In **Hoofdstuk 2** wordt een overzicht gegeven van polymeren en crosslink methoden die gebruikt worden voor het maken van hydrogelen. Ook wordt de toepassing van hydrogelen voor medicijn afgifte en tissue engineering beschreven. Tegenwoordig zijn tal van biodegradeerbare polymeren beschikbaar voor de bereiding van hydrogelen. Hydrogelen worden meer en meer ontworpen met toegevoegde functionaliteit om zo de natuurlijke extracellulaire matrix na te bootsen. Hiervoor zijn polymeren ontworpen met enzymatisch

Samenvatting

degradeerbare en/of cel adhesie eiwit sequenties. Recentelijk zijn meerdere crosslink methoden, fysisch zowel als chemisch, ontwikkeld voor de in situ bereiding van hydrogelen. Van de fysische crosslink methoden is stereocomplexatie, of te wel cokrystallisatie van poly(L-lactide) (PLLA) en poly(D-lactide) (PDLA), van water-oplosbare PLA blok copolymeren een veelbelovende benadering. Hydrogelen kunnen snel gevormd worden door stereocomplexatie onder fysiologische condities en kunnen gemakkelijk beladen worden met eiwitten zonder dat het eiwit wordt beschadigd. Bovendien zijn deze hydrogelen biodegradeerbaar door hydrolyse van de PLA blokken. Fotopolymerisatie is een veelgebruikte techniek voor de bereiding van chemisch gecrosslinkte hydrogelen. Deze crosslinktechniek geeft robuuste hydrogelen en de degradatiesnelheid van deze hydrogelen kan in een grote range gevarieerd kan worden. Het vormen van een hydrogel *in vivo* wordt echter bemoeilijkt doordat de huid het UV-licht voor een groot deel absorbeert. Deze crosslinktechniek kan verbeterd worden door combinatie van fotopolymerisatie met een snelle in situ crosslinktechniek. Michael type additie tussen thiolen en acrylaten of vinyl sulfonen is een veelbelovende chemische crosslinktechniek voor de in situ bereiding van hydrogelen. De reactie verloopt snel en is selectief voor thiolen onder fysiologische condities. Bio-functionele hydrogelen kunnen eenvoudig verkregen worden door reactie van de onverzadigde groepen met thiolbevattende bioactieve stoffen voor de geleringsreactie. In **Hoofdstuk 3** worden hydrogelen gebaseerd op poly(ethyleen glycol)-PLA (PEG-PLA) blok copolymeren beschreven. Deze hydrogelen kunnen snel in situ gevormd worden onder fysiologische condities door het mengen van oplossingen van equimolaire hoeveelheden van PEG-PLLA en PEG-PDLA copolymeren in water via stereocomplexatie tussen PLLA en PDLA blokken. Reologie metingen lieten zien dat stereocomplex hydrogelen gebaseerd op acht-arm PEG-PLA ster blok copolymeren verbeterde mechanische eigenschappen hebben vergeleken met hydrogelen gebaseerd op PLA-PEG-PLA triblok copolymeren. Dit komt door de hogere crosslink functionaliteit van de acht-arm PEG-PLA ster blok copolymeren. In **Hoofdstuk 4** wordt een gedetailleerde studie gedaan naar de geleringssnelheid en de mechanische eigenschappen van stereocomplex hydrogelen gebaseerd op acht-arm PEG-PLA ster blok copolymeren. Ook wordt het geleringsmechanisme onderzocht. Reologie metingen lieten zien dat de geleringstijd afneemt en de mechanische eigenschappen van stereocomplex hydrogelen toenemen met toenemende PLA blok lengte of polymeer concentratie. WAXS

metingen van stereocomplex hydrogelen bevestigden de aanwezigheid van stereocomplex kristallen. Cryo-TEM liet zien dat stereocomplex hydrogelen enigszins grotere “micellen” bevatten vergeleken met corresponderende oplossingen van het single enantiomeer in water. In **Hoofdstuk 5** wordt de afgifte van model eiwitten met verschillende groottes en van het farmaceutisch actieve eiwit recombinant human interleukin-2 (rhIL-2) door stereocomplex hydrogelen gebaseerd op acht-arm PEG-PLA ster blok copolymeren bestudeerd. Eiwit beladen hydrogelen konden eenvoudig verkregen worden door het mengen van eiwit bevattende oplossingen van PEG-PLLA en PEG-PDLA copolymeren in water. De *in vitro* afgifte van het relatief kleine eiwit lysozyme (d_h is 4.1 nm) verliep volgens eerste orde kinetiek, waarbij een hoge cumulatieve afgifte van lysozyme van ca. 90% in 10 dagen verkregen werd. Het afgegeven lysozyme behield de enzymatische activiteit, wat laat zien dat de gebruikte hydrogel bereidingsmethode eiwitvriendelijk is. Het grotere eiwit immunoglobuline G (IgG, d_h is 10.7 nm) kon *in vitro* afgegeven worden met bijna nulde orde kinetiek voor 16 dagen. RhIL-2 werd *in vitro* afgegeven met een bijna constante snelheid voor de periode van een week. Na de afgifte experimenten waren de hydrogelen compleet gedegradeerd en waren de oplossingen met de degradatieproducten helder. De therapeutische effectiviteit van rhIL-2 beladen stereocomplex hydrogelen werd gedemonstreerd met muizen die snelgroeiende, grote, kwaadaardige tumoren hadden. Echter, de cure rate van rhIL-2 beladen stereocomplex hydrogelen was lager, hoewel niet statistisch significant, vergeleken met de cure rate van een eenmalige injectie met vrij rhIL-2 aan het begin van de therapie (cure rates waren respectievelijk 30 en 70%). De behandeling zou verbeterd kunnen worden door combinatie van de langzame afgifte van rhIL-2 door stereocomplex hydrogelen met een eenmalige injectie van vrij rhIL-2 aan het begin van de therapie. Verdere studie is nodig voor optimalisatie van de dosis rhIL-2 in de hydrogel. Hydrogelen gebaseerd op acht-arm methacrylaat gefunctionaliseerde PEG-PLA ster blok copolymeren zijn beschreven in **Hoofdstuk 6**. De methacrylaat groep is gepositioneerd aan het uiteinde van de PLA keten of aan de PEG keten van de PEG-PLA-MA en PEG-PLA/MA copolymeren, respectievelijk. Deze hydrogelen kunnen snel *in situ* gevormd worden onder fysiologische condities door stereocomplexatie en kunnen vervolgens langzaam gefotopolymeriseerd worden bij lage initiator concentraties of licht intensiteit. Hierdoor wordt overmatige verhitting door de polymerisatie exotherm voorkomen. Stereocomplexatie hielp bij de fotopolymerisatie interessant genoeg, waardoor

Samenvatting

hydrogelen met een hogere opslagmodulus en langere degradatietijd verkregen werden. Met behulp van zwellingsproeven werd aangetoond dat de degradatietijd van PEG-PLA-MA stereo-foto hydrogelen (gecrosslinkt door een combinatie van stereocomplexatie en fotopolymerisatie) was verdubbeld ten opzichte van PEG-PLLA-MA hydrogelen die alleen door fotopolymerisatie gecrosslinkt waren (ca. 3 vs. 1.5 weken). PEG-MA/PLA stereo-foto hydrogelen degradeerden binnen 7 tot meer dan 16 weken, afhankelijk van de polymeerconcentratie. In **Hoofdstuk 7** worden hydrogelen beschreven die snel in situ gevormd kunnen worden onder fysiologische condities via Michael additie door het mengen van oplossingen van vinyl sulfon gefunctionaliseerd dextran (dex-VS) en multifunctioneel mercapto PEG (PEG-SH) in water. Dextranen met vinyl sulfon zijgroepen en een brede range van substitutiegraden werden gesynthetiseerd met behulp van een één-pot synthese procedure. De mechanische en degradatie eigenschappen van de hydrogelen konden goed gestuurd worden met de vinyl sulfon substitutiegraad, concentratie, dextran molgewicht en PEG thiol functionaliteit. Hydrogelen met gelijke mechanische eigenschappen, maar lagere degradatiesnelheden konden verkregen worden door een langere spacer tussen de thioether en de ester groepen te gebruiken. Reologie en zwellingsproeven lieten zien dat hydrogelen met een opslagmodulus van 3 tot 46 kPa en degradatietijden van 3 tot 21 dagen, respectievelijk, verkregen konden worden. Degradeerbare hydrogelen die snel in situ gevormd kunnen worden onder fysiologische condities via Michael additie door het mengen van oplossingen van dextran thiol en PEG tetra-acrylaat (PEG-4-Acr) of dex-VS in water worden beschreven in **Hoofdstuk 8**. Dextran thiolen konden eenvoudig gesynthetiseerd worden via een twee-stap synthese procedure, waarbij substitutiegraden variërend van 12 tot 25 konden worden verkregen. De mechanische en degradatie eigenschappen van de hydrogelen konden aangepast worden door variatie van de thiol substitutiegraad, concentratie, dextran molgewicht en type crosslinker (PEG-4-Acr of dex-VS). Reologie metingen lieten zien dat hydrogelen met opslagmoduli van 9 tot 100 kPa konden worden verkregen. De degradatietijden van dex-SH/PEG-4-Acr hydrogelen werden bepaald met zwellingsproeven en varieerden van 7 tot meer dan 21 weken. De degradatietijden van dex-SH/dex-VS hydrogelen varieerden van 3 tot 7 weken. In **Hoofdstuk 9** is de afgifte van model eiwitten met verschillende groottes en van basic fibroblast growth factor (bFGF) door dextran hydrogelen beschreven. Eiwit beladen hydrogelen konden snel in situ gevormd worden door het mengen van eiwit bevattende

oplossingen van dex-VS en tetrafunctioneel mercapto PEG. Het relatieve grote eiwit IgG kon worden afgegeven met bijna nulde orde kinetiek door de dextran hydrogelen, waarbij ca. 95% IgG werd afgegeven in 21 dagen. Dextran hydrogelen gaven het relatief kleine eiwit lysozyme af tot 40% in 14 dagen, waarbij het lysozyme de enzymatische activiteit volledig behield. Van belang is dat bFGF kwantitatief afgegeven werd in 28 dagen zonder een burst-effect. In **Appendix 1** zijn stereocomplex hydrogelen gebaseerd op PEG-PLA multi-blok copolymeren beschreven. Reologie metingen toonden aan dat deze hydrogelen verbeterde mechanische eigenschappen hebben vergeleken met hydrogelen gebaseerd op PLA-PEG-PLA triblok copolymeren, door de hogere crosslink functionaliteit van de PEG-PLA multi-blok copolymeren. In **Appendix 2** worden de resultaten beschreven van small angle neutron scattering (SANS) van acht-arm PEG-PLA ster blok copolymeren in water. De vorm van de experimentele scattering curves en de gevonden karakteristieke lengte konden benaderd worden door gebruik te maken van computational modeling. Het PEG-PLA molecuul werd gesimuleerd met een bead-spring model, waarbij de aantrekking tussen de PLA blokken en de afstoting tussen PLA en water gevarieerd konden worden.

Curriculum Vitae

Christine Hiemstra werd geboren op 15 februari 1978 te Drogeham. In 1996 behaalde ze haar VWO diploma aan het Lauwers College te Buitenpost. In 1996 begon ze aan de opleiding Chemische Technologie aan de Universiteit Twente te Enschede met Polymeer Chemie en Biomaterialen als hoofdrichting. Tijdens het vierde jaar heeft ze stage gelopen bij Baxter International te Nijvel (België). De stageopdracht was getiteld: 'De relatie tussen samenstelling, extrusiesnelheid, morfologie en mechanische eigenschappen van polymere blends'. Na deze stage begon ze met afstuderen bij de vakgroep Polymeer Chemie en Biomaterialen aan de Universiteit Twente van prof. dr. J. Feijen onder begeleiding van dr. F. Meng. De afstudeeropdracht had als titel: 'Synthese en karakterisering van kunstmatige cellen'. In 2002 behaalde zij Cum Laude haar universitair diploma. In dezelfde vakgroep Polymeer Chemie en Biomaterialen ging zij werken als assistent in opleiding onder begeleiding van prof. dr. J. Feijen en prof. dr. Z. Y. Zhong. Het promotieonderzoek was getiteld: In situ vorming van biodegradeerbare hydrogelen en hun toepassing voor eiwitafgifte. De resultaten van dit onderzoek staan beschreven in dit proefschrift.

